Synthesis of cyclic peptides as bioconjugation platforms

Peterse, E.

Synthesis of cyclic peptides as bioconjugation platforms

Proefschrift

ter verkrijging van
de graad van doctor aan de Universiteit Leiden,
op gezag van rector magnificus prof. dr. ir. H. Bijl,
volgens besluit van het college voor promoties
te verdedigen op dinsdag 29 juni 2021
klokke 13.45 uur

door

Evert Peterse

geboren te Wageningen
in 1991

Promotiecommissie

Promotor:	Prof. dr. H.S. Overkleeft
Co-promotor:	Dr. D.V. Filippov
Overige leden:	Prof. dr. G.A. van der Marel
	Prof. dr. M. van der Stelt
	Prof. dr. F.A. Ossendorp (Leiden UMC)
	Prof. dr. J. van Maarseveen (Universiteit van Amsterdam)
	Dr. S.I. van Kasteren
	Dr. A.L. Boyle

Printed by GVO Drukkers en Vormgevers
ISBN 978-94-6332-759-6

Table of contents

1

Synthesis and application of cyclic peptides

The identification of an adaptive immune system present in microbes has had a profound effect on science. Twenty years after their original discovery, clustered regularly interspaced short palindromic repeats (CRISPR) were recognized to provide acquired immunity against viruses and plasmids.[1–4] Identified in approximately 40% of sequenced bacterial genomes, CRISPR represents a family of DNA repeats separated by stretches of variable sequences termed spacers; short DNA sequences stemming from invading pathogens. Besides this immunological memory, a set of CRISPR-associated (Cas) genes completes the adaptive immune

system which encodes the protein machinery to carry out a directed immune response.[5] The first step in the CRISPR-Cas system is the identification, by Cas proteins, of a new spacer sequence from an invading pathogen which is then inserted into the CRISPR sequence. Expression of this sequence gives an RNA precursor that is subsequently processed so that each unit known as CRISPR RNA (crRNA) contains a single spacer flanked by a part of the repeat sequence. An active CRISPR-Cas complex is formed when this crRNA is combined with one or more Cas proteins. When a foreign nucleic acid is recognized by base-pairing with complementary crRNA sequences, the target is cleaved and degraded.[6]

The CRISPR-Cas system has since been transformed into a simple and efficient genome editing tool, awarded this year (2020) with the Nobel prize in chemistry.[7–10] The CRISPR-Cas9 system has been used to understand mechanisms of genetic diseases, validate disease targets, develop animal disease models, facilitate genetic engineering in plants and allow for more thorough epigenetic studies leading to over 6000 research papers within five years.[11–17] However, CRISPR-Cas does not mark the first time a microbial defense mechanism has had a major impact on science. Secondary metabolites produced by soil microbes have been a vast resource of antibiotics with over 55% of all antibiotics detected between 1945 and 1978 originating from the genus *Streptomyces*.[18] Since the early days of antibiotic research, it was hypothesized that these bioactive compounds act as a defense mechanism to protect the territory and resources from surrounding micro-organisms.[19] More recently, there have been reports that these secondary metabolites may function as signaling molecules as well.[20]

Since their introduction in the clinic, antibiotics have not only been used to treat infectious diseases, but have also found use in the treatment of other diseases, including cancer, and are applied in the context of organ transplants and open-heart surgery. Aided in part by antibiotics, the average human life expectancy has increased with 23 years when compared to 1910.[21] The discoveries of actinomycin, streptothricin and, most notably, streptomycin by the Waksman group in the 1940s kickstarted natural product discovery in the search for novel bioactive compounds. This has resulted in a myriad of bioactive compounds from bacteria, besides antibiotics also anti-cancer drugs, immunosuppressants, antifungals and anthelminthics.[22,23] Amongst these molecules is the class of macrocyclic peptide-based antibiotics, which are predominantly peptidic structures featuring a ring size larger than twelve atoms (*Figure 1*). In recent years, interest in these compounds as

therapeutics has been renewed and several novel macrocyclic peptides have entered clinical phase trials.[24,25]

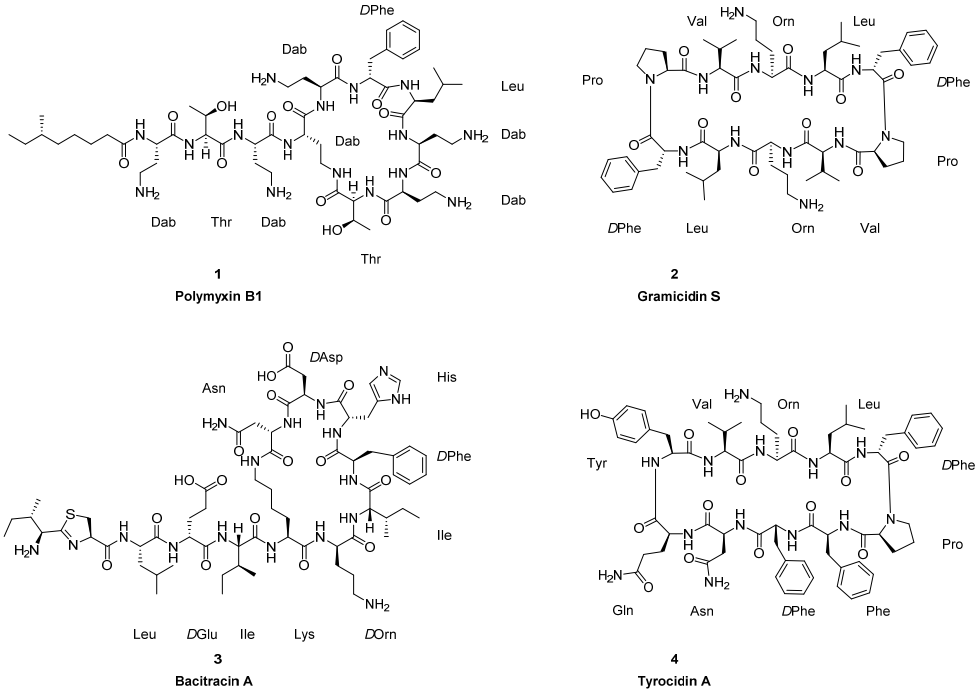

Figure 1. A selection of macrocyclic peptide-based antibiotics.

Syntheses of macrocyclic peptides were first performed to provide structural proof of natural compounds and to create new biologically active analogues.[26] More recently, synthetic cyclic peptides have also been employed to mimic functional domains from proteins and peptides to create peptidomimetic drugs. As an example, the antibiotic protegrin I adopts a well-defined β-hairpin conformation owing to the constraints induced by two disulfide bridges. The absence of one or both bridges leads to loss of the β-hairpin conformation and reduces the membranolytic activity.[27,28] However, significant hemolytic activity hinders the application of protegrin I as an antibiotic. The group of Robinson synthesized a number of cationic head-to-tail cyclic peptides (10 and 14-mers) that feature a β-hairpin structure induced by a L-Pro-D-Pro motif. Optimization of the most promising candidate eventually led to murepavadin lacking the hemolytic

properties of protegrin I but showing *Pseudomonas* specific antimicrobial activity and was projected to enter phase III clinical trials in 2017.[29–31]

The key step in synthetic approaches toward macrocyclic peptides is the macrocyclization reaction. The macrocyclization step most often comprises a lactamization, a lactonization (in case of depsipeptides – macrocyclic peptide-based compounds featuring an ester linkage in the backbone) or the formation of a disulfide bridge. Structurally more diverse macrocycles have been synthesized using other chemical bond forming steps, for instance oxadiazole formation or chemistries involving external stapling agents.[32,33] Depending on its functional groups, cyclization of a peptide can occur in four different ways: head-to-tail (C-terminus to N-terminus), head-to-side-chain, side-chain-to-tail and side-chain-to-side-chain. The most commonly employed strategy is solution-phase cyclization, where the linear peptide is synthesized on the resin and, after cleavage from the resin, is cyclized under dilute conditions (*Figure 2A*). To achieve a selective cyclization a minimum of three levels of orthogonality is required between the linker, the amino acid protecting groups not involved in the cyclization and the N-terminus for elongation. The advantage of this approach is that it enables the synthesis of cyclic peptides on a large scale. However, even under dilute conditions intermolecular reactions may occur to give cyclodimers and cyclooligomers.[34] Performing the cyclization when the peptide is still attached to the solid support remedies this problem owing to pseudo-dilution (*Figure 2B*). Polymer-bound intermediates favor intramolecular reactions over intermolecular ones owing to a low frequency of encounters between intermediates.[34,35] On-resin cyclization starts with the anchoring of an appropriate side-chain (most commonly Asx or Glx) or *via* backbone anchoring. After peptide elongation the sites for cyclization are deprotected orthogonally from the linker and side-chain protecting groups followed by cyclization. Cleavage from the resin and deprotection of applicable side-chains gives the cyclic peptide.

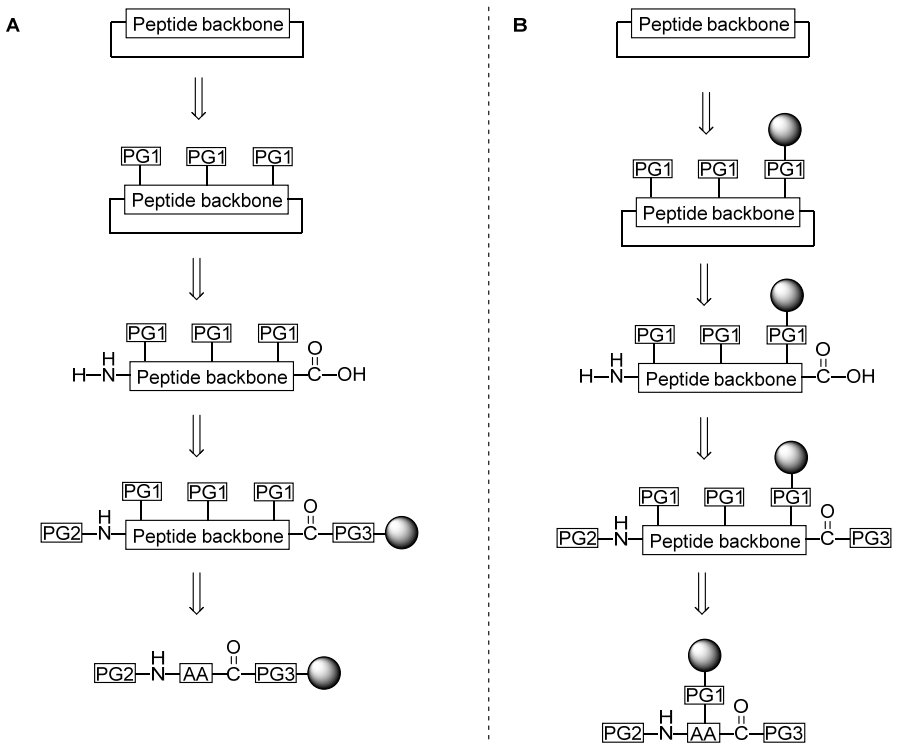

Figure 2. A. Off-resin cyclization strategy for head-to-tail cyclic peptides (PG = protecting group). *B.* The major alternative strategy for head-to-tail cyclic peptides involving on-resin cyclization for which a trifunctional amino acid is required.

Focusing on homodetic cyclic peptides (only amide-linkages connecting the constituent amino acids), both strategies have been employed to synthesize bioactive natural products. For example, the group of Bair utilized a solution-phase cyclization strategy in the synthesis of polymyxin B1 (*Figure 3*).[36] Polymyxin B1 is a side-chain-to-tail cyclic peptide consisting of ten amino acids and a lipophilic moiety at the N-terminus. It is derived from *Bacillus polymyxa* and has been used as a topical antibiotic for over 50 years.[37] Employing a standard Fmoc-based peptide synthesis, Bair and co-workers opted for the sasrin resin, as protected peptides can be liberated from this resin with dilute acid, and protected the Dab that participates in the cyclization with a Dde group. After furnishing linear peptide **6** using HBTU as the condensing agent, the Dde group was removed by three treatments of five minutes each with 2% (v/v) hydrazine in DMF after which the peptide was liberated from the resin using a mixture of TFA and DCM (1:99, TFA – DCM) to obtain compound **7**.

The macrocyclization was carried out with diphenylphosphoryl azide (DPPA) and DIPEA in acetonitrile for 48 hours to obtain protected cyclic peptide **8**. Lastly, global deprotection with 5% (v/v) H_2O in TFA afforded polymyxin B1 in a yield of 20% over 24 steps.

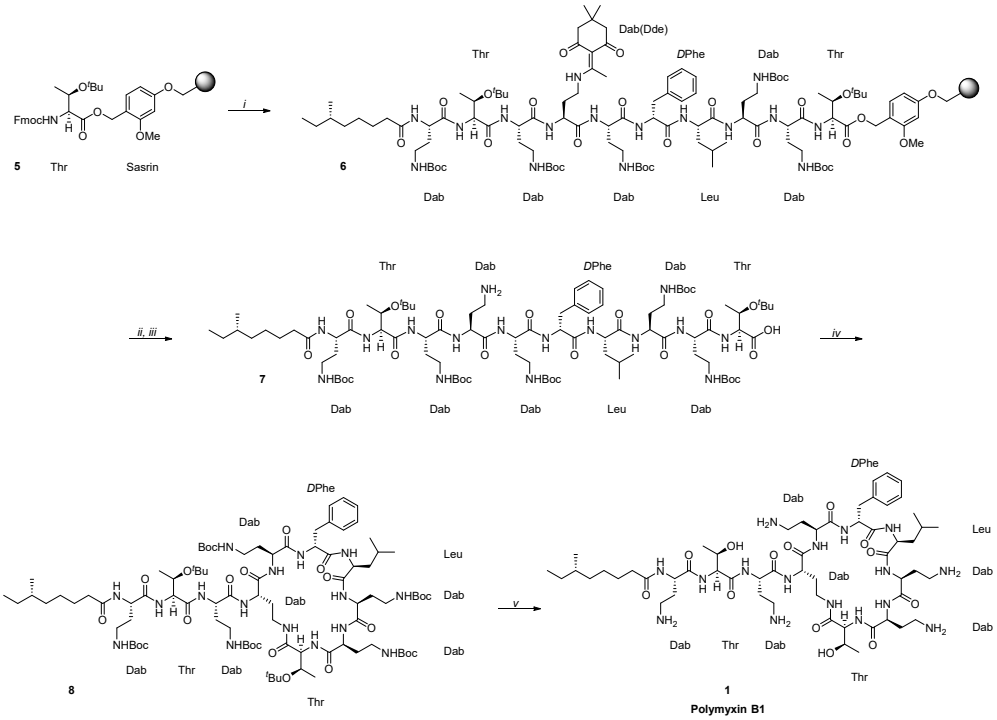

Figure 3. Solution-phase cyclization strategy for the synthesis of polymyxin B1. Reagents and conditions: (*i*) SPPS: (a) piperidine, DMF, rt, 2x, 5 and 15 min. (b) Fmoc-AA, HBTU, DIPEA, NMP, rt, 21 min. (*ii*) hydrazine – DMF (1:49), rt, 3x5 min. (*iii*) TFA – DCM (1:99), rt, 3x15 min. (*iv*) DPPA, DIPEA, MeCN, rt, 48 hrs (*v*) TFA – H_2O (95:5), rt, 1 hr, 20%.

Owing to several appealing characteristics as an antibiotic, gramicidin S has been the subject of numerous studies. Isolated from Russian soil *Bacillus brevis*, this head-to-tail cyclic decapeptide is active against both Gram-positive and Gram-negative bacteria with no observed resistance since its introduction into the clinic in the 40's of the 20th century.[38] Unfortunately, toxicity toward human red blood cells has limited its use to topical infections.[39–41] A range of analogues have been synthesized in an effort to mitigate the hemolysis caused by the parent compound.[42] As a consequence, both solution-phase cyclization strategies as well as on-resin cyclization approaches have been utilized to synthesize gramicidin S and its

analogues. The group of Ulrich employed a solution-phase cyclization strategy utilizing an Fmoc-based SPPS approach (*Figure 4*).[43] Orthogonality between linker and side-chain protecting groups was achieved by using a 2-chlorotrityl resin cleavable with acid and Dde moieties to protect the ornithine δ-amines that can be cleaved with hydrazine. The appropriate Fmoc amino acids were pre-activated with HCTU, 6-Cl-HOBt and DIPEA in DMF for two minutes after which it was coupled to the resin for two hours. After obtaining polymer-bound linear peptide **10**, the resin was subjected to a cleavage cocktail (185:10:5, TFA – TIPS – H_2O) giving decapeptide **11**. The macrocyclization was carried out with PyBOP acting as the condensing agent, HOBt as an additive, DIPEA as the base and DCM as the solvent. The solution was stirred for 20 hours after which the solvent was removed and the crude oil treated with 2% (v/v) hydrazine in THF for 16 hours to liberate the ornithine δ-amines. Ultimately, gramicidin S **2** was obtained in a yield of 69% over 23 steps.

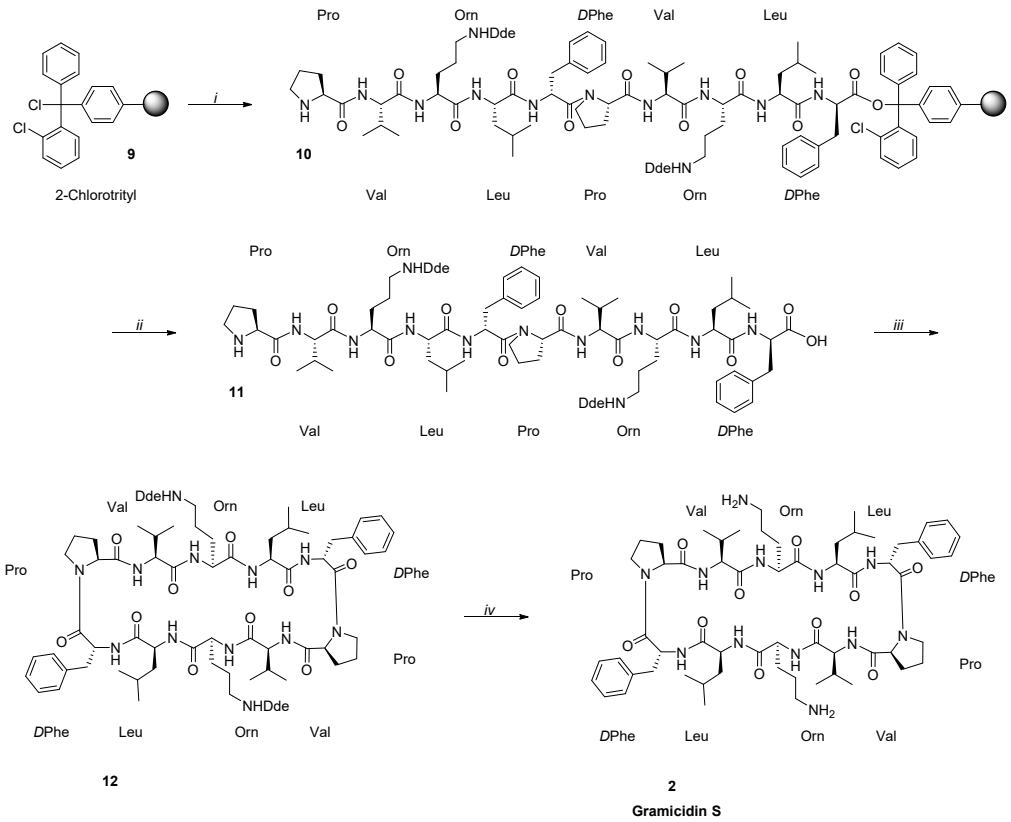

Figure 4. Solution-phase strategy for the synthesis of gramicidin S. Reagents and conditions: (*i*) SPPS: (a) piperidine, DMF, rt, 30 min. (b) Fmoc-AA, 6-Cl-HOBt, HCTU, DIPEA, NMP, rt, 2 hrs (*ii*) TFA – TIPS – H_2O (185:10:5), rt, 3.5 hrs (*iii*) PyBOP, HOBt, DIPEA, DCM, DMF, rt, 20 hrs (*iv*) hydrazine, THF, rt, 16 hrs, 69%.

Alternatively, an on-resin cyclization strategy to synthesize gramicidin S was utilized by the group of González-Muñiz (*Figure 5*).[44] Employing a resin functionalized with a para-hydroxybenzyl alcohol (PHB) linker, the ornithine ε-amine was anchored onto the solid support in two steps. First, the benzyl alcohol was activated with *N*,*N*′-disuccinimidyl carbonate and DMAP for two hours to give carbonate **14**. The resin was then reacted with the trifluoroacetate salt of Fmoc-Orn-OAll and DIPEA for four hours to afford anchored ornithine **15** in a 71% yield. After elongation of the peptide using solid-phase synthesis, the C-terminal allyl ester was deprotected with $Pd(PPh_3)_4$ and morpholine as the allyl acceptor followed by Fmoc deprotection with piperidine. With the N- and C-termini liberated, the cyclization was carried out with PyAOT, HOAt and DIPEA in DMF for two hours at which

point ninhydrin analysis showed no remaining free amino groups. Simultaneous cleavage from the resin and side-chain deprotection with 5% (v/v) H_2O in TFA furnished gramicidin S **2** in a yield of 10% over 22 steps.

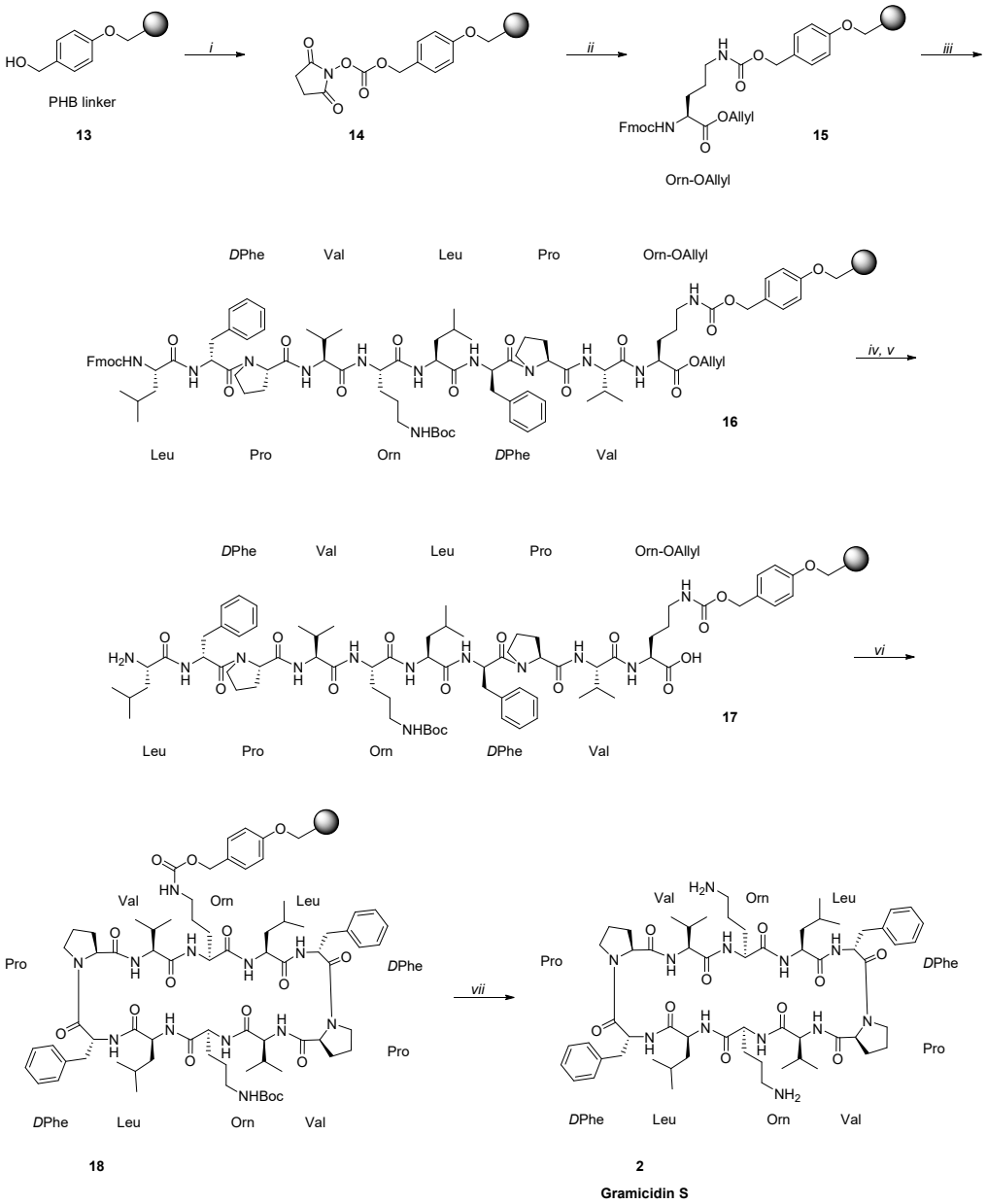

Figure 5. On-resin cyclization strategy for the synthesis of gramicidin S. Reagents and conditions: (*i*) *N*,*N*′-disuccinimidyl carbonate, DMAP, DMF, rt , 2 hrs (*ii*) Fmoc-Orn-OAll trifluoroacetate, DIPEA, DMF, rt, 4 hrs, 71% (*iii*) SPPS: (a) piperidine, DMF, rt, 2x1 min + 1x10 min (b) Fmoc-AA, TBTU, DIPEA, DMF, rt, 1 hr (*iv*) $Pd(PPh_3)_4$, DMSO, THF, 0.5 M aq. HCl, morpholine, rt, 2.5 hrs (*v*) piperidine, DMF, rt, 2x1 min + 1x10 min (*vi*) PyAOP, HOAt, DIPEA, DMF, rt, 2 hrs (*vii*) TFA – H_2O (19:1), rt, 2 hrs, 10%.

The synthesis of the antibiotic bacitracin A by the group of Griffin is another example of utilizing an on-resin cyclization approach (*Figure 6*).[45] Bacitracin A is a side-chain-to-tail cyclic peptide produced by *Bacillus subtilis* and is widely used as a component in topical antibacterial ointments.[46,47] For the synthesis of bacitracin A, Griffin and co-workers anchored the side-chain of Fmoc-Asp-OAll onto an acid-labile PAL resin, which gives an asparagine residue upon cleavage. Elongation of the peptide was performed using SPPS with HBTU and DIPEA as the coupling agents furnishing linear peptide **21** after ten cycles. The lysine ε-amine involved in the cyclization was protected with an alloc group, which was deprotected together with the C-terminal allyl ester with two treatments of $Pd(PPh_3)_4$. The cyclization was then performed with PyBOP, HOBt and DIPEA over 24 hours to give cyclic peptide **23**. After the N-terminal Fmoc was removed and further modified, bacitracin A **3** was liberated from the solid support with a cleavage cocktail (93:5:2, TFA – phenol – TIPS) in an overall yield of 24% over 24 steps.

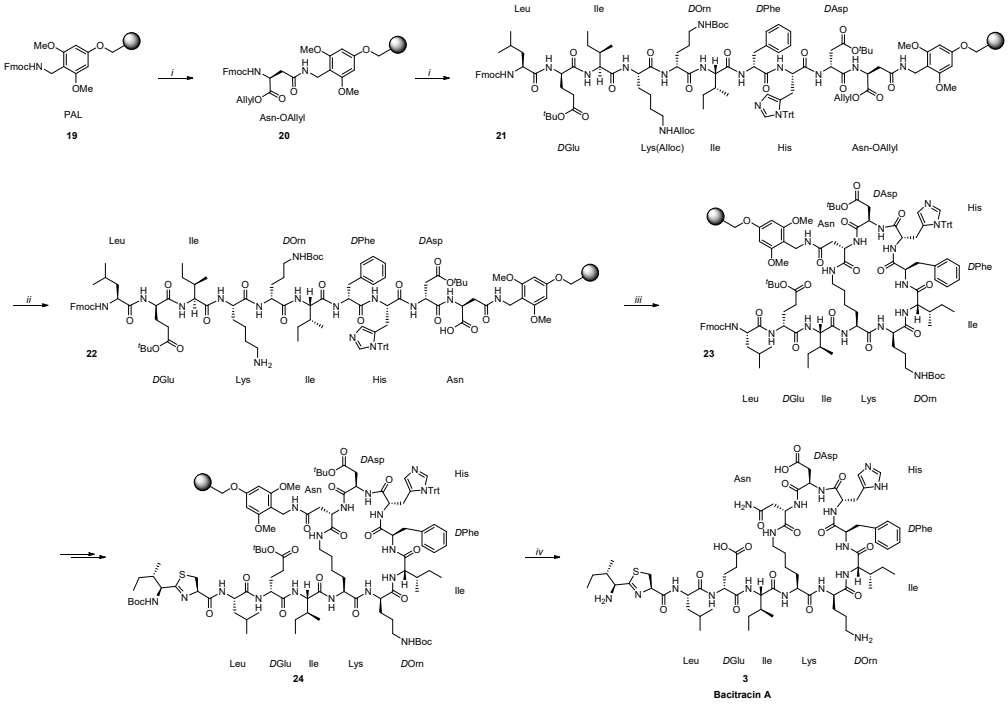

Figure 6. On-resin cyclization strategy for the synthesis of bacitracin A. Reagents and conditions: (*i*) SPPS: (a) HBTU, DIPEA, NMP, rt, 21 min (b) piperidine, DMF, rt, 1x5 min + 1x15 min (*ii*) $Pd(PPh_3)_4$, acetic acid, *N*-methylmorpholine, $CHCl_3$, rt, 1x4 hrs + 1x12 hrs (*iii*) PyBOP, HOBt, DIPEA, NMP, rt, 24 hrs (*iv*) TFA – phenol – TIPS (93:5:2), rt, 1 hr, 24%.

An interesting cleavage by cyclization approach toward cyclic peptides was reported by Yang and Moriello and applied to tyrocidine A by the group of Guo (*Figure 7*).[48,49] For this approach to be high-yielding a pre-organized conformation of the linear peptide is required.[50] Tyrocidine A is a cyclic decapeptide with antibacterial properties produced by *Bacillus brevis* and possesses a conformational preference to self-cyclize making it an ideal candidate for this approach.[47,51,52] First, Kenner's safety-catch resin was reacted with Fmoc-Leu-OH and DIC in the presence of 1-methylimidazole for 24 hours to give compound **26**. The peptide was elongated using SPPS with a combination of DIC and HOBt as the coupling reagents. The safety-catch linker was then activated by treatment with iodoacetonitrile and DIPEA in NMP for 24 hours. After activation, the linker could be cleaved with a nucleophile which was generated by global deprotection with a cleavage cocktail (88:5:5:2, TFA – phenol – TIPS – H_2O). Treatment with DIPEA stimulated cyclization and simultaneous liberation from the solid support giving tyrocidine A **4** in a yield of 25% over 22 steps.

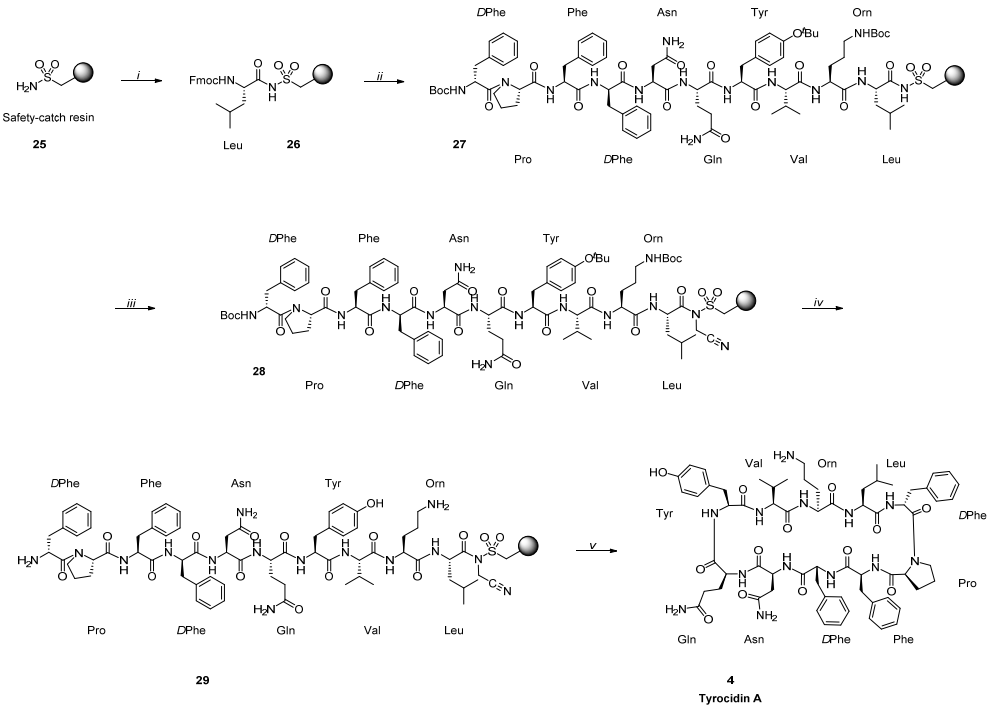

Figure 7. Strategy for synthesis of tyrocidin A involving simultaneous cyclization and cleavage from the resin. Reagents and conditions: (*i*) Fmoc-Leu-OH, DIC, 1-methylimidazole, DCM, DMF, rt, 24 hrs (*ii*) SPPS: (a) piperidine, DMF, rt, 30 min (b) Fmoc-AA (Boc-AA for last residue), DIC, HOBt, DMF, rt, 4 hrs (*iii*) iodoacetonitrile, DIPEA, NMP, rt, 24 hrs, (*iv*) TFA – phenol – TIPS – H_2O (88:5:5:2), rt, 2 hrs (*v*) DIPEA, THF, rt, 6 hrs, 25%.

With the available methods to synthesize them, exemplified by the syntheses described above, in combination with their reduced conformational mobility, cyclic peptides have seen a widespread usage as a multifunctional platform. A peptide template that serves as a structural motif was introduced by the group of Mutter and was termed regioselectively addressable functionalized template (RAFT) has seen considerable usage over the years (*Figure 8*).[53,54] RAFT is a cyclic decapeptide platform composed of two adjacent proline-glycine motifs as type II β-turn-inducers that constrain the backbone conformation in an antiparallel β sheet. This conformational restraint presents two separate spatial domains with residues 3-5-8-10 oriented in the upper plane and residues 4-9 in the opposite plane. Up to six lysine residues can be incorporated and are made regioselectively addressable by way of orthogonal protecting groups.[55]

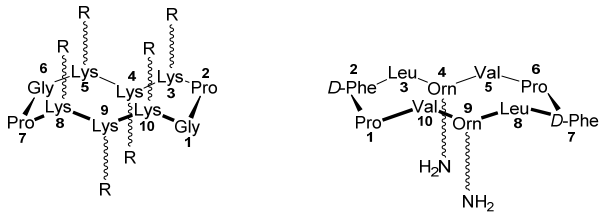

Figure 8. The regioselectively addressable functionalized template **30** as termed by Mutter and co-workers and gramicidin S **31** sharing structural similarities.

Similar to RAFT scaffold **30**, gramicidin S **31** adopts an antiparallel β sheet conformation which is closed by two type II′ β-turns. As shown by the crystal structure, the two ornithine residues present in gramicidin S are both oriented in the same plane making it suitable for the introduction of various functional groups.[56] For example, Martin-Pastor and co-workers functionalized gramicidin S by reacting the ornithine δ-amines with activated esters of achiral phosphines to create a chiral ligand for transition metal catalysis (*Figure 9*).[57] Rhodium(I) complexes were formed with phosphine-containing *para*-substituted gramicidin S **32** as well as the *meta*-variant. These complexes were found to be active in Rh-catalyzed asymmetric hydrogenation with up to 52% enantiomeric excess. The group of Kawai synthesized dinuclear Zn(II) complex **33** by reacting gramicidin S with 2-formylpyridine and $NaBH_3CN$ followed by addition of zinc chloride.[58] This dinuclear complex markedly accelerated the cleavage of the phosphodiester bond of RNA model substrate 2-hydroxypropyl *p*-nitrophenyl phosphate.

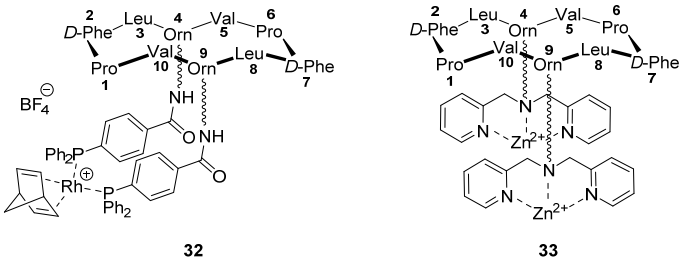

Figure 9. Examples of mono-functionalized cyclic peptides.

The RAFT template has been used by the group of Haehnel for the *de novo* synthesis of an antiparallel four helix bundle protein that is able to accommodate two bis-histidine ligated heme groups. Utilizing amphiphilic helices, Rau and Haehnel

synthesized water-soluble model **34** of the cytochrome *b* core consisting of two parallel heme-binding helices H1 alternated with two antiparallel helices H2 to shield the two hydrophobic heme binding sites (*Figure 10*).[59] The spectroscopic properties of the bound heme groups were found to resemble natural *b*-type cytochromes. For the synthesis, the cyclic decapeptide template was equipped with four protected cysteine residues with one level of orthogonality allowing for stepwise installation of the helices using a bromoacetyl-thiol coupling. Pifferi *et al.* designed and synthesized anticancer vaccines employing a RAFT scaffold with one plane creating a multivalent display of Tn antigen analogues and the opposite domain presenting an ovalbumin peptide containing T helper $CD4^+$ and $CD8^+$ epitopes, such as tetravalent scaffold **35**.[60] These constructs were designed to boost B cell activation and antibody production by effective clustering of the B-cell receptor through high-valency targeting. The synthesis was achieved by conjugating the GalNAc moieties to the scaffold through oxime ligation. A three-step procedure was then performed on the remaining lysine ε-amine (cysteine introduction, deprotection, heterodisulfide synthesis) to attach the peptide *via* disulfide bridge formation. Immunological evaluation showed the hexadecavalent construct to be the most promising generating potent and functional humoral and cellular immune responses with no observed toxicity.

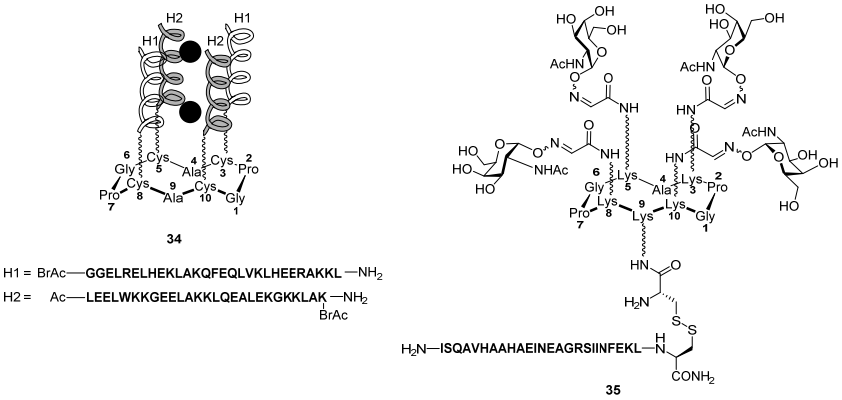

Figure 10. Examples of double functionalized cyclic peptides.

Delangle and co-workers designed a cyclodecapeptide scaffold to lower copper concentration in hepatocytes which is important in Wilson's disease.[61] Wilson's disease is a genetic disorder impairing copper transport in hepatocytes leading to cytosolic accumulation of copper and ultimately necrosis. This causes the release of

large amounts of copper into the blood stream damaging the membrane of red blood cells leading to hemolytic anemia.[62] The group of Delangle designed RAFT scaffold **36** with one plane decorated with GalNAc moieties to target the asialoglycoprotein receptor uniquely expressed on the surface of hepatocytes (*Figure 11*). The lower face of the RAFT scaffold is dedicated to soft metal ion complexation and is under normal conditions protected as a disulfide. Upon entering the reductive medium of the hepatic cells, the disulfide is reduced restoring the ability for copper chelation. The scaffold is also equipped with the fluorophore TRITC to visualize the uptake of the compound in hepatic cell lines. Its synthesis was performed by SPPS on a 2-chlorotrityl chloride resin. On-resin oxidation of the linear peptide furnished the disulfide after which the peptide was cleaved from the resin and subsequently cyclized. The GalNAc moieties were installed by oxime ligation after which the D-Lys ε-amine was reacted with tetramethylrhodamine isothiocyanate to give peptide **36**. Five different bioorthogonal conjugations were used by the group of Renaudet to synthesize well-defined scaffold **37**.[63] A heteroglycocluster of four different carbohydrates comprises one plane of the scaffold while presenting the TLR9 ligand CpG oligodeoxynucleotide (CpG ODN) on the other side. First, β-Glc hydroxylamine was conjugated to the RAFT scaffold by oxime ligation followed by attachment of a GlcNAc thiol to an alloc group by a photo-induced thiol-ene coupling. A copper-catalyzed alkyne-azide cycloaddition (CuAAC) was then performed between α-GalNAc propargyl and azidolysine after which α-Man thiol was coupled to chloroacetamide in an S_N2 reaction to complete the heteroglycocluster. Next, the lysine ε-amine facing the opposite side was functionalized with a hydroxylamine which is then coupled to CpG ODN carrying an aldehyde at the 5′-end obtaining RAFT scaffold **37**.

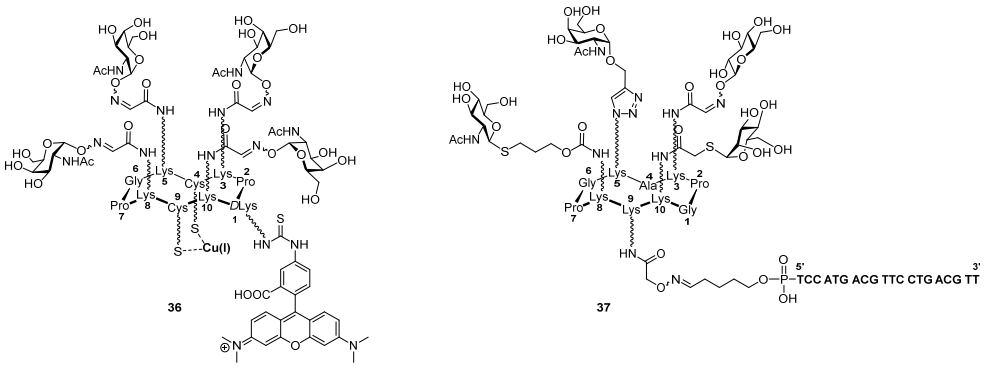

Figure 11. Examples of higher-order functionalized cyclic peptides.

The RAFT scaffolds described above all employ a solution-phase cyclization strategy with a representative example shown in *Figure 12*. The synthesis of antiparallel four-helix bundle protein **34** by Rau and Haehnel started from the extremely acid-sensitive 4-carboxytrityl resin which was preloaded with a glycine residue and the peptide was elongated using Fmoc-based solid-phase synthesis. Special care was taken to avoid racemization of the cysteine residues by introducing them as the symmetrical anhydrides under neutral conditions. The cysteine residues were alternately protected with the trityl (Trt) and acetamidomethyl (Acm) groups that serve as selectively addressable functional groups. The linear peptide was then cleaved from the resin with a cleavage cocktail (5:1:4, AcOH – MeOH – DCM) leaving the side-chain protections intact. Cyclization was performed with TBTU and DIPEA in DMF to give cyclic peptide **41**. After the trityl groups were removed with strong acid, the free thiols were conjugated with the bromoacetamide group present on helix H1 in an S_N2 fashion to obtain functionalized peptide **44**. Deprotection of the Acm groups were achieved with mercury(II) acetate and the free thiols were subsequently reacted with the bromoacetamide group present on helix H2 to give four-helix bundle protein **45**. Finally, incorporation of the heme groups furnished bis-heme binding protein **34** with the spectral properties resembling the natural cytochrome *b*.

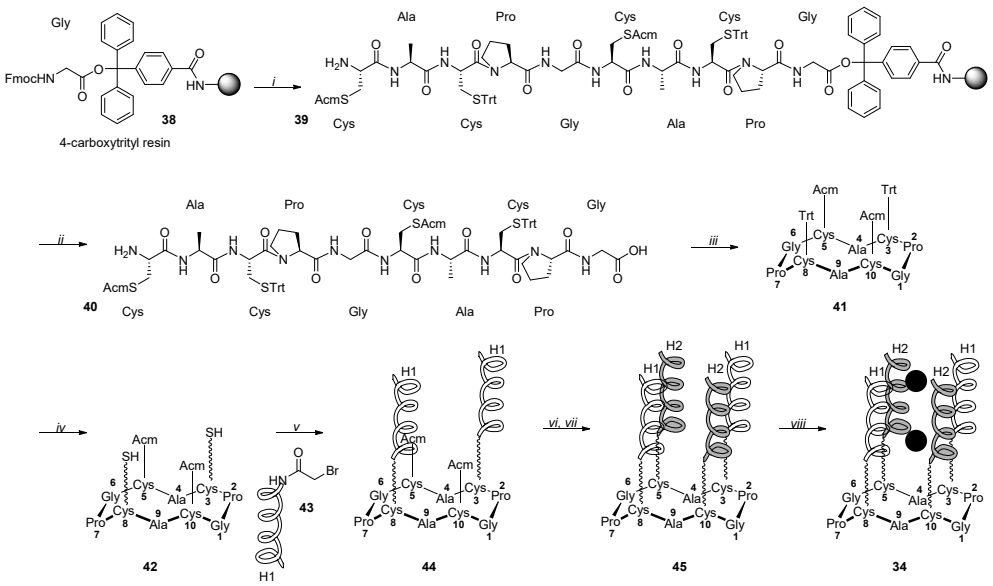

Figure 12. Synthesis of water-soluble model **34** of the cytochrome *b* core. Reagents and conditions: (*i*) SPPS: (a) piperidine, DMF, rt, 7 min. (b) Fmoc-AA, TBTU, DIPEA, DMF, rt, 30 min. or Fmoc-Cys symmetrical anhydride, DMF, rt, 30 min. (*ii*) AcOH – MeOH – DCM (5:1:4), rt, 2 hrs (*iii*) TBTU, DIPEA, DMF, rt, 8 hrs (*iv*) TFA – dithiothreitol (19:1), rt, 30 min. (*v*) 3:2 (v/v) 0.15 M sodium phosphate buffer (pH 7.5) – MeCN, rt, 3 hrs (*vi*) Hg(II)OAc, ammonium acetate buffer (pH 4), rt, 1 hr, then dithiothreitol, rt, 4 hrs (*vii*) H2, 3:2 (v/v) 0.15 M sodium phosphate buffer (pH 7.5) – MeCN, rt, 4 hrs (*viii*) Fe(III)-protoporphyrin IX (heme), DMSO, 50 mM Tris-HCl buffer (pH 8), rt, 30 min.

Thesis outline

This thesis features an on-resin cyclization strategy to synthesize several RAFT scaffolds based on gramicidin S. In **Chapter 2** a method for anchoring lysine ε- and ornithine δ-amines to a nucleophilic solid support is described. The method is used in the synthesis of several head-to-tail cyclic peptides and compared to other reported syntheses. Utilizing this method, **Chapter 3** describes the synthesis of various RAFT scaffolds equipped with two chemoselective handles in differing orientations. Several TLR ligands are synthesized with their chemoselective counterparts to study the effect of orientation on synergy between these ligands. Expanding upon these scaffolds, **Chapter 4** entails the synthesis of gramicidin-based constructs bearing three orthogonal chemoselective handles in various orientation. TLR constructs bearing the additional chemoselective counterpart are also synthesized. The synthesis of a well-defined fusion protein through employing a chemical ligation strategy is the subject in **Chapter 5**. The emphasis is put on late-stage derivatization of the individual proteins for which a two-component linker

system is designed. The linker system is then applied to conjugate two camelid antibodies together. Finally, **Chapter 6** summarizes the content of this Thesis followed by future prospects.

References

(1) Ishino, Y.; Shinagawa, H.; Makino, K.; Amemura, M.; Nakata, A. Nucleotide Sequence of the Iap Gene, Responsible for Alkaline Phosphatase Isozyme Conversion in Escherichia Coli, and Identification of the Gene Product. *J. Bacteriol.* **1987**, *169* (12), 5429–5433. https://doi.org/10.1128/jb.169.12.5429-5433.1987.

(2) Mojica, F. J. M.; Díez-Villaseñor, C.; García-Martínez, J.; Soria, E. Intervening Sequences of Regularly Spaced Prokaryotic Repeats Derive from Foreign Genetic Elements. *J. Mol. Evol.* **2005**, *60* (2), 174–182. https://doi.org/10.1007/s00239-004-0046-3.

(3) Bolotin, A.; Quinquis, B.; Sorokin, A.; Ehrlich, S. D. Clustered Regularly Interspaced Short Palindrome Repeats (CRISPRs) Have Spacers of Extrachromosomal Origin. *Microbiol. Read. Engl.* **2005**, *151* (Pt 8), 2551–2561. https://doi.org/10.1099/mic.0.28048-0.

(4) Pourcel, C.; Salvignol, G.; Vergnaud, G. CRISPR Elements in Yersinia Pestis Acquire New Repeats by Preferential Uptake of Bacteriophage DNA, and Provide Additional Tools for Evolutionary Studies. *Microbiol. Read. Engl.* **2005**, *151* (Pt 3), 653–663. https://doi.org/10.1099/mic.0.27437-0.

(5) Horvath, P.; Barrangou, R. CRISPR/Cas, the Immune System of Bacteria and Archaea. *Science* **2010**, *327* (5962), 167–170. https://doi.org/10.1126/science.1179555.

(6) Amitai, G.; Sorek, R. CRISPR-Cas Adaptation: Insights into the Mechanism of Action. *Nat. Rev. Microbiol.* **2016**, *14* (2), 67–76. https://doi.org/10.1038/nrmicro.2015.14.

(7) Jinek, M.; Chylinski, K.; Fonfara, I.; Hauer, M.; Doudna, J. A.; Charpentier, E. A Programmable Dual-RNA–Guided DNA Endonuclease in Adaptive Bacterial Immunity. *Science* **2012**, *337* (6096), 816–821. https://doi.org/10.1126/science.1225829.

(8) Mali, P.; Aach, J.; Stranges, P. B.; Esvelt, K. M.; Moosburner, M.; Kosuri, S.; Yang, L.; Church, G. M. CAS9 Transcriptional Activators for Target Specificity Screening and Paired Nickases for Cooperative Genome Engineering. *Nat. Biotechnol.* **2013**, *31* (9), 833–838. https://doi.org/10.1038/nbt.2675.

(9) Cho, S. W.; Kim, S.; Kim, J. M.; Kim, J.-S. Targeted Genome Engineering in Human Cells with the Cas9 RNA-Guided Endonuclease. *Nat. Biotechnol.* **2013**, *31* (3), 230–232. https://doi.org/10.1038/nbt.2507.

(10) Cong, L.; Ran, F. A.; Cox, D.; Lin, S.; Barretto, R.; Habib, N.; Hsu, P. D.; Wu, X.; Jiang, W.; Marraffini, L. A.; Zhang, F. Multiplex Genome Engineering Using CRISPR/Cas Systems. *Science* **2013**, *339* (6121), 819–823. https://doi.org/10.1126/science.1231143.

(11) Lino, C. A.; Harper, J. C.; Carney, J. P.; Timlin, J. A. Delivering CRISPR: A Review of the Challenges and Approaches. *Drug Deliv.* **2018**, *25* (1), 1234–1257. https://doi.org/10.1080/10717544.2018.1474964.

(12) Fellmann, C.; Gowen, B. G.; Lin, P.-C.; Doudna, J. A.; Corn, J. E. Cornerstones of CRISPR-Cas in Drug Discovery and Therapy. *Nat. Rev. Drug Discov.* **2017**, *16* (2), 89–100. https://doi.org/10.1038/nrd.2016.238.

(13) Findlay, G. M.; Boyle, E. A.; Hause, R. J.; Klein, J.; Shendure, J. Saturation Editing of Genomic Regions by Multiplex Homology-Directed Repair. *Nature* **2014**, *513* (7516), 120–123. https://doi.org/10.1038/nature13695.

(14) Shalem, O.; Sanjana, N. E.; Hartenian, E.; Shi, X.; Scott, D. A.; Mikkelson, T.; Heckl, D.; Ebert, B. L.; Root, D. E.; Doench, J. G.; Zhang, F. Genome-Scale CRISPR-Cas9 Knockout Screening in Human Cells. *Science* **2014**, *343* (6166), 84–87. https://doi.org/10.1126/science.1247005.

(15) Yang, H.; Wang, H.; Shivalila, C. S.; Cheng, A. W.; Shi, L.; Jaenisch, R. One-Step Generation of Mice Carrying Reporter and Conditional Alleles by CRISPR/Cas-Mediated Genome Engineering. *Cell* **2013**, *154* (6), 1370–1379. https://doi.org/10.1016/j.cell.2013.08.022.

(16) Raitskin, O.; Patron, N. J. Multi-Gene Engineering in Plants with RNA-Guided Cas9 Nuclease. *Curr. Opin. Biotechnol.* **2016**, *37*, 69–75. https://doi.org/10.1016/j.copbio.2015.11.008.

(17) Yao, S.; He, Z.; Chen, C. CRISPR/Cas9-Mediated Genome Editing of Epigenetic Factors for Cancer Therapy. *Hum. Gene Ther.* **2015**, *26* (7), 463–471. https://doi.org/10.1089/hum.2015.067.

(18) Williams, S. T.; Vickers, J. C. The Ecology of Antibiotic Production. *Microb. Ecol.* **1986**, *12* (1), 43–52. https://doi.org/10.1007/BF02153221.

(19) Waksman, S. A. Antagonistic Relations of Microörganisms. *Bacteriol. Rev.* **1941**, *5* (3), 231–291.

(20) Romero, D.; Traxler, M. F.; López, D.; Kolter, R. Antibiotics as Signal Molecules. *Chem. Rev.* **2011**, *111* (9), 5492–5505. https://doi.org/10.1021/cr2000509.

(21) Hutchings, M. I.; Truman, A. W.; Wilkinson, B. Antibiotics: Past, Present and Future. *Curr. Opin. Microbiol.* **2019**, *51*, 72–80. https://doi.org/10.1016/j.mib.2019.10.008.

(22) Katz, L.; Baltz, R. H. Natural Product Discovery: Past, Present, and Future. *J. Ind. Microbiol. Biotechnol.* **2016**, *43* (2–3), 155–176. https://doi.org/10.1007/s10295-015-1723-5.

(23) Traxler, M. F.; Kolter, R. Natural Products in Soil Microbe Interactions and Evolution. *Nat. Prod. Rep.* **2015**, *32* (7), 956–970. https://doi.org/10.1039/c5np00013k.

(24) Luther, A.; Bisang, C.; Obrecht, D. Advances in Macrocyclic Peptide-Based Antibiotics. *Bioorg. Med. Chem.* **2018**, *26* (10), 2850–2858. https://doi.org/10.1016/j.bmc.2017.08.006.

(25) Cochrane, S. A.; Vederas, J. C. Lipopeptides from Bacillus and Paenibacillus Spp.: A Gold Mine of Antibiotic Candidates. *Med. Res. Rev.* **2016**, *36* (1), 4–31. https://doi.org/10.1002/med.21321.

(26) Davies, J. S. The Cyclization of Peptides and Depsipeptides. *J. Pept. Sci.* **2003**, *9* (8), 471–501. https://doi.org/10.1002/psc.491.

(27) Harwig, S. S. L.; Waring, A.; Yang, H. J.; Cho, Y.; Tan, L.; Lehrer, R. I. Intramolecular Disulfide Bonds Enhance the Antimicrobial and Lytic Activities of Protegrins at Physiological Sodium Chloride Concentrations. *Eur. J. Biochem.* **1996**, *240* (2), 352–357. https://doi.org/10.1111/j.1432-1033.1996.0352h.x.

(28) Chen, J.; Falla, T. J.; Liu, H.; Hurst, M. A.; Fujii, C. A.; Mosca, D. A.; Embree, J. R.; Loury, D. J.; Radel, P. A.; Chang, C. C.; Gu, L.; Fiddes, J. C. Development of Protegrins for the Treatment and Prevention of Oral Mucositis: Structure–Activity Relationships of Synthetic Protegrin Analogues. *Pept. Sci.* **2000**, *55* (1), 88–98. https://doi.org/10.1002/1097-0282(2000)55:1<88::AID-BIP80>3.0.CO;2-K.

(29) Shankaramma, S. C.; Athanassiou, Z.; Zerbe, O.; Moehle, K.; Mouton, C.; Bernardini, F.; Vrijbloed, J. W.; Obrecht, D.; Robinson, J. A. Macrocyclic Hairpin Mimetics of the Cationic Antimicrobial Peptide Protegrin I: A New Family of Broad-Spectrum Antibiotics. *ChemBioChem* **2002**, *3* (11), 1126–1133. https://doi.org/10.1002/1439-7633(20021104)3:11<1126::AID-CBIC1126>3.0.CO;2-I.

(30) Srinivas, N.; Jetter, P.; Ueberbacher, B. J.; Werneburg, M.; Zerbe, K.; Steinmann, J.; Meijden, B. V. der; Bernardini, F.; Lederer, A.; Dias, R. L. A.; Misson, P. E.; Henze, H.; Zumbrunn, J.; Gombert, F. O.; Obrecht, D.; Hunziker, P.; Schauer, S.; Ziegler, U.; Käch, A.; Eberl, L.; Riedel, K.; DeMarco, S. J.; Robinson, J. A. Peptidomimetic Antibiotics Target Outer-Membrane Biogenesis in Pseudomonas Aeruginosa. *Science* **2010**, *327* (5968), 1010–1013. https://doi.org/10.1126/science.1182749.

(31) Luther, A.; Moehle, K.; Chevalier, E.; Dale, G.; Obrecht, D. Protein Epitope Mimetic Macrocycles as Biopharmaceuticals. *Curr. Opin. Chem. Biol.* **2017**, *38*, 45–51. https://doi.org/10.1016/j.cbpa.2017.02.004.

(32) White, C. J.; Yudin, A. K. Contemporary Strategies for Peptide Macrocyclization. *Nat. Chem.* **2011**, *3* (7), 509–524. https://doi.org/10.1038/nchem.1062.

(33) Wu, J.; Tang, J.; Chen, H.; He, Y.; Wang, H.; Yao, H. Recent Developments in Peptide Macrocyclization. *Tetrahedron Lett.* **2018**, *59* (4), 325–333. https://doi.org/10.1016/j.tetlet.2017.12.035.

(34) *Peptides: Design, Synthesis, and Biological Activity*; Basava, C., Anantharamaiah, G. M., Eds.; Birkhäuser Basel, 1994. https://doi.org/10.1007/978-1-4615-8176-5.

(35) Mazur, S.; Jayalekshmy, P. Chemistry of Polymer-Bound o-Benzyne. Frequency of Encounter between Substituents on Crosslinked Polystyrenes. *J. Am. Chem. Soc.* **1979**, *101* (3), 677–683. https://doi.org/10.1021/ja00497a032.

(36) Sharma, S. K.; Wu, A. D.; Chandramouli, N.; Fotsch, C.; Kardash, G.; Bair, K. W. Solid-Phase Total Synthesis of Polymyxin B1. *J. Pept. Res.* **1999**, *53* (5), 501–506. https://doi.org/10.1034/j.1399-3011.1999.00045.x.

(37) Stansly, P. G. The Polymyxins: A Review and Assessment. *Am. J. Med.* **1949**, *7* (6), 807–818. https://doi.org/10.1016/0002-9343(49)90419-2.

(38) Gause, G. F.; Brazhnikova, M. G. Gramicidin S and Its Use in the Treatment of Infected Wounds. *Nature* **1944**, *154* (3918), 703–703. https://doi.org/10.1038/154703a0.

(39) Kondejewski, L. H.; Farmer, S. W.; Wishart, D. S.; Hancock, R. E. W.; Hodges, R. S. Gramicidin S Is Active against Both Gram-Positive and Gram-Negative Bacteria. *Int. J. Pept. Protein Res.* **1996**, *47* (6), 460–466. https://doi.org/10.1111/j.1399-3011.1996.tb01096.x.

(40) Berditsch, M.; Lux, H.; Babii, O.; Afonin, S.; Ulrich, A. S. Therapeutic Potential of Gramicidin S in the Treatment of Root Canal Infections. *Pharmaceuticals* **2016**, *9* (3). https://doi.org/10.3390/ph9030056.

(41) Wadsten, C. J.; Bertilsson, C. A.; Sieradzki, H.; Edström, S. A Randomized Clinical Trial of Two Topical Preparations (Framycitin/Gramicidin and Oxytetracycline/Hydrocortisone with Polymyxin B) in the Treatment of External Otitis. *Arch. Otorhinolaryngol.* **1985**, *242* (2), 135–139. https://doi.org/10.1007/BF00454412.

(42) Guan, Q.; Huang, S.; Jin, Y.; Campagne, R.; Alezra, V.; Wan, Y. Recent Advances in the Exploration of Therapeutic Analogues of Gramicidin S, an Old but Still Potent Antimicrobial Peptide. *J. Med. Chem.* **2019**, *62* (17), 7603–7617. https://doi.org/10.1021/acs.jmedchem.9b00156.

(43) Wadhwani, P.; Afonin, S.; Ieronimo, M.; Buerck, J.; Ulrich, A. S. Optimized Protocol for Synthesis of Cyclic Gramicidin S: Starting Amino Acid Is Key to High Yield. *J. Org. Chem.* **2006**, *71* (1), 55–61. https://doi.org/10.1021/jo051519m.

(44) Andreu, D.; Ruiz, S.; Carreño, C.; Alsina, J.; Albericio, F.; Jiménez, M. Á.; de la Figuera, N.; Herranz, R.; García-López, M. T.; González-Muñiz, R. IBTM-Containing Gramicidin S Analogues: Evidence for IBTM as a Suitable Type II′ β-Turn Mimetic1,2. *J. Am. Chem. Soc.* **1997**, *119* (44), 10579–10586. https://doi.org/10.1021/ja9705755.

(45) Lee, J.; Griffin, J. H.; Nicas, T. I. Solid-Phase Total Synthesis of Bacitracin A. *J. Org. Chem.* **1996**, *61* (12), 3983–3986. https://doi.org/10.1021/jo960580b.

(46) Johnson, B. A.; Anker, H.; Meleney, F. L. Bacitracin: A New Antibiotic Produced by a Member of the B. Subtilis Group. *Science* **1945**, *102* (2650), 376–377. https://doi.org/10.1126/science.102.2650.376.

(47) Ressler, C.; Kashelikar, D. V. Identification of Asparaginyl and Glutaminyl Residues in Endo Position in Peptides by Dehydration-Reduction1. *J. Am. Chem. Soc.* **1966**, *88* (9), 2025–2035. https://doi.org/10.1021/ja00961a032.

(48) Yang, L.; Morriello, G. Solid Phase Synthesis of 'Head-to-Tail' Cyclic Peptides Using a Sulfonamide 'Safety-Catch' Linker: The Cleavage by Cyclization Approach. *Tetrahedron Lett.* **1999**, *40* (47), 8197–8200. https://doi.org/10.1016/S0040-4039(99)01701-3.

(49) Qin, C.; Bu, X.; Wu, X.; Guo, Z. A Chemical Approach to Generate Molecular Diversity Based on the Scaffold of Cyclic Decapeptide Antibiotic Tyrocidine A. *J. Comb. Chem.* **2003**, *5* (4), 353–355. https://doi.org/10.1021/cc0300255.

(50) Qin, C.; Xu, C.; Zhang, R.; Niu, W.; Shang, X. On-Resin Cyclization and Antimicrobial Activity of Laterocidin and Its Analogues. *Tetrahedron Lett.* **2010**, *51* (9), 1257–1261. https://doi.org/10.1016/j.tetlet.2009.11.007.

(51) Hotchkiss, R. D.; Dubos, R. J. Bactericidal Fractions from an Aerobic Sporulating Bacillus. *J. Biol. Chem.* **1940**, *136* (3), 803–804.

(52) Bu, X.; Wu, X.; Xie, G.; Guo, Z. Synthesis of Tyrocidine A and Its Analogues by Spontaneous Cyclization in Aqueous Solution. *Org. Lett.* **2002**, *4* (17), 2893–2895. https://doi.org/10.1021/ol0263191.

(53) Silla, U.; Mutter, M. Topological Templates as Tool in Molecular Recognition and Peptide Mimicry: Synthesis of a TASK Library. *J. Mol. Recognit.* **1995**, *8* (1–2), 29–34. https://doi.org/10.1002/jmr.300080105.

(54) Dumy, P.; Eggleston, I. M.; Cervigni, S.; Sila, U.; Sun, X.; Mutter, M. A Convenient Synthesis of Cyclic Peptides as Regioselectively Addressable Functionalized Templates (RAFT). *Tetrahedron Lett.* **1995**, *36* (8), 1255–1258. https://doi.org/10.1016/0040-4039(94)02481-P.

(55) Dumy, P.; Eggleston, I. M.; Esposito, G.; Nicula, S.; Mutter, M. Solution Structure of Regioselectively Addressable Functionalized Templates: An NMR and Restrained Molecular Dynamics Investigation. *Biopolymers* **1996**, *39* (3), 297–308. https://doi.org/10.1002/(sici)1097-0282(199609)39:3<297::aid-bip3>3.0.co;2-j.

(56) Llamas-Saiz, A. L.; Grotenbreg, G. M.; Overhand, M.; van Raaij, M. J. Double-Stranded Helical Twisted β-Sheet Channels in Crystals of Gramicidin S Grown in the Presence of Trifluoroacetic and Hydrochloric Acids. *Acta Crystallogr. D Biol. Crystallogr.* **2007**, *63* (3), 401–407. https://doi.org/10.1107/S0907444906056435.

(57) Guisado-Barrios, G.; Muñoz, B. K.; Kamer, P. C. J.; Lastdrager, B.; Marel, G. van der; Overhand, M.; Vega-Vázquez, M.; Martin-Pastor, M. Cyclic Decapeptide Gramicidin S Derivatives Containing Phosphines: Novel Ligands for Asymmetric Catalysis. *Dalton Trans.* **2013**, *42* (6), 1973–1978. https://doi.org/10.1039/C2DT31782F.

(58) Yamada, K.; Takahashi, Y.; Yamamura, H.; Araki, S.; Saito, K.; Kawai, M. Phosphodiester Bond Cleavage Mediated by a Cyclic β-Sheet Peptide-Based Dinuclear Zinc(II) Complex. *Chem. Commun.* **2000**, No. 14, 1315–1316. https://doi.org/10.1039/B003370G.

(59) Rau, H. K.; Haehnel, W. Design, Synthesis, and Properties of a Novel Cytochrome b Model. *J. Am. Chem. Soc.* **1998**, *120* (3), 468–476. https://doi.org/10.1021/ja973018r.

(60) Pifferi, C.; Ruiz-de-Angulo, A.; Goyard, D.; Tiertant, C.; Sacristán, N.; Barriales, D.; Berthet, N.; Anguita, J.; Renaudet, O.; Fernández-Tejada, A. Chemical Synthesis and Immunological Evaluation of New Generation Multivalent Anticancer Vaccines Based on a Tn Antigen Analogue. *Chem. Sci.* **2020**, *11* (17), 4488–4498. https://doi.org/10.1039/D0SC00544D.

(61) Pujol, A. M.; Cuillel, M.; Renaudet, O.; Lebrun, C.; Charbonnier, P.; Cassio, D.; Gateau, C.; Dumy, P.; Mintz, E.; Delangle, P. Hepatocyte Targeting and Intracellular Copper Chelation by a Thiol-Containing Glycocyclopeptide. *J. Am. Chem. Soc.* **2011**, *133* (2), 286–296. https://doi.org/10.1021/ja106206z.

(62) Sarkar, B. Treatment of Wilson and Menkes Diseases. *Chem. Rev.* **1999**, *99* (9), 2535–2544. https://doi.org/10.1021/cr980446m.

(63) Thomas, B.; Fiore, M.; Daskhan, G. C.; Spinelli, N.; Renaudet, O. A Multi-Ligation Strategy for the Synthesis of Heterofunctionalized Glycosylated Scaffolds. *Chem. Commun.* **2015**, *51* (25), 5436–5439. https://doi.org/10.1039/C4CC05451B.

2

Protocol for side-chain anchoring of the ornithine δ-amine and the lysine ε-amine in the synthesis of macrocyclic peptides

Macrocycles are defined as organic compounds featuring twelve or more atoms in their cyclic structure. Macrocycles are abundant in nature and have received considerable interest from the organic synthesis community both because of their synthetic challenge as well as their promising biological properties.[1–3] Compared to their linear counterparts, macrocycles are conformationally much more constrained. This may be of considerable biological and biomedical advantage, for instance when the conformational preference in solution matches that of the bioactive conformation when bound to a pharmacological target.[4] Macrocycles are

relatively large, and natural ones often quite polar, features that do not comply with Lipinski's rule of five traditionally used to evaluate the chance of success of potential clinical candidates.[5] Recent years however have witnessed the development of several compounds that notwithstanding the fact that they fall short of these benchmarks, have reached the clinic.[6,7] Many of these are macrocycles, further spurning academic interest in these compounds, as well as their synthesis.[8–12]

Cyclic peptides encompass a major class of macrocyclic compounds, varying widely in structure, ring size, functional group patterns and biological activities. Cyclic peptides, and indeed macrocycles in general, have found wide application as antibiotics, ever since the discovery of gramicidin S and tyrothricin in the 1940's. Tyrothricin is a mixture of peptides first isolated from the species *Aneurinibacillus migulanus* (formerly known as *Bacillus brevis*) and contains the cyclic decapeptide tyrocidine. In an effort to isolate tyrothricin from Russian soil *B. brevis*, Gause *et al.* discovered gramicidin S, which already for decades is prescribed as antibiotic for topical infections.[13,14] Both tyrocidine and gramicidin S belong to the so-called head-to-tail cyclic peptide compounds, also subject of the synthesis studies described in this chapter, in which the macrocycle is exclusively made up from the peptide backbone. Cyclic peptides exist as well in which amino acid side chain functionalities partake in macrocyclic structure.

Compared to the synthesis of linear peptides, the synthesis of head-to-tail cyclic peptides is inherently more complicated, predominantly due to the need to condense, at one stage or another in the synthetic procedure, the N-terminal amine with the C-terminal carboxylate to form an amide. This cyclization may occur either on-resin (whence a solid phase peptide synthesis procedure is followed, which is often the case) or off-resin, and both procedures require additional functional (protective) group manipulations compared to the solid phase synthesis of standard, linear peptides (*Figure 1*). On-resin cyclisation for instance requires immobilization of the first amino acid building block through a side chain functionality, rather than the carboxylate, as is standard practice in the solid phase synthesis of linear peptides. Off-resin cyclisation requires the use of side chain amine/carboxylate protective groups orthogonal to the N-terminal one and that can withstand conditions to cleave the linear precursor from the resin. A major intrinsic advantage of on-resin cyclization is that due to the inherent pseudo-dilution effect, the occurrence of intermolecular condensations is diminished compared to that of in solution procedures.[15] Of note as well are simultaneous cyclization/cleavage procedures that

have seen some usage but that appear limited in application to relatively simple macrocyclic peptides.[16,17]

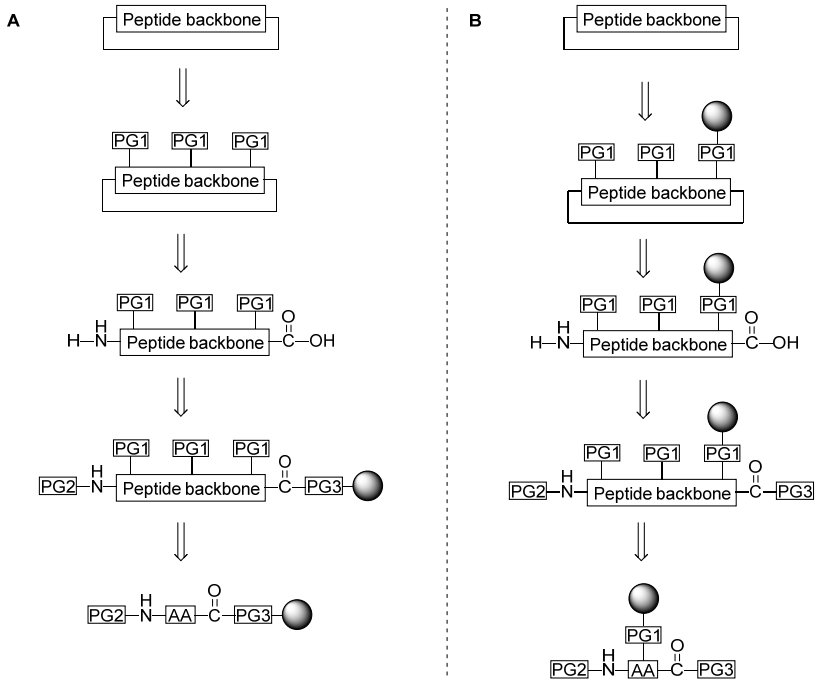

Figure 1. A. Off-resin cyclization strategy for the synthesis of head-to-tail cyclic peptides. *B.* The major alternative strategy for head-to-tail cyclic peptides involving on-resin cyclization for which a trifunctional amino acid is required. (PG = protecting group, AA = amino acid)

The research described in this Chapter entails the development of optimized protocols for the synthesis of head-to-tail cyclic peptides through on-resin cyclization, with particular focus on the nature of the amino acid selected for attachment to the resin through its side chain, the nature of the connecting functionality and the chemistry used to bring the linkage about. Such a chain anchoring methodology requires amino acids with three functional groups that can be addressed individually, and for which new chemistries may need to be developed. Anchoring through carboxamide or carboxylic acid side-chain functionalities (leading to aspartate/glutamate/asparagine/glutamine residues in the final products) can be achieved using established peptide coupling methodologies.[18,19] Other amino acids that have been attached to a resin *via* their side-chain and for which new chemistries have been developed include cysteine[20],

histidine[21,22], serine[23,24], threonine[23,24], tyrosine[25], lysine[26,27], tryptophan[28], arginine[29] and phenylalanine.[30]

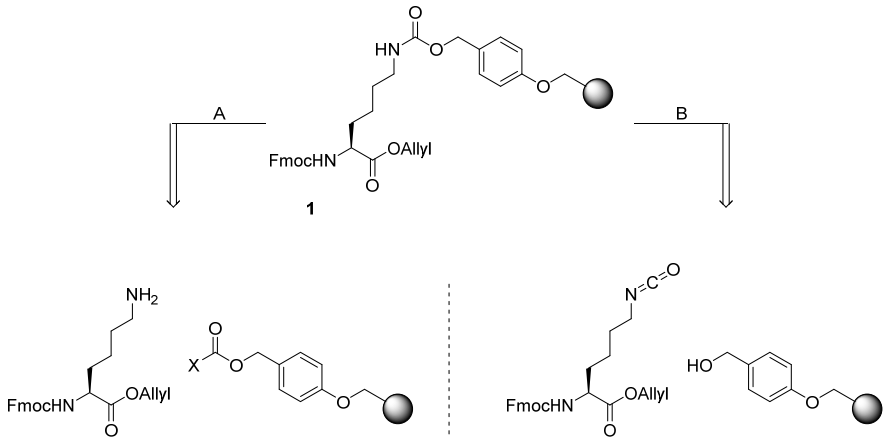

Figure 2. A. Conventional approach of lysine side-chain anchoring that involves an electrophilic resin. *B.* Strategy with a nucleophilic resin resulting in the same linkage.

The work presented in this Chapter entails utilizing the ornithine δ-amine as well as the lysine ε-amine for anchoring to a solid support through an acid-labile functionality. For this purpose, the para-hydroxymethylphenyloxy (Wang) linker in combination with a carbamate as connecting functionality was selected (*Figure 2*). This side chain anchoring system features in several literature studies, in which it was created through nucleophilic attack of the free lysine ε-amine onto an activated carbonate as depicted in *Figure 2, route A*.[26,27] Carbamates can however also be generated by reacting an alcohol with an isocyanate (*Figure 2 route B*) and, since this strategy has not been implemented in the generation of neither anchored lysine ε-amine **1** nor anchored ornithine δ-amine **2** exploration of this route became subject of studies presented in this Chapter (*Figure 2 & 3*). Thus, results here entail the preparation of **1** and **2** following *route B* in efficiencies at least equal to those reported in the literature based on *route A* as well as implementation of anchored ornithine δ-amine **2** in the synthesis of four representative head-to-tail cyclic peptide antibiotics, including gramicidin S and tyrocidine (*Figure 3*).

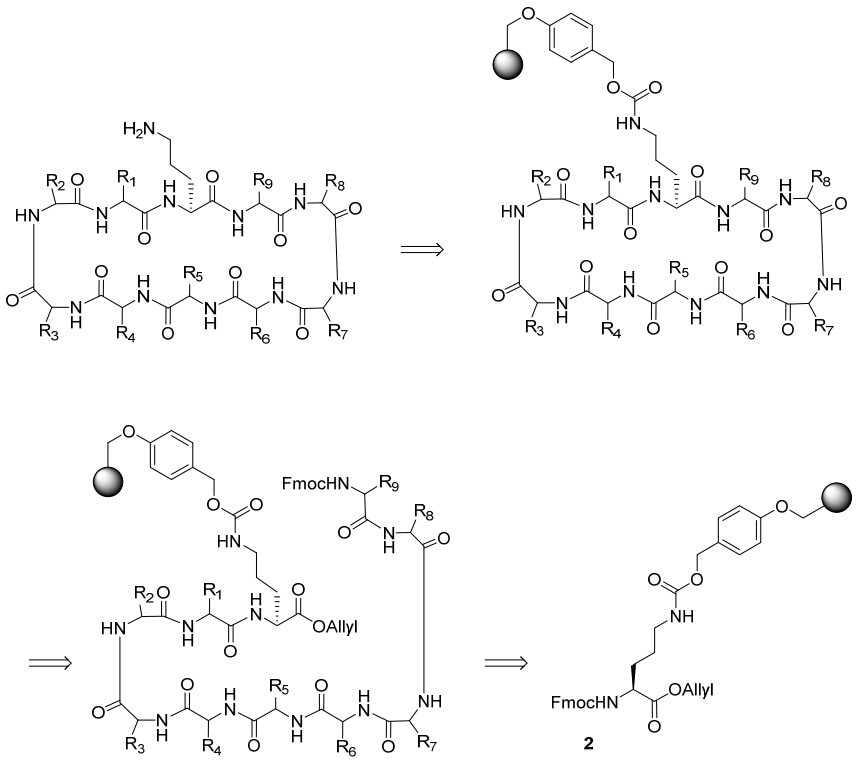

Figure 3. Retrosynthesis of head-to-tail cyclic peptides using an on-resin cyclization strategy.

The target cyclic peptides were selected to allow for comparison of the efficiency (yield, purity) of the investigated synthesis procedure to that of published literature syntheses. As the initial testing will be performed on lysine as opposed to ornithine, due to its availability at cheaper cost, investigating whether the conditions used for the formation of **1** hold true for the formation of anchored ornithine δ-amine **2** is necessary. If true, the construction of the target peptides follows the strategy outlined for on-resin cyclization (*Figure 1B & 3*). Starting from **2** equipped with an N-terminal Fmoc group and a C-terminal allyl protecting group, the peptide is elongated following Fmoc-based solid phase peptide synthesis (SPPS) procedures using amino acids with the appropriate acid-labile protecting groups. After deprotection of the N- and C-terminal protecting groups, the peptide is cyclized in an on-resin fashion. Final global deprotection is envisaged under acidic conditions that also result in removal of the para-alkoxybenzyl group and subsequent

decarboxylation – liberation, in other words, of the ornithine-containing cyclic peptide from the resin.

Results and discussion

As the first research objective, the synthesis of a suitably and orthogonally protected lysine residue for ensuing side chain anchoring to resins was undertaken. Starting from *N*-α-Fmoc-*N*-ε-Boc lysine **3** (the standard lysine building block commonly applied in Fmoc-based solid phase peptide synthesis), alkylation of the carboxylate with allyl bromide and silver carbonate as the base afforded fully and orthogonally protected lysine **4** (*Scheme 1*).

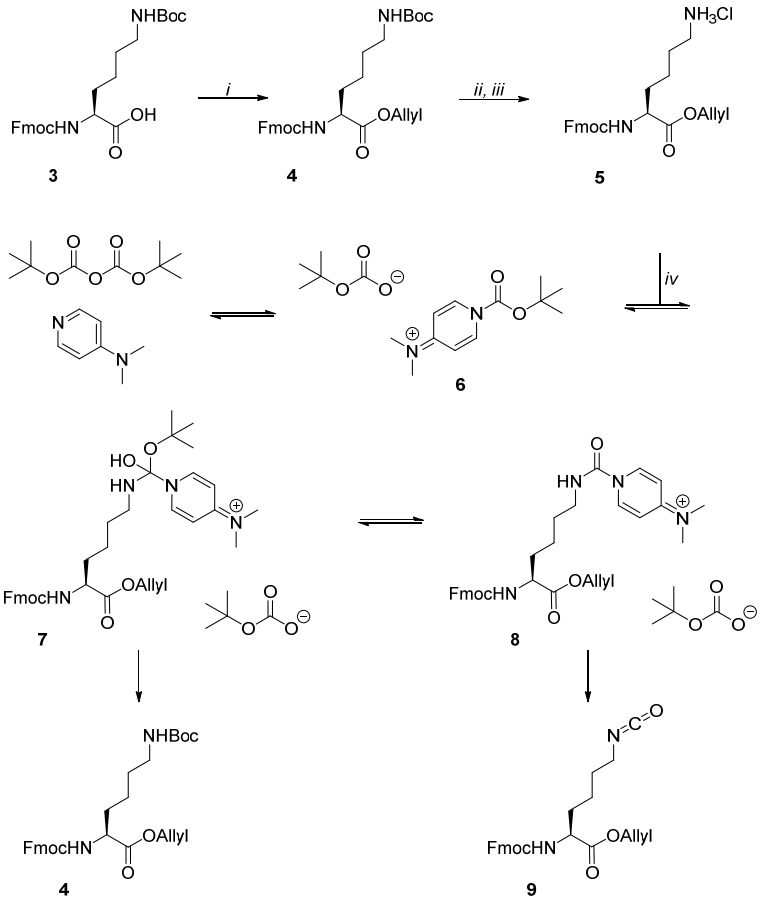

Scheme 1. Postulated mechanism by Knölker and co-workers to convert a free amine to the isocyanate applied to starting material **5**.[31] Reagents and conditions: (*i*) Ag_2CO_3, allyl bromide, DMF, 0 °C to rt, 2.5 hrs, 95% (*ii*) $SnCl_4$, DCM, EA, rt, 1 hr, 88% (*iii*) DMAP, MeCN, rt, 5 min. (*iv*) Boc_2O, DMAP, MeCN, rt, 10 min., 68% (**3**).

With orthogonally protected lysine **4** in hand, the synthesis of the isocyanate was envisioned *via* the free amine followed by conversion to the isocyanate using the procedure originally reported by Knölker *et al.*[31] In this procedure, a free amine is added to a mixture of 4-dimethylaminopyridine and di-*tert*-butyldicarbonate in which *N*-acylpyridinium ion **6** is postulated to be transiently formed. The mechanism postulated by the authors involves the formation of tetrahedral intermediate **7**. At this stage, loss of the pyridinium ion may occur resulting in the formation of *N*-Boc protected amine **3**. However, the authors propose, based on the products they observed, that *tert*-butanol is liberated leading to intermediate **8**.

Finally, loss of the pyridinium ion generates isocyanate **9** together with regeneration of DMAP. In order to investigate this method, *tert*-butyl carbamate **4** was first deprotected using tin(IV) chloride to furnish ammonium chloride **5** in 88% yield. The free amine was generated by treatment with DMAP in MeCN and the solution was subsequently added to a mixture of DMAP and di-*tert*-butyldicarbonate (1:1.4, DMAP – Boc_2O). The solution was stirred for 10 minutes, concentrated and the residue purified by silica gel column chromatography. However, instead of isocyanate **9** urethane **4** was found to be formed as the major product (68% isolated yield).

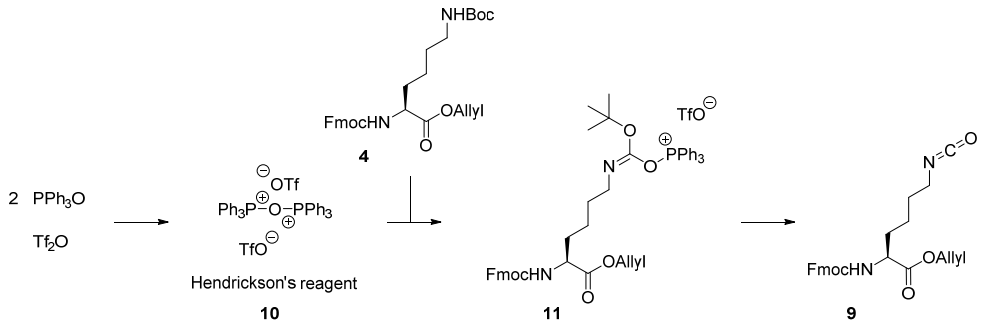

Scheme 2. Postulated mechanism by Cho and co-workers to convert *N*-Boc urethane to isocyanate applied to starting material **4.** Reagents and conditions: (*i*) PPh_3O, Tf_2O, DCM, 0 °C, 30 min, then **4**, DCM, 0 °C to rt, 3 hrs, 19%.

In an alternative procedure, carbamates themselves can be directly transformed into isocyanates following a variety of literature procedures.[32–36] As lysine **4** encompasses two carbamates (N-α-Fmoc and N-ε-Boc), any successful method to turn **4** into **9** should transform the latter carbamate into the isocyanate while leaving the former untouched. Cho and co-workers described a method to convert an *N*-Boc carbamate to an isocyanate (*Scheme 2*).[37] The procedure involves the use of Hendrickson's dehydrating reagent **10**, which is formed by reacting two equivalents of triphenylphosphine oxide with one equivalent of triflic anhydride.[38,39] From this work, in which they investigated a number of carbamates varying in the nature of the oxygen alkyl substituent it could be concluded that the efficiency of the transformation correlates with the acid lability of the carbamate. The authors suggest that the triflic acid that is formed during the reaction aids the conversion of **11** into isocyanate **9** by removing the acid-labile *tert*-butyl group. It was therefore hypothesized that the methodology should be applicable to convert lysine **4** into isocyanate **9**, thus to transform the acid-labile *O*-^{t}Bu carbamate while leaving the acid-stabile *O*-fluorenylmethyl carbamate intact.

To test this hypothesis, Hendrickson reagent was prepared *in situ* by mixing triphenylphosphine oxide and triflic anhydride after which a solution of *N*-Boc carbamate **4** in dichloromethane was added. The reaction proceeded in a clean fashion and after three hours all starting material had been converted and the formation of a more apolar compound was observed by TLC analysis. A sample of the crude reaction mixture was subjected to IR spectroscopy which revealed a strong peak at 2262 cm^{-1} strongly suggesting the formation of an isocyanate. For further examination, this compound was isolated by silica gel column chromatography by directly applying the crude solution onto the column affording an orange oil in a 19% yield. Characterization by ^{1}H NMR spectroscopy showed the presence of the fluorenylmethyl group as well as the absence of the *tert*-butyl group. The ^{13}C NMR spectrum displayed a new peak at 122 ppm characteristic for an isocyanate carbon. Conclusive evidence was obtained using heteronuclear multiple-bond correlation spectroscopy (HMBC) showing correlation between the isocyanate carbon and the ε-protons of the lysine, while no correlation was observed with the α-proton indicating that the Fmoc-carbamate was intact. During column chromatography, besides isolation of isocyanate **9**, a significant amount of the corresponding amine was obtained. Since no amine was formed during the reaction according to TLC, it is likely that the isocyanate degraded on the column. Therefore, it was decided to forego the purification step and add the isocyanate as a crude solution to Wang-type resin **12** (*Table 1*).

Usage of the crude isocyanate solution to furnish side-chain anchored resin **1** necessitated neutralization of the triflic acid that is generated during the reaction. Fortunately, tertiary amines act as a catalyst in the reaction between isocyanates and alcohols so it was envisioned to catch two birds with one stone.[40] The catalytic activity of tertiary amines generally increases as basicity increases. However, the presence of the base-labile Fmoc group limits the choice of catalysts. As the first attempt *N*-methylmorpholine was chosen because of its use as catalyst in the polyurethane industry as well as base in Fmoc-based SPPS.[41] Thus, isocyanate **9** was synthesized as before and 8.5 equivalents *N*-methylmorpholine were added to the solution (7.2 equivalents to neutralize the triflic acid and the remaining 1.3 equivalents to act as catalyst). TentaGel S PHB resin **12** was co-evaporated three times with 1,4-dioxane to remove traces of water. The solution containing isocyanate **9** was transferred to a reaction vessel containing resin **12** and the suspension was shaken for 17 hours. The suspension was filtered and washed with dichloromethane

followed by diethyl ether to shrink the resin. The resin was dried under vacuum and two samples (5 – 10 mg) were taken to determine the loading. Each sample was swollen in DMF (0.80 mL) for 20 minutes followed by addition of piperidine (0.20 mL) and the resulting suspension was shaken for another 20 minutes. The sample was filtrated into a volumetric flask, the resin washed with additional 20% (v/v) piperidine in DMF and subsequently diluted with 20% (v/v) piperidine in DMF to a total volume of 10 mL. The absorption of this solution at 301.0 nm was measured against a blank 20% (v/v) piperidine in DMF solution using a Shimadzu UV-1601 UV-VIS spectrometer with a Quartz cuvette. The loading was determined with the formula described by Eissler *et al.* and the yield was calculated by multiplying the loading substitution with the dry weight of the resin.[42] Less than 5% loading yield was obtained in this way (*Table 1, entry 1*) and alternative conditions involving a variety of catalysts were explored next.

Table 1. Screening of catalysts in the condensation of isocyanate 9 and resin-bound alcohol 12.[a]

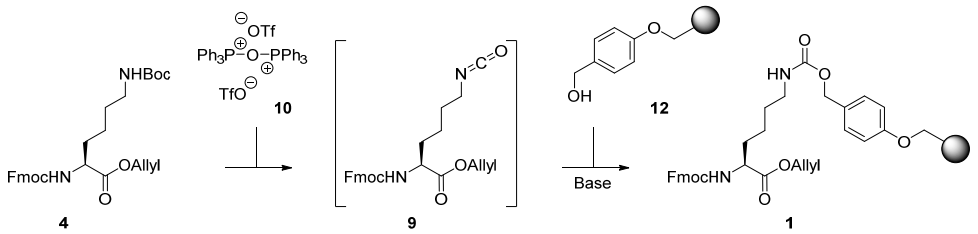

Entry	Catalyst	Equivalents	Base	Excess[b]	Yield
1	–	–	*N*-methylmorpholine	1.3	<5%
2	–	–	1-methylimidazole	1.3	<5%
3	–	–	DMAP	1.3	Fmoc cleavage
4	$Ti(O^tBu)_4$	1.0	*N*-methylmorpholine	0.3	55%
5	$Ti(O^tBu)_4$	3.0	*N*-methylmorpholine	0.3	57%
6	Zr(IV)acac	1.0	*N*-methylmorpholine	0.3	94%
7	Dibutyltindilaurate	1.0	*N*-methylmorpholine	0.3	>99%
8	Dibutyltindilaurate	1.0	1-methylimidazole	0.3	44%

[a] Reactions were performed at a 0.1 mmol scale with 3.0 equivalents of **4** compared to resin **12** over 17 hrs. [b] Excess in equivalents compared to resin **12**.

Yoganathan *et al.* described the use of nucleophilic catalysts 1-methylimidazole and 4-dimethylaminopyridine (DMAP) in the condensation of alcohols with isocyanates.[43] Inspired by these literature precedents, both catalysts were assessed in their efficacy to condense **4** with resin **12** to provide **1**. Concerning the compatibility with the Fmoc group, 1-methylimidazole was expected to cause no issues as it has been used in the presence of an Fmoc group previously.[44] With respect to DMAP it had been shown that a 10% (w/v) solution of this base in DMF can cleave the Fmoc group with a half-life time of 85 minutes.[45] A redeeming quality was that Yoganathan and co-workers observed complete conversion in the condensation with 10 mol% DMAP in 60 minutes. Using 1-methylimidazole as the catalyst and base furnished anchored lysine **1** in less than a 5% yield (*Entry 2*) whereas using DMAP led to partial Fmoc cleavage (*Entry 3*). Attention was then shifted to a procedure by the group of Arbour, who applied titanium(IV) *tert*-butoxide to catalyze the condensation of alcohols with isocyanates.[46] By separating the function of base and catalyst, *N*-methylmorpholine was chosen as the base as it apparently did not catalyze the transformation. In the first instance, 55% yield of resin-bound lysine was obtained with this catalyst (*Entry 4*). Increasing the amount of catalyst to 3.0 equivalents did not lead to a significant increase of the yield affording side-chain anchored lysine **1** in a 57% yield (*Entry 5*).

Two catalysts were finally attempted that originate from the field of polyurethane chemistry, namely zirconium(IV) acetylacetonate and dibutyltin dilaurate.[47,48] With *N*-methylmorpholine as the base, both compounds proved highly effective in catalyzing the desired transformation, giving anchored lysine **1** in a 94% yield for zirconium(IV) acetylacetonate and >99% yield for dibutyltin dilaurate (*Entry 6 & 7)*. Comparing the two catalysts, dibutyltin dilaurate is more efficient in the synthesis of the urethane while zirconium(IV) acetylacetonate is considerably less toxic.[49,50] To assess the influence of the base, *N*-methylmorpholine was substituted for 1-methylimidazole while using dibutyltin dilaurate as the catalyst. This substitution proved detrimental giving urethane **1** in 44% yield (*Entry 8*). This result highlights the influence of the base and further research is necessary to determine the most effective base-catalyst combination.

For the synthesis of the targeted head-to-tail cyclic peptides, first the method had to be applied to ornithine. Therefore, the C-terminus of *N*-α-Fmoc-*N*-δ-Boc ornithine **13** was protected as the allyl ester using allyl bromide and silver carbonate to furnish fully protected ornithine **14** in a 91% yield (*Scheme 3*).

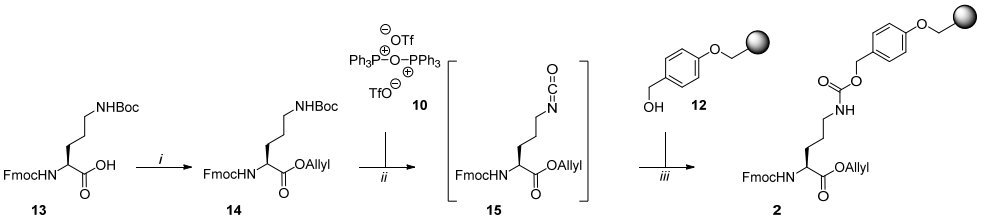

Scheme 3. Reagents and conditions: (*i*) Ag_2CO_3, allyl bromide, DMF, 0 °C to rt, 2.5 hrs, 91% (*ii*) DCM, rt, 15 min. (*iii*) dibutyltin dilaurate, *N*-methylmorpholine, DCM, rt, 24 hrs, 94%.

Using the same procedure as for lysines, *N*-Boc carbamate **14** was converted into isocyanate **15** by Hendrickson's reagent **10**. To the crude solution containing the isocyanate was added *N*-methylmorpholine and dibutyltin dilaurate and the mixture was transferred to a vessel containing TentaGel S PHB resin **12**. After shaking for 24 hours, ornithine-bound resin **2** was obtained in 94% yield. With both resin **2** and lysine-bound resin **1** in hand, the synthesis of the head-to-tail cyclic peptides was started. Methods for allyl deprotection and on-resin cyclization were first conducted on lysine-bound resin **1** and the peptide fragments examined by LC-MS after a sample of the resin was treated to a cleavage cocktail. Suitable conditions were then applied to resin **2** to minimize byproduct formation and incomplete conversions during the synthesis of the first target, gramicidin S.

The synthesis of gramicidin S **20** started with nine peptide coupling cycles on a Protein Technologies Tribute automated peptide synthesizer (*Scheme 4*). Each cycle started with two treatments of 20% (v/v) piperidine in DMF for three minutes to remove the Fmoc group. After a series of washing steps, condensation was achieved by reacting the appropriate partially protected amino acid with deprotected resin-bound peptide using HCTU as the activator and Hünig's base as the base for one hour at room temperature. Unreacted amines were capped by two treatments of 10% (v/v) Ac_2O in DMF for three minutes. After nine such cycles, fully protected linear peptide **16** was obtained.

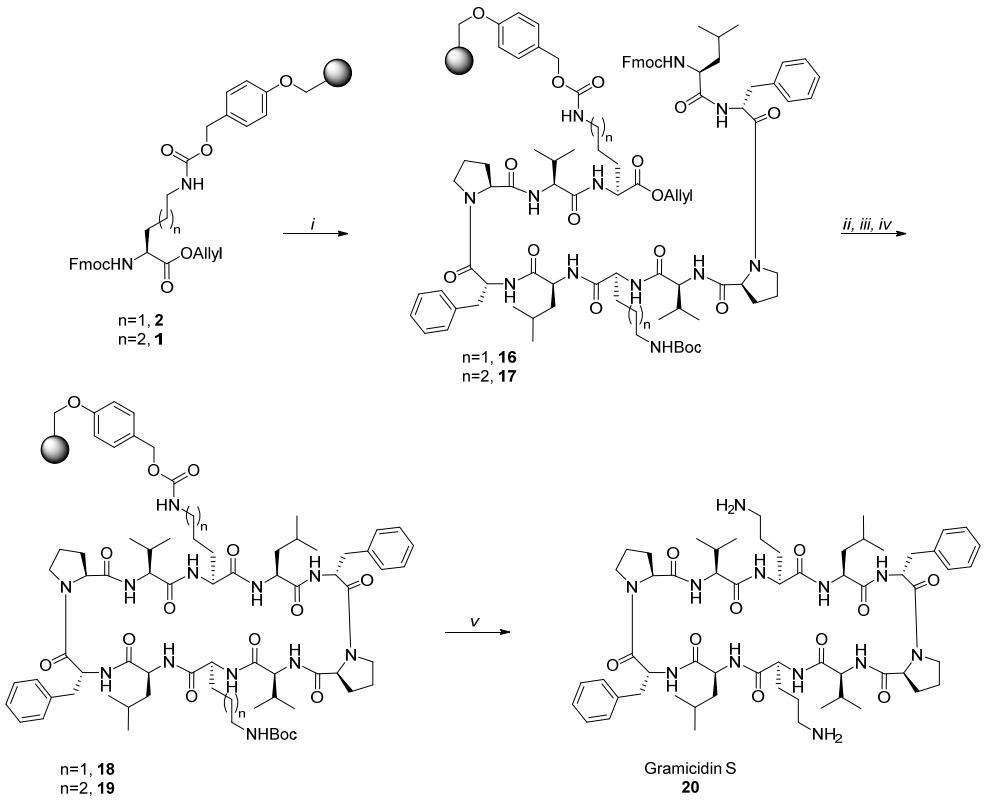

Scheme 4. Reagents and conditions: (*i*) SPPS: (a) piperidine, DMF, rt, 2x3 min. (b) Fmoc-AA-OH, HCTU, DIPEA, DMF, rt, 1 hr (c) Ac_2O, DMF, rt, 2x3 min. (*ii*) $Pd(PPh_3)_4$, $PhSiH_3$, DCM, DMF, rt, 1.5 hrs (*iii*) piperidine, DMF, rt, 2x10 min. (*iv*) benzotriazole-1-yl-oxy-tris-pyrrolidino-phosphonium hexafluorophosphate, 1-hydroxybenzotriazole hydrate, *N*-methylmorpholine, DMF, rt, 2.5 hrs (*v*) TFA – TIPS – H_2O (38:1:1), rt, 3 hrs, 43%.

The synthesis of gramicidin S was continued manually by deprotecting the allyl group. The allyl ester was deprotected before cleavage of the Fmoc-group since the free amine would poison the palladium catalyst.[51] Complete removal of the allyl was observed (as established by cleavage from the resin of a fraction of reacted immobilized peptide **17**) after treatment with palladium tetrakis(triphenylphosphine) with phenylsilane as the allyl group scavenger for 90 minutes. Two treatments with 20% (v/v) piperidine in DMF for ten minutes furnished the liberated N-terminus. For the key on-resin cyclization step, the phosphonium salt benzotriazol-1-yl-oxytripyrrolidinophosphonium hexafluorophosphate was chosen as the coupling reagent over uronium- and aminium-based salts as phosphonium-based coupling reagents do not suffer from

the formation of guanidine derivatives as has been reported for the uronium- and aminium-based reagents.[52,53] 1-Hydroxybenzotriazole was also added to provide more efficient coupling and to lower racemization of the activated amino acid.[54] Cyclization under these conditions plus *N*-methylmorpholine as the base was applied to resin **16** and the suspension was shaken for 2.5 hours. Liberation of gramicidin S **20** from the resin was achieved by treating resin **18** with a cleavage cocktail (38:1:1, TFA – TIPS – H_2O) for three hours. The suspension was filtered and the resin was washed with additional cleavage cocktail. The crude peptide was obtained by evaporation and subsequent purification by size exclusion chromatography afforded gramicidin S in 43% yield.

Analysis by analytical reversed-phase HPLC revealed gramicidin S was obtained with a purity of 96% (*Table 2, entry 1*). In comparison, an on-resin cyclization approach by Andreu and co-workers furnished gramicidin S in a 24% yield with a purity of *ca.* 90%.[55] The major difference in their approach is the method of resin anchoring of the ornithine residue which involved transforming the resin into an activated carbonate species before treatment with ornithine δ-amine (*Figure 2A*). Extensive research investigating an off-resin cyclization strategy in the synthesis of gramicidin S was conducted by Wadhwani *et al.*[56] The highest yield and purity were obtained when the peptide synthesis was started from the D-phenylalanine residue affording gramicidin S in a 69% overall yield with a 95% purity. When the solid-phase synthesis started with Fmoc-Orn(Dde)-OH the yield and purity dropped to 17% and 70% respectively.

Table 2. Synthesis of cyclic peptides using side-chain anchoring.

Entry	Peptide	Yield[a]	Purity[b]
1	*cyclo*(-Leu-*D*Phe-Pro-Val-Orn-)$_2$ Gramicidin S	43%	96%
2	*cyclo*(-Leu-*D*Phe-Pro-Phe-*D*Phe-Asn-Gln-Tyr-Val-Orn-) Tyrocidin A	66%	73%
3	*cyclo*(-Leu-*D*Tyr-Pro-Phe-*D*Phe-Asn-Asp-Tyr-Val-Orn-) Loloatin A	59%	93%
4	*cyclo*(-Leu-*D*Phe-Pro-Leu-*D*Trp-Asn-Gln-Tyr-Val-Orn-) Streptocidin A	40%	53%

[a] Yield after size exclusion chromatography, [b] Chromatographic purity based on area percentage.

To investigate the scope of the procedure described for the synthesis of gramicidin S, three additional natural head-to-tail cyclic peptides that also feature ornithine residues, namely tyrocidin A, loloatin A and streptocidin A, were synthesized in the same manner.[14,57–59] Tyrocidin A was obtained in a 66% yield with a purity of 73% (*Entry 2*). In the synthesis of tyrocidin A, a concurrent cyclization and cleavage approach was employed by Ösapay and co-workers using the Kaiser oxime resin furnishing tyrocidin A in a yield of 55% with a >95% purity.[60] This strategy has also been employed by the group of Guo in the syntheses of gramicidin S (25% yield, 87% purity), tyrocidin A (25% yield, >95% purity), loloatin A (28% yield, 90% purity) and streptocidin A (16% yield, 94% purity).[61–64] The syntheses of loloatin A and streptocidin A were achieved in a 59% and 40% yield with a purity of 93% and 53% respectively (*Entry 3&4*). A reported synthesis of loloatin A by Scherkenbeck *et al.* also employed an on-resin cyclization strategy but here the side-chain of the asparagine residue was used to anchor the growing peptide to the resin.[65] This strategy gave loloatin A in an overall yield of 31% with a 97% purity. Tyrocidin and streptocidin were obtained in a lower purity, which based on the observed masses of the formed product mixtures may be because in both cases incomplete detritylation of the -Asn-Gln- motif had occurred. Perhaps longer exposure to trifluoroacetic acid could alleviate this problem. The synthesis of streptocidin A in turn appeared accompanied by formation of other minor byproducts as well.

Conclusion

In the synthesis of cyclic peptides, the methods for side-chain anchoring of amino acids are limited. In this Chapter, the δ- and ε-amine of ornithine and lysine respectively was successfully anchored to a Wang-type resin. With this method, the properties of the linker remain unaffected compared to coupling to the respective C-terminus as exposure to trifluoroacetic acid liberates the amine accompanied by formation of carbon dioxide. The method involves the formation of an isocyanate which was readily achieved from the *N*-Boc carbamate using Hendrickson's reagent following a procedure by Cho *et al*.[37] In the coupling of the isocyanate to a TentaGel Wang-type resin, dibutyltin dilaurate and zirconium(IV) acetylacetonate were found to be efficient in catalyzing this transformation with *N*-methylmorpholine acting as the base. The choice of base proved to be influential as 1-methylimidazole hampered the catalysis of dibutyltin dilaurate. The side-chain anchoring procedure was then applied to the synthesis of several natural head-to-tail cyclic peptides including gramicidin S and tyrocidin A. The peptides were synthesized in 40-66%

yields with a purity ranging from 53-96%, results that compare well to those reported in the literature on alternative synthesis procedures. A lower purity was observed for the synthesis of tyrocidine A and streptocidin A and was believed to be due to incomplete detritylation of the -Asn-Gln- motif. Longer treatment with trifluoroacetic acid might achieve full deprotection.

General information

Materials, reactions and purification

Standard Fmoc-amino acids and resins for solid-phase peptide synthesis (SPPS), amino acids for solution-phase synthesis and peptide coupling reagents 2-(6-chloro-1*H*-benzotriazole-1-yl)-1,1,3,3-tetramethyluronium hexafluorophosphate (HCTU), *N*,*N*'-diisopropylcarbodiimide (DIC), 1-ethyl-3-(3-dimethylaminopropyl) carbodiimide hydrochloride (EDC), ethyl cyano(hydroxyimino)acetate (Oxyma Pure) and 1-hydroxybenzotriazole (HOBt) were purchased from Novabiochem or Sigma-Aldrich. Fmoc-D-Tyr(^{t}Bu)-OH, Fmoc-D-Trp(Boc)-OH were acquired from Iris Biotech. The resins TentaGel S PHB (0.27 mmol/g) and TentaGel S AC (0.23 mmol/g) were bought from Rapp Polymere. All other chemicals were purchased from Acros, Sigma Aldrich, VWR, Fluka, Merck and Fisher Scientific and used as received unless stated otherwise. Tetrahydrofuran (THF), *N*,*N*-dimethylformamide (DMF), dichloromethane (DCM), 1,4-dioxane and toluene were stored over molecular sieves before use. Commercially available ACS grade solvents were used for column chromatography without any further purification, except for toluene and ethyl acetate which were distilled prior to use. All reactions were carried out under a nitrogen atmosphere, unless indicated otherwise. Reaction progress and chromatography fractions were monitored by thin layer chromatography (TLC) on silica-gel-coated aluminium sheets with a F254 fluorescent indicator purchased from Merck (Silica gel 60 F_{254}). Visualization was achieved by UV absorption by fluorescence quenching, permanganate stain (4 g $KMnO_4$ and 2 g K_2CO_3 in 200 mL of H_2O), ninhydrin stain (0.6 g ninhydrin and 10 mL acetic acid in 200 mL ethanol). Silica gel column chromatography was performed using Screening Devices silica gel 60 (particle size of 40 – 63 μm, pore diameter of 60 Å) with the indicated eluent. Analytical reversed-phase high-performance liquid chromatography (RP-HPLC) was performed on a Thermo Finnigan Surveyor HPLC system with a Phenomenex Gemini C_{18} column (4.6 mm x 50 mm, 3 μm particle size) with a flow rate of 1 mL/min and a solvent gradient of 10-90% solvent B over 8 min coupled to a LCQ Advantage Max (Thermo Finnigan) ion-trap spectrometer (ESI^+). Preparative RP-HPLC was performed with a GX-281 Liquid Handler and a 331 and 332-H2 primary and secondary solvent pump respectively with a Phenomenex Gemini C_{18} column (250 x 10.0 mm, 3 μm particle size) with a flow rate of 5 mL/min and solvent gradients as described for each compound. All HPLC solvents were filtered with a Millipore filtration system equipped with a 0.22 μm nylon membrane filter prior to use. HPLC solvent compositions: solvent A is H_2O; solvent B is MeCN; solvent C is 1.0% TFA in H_2O at a continuous 10% of the volume throughout the run.

Characterization

Nuclear magnetic resonance (^{1}H and ^{13}C APT NMR) spectra were recorded on a Brüker DPX-300, Brüker AV-400, Brüker DMX-400, Brüker AV-500 or Brüker DMX-600 in the given solvent. Chemical shifts are reported in parts per million (ppm) with the residual solvent or tetramethylsilane (0 ppm) as reference. High-resolution mass spectrometry (HRMS) analysis was performed with a Thermo Finnigan LTQ Orbitrap mass spectrometer equipped with an electronspray ion source in positive mode (source voltage 3.5 kV, sheath gas flow 10 ml/min, capillary temperature 250 °C) with resolution R = 60000 at m/z 400 (mass range m/z = 150 – 2000) and dioctyl phthalate (m/z = 391.28428) as a "lock mass". The high-resolution mass spectrometer was calibrated prior to measurements with a Thermo Finnigan calibration mixture. Nominal and exact m/z values are reported in daltons.

Solid-phase peptide synthesis

General methodology

Manual solid-phase peptide synthesis

Manual amino acid couplings were carried out using a fritted reaction syringe equipped with a plunger and syringe cap or a manual reaction vessel (SHG-20260-PI, 60 mL) purchased from Peptides International. The syringe was shaken using either a Heidolph Multi Reax vortexer set at 1000 rpm or a St. John Associates 180° Flask Shaker (model no. A5-6027). Fmoc deprotection was achieved by agitating the resin with 20% (v/v) piperidine in DMF (2 x 10 min.). After draining the reaction vessel, the resin was washed with DMF (6 x 30 sec.). The appropriately side-chain protected Fmoc-amino acid (5.0 equiv.) in DMF (5.0 mL) was pre-activated with HCTU (5.0 equiv.) and DIPEA (10 equiv.) for 5 min, then added to resin and agitated for 60 min. After draining the reaction vessel, the resin was washed with DMF (4 x 30 sec.). The completion of all couplings was assessed by a Kaiser test and double coupling was performed as needed.

Automated solid-phase peptide synthesis

The automated peptide coupling was performed on a CEM Liberty Blue microwave peptide synthesizer or a Protein Technologies Tribute peptide synthesizer using standard Fmoc protected amino acids. For the Tribute peptide

synthesizer, amino acids were presented as solids and 0.20 M HCTU in DMF was used as activator, 0.50 M DIPEA in DMF as the activator base, 20% (v/v) piperidine in DMF as the deprotection agent and a 90:10, DMF – Ac_2O mixture as the capping agent. Coupling of each amino acid occurred at room temperature for 1 hr followed by a capping step (2x 3 min.) betwixt two washing steps. Subsequently, Fmoc was deprotected using the deprotection agent (2x 3 min.) followed by two more washing steps. For the Liberty Blue microwave synthesizer, amino acids were presented as a solution (0.20 M in DMF) and 0.50 M DIC in DMF was used as activator, 1.0 M Oxyma Pure in DMF as additive and 20% (v/v) piperidine in DMF as the deprotection agent. Amino acid coupling in the microwave synthesizer occurred at 90 °C for 2 min. followed by Fmoc deprotection at 90 °C using the aforementioned deprotection agent (2x 90 sec.) and two washing steps.

Loading calculation

Resin was dried before loading calculation by washing with DCM (3x 30 sec.) and Et_2O (3x 30 sec.) followed by purging with N_2. A small amount of resin (5 – 10 mg) was weighed and DMF (0.80 mL) was added and the resin was swollen for 20 min. Piperidine (0.20 mL) was then added and shaken for 20 min. Following the deprotection, the suspension was filtered and diluted with 20% (v/v) piperidine in DMF to a total volume of 10 mL in a volumetric flask. The absorption of this solution was measured against a blank 20% (v/v) piperidine in DMF solution using a Shimadzu UV-1601 UV-VIS spectrometer with a Quartz cuvette (optical pathway = 1 cm). The loading was then calculated using the following equation[42]:

$$\text{Loading}_{\text{resin}} = \frac{A_{301.0\,\text{nm}} * 10^6\ \text{mmol mol}^{-1}\ \text{mg g}^{-1} * V * D}{\varepsilon_{301.0\,\text{nm}} * m_{\text{resin}} * l}$$

where:

$\text{Loading}_{\text{resin}}$	= Fmoc substitution in mmol/g
$A_{301.0\,\text{nm}}$	= Absorption of sample at 301.0 nm
10^6 mmol mol^{-1} mg g^{-1}	= Conversion factor of mmol to mol and mg^{-1} to g^{-1}
V	= Total volume in L
D	= Dilution factor
$\varepsilon_{301.0\,\text{nm}}$	= Molar absorption coefficient at 301.0 nm (8021 L mol^{-1} cm^{-1})
m_{resin}	= sample weight of the resin in mg
l	= optical path length of the cell in cm

Fmoc-Lys(Boc)-OAllyl

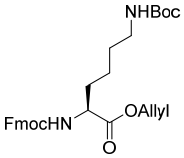

4

Standard Fmoc-protected lysine building block **3** (4.7 g, 10 mmol, 1.0 equiv.) was dissolved in DMF (40 mL, 0.25 M) and the solution was cooled to 0 °C. Silver carbonate (3.6 g, 13 mmol, 1.3 equiv.) was added and the reaction was stirred for 15 min. The cooling bath was removed, allyl bromide (4.0 mL, 46 mmol, 4.6 equiv.) was added and the mixture was stirred for an additional 2.5 hrs. The suspension was then filtered, diluted with EA and subsequently washed with 10% (w/v) aq. $KHSO_4$ and H_2O. The organic layer was dried ($MgSO_4$), filtered and the volatiles were removed under reduced pressure. Purification by silica gel column chromatography (1:4, EA – Pentane to 3:2, EA – Pentane) furnished allyl ester **4** (4.8 g, 9.5 mmol, 95%) as a white solid.

^{1}H NMR (400 MHz, $CDCl_3$) δ 7.77 (d, *J* = 7.5 Hz, 2H, C*H*-arom), 7.65 – 7.52 (m, 2H, C*H*-arom), 7.40 (t, *J* = 7.5 Hz, 2H, C*H*-arom), 7.32 (tt, *J* = 7.5, 1.3 Hz, 2H, C*H*-arom), 5.91 (ddt, *J* = 16.4, 10.3, 5.8 Hz, 1H, OCH_2CH=CH_2), 5.45 – 5.23 (m, 3H, N*H*Fmoc, OCH_2CH=CH_2), 4.68 – 4.62 (m, 2H, OCH_2CH=CH_2), 4.57 (s, 1H, N*H*Boc), 4.47 – 4.33 (m, 3H, CH_2-Fmoc, α-Lys), 4.23 (t, *J* = 7.0 Hz, 1H, C*H*-Fmoc), 3.16 – 3.07 (m, 2H, ε-Lys), 1.95 – 1.82 (m, 1H, β-Lys), 1.79 – 1.67 (m, 1H, β-Lys), 1.43 (s, 13H, δ-Lys, CH_3-Boc, γ-Lys).

^{13}C NMR (101 MHz, $CDCl_3$) δ 172.3 (*C*OOAllyl), 156.2 (*C*=O-Boc), 156.1 (*C*=O-Fmoc), 144.0 (*C*q-arom), 143.9 (*C*q-arom), 141.4 (*C*q-arom), 131.6 (OCH_2CH=CH_2), 127.8 (CH-arom), 127.2 (CH-arom), 125.2 (CH-arom), 120.1 (CH-arom), 120.1 (CH-arom), 119.2 (OCH_2CH=CH_2), 83.0 (*C*(CH_3)$_3$), 67.2 (CH_2-Fmoc), 66.2 (OCH_2CH=CH_2), 53.9 (α-Lys), 47.3 (*C*H-Fmoc), 40.2 (ε-Lys), 32.3 (β-Lys), 29.7 (δ-Lys), 28.5 (CH_3-Boc), 22.5 (γ-Lys).

HRMS (ESI-Orbitrap) calcd. for $C_{29}H_{36}N_2O_6Na$ $[M+Na]^+$ 531.24656, found 531.24641.

Fmoc-Lys-OAllyl

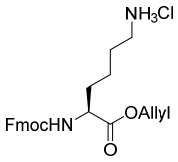

5

Boc-protected amine **4** (50 mg, 98 μmol, 1.0 equiv.) was dissolved in EA (0.98 mL, 0.10 M) and $SnCl_4$ (1.0 M in DCM, 0.39 mL, 0.39 mmol, 4.0 equiv.) was added. The reaction was stirred at room temperature for 1 hr. Afterwards, the reaction mixture was evaporated and dissolved in a small amount of MeOH. Product crashed out upon addition of Et_2O and was collected by filtration affording amine **5** (38 mg, 86 μmol, 88%) as the hydrochloric acid salt.

^{1}H NMR (400 MHz, MeOD) δ 7.79 (d, *J* = 7.5 Hz, 2H, C*H*-arom), 7.66 (t, *J* = 7.5 Hz, 2H, C*H*-arom), 7.39 (t, *J* = 7.4 Hz, 2H, C*H*-arom), 7.30 (t, *J* = 7.4 Hz, 2H, C*H*-arom), 5.93 (ddt, *J* = 16.1, 10.8, 5.6 Hz, 1H, OCH_2CH=CH_2), 5.32 (dq, *J* = 17.2, 1.7 Hz, 1H, OCH_2CH=CH_2), 5.21 (dq, *J* = 10.5, 1.4 Hz, 1H, OCH_2CH=CH_2), 4.62 (dt, *J* = 5.6, 1.5 Hz, 2H, OCH_2CH=CH_2), 4.43 – 4.28 (m, 2H, CH_2-Fmoc), 4.25 – 4.16 (m, 2H, C*H*-Fmoc, α-Lys), 2.97 – 2.85 (m, 2H, ε-Lys), 1.95 – 1.82 (m, 1H, β-Lys), 1.80 – 1.62 (m, 3H, β-Lys, δ-Lys), 1.56 – 1.38 (m, 2H, γ-Lys).

^{13}C NMR (101 MHz, MeOD) δ 173.5 (*C*OOAllyl), 158.7 (*C*=O-Fmoc), 145.2 (*C*q-arom), 142.5 (*C*q-arom), 133.3 (OCH_2CH=CH_2), 128.8 (*C*H-arom), 128.1 (*C*H-arom), 126.2 (*C*H-arom), 126.1 (*C*H-arom), 120.9 (*C*H-arom), 118.7 (OCH_2CH=CH_2), 67.9 (CH_2-Fmoc), 66.7 OCH_2CH=CH_2), 55.2 (α-Lys), 48.3 (*C*H-Fmoc), 40.5 (ε-Lys), 31.9 (β-Lys), 27.9 (δ-Lys), 23.8 (γ-Lys).

Fmoc-Lys(CO)-OAllyl

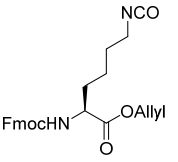

9

Triphenylphosphine oxide (0.16 g, 0.58 mmol, 2.4 equiv.) was dissolved in DCM (8.0 mL, 30 mM) and the solution was cooled to 0 °C. Triflic anhydride (48 μL, 0.29 mmol, 1.2 equiv.) was added and the reaction was stirred at 0 °C for 30 min. during which time a white precipitate was formed. Lysine building block **4** (0.12 g, 0.24 mmol, 1.0 equiv.) was added to the suspension and the reaction was stirred for 3 hrs allowing the mixture to gradually warm to room temperature. The solution was loaded onto a silica gel column and purified by silica gel column chromatography (1:4, EA – Pentane) to give isocyanate **9** (20 mg, 46 μmol, 19%) as an orange oil.

^{1}H NMR (500 MHz, $CDCl_3$) δ 7.79 – 7.73 (m, 2H, C*H*-arom), 7.63 – 7.54 (m, 2H, C*H*-arom), 7.40 (tt, *J* = 7.5, 1.5 Hz, 2H, C*H*-arom), 7.31 (tt, *J* = 7.5, 1.1 Hz, 2H, C*H*-arom), 5.91 (ddt, *J* = 16.6, 11.0, 5.9 Hz, 1H, OCH_2CH=CH_2), 5.39 – 5.22 (m, 3H, N*H*Fmoc, OCH_2CH=CH_2), 4.68 – 4.61 (m, 2H, OCH_2CH=CH_2), 4.45 – 4.34 (m, 3H, CH_2-Fmoc, α-Lys), 4.22 (t, *J* = 7.0 Hz, 1H, C*H*-Fmoc), 3.31 (t, *J* = 6.6 Hz, 2H, ε-Lys), 1.93 – 1.85 (m, 1H, β-Lys), 1.76 – 1.57 (m, 3H, β-Lys, δ-Lys), 1.55 – 1.36 (m, 2H, γ-Lys).

^{13}C NMR (126 MHz, $CDCl_3$) δ 172.1 (*C*OOAllyl), 156.0 (*C*=O-Fmoc), 144.0 (*C*q-arom), 143.8 (*C*q-arom), 141.4 (*C*q-arom), 131.5 (OCH_2CH=CH_2), 127.9 (*C*H-arom), 127.2 (*C*H-arom), 125.2 (*C*H-arom), 122.1 (N*C*O), 120.1 (*C*H-arom), 120.1 (*C*H-arom), 119.3 (OCH_2CH=CH_2), 67.1 (CH_2-Fmoc), 66.3 (OCH_2CH=CH_2), 53.7 (α-Lys), 47.3 (*C*H-Fmoc), 42.8 (ε-Lys), 32.2 (β-Lys), 30.7 (δ-Lys), 22.3 (γ-Lys).

IR (thin film) ν (cm^{-1}) 2262, 1719, 1700, 1451, 1183, 1085, 759, 741.

Fmoc-Lys(TentaGel S PHB)-OAllyl

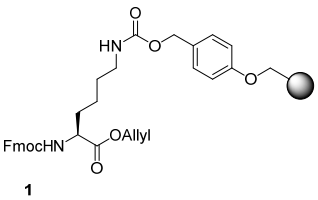

1

A solution containing triphenylphosphine oxide (0.20 g, 0.72 mmol, 7.2 equiv.) in DCM (3.0 mL, 0.12 M) was cooled to 0 °C and triflic anhydride (1.0 M in DCM, 0.36 mL, 0.36 mmol, 3.6 equiv.). The reaction was stirred at 0 °C for 30 min. during which a white precipitate was formed. A solution of *N*-Boc protected lysine **4** (0.15 g, 0.30 mmol, 3.0 equiv.) in DCM (0.34 mL, 0.88 M) was then added to the suspension and the cooling bath was removed. The reaction was stirred for 5 min. followed by the addition of *N*-methylmorpholine (83 μL, 0.75 mmol, 7.5 equiv.) and dibutyltin dilaurate (59 μL, 0.10 mmol, 1.0 equiv.). The solution was transferred to TentaGel S PHB resin (0.27 mmol/g, 0.37 g, 0.10 mmol, 1.0 equiv.) which was co-evaporated previously with 1,4-dioxane (3x) and the suspension was shaken for 18 hrs. The suspension was filtered and the resin was washed with DCM (4x) and Et_2O (4x). Drying the resin over N_2 afforded functionalized resin **1** (0.43 g, 0.10 mmol, >99%) with a loading of 0.24 mmol/g. A fraction of the resin (5.0 mg) was subjected to a cleavage cocktail (190:5:5, TFA – H_2O – TIPS) for 2 hrs and analyzed by LC-MS.

LC-MS (ESI^+) calcd. for $C_{24}H_{29}N_2O_4$ $[M+H]^+$ 409.21, observed 409.25 with a retention time of 5.34 min.

Fmoc-Leu-*D*Phe-Pro-Val-Lys(Boc)-Leu-*D*Phe-Pro-Val-Lys(TentaGel S PHB)-OH

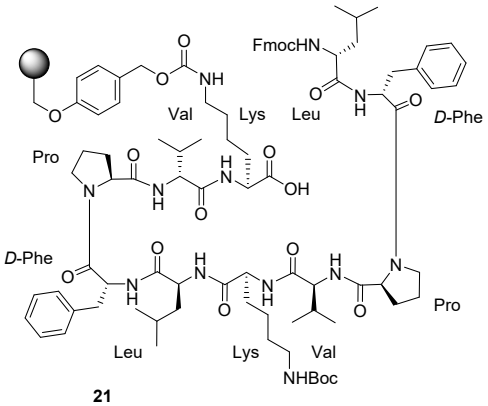

21

Functionalized resin **1** (0.43 g, 0.10 mmol, 1.0 equiv.) was elongated using the Tribute peptide synthesizer. Afterwards, the resin was washed with DCM (4x), Et_2O (4x) and dried over N_2. Resin was suspended in a mixture of DCM and DMF (1:1, DCM – DMF, 4.0 mL, 25 mM) and swollen for 20 min. Phenylsilane (31 µL, 0.25 mmol, 2.5 equiv.) and $Pd(PPh_3)_4$ (29 mg, 25 µmol, 25 mol%) were added and the resin was shaken for 90 min. while being protected from light. The suspension was filtered and the resin was washed with DCM (3x), 0.50% (w/v) sodium diethyldithiocarbamate in DMF (2x) and DMF (3x). A small amount of resin (5.0 mg) was subjected to a cleavage cocktail (190:5:5, TFA – H_2O – TIPS) for 2 hrs and analyzed by LC-MS.

LC-MS (ESI^+) calcd. for $C_{77}H_{108}N_{12}O_{13}$ $[M+H]^+$ 1408.82, observed 1409.73 with a retention time of 6.96 min.

H-Leu-*D*Phe-Pro-Val-Lys(Boc)-Leu-*D*Phe-Pro-Val-Lys(TentaGel S PHB)-OH

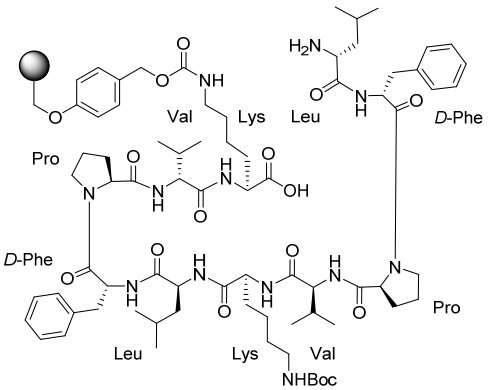

22

To decapeptide **21** was added 20% (v/v) piperidine in DMF (5.0 mL, 20 mM) and the resin was shaken for 10 min. Resin was filtered and 20% (v/v) piperidine in DMF (5.0 mL, 20 mM) was added. Resin was shaken for 10 min. Afterwards, the resin was filtered and washed with DMF (6x). A small amount of resin (5.0 mg) was subjected to a cleavage cocktail (190:5:5, TFA – H_2O – TIPS) for 2 hrs and analyzed by LC-MS.

LC-MS (ESI^+) calcd. for $C_{62}H_{99}N_{12}O_{11}$ $[M+H]^+$ 1187.76, observed 1187.60 with a retention time of 5.31 min.

***cyclo*(-Leu-*D*Phe-Pro-Val-Lys(Boc)-Leu-*D*Phe-Pro-Val-Lys(TentaGel S PHB)-)**

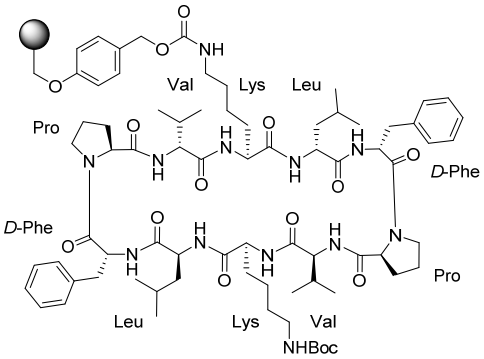

19

To decapeptide **22** was added DMF (4.0 mL, 25 mM). Subsequently, 1-hydroxybenzotriazole hydrate (68 mg, 0.50 mmol, 5.0 equiv.), benzotriazole-1-yl-oxy-tris-pyrrolidino-phosphonium hexafluorophosphate (0.26 g, 0.50 mmol, 5.0 equiv.) and *N*-methylmorpholine (0.11 mL, 1.0 mmol, 10 equiv.) were added to the suspension and the reaction was stirred for 2.5 hrs. The suspension was filtered and the residue was washed with DMF (3x) and DCM (3x). A cleavage mixture (190:5:5, TFA – H_2O – TIPS) was added to a small amount of resin (5.0 mg) and shaken for 2 hrs. The suspension was filtered and the filtrate was analyzed by LC-MS.

LC-MS (ESI$^+$) calcd. for $C_{62}H_{97}N_{12}O_{10}$ $[M+H]^+$ 1169.74, observed 1169.67 with a retention time of 7.13 min.

Fmoc-Orn(Boc)-OAllyl

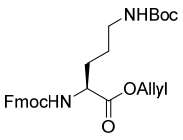

14

Fmoc-Orn(Boc)-OH **13** (2.0 g, 4.4 mmol, 1.0 equiv.) was dissolved in DMF (18 mL, 0.25 M) and cooled to 0 °C. Silver carbonate (1.6 g, 5.7 mmol, 1.3 equiv.) was added and the reaction was stirred for 15 min. Allyl bromide (1.8 mL, 20 mmol, 4.6 equiv.) was added, cooling bath was removed and the mixture was stirred at room temperature for 3 hrs. The suspension was filtered and the filtrate was diluted with DCM and subsequently washed with 10% (w/v) aq. $KHSO_4$. The organic phase was dried ($MgSO_4$), filtered and the volatiles were removed under reduced pressure. Purification by silica gel column chromatography (1:4, EA – Pentane to 2:3, EA – Pentane) afforded allyl ester **14** (2.0 g, 4.1 mmol, 91%) as a white solid.

^{1}H NMR (400 MHz, $CDCl_3$) δ 7.77 (dq, *J* = 7.7, 1.0 Hz, 2H, C*H*-arom), 7.64 – 7.57 (m, 2H, C*H*-arom), 7.41 (tq, *J* = 7.5, 1.0 Hz, 2H, C*H*-arom), 7.32 (tt, *J* = 7.4, 1.2 Hz, 2H, C*H*-arom), 5.91 (ddt, *J* = 16.4, 10.9, 5.8 Hz, 1H, OCH_2CH=CH_2), 5.45 (d, *J* = 8.3 Hz, 1H, N*H*Fmoc), 5.37 – 5.24 (m, 2H, OCH_2CH=CH_2), 4.65 (d, *J* = 5.8 Hz, 2H, OCH_2CH=CH_2), 4.57 (s, 1H, N*H*Boc), 4.45 – 4.36 (m, 3H, CH_2-Fmoc, α-Orn), 4.22 (t, *J* = 6.9 Hz, 1H, C*H*-Fmoc), 3.22 – 3.10 (m, 2H, δ-Orn), 1.96 – 1.84 (m, 1H, β-Orn), 1.77 – 1.49 (m, 3H, β-Orn, γ-Orn), 1.44 (s, 9H, CH_3-Boc).

^{13}C NMR (101 MHz, $CDCl_3$) δ 172.1 (*C*OOAllyl), 156.1 (*C*=O-Boc), 156.1 (*C*=O-Fmoc), 143.9 (*C*q-arom), 141.5 (*C*q-arom), 131.6 (OCH_2CH=CH_2), 127.9 (*C*H-arom), 127.2 (*C*H-arom), 125.2 (*C*H-arom), 120.1 (*C*H-arom), 120.1 (*C*H-arom), 119.3 (OCH_2CH=CH_2), 67.1 (CH_2-Fmoc), 66.2 (OCH_2CH=CH_2), 53.8 (α-Orn), 47.3 (*C*H-Fmoc), 40.1 (δ-Orn), 30.0 (β-Orn), 28.5 (CH_3-Boc), 26.3 (γ-Orn).

HRMS (ESI-Orbitrap) calcd. for $C_{28}H_{34}N_2O_6Na$ $[M+Na]^+$ 517.23091, found 517.23091.

Fmoc-Orn(TentaGel S PHB)-OAllyl

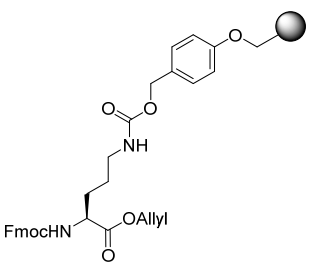

2

A solution containing triphenyl phosphine oxide (1.0 g, 3.6 mmol, 7.2 equiv.) in DCM (14 mL, 0.26 M) was cooled to 0 °C and triflic anhydride (1.0 M in DCM, 1.8 mL, 1.8 mmol, 3.6 equiv.) was added. The reaction was stirred at 0 °C for 30 min. forming a white precipitate. A solution of allyl ester **8** (0.74 g, 1.5 mmol, 3.0 equiv.) in DCM (1.7 mL, 0.88 M) was added and the cooling bath was removed. The reaction was stirred at room temperature for 15 min. followed by the addition of *N*-methylmorpholine (0.41 mL, 3.8 mmol, 7.5 equiv.) and dibutyltin dilaurate (0.30 mL, 0.5 mmol, 1.0 equiv.). The solution was transferred to TentaGel S PHB resin (0.27 mmol/g, 1.9 g, 0.50 mmol, 1.0 equiv.) which was previously co-evaporated with 1,4-dioxane (3x) and the suspension was shaken for 24 hrs. The reaction mixture was filtered and the resin was washed with DCM (4x) and Et_2O (4x). Drying the resin over N_2 furnished functionalized resin **2** (2.1 g, 0.47 mmol, 94%) with a loading of 0.23 mmol/g.

Gramicidin S
***cyclo*(-Leu-*D*Phe-Pro-Val-Orn-)$_2$**

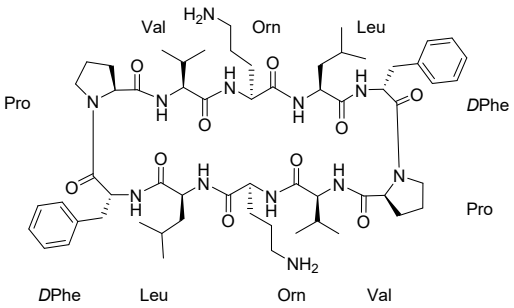

20

Functionalized resin **2** (0.44 g, 0.10 mmol, 1.0 equiv.) was elongated using the Tribute peptide synthesizer. Afterwards, the resin was washed with DMF (4x) and DCM (4x). Resin was suspended in a mixture of DCM and DMF (1:1, DCM – DMF, 4.0 mL, 25 mM) and phenylsilane (31 μL, 0.25 mmol, 2.5 equiv.) and $Pd(PPh_3)_4$ (29 mg, 25 μmol, 25 mol%) were added. The resin was shaken for 90 min. while being protected from light. The suspension was filtered and the resin was washed with DCM (3x), 0.50% (w/v) sodium diethyldithiocarbamate in DMF (2x) and DMF (3x). To the resin was added 20% (v/v) piperidine in DMF (5.0 mL, 20 mM) and the resin was shaken for 10 min. Suspension was filtered and 20% (v/v) piperidine in DMF (5.0 mL, 20 mM) was added to the residue. Resin was shaken for 10 min. followed by filtration and washing with DMF (6x). To the resin was added DMF (4.0 mL, 25 mM). Subsequently, 1-hydroxybenzotriazole hydrate (68 mg, 0.50 mmol, 5.0 equiv.), benzotriazole-1-yl-oxy-tris-pyrrolidino-phosphonium hexafluorophosphate (0.26 g, 0.50 mmol, 5.0 equiv.) and *N*-methylmorpholine (0.11 mL, 1.0 mmol, 10 equiv.) were added to the suspension and the reaction was stirred for 2.5 hrs. The suspension was filtered and the residue was washed with DMF (3x) and DCM (6x). A cleavage mixture (190:5:5, TFA – H_2O – TIPS, 10 mL, 10 mM) was then added to the resin and the resulting suspension was shaken for 3 hrs. The suspension was filtered and the volatiles of the filtrate were removed under a stream of N_2. Residue was dissolved in a mixture of DCM and MeOH (1:1, MeOH – DCM) and purified by size exclusion chromatography (Sephadex LH-20, 1:1, MeOH – DCM) to give gramicidin S **20** (49 mg, 43 μmol, 43%) as a white solid.

^{1}H NMR (400 MHz, CD_3OH, 4.94 ppm suppressed) δ 8.94 (br s, 2H, N*H*-*D*Phe), 8.72 (dd, *J* = 12.0, 9.4 Hz, 4H, N*H*-Leu, N*H*-Orn), 7.71 (d, *J* = 9.0 Hz, 2H, N*H*-Val), 7.37 – 7.20 (m, 10H, C*H*-arom-*D*Phe), 4.66 (q, *J* = 7.6 Hz, 2H, α-Leu), 4.54 – 4.45 (m, 2H, α-*D*Phe), 4.37 – 4.32 (m, 2H, α-Pro), 4.15 (t, *J* = 8.8 Hz, 2H, α-Val), 3.73 (t, *J* = 9.5 Hz, 2H, δ-Pro), 3.15 – 2.82 (m, 8H, β-*D*Phe, δ-Orn, β-*D*Phe, δ-Orn), 2.50 – 2.42 (m, 2H, δ-Pro), 2.32 – 2.22 (m, 2H, β-Val), 2.09 – 1.96 (m, 4H, β-Pro, β-Orn), 1.81 – 1.34 (m, 18H, β-Orn, γ-Pro, β-Pro, γ-Pro, γ-Orn, β-Leu, γ-Leu, β-Leu), 0.98 – 0.84 (m, 24H, γ-Val, δ-Leu).
Note: α-Orn is in the suppressed region of 4.94 ppm.
^{13}C NMR (101 MHz, CD_3OH) δ 173.5 (*C*ONH), 173.5 (*C*ONH), 173.4 (*C*ONH), 172.8 (*C*ONH), 172.4 (*C*ONH), 136.8 (*C*q-arom-*D*Phe), 130.3 (*C*H-arom-*D*Phe), 129.6 (*C*H-arom-*D*Phe), 128.5 (*C*H-arom-*D*Phe), 61.9 (α-Pro), 60.3 (α-Val), 55.9 (α-*D*Phe), 52.4 (α-Orn), 51.4 (α-Leu), 47.9 (δ-Pro), 42.0 (β-Leu), 40.5 (δ-Orn), 31.9 (β-Val), 30.2 (β-Orn), 28.0 (β-Pro), 26.8 (γ-Orn), 25.6 (γ-Val), 24.4 (γ-Pro), 23.1 (δ-Leu), 23.0 (δ-Leu), 19.6 (γ-Val), 19.4 (γ-Val).
HRMS (ESI-Orbitrap) calcd. for $C_{60}H_{93}N_{12}O_{10}$ $[M+H]^+$ 1141.71321, found 1141.68680.

Loloatin A
***cyclo*(-Leu-*D*Tyr-Pro-Phe-*D*Phe-Asn-Asp-Tyr-Val-Orn-)**

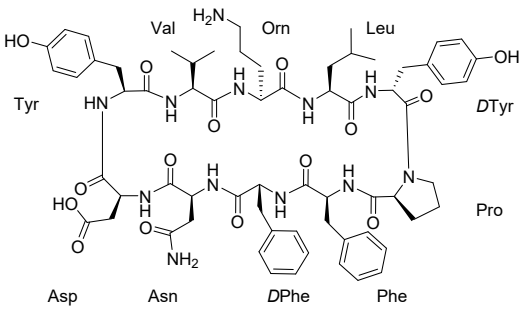

23

Functionalized resin **2** (0.44 g, 0.10 mmol, 1.0 equiv.) was elongated using the Tribute peptide synthesizer. Afterwards, the resin was washed with DMF (4x) and DCM (4x). Resin was suspended in a mixture of DCM and DMF (1:1, DCM – DMF, 4.0 mL, 25 mM) and phenylsilane (31 μL, 0.25 mmol, 2.5 equiv.) and $Pd(PPh_3)_4$ (29 mg, 25 μmol, 25 mol%) were added. The resin was shaken for 90 min. while being protected from light. The suspension was filtered and the resin was washed with DCM (3x), 0.50% (w/v) sodium diethyldithiocarbamate in DMF (2x) and DMF (3x). To the resin was added 20% (v/v) piperidine in DMF (5.0 mL, 20 mM) and the resin was shaken for 10 min. Suspension was filtered and 20% (v/v) piperidine in DMF (5.0 mL, 20 mM) was added to the residue. Resin was shaken for 10 min. followed by filtration and washing with DMF (6x). To the resin was added DMF (4.0 mL, 25 mM). Subsequently, 1-hydroxybenzotriazole hydrate (68 mg, 0.50 mmol, 5.0 equiv.), benzotriazole-1-yl-oxy-tris-pyrrolidino-phosphonium hexafluorophosphate (0.26 g, 0.50 mmol, 5.0 equiv.) and *N*-methylmorpholine (0.11 mL, 1.0 mmol, 10 equiv.) were added to the suspension and the reaction was stirred for 2.5 hrs. The suspension was filtered and the residue was washed with DMF (3x) and DCM (6x). A cleavage mixture (190:5:5, TFA – H_2O – TIPS, 10 mL, 10 mM) was then added to the resin and the resulting suspension was shaken for 3 hrs. The suspension was filtered and the volatiles of the filtrate were removed under a stream of N_2. Residue was dissolved in a mixture of DCM and MeOH (1:1, MeOH – DCM) and purified by size exclusion chromatography (Sephadex LH-20, 1:1, MeOH – DCM) to give loloatin A **23** (76 mg, 59 μmol, 59%) as a white solid.

^{1}H NMR (400 MHz, CD_3OH, 4.94 ppm suppressed) δ 9.52 – 9.33 (m, 2H, N*H*-Asn, N*H*-*D*Tyr), 9.23 (s, 1H, N*H*-Orn), 9.00 (br s, 1H, N*H*-*D*Phe), 8.86 (d, *J* = 9.4 Hz, 1H, N*H*-Tyr), 8.63 (d, *J* = 8.7 Hz, 1H, N*H*-Leu), 8.43 (d, *J* = 4.3 Hz, 1H, N*H*-Asp), 8.14 (s, 1H, δ-Asn), 7.93 (d, *J* = 8.9 Hz, 1H, N*H*-Val), 7.64 – 7.49 (m, 2H, δ-Asn, N*H*-Phe), 7.26 – 7.11 (m, 10H, C*H*-arom-Phe, C*H*-arom-*D*Phe), 7.05 (d, *J* = 8.1 Hz, 2H, C*H*-arom-*D*Tyr), 6.81 (d, *J* = 8.1 Hz, 2H, C*H*-arom-Tyr), 6.69 (d, *J* = 8.1 Hz, 2H, C*H*-arom-*D*Tyr), 6.46 (d, *J* = 8.0 Hz, 2H, C*H*-arom-Tyr), 5.94 – 5.83 (m, 1H, α-*D*Phe), 5.53 – 5.45 (m, 1H, α-Orn), 4.68 (s, 1H, α-Asn), 4.60 – 4.51 (m, 2H, α-Tyr, α-Phe), 4.47 – 4.38 (m, 2H, α-*D*Tyr, α-Asp), 4.15 (d, *J* = 8.1 Hz, 1H, α-Pro), 3.42 – 3.33 (m, 3H, β-Asn, β-*D*Phe, δ-Pro), 3.27 – 2.75 (m, 8H, β-Asn, β-*D*Tyr, β-Tyr, δ-Orn, β-*D*Phe, δ-Orn), 2.58 – 2.49 (m, 1H, β-Asp), 2.46 – 2.14 (m, 7H, β-Asp, β-Phe, δ-Pro, β-Orn, β-Phe, β-Val), 1.89 – 1.43 (m, 6H, γ-Orn, β-Leu, γ-Leu, β-Leu, β-Pro), 1.38 – 1.32 (m, 1H, β-Pro), 1.19 – 1.04 (m, 13H, γ-Val, γ-Pro, δ-Leu), 0.46 (s, 1H, γ-Pro).

Note: α-Leu and α-Val are in the suppressed region of 4.94 ppm.

^{13}C NMR (101 MHz, CD_3OH) δ 175.2 (*C*OOH), 173.8 (*C*ONH_2), 173.7 (*C*ONH), 173.7 (*C*ONH), 173.5 (*C*ONH), 173.4 (*C*ONH), 173.3 (*C*ONH), 172.9 (*C*ONH), 172.8 (*C*ONH), 172.1 (*C*ONH), 172.1 (*C*ONH), 172.0 (*C*ONH), 157.9 (*C*qOH-Tyr), 157.2 (*C*qOH-Tyr), 138.9 (*C*q-Phe), 138.8 (*C*q-Phe), 131.6 (*C*H-arom-Tyr), 130.8 (*C*H-arom-Phe), 130.6 (*C*H-arom-Phe), 130.0 (*C*H-arom-Phe), 129.2 (*C*H-arom-Phe), 129.0 (*C*q-arom-Tyr), 127.6 (*C*H-arom-Phe), 127.2 (*C*q-arom-Tyr), 116.2 (*C*H-arom-Tyr), 116.1 (*C*H-arom-Tyr), 61.4 (α-Pro), 59.5 (α-Tyr), 58.5 (α-Val), 56.3 (α-*D*Tyr), 55.3 (α-Phe), 54.7 (α-*D*Phe), 54.1 (α-Asp), 52.6 (α-Orn), 52.3 (α-Leu), 50.9 (α-Asn), 47.6 (δ-Pro), 43.1 (β-Leu), 41.3 (β-*D*Phe), 40.6 (δ-Orn), 38.7 (β-Phe), 38.2 (β-Tyr), 37.3 (β-*D*Tyr), 36.6 (β-Asn), 36.5 (β-Asp), 33.2 (β-Val), 32.9 (β-Orn), 29.7 (β-Pro), 26.2 (γ-Leu), 24.4 (γ-Orn), 23.8 (δ-Leu), 23.3 (γ-Pro), 22.9 (δ-Leu), 19.6 (γ-Val), 19.1 (γ-Val).

HRMS (ESI-Orbitrap) calcd. for $C_{65}H_{88}N_{12}O_{15}$ $[M+H]^+$ 1273.62519, found 1273.62505.

Tyrocidin A
***cyclo*(-Leu-*D*Phe-Pro-Phe-*D*Phe-Asn-Gln-Tyr-Val-Orn-)**

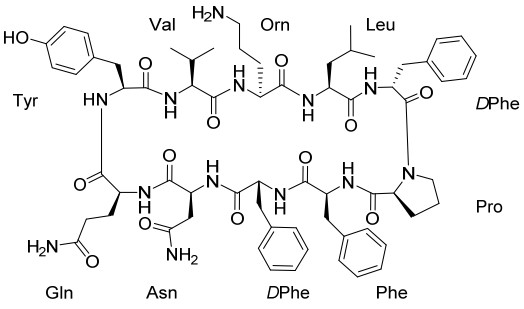

24

Functionalized resin **2** (0.40 g, 90 μmol, 1.0 equiv.) was elongated using the Tribute peptide synthesizer. Afterwards, the resin was washed with DMF (4x) and DCM (4x). Resin was suspended in a mixture of DCM and DMF (1:1, DCM – DMF, 4.0 mL, 23 mM) and phenylsilane (31 μL, 0.25 mmol, 2.8 equiv.) and $Pd(PPh_3)_4$ (29 mg, 25 μmol, 28 mol%) were added. The resin was shaken for 90 min. while being protected from light. The suspension was filtered and the resin was washed with DCM (3x), 0.50% (w/v) sodium diethyldithiocarbamate in DMF (2x) and DMF (3x). To the resin was added 20% (v/v) piperidine in DMF (5.0 mL, 20 mM) and the resin was shaken for 10 min. Suspension was filtered and 20% (v/v) piperidine in DMF (5.0 mL, 18 mM) was added to the residue. Resin was shaken for 10 min. followed by filtration and washing with DMF (6x). To the resin was added DMF (4.0 mL, 23 mM). Subsequently, 1-hydroxybenzotriazole hydrate (68 mg, 0.50 mmol, 5.6 equiv.), benzotriazole-1-yl-oxy-tris-pyrrolidino-phosphonium hexafluorophosphate (0.26 g, 0.50 mmol, 5.6 equiv.) and *N*-methylmorpholine (0.11 mL, 1.0 mmol, 11 equiv.) were added to the suspension and the reaction was stirred for 2.5 hrs. The suspension was filtered and the residue was washed with DMF (3x) and DCM (6x). A cleavage mixture (190:5:5, TFA – H_2O – TIPS, 10 mL, 9.0 mM) was then added to the resin and the resulting suspension was shaken for 3 hrs. The suspension was filtered and the volatiles of the filtrate were removed under a stream of N_2. Residue was dissolved in a mixture of DCM and MeOH (1:1, MeOH – DCM) and purified by size exclusion chromatography (Sephadex LH-20, 1:1, MeOH – DCM) to give tyrocidin A- **24** (75 mg, 59 μmol, 66%) as a white solid.

^{1}H NMR (400 MHz, CD_3OH, 4.94 ppm suppressed) δ 9.40 – 9.27 (m, 2H, N*H*-Asn, N*H*-*D*Phe), 9.15 – 9.02 (m, 2H, N*H*-Orn, N*H*-Gln), 8.92 (d, *J* = 9.7 Hz, 1H, N*H*-*D*Phe), 8.74 (d, *J* = 9.8 Hz, 1H, N*H*-Tyr), 8.50 (br s, 1H, N*H*-Leu), 8.10 (s, 1H, δ-Asn), 7.88 (d, *J* = 9.1 Hz, 1H, N*H*-Val), 7.57 (s, 1H, δ-Asn), 7.52 (d, *J* = 9.0 Hz, 1H, N*H*-Phe), 7.37 (d, *J* = 2.4 Hz, 1H, ε-Gln), 7.34 – 7.10 (m, 15H, C*H*-arom-Phe, C*H*-arom-*D*Phe), 6.91 (d, *J* = 2.3 Hz, 1H, ε-Gln), 6.86 (d, *J* = 8.0 Hz, 2H, C*H*-arom-Tyr), 6.50 (d, *J* = 7.8 Hz, 2H, C*H*-arom-Tyr), 5.87 – 5.77 (m, 1H, α-*D*Phe), 5.47 (q, *J* = 8.2 Hz, 1H, α-Orn), 4.70 – 4.51 (m, 3H, α-Asn, α-Tyr, α-Phe), 4.49 – 4.43 (m, 1H, α-*D*Phe), 4.13 (d, *J* = 8.0 Hz, 1H, α-Pro), 4.04 (q, *J* = 5.8, 5.1 Hz, 1H, α-Gln), 3.39 – 3.32 (m, 2H, δ-Pro, β-Asn), 3.30 – 3.04 (m, 6H, β-*D*Phe, β-Asn, β-*D*Phe, β-Tyr), 3.01 – 2.79 (m, 3H, δ-Orn, β-*D*Phe, δ-Orn), 2.41 (t, *J* = 13.2 Hz, 1H, β-Phe), 2.33 – 1.87 (m, 7H, β-Phe, δ-Pro, β-Val, β-Orn, γ-Gln, β-Orn), 1.85 – 1.55 (m, 6H, γ-Orn, β-Leu, β-Gln, γ-Leu), 1.52 – 1.41 (m, 2H, β-Pro, β-Leu), 1.37 – 1.33 (m, 1H, β-Pro), 1.15 – 1.00 (m, 13H, γ-Val, γ-Pro, δ-Leu), 0.48 – 0.34 (m, 1H, γ-Pro).

Note: α-Leu and α-Val are in the suppressed region of 4.94 ppm.

^{13}C NMR (101 MHz, CD_3OH) δ 178.4 (*C*ONH_2-Gln), 175.1 (*C*ONH_2-Asn), 173.9 (*C*ONH), 173.8 (*C*ONH), 173.4 (*C*ONH), 173.4 (*C*ONH), 173.3 (*C*ONH), 173.1 (*C*ONH), 173.0 (*C*ONH), 172.9 (*C*ONH), 172.2 (*C*ONH), 172.0 (*C*ONH), 157.2 (*C*qOH-Tyr), 138.9 (*C*q-*D*Phe), 138.7 (*C*q-*D*Phe), 136.8 (*C*q-Phe), 130.9 (*C*H-arom-Tyr), 130.8 (*C*H-arom-Phe), 130.5 (*C*H-arom-Phe), 130.0 (*C*H-arom-Phe), 129.5 (*C*H-arom-Phe), 129.3 (*C*H-arom-Phe), 129.2 (*C*H-arom-Phe), 129.1 (*C*q-arom-Tyr), 128.4 (*C*H-arom-Phe), 127.7 (*C*H-arom-Phe), 127.6 (*C*H-arom-Phe), 116.3 (*C*H-arom-Tyr), 61.4 (α-Pro), 59.6 (α-Val), 58.3 (α-Tyr), 56.7 (α-Gln), 56.0 (α-*D*Phe), 55.4 (α-Phe), 54.6 (α-*D*Phe), 52.4 (α-Orn), 52.3 (α-Leu), 50.9 (α-Asn), 47.6 (δ-Pro), 42.9 (β-Leu), 41.4 (β-*D*Phe), 40.6 (δ-Orn), 38.7 (β-Phe), 38.3 (β-Tyr), 37.3 (β-*D*Phe), 36.5 (β-Asn), 33.2 (β-Val), 32.6 (β-Orn), 31.6 (γ-Gln), 29.9 (β-Pro), 26.8 (β-Gln), 26.3 (γ-Leu), 24.4 (γ-Orn), 23.8 (δ-Leu), 23.3 (γ-Pro), 22.7 (δ-Leu), 19.5 (γ-Val), 19.1 (γ-Val).

HRMS (ESI-Orbitrap) calcd. for $C_{66}H_{88}N_{13}O_{13}$ $[M+H]^+$ 1270.66191, found 1270.66186.

Streptocidin A
***cyclo*(-Leu-*D*Phe-Pro-Leu-*D*Trp-Asn-Gln-Tyr-Val-Orn-)**

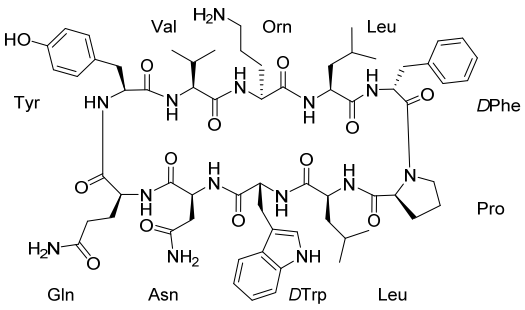

25

Functionalized resin **2** (0.40 g, 90 μmol, 1.0 equiv.) was elongated using the Tribute peptide synthesizer. Afterwards, the resin was washed with DMF (4x) and DCM (4x). Resin was suspended in a mixture of DCM and DMF (1:1, DCM – DMF, 4.0 mL, 23 mM) and phenylsilane (31 μL, 0.25 mmol, 2.8 equiv.) and $Pd(PPh_3)_4$ (29 mg, 25 μmol, 28 mol%) were added. The resin was shaken for 90 min. while being protected from light. The suspension was filtered and the resin was washed with DCM (3x), 0.50% (w/v) sodium diethyldithiocarbamate in DMF (2x) and DMF (3x). To the resin was added 20% (v/v) piperidine in DMF (5.0 mL, 20 mM) and the resin was shaken for 10 min. Suspension was filtered and 20% (v/v) piperidine in DMF (5.0 mL, 18 mM) was added to the residue. Resin was shaken for 10 min. followed by filtration and washing with DMF (6x). To the resin was added DMF (4.0 mL, 23 mM). Subsequently, 1-hydroxybenzotriazole hydrate (68 mg, 0.50 mmol, 5.6 equiv.), benzotriazole-1-yl-oxy-tris-pyrrolidino-phosphonium hexafluorophosphate (0.26 g, 0.50 mmol, 5.6 equiv.) and *N*-methylmorpholine (0.11 mL, 1.0 mmol, 11 equiv.) were added to the suspension and the reaction was stirred for 2.5 hrs. The suspension was filtered and the residue was washed with DMF (3x) and DCM (6x). A cleavage mixture (190:5:5, TFA – H_2O – TIPS, 10 mL, 9.0 mM) was then added to the resin and the resulting suspension was shaken for 3 hrs. The suspension was filtered and the volatiles of the filtrate were removed under a stream of N_2. Residue was dissolved in a mixture of DCM and MeOH (1:1, MeOH – DCM) and purified by size exclusion chromatography (Sephadex LH-20, 1:1, MeOH – DCM) to give streptocidin A- **25** (45 mg, 35 μmol, 40%) as a white solid.

^{1}H NMR (400 MHz, CD_3OH, 4.94 ppm suppressed) δ 10.40 (s, 1H, N*H*-arom-Trp), 9.45 (d, *J* = 7.5 Hz, 1H, N*H*-Asn), 9.22 (br s, 1H, N*H*-*D*Phe), 9.07 (s, 1H, N*H*-Gln), 8.98 (br s, 1H, N*H*-Orn), 8.80 (d, *J* = 9.7 Hz, 1H, N*H*-Tyr), 8.38 – 8.27 (m, 1H, N*H*-Leu), 8.22 (d, *J* = 9.5 Hz, 1H, N*H*-*D*Trp), 8.08 (s, 1H, δ-Asn), 7.89 (d, *J* = 9.2 Hz, 1H, N*H*-Val), 7.60 (d, *J* = 8.0 Hz, 1H, C*H*-arom-*D*Trp), 7.54 (s, 1H, δ-Asn), 7.43 – 7.39 (m, N*H*-Leu), 7.39 (s, 1H, ε-Gln)), 7.34 – 7.20 (m, 6H, C*H*-arom-*D*Phe, C*H*-arom-*D*Trp), 7.09 – 6.96 (m, 2H, C*H*-arom-*D*Trp), 6.93 (s, 1H, ε-Gln), 6.90 – 6.82 (m, 3H, C*H*-arom-*D*Trp, C*H*-arom-Tyr), 6.55 – 6.44 (m, 2H, C*H*-arom-Tyr), 5.87 – 5.74 (m, 1H, α-*D*Trp), 5.55 – 5.45 (m, 1H, α-Orn), 4.75 – 4.64 (m, 1H, α-Asn), 4.63 – 4.55 (m, 1H, α-Tyr), 4.47 – 4.39 (m, 1H, α-*D*Phe), 4.26 – 4.20 (m, 1H, α-Pro), 4.17 – 4.08 (m, 1H, α-Leu), 4.05 (q, *J* = 6.1, 5.2 Hz, 1H, α-Gln), 3.62 – 3.56 (m, 1H, δ-Pro), 3.29 – 3.21 (m, 2H, β-Asn, β-*D*Trp), 3.19 – 2.96 (m, 7H, β-Asn, β-*D*Trp, β-Tyr, β-*D*Phe, δ-Orn), 2.91 – 2.78 (m, 1H, δ-Orn), 2.35 (q, *J* = 8.6 Hz, 1H, δ-Pro), 2.27 – 2.21 (m, 1H, β-Val), 2.07 – 1.96 (m, 4H, β-Orn, γ-Gln, β-Orn), 1.92 – 1.86 (m, 1H, β-Pro), 1.84 – 1.70 (m, 4H, γ-Orn, β-Gln), 1.65 – 1.35 (m, 5H, β-Pro, γ-Pro, γ-Leu, β-Leu), 1.28 – 1.17 (m, 2H, β-Leu, γ-Leu), 1.14 (d, *J* = 6.7 Hz, 3H, γ-Val), 1.11 (d, *J* = 6.8 Hz, 3H, γ-Val), 1.02 – 0.92 (m, 7H, δ-Leu, β-Leu), 0.63 (d, *J* = 6.6 Hz, 6H, δ-Leu), -0.15 (s, 1H, β-Leu).

Note: α-Leu and α-Val are in the suppressed region of 4.94 ppm.

^{13}C NMR (101 MHz, CD_3OH) δ 179.4 ($CONH_2$-Gln), 178.4 ($CONH_2$-Asn), 175.1 (*C*ONH), 174.7 (*C*ONH), 174.5 (*C*ONH), 174.0 (*C*ONH), 173.9 (*C*ONH), 173.3 (*C*ONH), 173.1 (*C*ONH), 173.0 (*C*ONH), 172.1 (*C*ONH), 172.0 (*C*ONH), 157.2 (*C*q-OH-Tyr), 138.2 (*C*q-arom-*D*Phe), 136.8 (*C*q-arom-*D*Trp), 130.9 (*C*H-arom-Tyr), 130.7 (*C*H-arom-*D*Phe), 130.5 (*C*H-arom-*D*Phe), 129.5 (*C*H-arom-*D*Phe), 129.1 (*C*q-arom-Tyr), 128.4 (*C*q-arom-*D*Trp), 125.3 (*C*H-arom-*D*Trp), 122.5 (*C*H-arom-*D*Trp), 120.1 (*C*H-arom-*D*Trp), 120.0 (*C*H-arom-*D*Trp), 116.2 (*C*H-arom-Tyr), 112.2 (*C*H-arom-*D*Trp), 111.1 (*C*q-arom-*D*Trp), 61.7 (α-Pro), 59.6 (α-Val), 58.3 (α-Tyr), 56.6 (α-Gln), 56.0 (α-*D*Phe), 53.2 (α-*D*Trp), 52.6 (α-Orn), 52.4 (α-Leu), 52.4 (α-Leu), 50.9 (α-Asn), 47.7 (δ-Pro), 42.3 (β-Leu), 40.6 (δ-Orn), 40.4 (β-Leu), 38.2 (β-Tyr), 37.8 (β-*D*Phe), 36.5 (β-Asn), 33.0 (β-Val), 32.9 (β-Orn), 31.6 (γ-Gln), 31.6 (β-Trp), 30.1 (β-Pro), 26.7 (β-Gln), 26.2 (γ-Leu), 25.5 (γ-Leu), 24.3 (γ-Orn), 24.0 (δ-Leu), 23.6 (γ-Pro), 23.4 (δ-Leu)), 22.2 (δ-Leu), 20.7 (δ-Leu), 19.5 (γ-Val), 19.3 (γ-Val).

HRMS (ESI-Orbitrap) calcd. for $C_{65}H_{91}N_{14}O_{13}$ $[M+H]^+$ 1275.68846, found 1275.68889.

References

(1) Brandt, W.; Haupt, V. J.; Wessjohann, L. A. Chemoinformatic Analysis of Biologically Active Macrocycles. *Curr. Top. Med. Chem.* **2010**, *10* (14), 1361–1379. https://doi.org/10.2174/156802610792232060.

(2) Abdalla, M. A.; McGaw, L. J. Natural Cyclic Peptides as an Attractive Modality for Therapeutics: A Mini Review. *Molecules* **2018**, *23* (8), 2080. https://doi.org/10.3390/molecules23082080.

(3) Wessjohann, L. A.; Bartelt, R.; Brandt, W. Natural and Nature-Inspired Macrocycles. In *Practical Medicinal Chemistry with Macrocycles*; John Wiley & Sons, Ltd, 2017; pp 77–100. https://doi.org/10.1002/9781119092599.ch4.

(4) Giordanetto, F.; Kihlberg, J. Macrocyclic Drugs and Clinical Candidates: What Can Medicinal Chemists Learn from Their Properties? *J. Med. Chem.* **2014**, *57* (2), 278–295. https://doi.org/10.1021/jm400887j.

(5) Lipinski, C. A.; Lombardo, F.; Dominy, B. W.; Feeney, P. J. Experimental and Computational Approaches to Estimate Solubility and Permeability in Drug Discovery and Development Settings. *Adv. Drug Deliv. Rev.* **1997**, *23* (1), 3–25. https://doi.org/10.1016/S0169-409X(96)00423-1.

(6) Shultz, M. D. Two Decades under the Influence of the Rule of Five and the Changing Properties of Approved Oral Drugs. *J. Med. Chem.* **2019**, *62* (4), 1701–1714. https://doi.org/10.1021/acs.jmedchem.8b00686.

(7) Doak, B. C.; Over, B.; Giordanetto, F.; Kihlberg, J. Oral Druggable Space beyond the Rule of 5: Insights from Drugs and Clinical Candidates. *Chem. Biol.* **2014**, *21* (9), 1115–1142. https://doi.org/10.1016/j.chembiol.2014.08.013.

(8) Driggers, E. M.; Hale, S. P.; Lee, J.; Terrett, N. K. The Exploration of Macrocycles for Drug Discovery — an Underexploited Structural Class. *Nat. Rev. Drug Discov.* **2008**, *7* (7), 608–624. https://doi.org/10.1038/nrd2590.

(9) Marsault, E.; Peterson, M. L. Macrocycles Are Great Cycles: Applications, Opportunities, and Challenges of Synthetic Macrocycles in Drug Discovery. *J. Med. Chem.* **2011**, *54* (7), 1961–2004. https://doi.org/10.1021/jm1012374.

(10) Liras, S.; Mcclure, K. F. Permeability of Cyclic Peptide Macrocycles and Cyclotides and Their Potential as Therapeutics. *ACS Med. Chem. Lett.* **2019**, *10* (7), 1026–1032. https://doi.org/10.1021/acsmedchemlett.9b00149.

(11) Mortensen, K. T.; Osberger, T. J.; King, T. A.; Sore, H. F.; Spring, D. R. Strategies for the Diversity-Oriented Synthesis of Macrocycles. *Chem. Rev.* **2019**, *119* (17), 10288–10317. https://doi.org/10.1021/acs.chemrev.9b00084.

(12) Terrett, N. K. Methods for the Synthesis of Macrocycle Libraries for Drug Discovery. *Drug Discov. Today Technol.* **2010**, *7* (2), e97–e104. https://doi.org/10.1016/j.ddtec.2010.06.002.

(13) Gause, G. F.; Brazhnikova, M. G. Gramicidin S and Its Use in the Treatment of Infected Wounds. *Nature* **1944**, *154* (3918), 703–703. https://doi.org/10.1038/154703a0.

(14) Hotchkiss, R. D.; Dubos, R. J. Bactericidal Fractions from an Aerobic Sporulating Bacillus. *J. Biol. Chem.* **1940**, *136* (3), 803–804.

(15) Mazur, S.; Jayalekshmy, P. Chemistry of Polymer-Bound o-Benzyne. Frequency of Encounter between Substituents on Crosslinked Polystyrenes. *J. Am. Chem. Soc.* **1979**, *101* (3), 677–683. https://doi.org/10.1021/ja00497a032.

(16) Yang, L.; Morriello, G. Solid Phase Synthesis of 'Head-to-Tail' Cyclic Peptides Using a Sulfonamide 'Safety-Catch' Linker: The Cleavage by Cyclization Approach. *Tetrahedron Lett.* **1999**, *40* (47), 8197–8200. https://doi.org/10.1016/S0040-4039(99)01701-3.

(17) Ösapay, G.; Profit, A.; Taylor, J. W. Synthesis of Tyrocidine a: Use of Oxime Resin for Peptide Chain Assembly and Cyclization. *Tetrahedron Lett.* **1990**, *31* (43), 6121–6124. https://doi.org/10.1016/S0040-4039(00)97003-5.

(18) Trzeciak, A.; Bannwarth, W. Synthesis of 'Head-to-Tail' Cyclized Peptides on Solid Support by Fmoc Chemistry. *Tetrahedron Lett.* **1992**, *33* (32), 4557–4560. https://doi.org/10.1016/S0040-4039(00)61311-4.

(19) McMurray, J. S. Solid Phase Synthesis of a Cyclic Peptide Using Fmoc Chemistry. *Tetrahedron Lett.* **1991**, *32* (52), 7679–7682. https://doi.org/10.1016/0040-4039(91)80563-L.

(20) Barany, G.; Han, Y.; Hargittai, B.; Liu, R.-Q.; Varkey, J. T. Side-Chain Anchoring Strategy for Solid-Phase Synthesis of Peptide Acids with C-Terminal Cysteine. *Pept. Sci.* **2003**, *71* (6), 652–666. https://doi.org/10.1002/bip.10593.

(21) Isied, S. S.; Kuehn, C. G.; Lyon, J. M.; Merrifield, R. B. Specific Peptide Sequences for Metal Ion Coordination. 1. Solid-Phase Synthesis of Cyclo-(Gly-His)3. *J. Am. Chem. Soc.* **1982**, *104* (9), 2632–2634. https://doi.org/10.1021/ja00373a049.

(22) Alcaro, M. C.; Orfei, M.; Chelli, M.; Ginanneschi, M.; Papini, A. M. Solid-Phase Approach to the Synthesis of Cyclen Scaffolds from Cyclotetrapeptides. *Tetrahedron Lett.* **2003**, *44* (28), 5217–5219. https://doi.org/10.1016/S0040-4039(03)01213-9.

(23) Yan, L. Z.; Edwards, P.; Flora, D.; Mayer, J. P. Synthesis of Cyclic Peptides through Hydroxyl Side-Chain Anchoring. *Tetrahedron Lett.* **2004**, *45* (5), 923–925. https://doi.org/10.1016/j.tetlet.2003.11.107.

(24) Alsina, J.; Chiva, C.; Ortiz, M.; Rabanal, F.; Giralt, E.; Albericio, F. Active Carbonate Resins for Solid-Phase Synthesis through the Anchoring of a Hydroxyl Function. Synthesis of Cyclic and Alcohol Peptides. *Tetrahedron Lett.* **1997**, *38* (5), 883–886. https://doi.org/10.1016/S0040-4039(96)02431-8.

(25) Cabrele, C.; Langer, M.; Beck-Sickinger, A. G. Amino Acid Side Chain Attachment Approach and Its Application to the Synthesis of Tyrosine-Containing Cyclic Peptides. *J. Org. Chem.* **1999**, *64* (12), 4353–4361. https://doi.org/10.1021/jo982402j.

(26) Alsina, J.; Rabanal, F.; Giralt, E.; Albericio, F. Solid-Phase Synthesis of "Head-to-Tail" Cyclic Peptides via Lysine Side-Chain Anchoring. *Tetrahedron Lett.* **1994**, *35* (51), 9633–9636. https://doi.org/10.1016/0040-4039(94)88531-1.

(27) Breipohl, G.; Knolle, J.; Geiger, R. Solid Phase Synthesis of Peptide Aminoalkylamides Development and Application of New Linking Agents. *Tetrahedron Lett.* **1987**, *28* (46), 5647–5650. https://doi.org/10.1016/S0040-4039(00)96803-5.

(28) Torres-García, C.; Díaz, M.; Blasi, D.; Farràs, I.; Fernández, I.; Ariza, X.; Farràs, J.; Lloyd-Williams, P.; Royo, M.; Nicolás, E. Side Chain Anchoring of Tryptophan to Solid Supports Using a Dihydropyranyl Handle: Synthesis of Brevianamide F. *Int. J. Pept. Res. Ther.* **2012**, *18* (1), 7–19. https://doi.org/10.1007/s10989-011-9274-8.

(29) Beythien, J.; Barthélémy, S.; Schneeberger, P.; White, P. D. A Novel Solid-Phase Linker Strategy for the Side-Chain Anchoring of Arginine: An Expeditious Route to Arginine 7-Amido-4-Methylcoumarins. *Tetrahedron Lett.* **2006**, *47* (18), 3009–3012. https://doi.org/10.1016/j.tetlet.2006.03.019.

(30) Lee, Y.; Silverman, R. B. Efficient Solid-Phase Synthesis of Compounds Containing Phenylalanine and Its Derivatives via Side-Chain Attachment to the Polymer Support. *J. Am. Chem. Soc.* **1999**, *121* (36), 8407–8408. https://doi.org/10.1021/ja991679d.

(31) Knölker, H.-J.; Braxmeier, T.; Schlechtingen, G. A Novel Method for the Synthesis of Isocyanates Under Mild Conditions. *Angew. Chem. Int. Ed. Engl.* **1995**, *34* (22), 2497–2500. https://doi.org/10.1002/anie.199524971.

(32) Valli, V. L. K.; Alper, H. A Simple, Convenient, and Efficient Method for the Synthesis of Isocyanates from Urethanes. *J. Org. Chem.* **1995**, *60* (1), 257–258. https://doi.org/10.1021/jo00106a044.

(33) Butler, D. C. D.; Alper, H. Synthesis of Isocyanates from Carbamate Esters Employing Boron Trichloride. *Chem. Commun.* **1998**, No. 23, 2575–2576. https://doi.org/10.1039/A807287F.

(34) Chong, P. Y.; Janicki, S. Z.; Petillo, P. A. Multilevel Selectivity in the Mild and High-Yielding Chlorosilane-Induced Cleavage of Carbamates to Isocyanates. *J. Org. Chem.* **1998**, *63* (23), 8515–8521. https://doi.org/10.1021/jo981816+.

(35) Gastaldi, S.; Weinreb, S. M.; Stien, D. Diiodosilane: A Reagent for Mild, Efficient Conversion of Carbamates to Ureas via Isocyanates. *J. Org. Chem.* **2000**, *65* (10), 3239–3240. https://doi.org/10.1021/jo9919714.

(36) Greber, G.; Kricheldorf, H. R. A New Synthesis of Isocyanates and Isothiocyanates. *Angew. Chem. Int. Ed. Engl.* **1968**, *7* (12), 941–941. https://doi.org/10.1002/anie.196809411.

(37) Cho, H.; Lee, J. O.; Hwang, S.; Seo, J. H.; Kim, S. Hendrickson-Reagent-Mediated Conversion of N-Boc Carbamates to Isocyanates: Applications for the Synthesis of 3,4-Dihydroisoquinolin-1-Ones and Ureas. *Asian J. Org. Chem.* **2016**, *5* (2), 287–292. https://doi.org/10.1002/ajoc.201500462.

(38) Hendrickson, J. B.; Schwartzman, S. M. Triphenyl Phosphine Ditriflate: A General Oxygen Activator. *Tetrahedron Lett.* **1975**, *16* (4), 277–280. https://doi.org/10.1016/S0040-4039(00)71842-9.

(39) Atle, A.; Thor, G.; Steinar, H. The Reaction of Trifluoromethanesulphonicanhydride with Phosphoryl Compounds. *Tetrahedron Lett.* **1979**, *20* (24), 2263–2264. https://doi.org/10.1016/S0040-4039(01)93693-7.

(40) Silva, A. L.; Bordado, J. C. Recent Developments in Polyurethane Catalysis: Catalytic Mechanisms Review. *Catal. Rev.* **2004**, *46* (1), 31–51. https://doi.org/10.1081/CR-120027049.

(41) Hansén, L.; Åkesson, B.; Sollenberg, J.; Lundh, T. Determination of N-Methylmorpholine in Air Samples from a Polyurethane Foam Factory: Comparison between Two Methods Using Gas Chromatography and Isotachophoresis for Analysis. *Scand. J. Work. Environ. Health* **1986**, *12* (1), 66–69.

(42) Eissler, S.; Kley, M.; Bächle, D.; Loidl, G.; Meier, T.; Samson, D. Substitution Determination of Fmoc-Substituted Resins at Different Wavelengths. *J. Pept. Sci.* **2017**, *23* (10), 757–762. https://doi.org/10.1002/psc.3021.

(43) Yoganathan, S.; Miller, S. J. N-Methylimidazole-Catalyzed Synthesis of Carbamates from Hydroxamic Acids via the Lossen Rearrangement. *Org. Lett.* **2013**, *15* (3), 602–605. https://doi.org/10.1021/ol303424b.
(44) Coin, I.; Beyermann, M.; Bienert, M. Solid-Phase Peptide Synthesis: From Standard Procedures to the Synthesis of Difficult Sequences. *Nat. Protoc.* **2007**, *2* (12), 3247–3256. https://doi.org/10.1038/nprot.2007.454.
(45) Atherton, E.; Logan, C. J.; Sheppard, R. C. Peptide Synthesis. Part 2. Procedures for Solid-Phase Synthesis Using Nα-Fluorenylmethoxycarbonylamino-Acids on Polyamide Supports. Synthesis of Substance P and of Acyl Carrier Protein 65–74 Decapeptide. *J. Chem. Soc. Perkin 1* **1981**, No. 0, 538–546. https://doi.org/10.1039/P19810000538.
(46) Spino, C.; Joly, M.-A.; Godbout, C.; Arbour, M. Ti-Catalyzed Reactions of Hindered Isocyanates with Alcohols. *J. Org. Chem.* **2005**, *70* (15), 6118–6121. https://doi.org/10.1021/jo050712d.
(47) Hostettler, Fritz.; Cox, E. F. Organotin Compounds in Isocyanate Reactions. Catalysts for Urethane Technology. *Ind. Eng. Chem.* **1960**, *52* (7), 609–610. https://doi.org/10.1021/ie50607a032.
(48) Blank, W. J.; He, Z. A.; Hessell, E. T. Catalysis of the Isocyanate-Hydroxyl Reaction by Non-Tin Catalysts. *Prog. Org. Coat.* **1999**, *35* (1), 19–29. https://doi.org/10.1016/S0300-9440(99)00006-5.
(49) Lewis Sr., R. J. *Sax's Dangerous Properties of Industrial Materials, 5 Volume Set*, 12 edition.; Wiley: Hoboken, New Jersey, 2012.
(50) Sunday, A. O.; Alafara, B. A.; Oladele, O. G. Toxicity and Speciation Analysis of Organotin Compounds. *Chem. Speciat. Bioavailab.* **2012**, *24* (4), 216–226. https://doi.org/10.3184/095422912X13491962881734.
(51) Maxted, E. B. The Poisoning of Metallic Catalysts. In *Advances in Catalysis*; Frankenburg, W. G., Komarewsky, V. I., Rideal, E. K., Emmett, P. H., Taylor, H. S., Eds.; Academic Press, 1951; Vol. 3, pp 129–178. https://doi.org/10.1016/S0360-0564(08)60106-6.
(52) Story, S. C.; Aldrich, J. V. Side-Product Formation during Cyclization with HBTU on a Solid Support. *Int. J. Pept. Protein Res.* **1994**, *43* (3), 292–296. https://doi.org/10.1111/j.1399-3011.1994.tb00393.x.
(53) Albericio, F.; Bofill, J. M.; El-Faham, A.; Kates, S. A. Use of Onium Salt-Based Coupling Reagents in Peptide Synthesis1. *J. Org. Chem.* **1998**, *63* (26), 9678–9683. https://doi.org/10.1021/jo980807y.
(54) Hudson, D. Methodological Implications of Simultaneous Solid-Phase Peptide Synthesis. 1. Comparison of Different Coupling Procedures. *J. Org. Chem.* **1988**, *53* (3), 617–624. https://doi.org/10.1021/jo00238a026.
(55) Andreu, D.; Ruiz, S.; Carreño, C.; Alsina, J.; Albericio, F.; Jiménez, M. Á.; de la Figuera, N.; Herranz, R.; García-López, M. T.; González-Muñiz, R. IBTM-Containing Gramicidin S Analogues: Evidence for IBTM as a Suitable Type II′ β-Turn Mimetic1,2. *J. Am. Chem. Soc.* **1997**, *119* (44), 10579–10586. https://doi.org/10.1021/ja9705755.
(56) Wadhwani, P.; Afonin, S.; Ieronimo, M.; Buerck, J.; Ulrich, A. S. Optimized Protocol for Synthesis of Cyclic Gramicidin S: Starting Amino Acid Is Key to High Yield. *J. Org. Chem.* **2006**, *71* (1), 55–61. https://doi.org/10.1021/jo051519m.
(57) Krachkovskii, S. A.; Sobol', A. G.; Ovchinnikova, T. V.; Tagaev, A. A.; Yakimenko, Z. A.; Azizbekyan, R. R.; Kuznetsova, N. I.; Shamshina, T. N.; Arseniev, A. S. Isolation, Biological Properties, and Spatial Structure of Antibiotic Loloatin A. *Russ. J. Bioorganic Chem.* **2002**, *28* (4), 269–273. https://doi.org/10.1023/A:1019531505769.
(58) Gebhardt, K.; Pukall, R.; Fiedler, H.-P. Streptocidins A-D, Novel Cyclic Decapeptide Antibiotics Produced by Streptomyces Sp. Tü 6071. *J. Antibiot. (Tokyo)* **2001**, *54* (5), 428–433. https://doi.org/10.7164/antibiotics.54.428.
(59) Gerard, J. M.; Haden, P.; Kelly, M. T.; Andersen, R. J. Loloatins A−D, Cyclic Decapeptide Antibiotics Produced in Culture by a Tropical Marine Bacterium. *J. Nat. Prod.* **1999**, *62* (1), 80–85. https://doi.org/10.1021/np980219f.
(60) Ösapay, G.; Profit, A.; Taylor, J. W. Synthesis of Tyrocidine a: Use of Oxime Resin for Peptide Chain Assembly and Cyclization. *Tetrahedron Lett.* **1990**, *31* (43), 6121–6124. https://doi.org/10.1016/S0040-4039(00)97003-5.
(61) Bu, X.; Wu, X.; Ng, N. L. J.; Mak, C. K.; Qin, C.; Guo, Z. Synthesis of Gramicidin S and Its Analogues via an On-Resin Macrolactamization Assisted by a Predisposed Conformation of the Linear Precursors. *J. Org. Chem.* **2004**, *69* (8), 2681–2685. https://doi.org/10.1021/jo035712x.
(62) Qin, C.; Bu, X.; Wu, X.; Guo, Z. A Chemical Approach to Generate Molecular Diversity Based on the Scaffold of Cyclic Decapeptide Antibiotic Tyrocidine A. *J. Comb. Chem.* **2003**, *5* (4), 353–355. https://doi.org/10.1021/cc0300255.
(63) Ding, Y.; Qin, C.; Guo, Z.; Niu, W.; Zhang, R.; Li, Y. Solid-Phase Total Synthesis and Antimicrobial Activities of Loloatins A–D. *Chem. Biodivers.* **2007**, *4* (12), 2827–2834. https://doi.org/10.1002/cbdv.200790232.

(64) Qin, C.; Zhong, X.; Ng, N. L.; Bu, X.; Chan, W. S.; Guo, Z. Facile Solid-Phase Synthesis of Cyclic Decapeptide Antibiotic Streptocidins A–D. *Tetrahedron Lett.* **2004**, *45* (1), 217–220. https://doi.org/10.1016/j.tetlet.2003.10.134.

(65) Scherkenbeck, J.; Chen, H.; Haynes, R. K. Solid-Phase Syntheses of Loloatins A−C. *Eur. J. Org. Chem.* **2002**, *2002* (14), 2350–2355. https://doi.org/10.1002/1099-0690(200207)2002:14<2350::AID-EJOC2350>3.0.CO;2-R.

3

Design and synthesis of gramicidin S derivatives bearing chemoselective handles in different orientations

For a vaccine to elicit an effective immune response, an antigen alone is not sufficient. Immunostimulatory compounds or adjuvants improve the immunogenicity of vaccines and such agents have been added in most formulations either through accidental means owing to the material used or deliberately.[1,2] The first hint for adjuvanticity occurred in 1926 when Glenny *et al.* reported that an antigen that was precipitated onto insoluble particles of aluminum potassium sulphate before immunization induced better antibody responses in guinea pigs than the soluble antigen alone.[3] Since this discovery aluminum salts have been used

in clinical vaccines worldwide as the principle adjuvants.[4] The research on adjuvants took another step forward starting from 1989 when Janeway hypothesized the existence of pattern recognition receptors (PRRs) that would recognize certain pathogen-associated molecular patterns (PAMPs) not found in the host.[5] This hypothesis was validated in the 1990s with the discovery of Toll-like receptors (TLRs), which upon pathogen detection induce the production of cytokines and type I interferons in the host.[6]

Extensive research has been conducted on Toll-like receptors, which is the first discovered family of PRRs with ten receptors being identified in humans (TLR1-TLR10). TLRs are transmembrane proteins either located on the plasma membrane or the endosome of dendritic cells, macrophages, lung epithelial cells and B cells (*Table 1*).[7] The extracellular domain is shaped like a horseshoe bearing leucine-rich repeats that surrounds variable binding regions capable of recognizing various PAMPs. TLRs bind their agonist, as a homo- or heterodimer along with a co-receptor or accessory molecule, initiating a signalling cascade leading to the expression of inflammatory cytokines and triggering an adaptive immune response.[8] TLR10 is the only exception and has been shown to exhibit immunosuppressive properties on B cells.[9]

Table 1. Overview of the family of immunostimulatory Toll-like receptors in humans.[6,10]

Entry	Receptor	Location	Agonist	Synthetic analog
1	TLR1/2	Plasma membrane	Triacylated lipopeptides	Pam_3CSK_4
2	TLR2/6	Plasma membrane	Diacylated lipopeptides	Pam_2CGDPKHPKSF (FSL-1)
3	TLR3	Endosome	Double-stranded RNA	Poly(I:C)
4	TLR4	Plasma membrane	Lipopolysaccharide	Monophosphoryl lipid A (MPL)
5	TLR5	Plasma membrane	Flagellin	–
6	TLR7/8	Endosome	Single-stranded RNA	Resiquimod
7	TLR9	Endosome	CpG-rich hypomethylated DNA	CpG oligodeoxynucleotide

Considerable efforts have gone into the synthesis of analogues and the isolation of fragments of the native agonists of TLRs to identify compounds capable of binding to the receptor and stimulating an immune response.[10] A noteworthy example is monophosphoryl lipid A (MPL) which is obtained through a series of hydrolysis steps from lipopolysaccharide (LPS) of *Salmonella minnesota* R595 and has been shown to have an immunostimulatory effect. Compared to LPS, MPL exhibits not only reduced potencies, but also reduced the toxicity, allowing MPL to be used safely in humans at correct doses.[11] MPL has since found its way as an adjuvant into the human papilloma virus (HPV) vaccine as part of adjuvant system AS04.[2] Another example is the use of TLR2/6 agonist lipoteichoic acid (LTA) from *Staphylococcus aureus* and variants by Stadelmaier *et al.* in an effort to assess the active component of LTA stimulation of the immune system.[12]

With the availability of known TLR agonists, research on cross-talk between the receptors was intensified as the triggering of a single TLR is rarely sufficient to stimulate an effective immune response to protect the host from infection.[13] As a result of these research efforts both synergistic and antagonistic effects have been shown for soluble, conjugated as well as encapsulated combinations of PRR ligands.[14–17] Recently, the group of Esser-Kahn reported on the significance of the linker length between the covalently connected pairs of different TLR-agonists for the ability of such a conjugate to trigger NF-κB pathway and to induce IL-6 production. It turned out that different agonist pairs preferred different spatial presentation.[18] Much research is, however, needed to establish the effect of the orientation of TLR agonists in their ability to stimulate an immune response. The work described in this Chapter aims to design and synthesize a suitable scaffold, to which different TLR ligands can be attached, in order to further probe the influence of their spatial positioning on the immunogenicity of the covalent cluster of TLR-agonists. Inspiration was drawn from a concept introduced by the group of Mutter and termed regioselective addressable functionalized template (RAFT) which was

employed as a tertiary structure-inducing device in *de novo* protein design (*Figure 1*).[19,20]

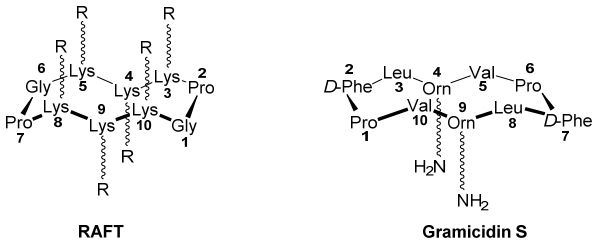

Figure 1. Comparison of the amino acid composition of the regioselective addressable functionalized template platform introduced by the group of Mutter and gramicidin S with lysines instead of the naturally occurring ornithines.

RAFT is a cyclic decapeptide platform composed of two adjacent proline-glycine motifs as type II β-turn-inducers that constrain the backbone conformation in an antiparallel β sheet. This conformational restraint presents two separate spatial domains with residues 3-5-8-10 oriented in the lower plane and residues 4-9 in the opposite plane. Up to six lysine residues can be incorporated and are made regioselectively addressable by way of orthogonal protecting groups.[21] In recent years, the RAFT platform has received interest for its potential as a vaccine scaffold offering improved stability against degradation compared to linear peptides and the ease of introducing a multivalent carbohydrate presentation.[22,23]

The work presented in this Chapter entails the synthesis of a RAFT platform, with a pair of major alterations over the original, as a scaffold for TLR agonist ligation in different orientations. First, a derivative of the cyclic decapeptide gramicidin S is used as the basis for the scaffold bearing two lysine groups (instead of the naturally occurring ornithine groups) which can be used for functionalization with two TLR substrates (*Figure 1*). Gramicidin S adopts the same antiparallel β sheet conformation, which is closed by two type II′ β-turns and is highly stabilized by four intramolecular hydrogens bonds involving the backbone as confirmed by crystal structure analysis.[24] Asano and co-workers showed that the secondary structure is not perturbed by substitution of the ornithine moieties with leucine residues proving the conformation is rigid and allows for shuffling of amino acid residues 3-4-5 and 8-9-10.[25] The second alteration is the way of regioselectively addressing the lysine side-chains by replacing the orthogonal protecting groups with orthogonal

ligation handles, opting for a maleimido-group and the strained cyclooctyne bicyclo[6.1.0]non-4-yne (BCN) (**1**, *Figure 2*).

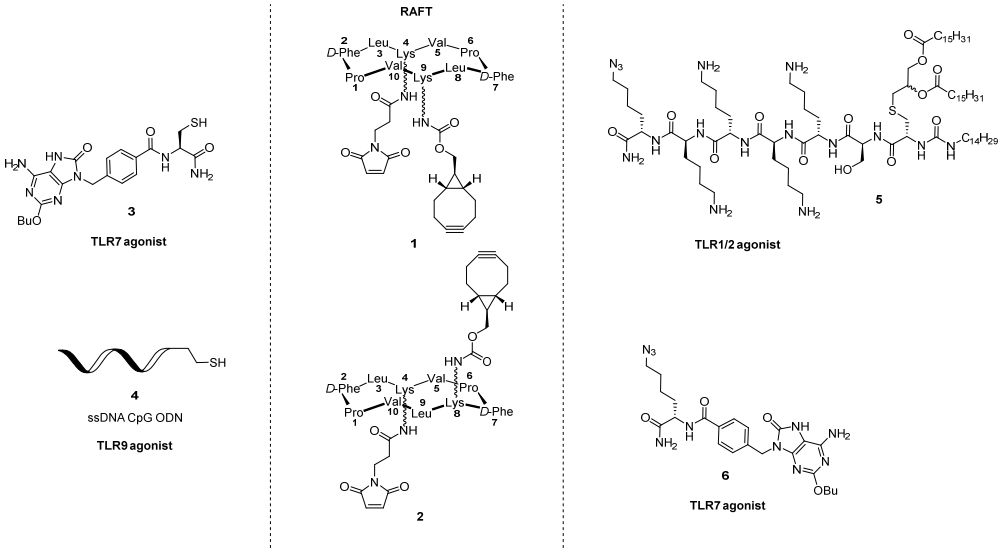

Figure 2. Design of the RAFT scaffold bearing two chemoselective groups and various TLR agonists functionalized with their chemoselective counterpart.

With these design choices RAFT scaffolds **1** and **2** were envisioned bearing two chemoselective handles in different orientations. Scaffold **1** has the ligation handles on the same face of the macrocycle while RAFT **2** has them on the opposite faces. TLR7 and TLR9 agonists were designed with a free thiol as the ligation partner for the maleimido-group, while TLR1/2 and TLR7 agonists were equipped with an azide as the complementary group for the strained alkyne. Overall, this gives rise to the possibility of obtaining dual TLR1/2-7, TLR1/2-9 and TLR7-9 agonists on two scaffolds for a total of six different entities. For the synthesis of the ligands, suitably modified to include a free thiol group or an azide moiety, the known syntheses previously developed in-house for the preparation of TLR1/2 agonist UPam and TLR7 agonist 9-benzyl-8-oxo-2-butoxy-adenine could be used as the starting point.[26,27]

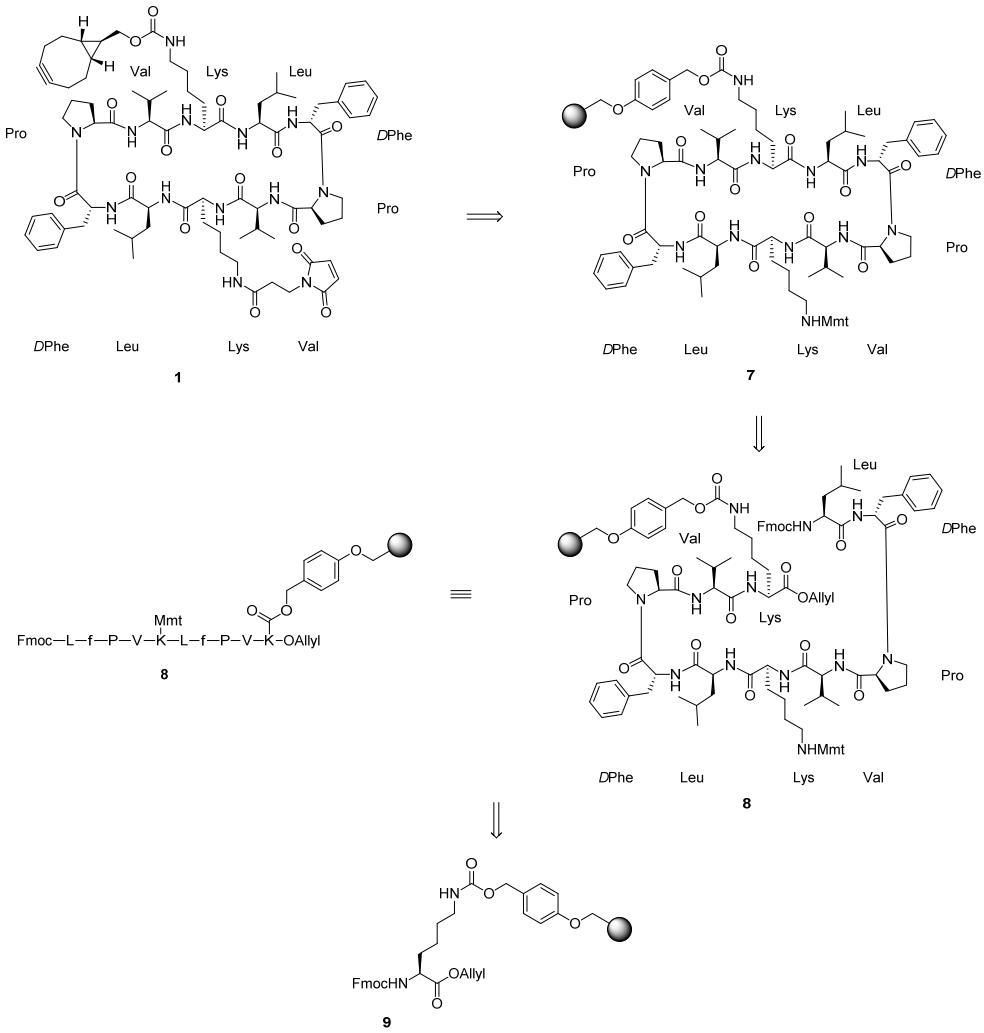

Figure 3. Retrosynthesis of regioselectively addressable template **1** based on gramicidin S.

The synthesis of RAFT scaffold **1**, and in a similar manner scaffold **2**, was envisioned *via* an on-resin cyclization strategy employing the procedure for anchoring the lysine ε-amine to the resin as described in the previous Chapter (*Figure 3*). The added benefit of using this procedure is the ease of functionalizing the side-chain of the non-anchored lysine. Starting from lysine functionalized resin **9**, elongation will be achieved by Fmoc-based automated solid-phase peptide synthesis (SPPS) to furnish linear peptide **8** bearing three orthogonal protecting groups and the linker to the

resin. Palladium-catalyzed deprotection of the C-terminal allyl group and N-terminal Fmoc deprotection with piperidine will allow for on-resin cyclization which will afford cyclic peptide **7**. The first orthogonal ligation handle will be installed by first deprotecting the monomethoxytrityl (Mmt) group using weak acidic conditions followed by functionalization of the lysine ε-amine with a maleimido-group. The cyclic peptide will be cleaved off the resin by treatment with a strong acid simultaneously liberating the second lysine ε-amine which will then be functionalized with a BCN moiety giving scaffold **1**.

Results and discussion

The construction of scaffolds bearing chemoselective handles in different orientations is preceded by the synthesis of the TLR agonists bearing complementary handles and in particular TLR7 ligands **3** and **6** (*Scheme 1*).

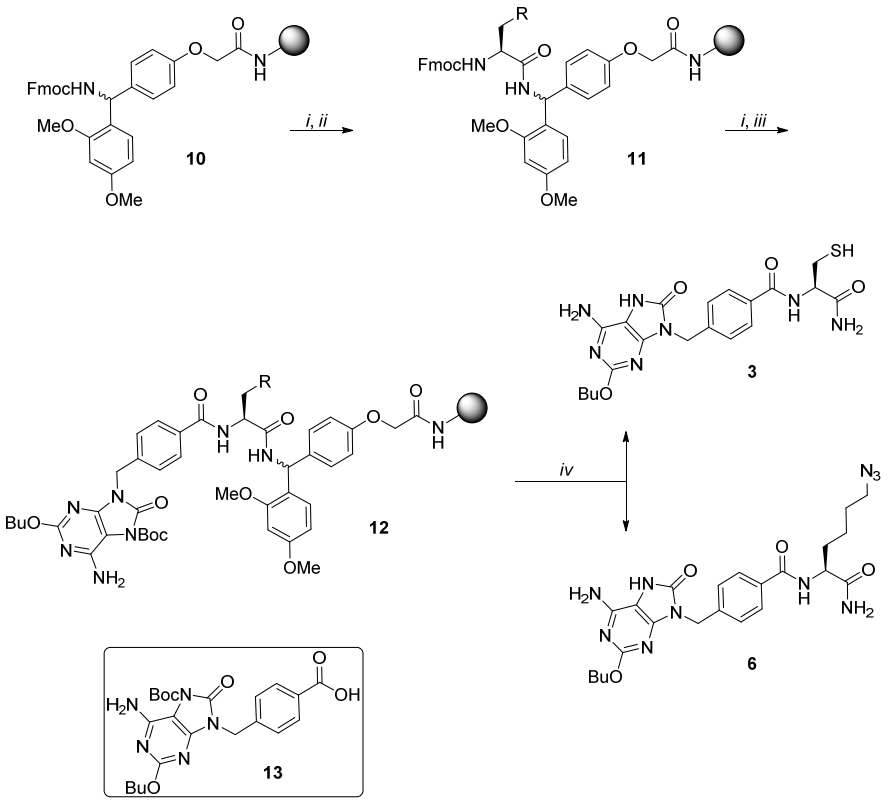

Scheme 1. Reagents and conditions: (*i*) piperidine, DMF, rt, 2x10 min (*ii*) Fmoc-AA-OH, HCTU, DIPEA, DMF, rt, 1 hr (*iii*) 4-((6-amino-2-butoxy-7-(tert-butoxycarbonyl)-8-oxo-7,8-dihydro-9*H*-purin-9-yl)methyl)benzoic acid, HCTU, DIPEA, DMF, rt, 17 hrs (*iv*) TFA – H_2O – TIPS (190:5:5), rt, 3 hrs, 39% (**3**), 61% (**6**).

Starting from TentaGel S RAM **10**, the Fmoc-group was deprotected with two treatments of 20% (v/v) piperidine in DMF. The liberated amine was then condensed with either Fmoc-Lys(N_3)-OH or Fmoc-Cys(Trt)-OH, using HCTU and DIPEA in DMF for one hour. After another cycle of Fmoc deprotection, adenine derivative **13** was introduced by treatment with peptide coupling reagent HCTU and DIPEA for 17 hours. Compound **13** bears a Boc protecting group to increase its solubility and make it suitable for SPPS.[27] Liberation of the target molecules **3** and **6** from the resin was achieved by treating the resin with a cleavage cocktail (190:5:5, TFA – TIPS – H_2O) for three hours. The suspension was filtered and the resin was washed with an additional treatment with the cleavage cocktail. The crude compounds were obtained by evaporation and subsequent purification by reversed-phase HPLC delivering TLR7 ligands **3** and **6** in a yield of 39% and 61% respectively.

Next, the attention was shifted to the synthesis of TLR1/2 agonist UPam **5** bearing an azido group for ligation purposes (*Scheme 2*).

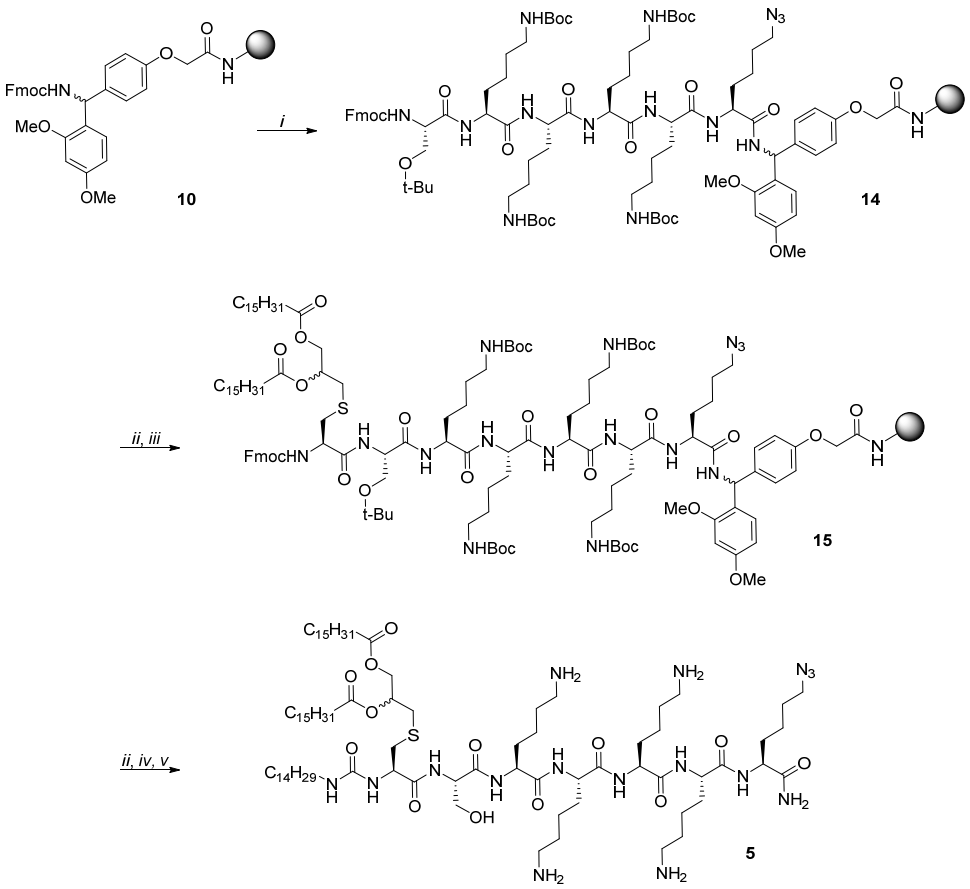

Scheme 2. Reagents and conditions: (*i*) SPPS: (a) piperidine, DMF, rt, 2x3 min. (b) Fmoc-AA-OH, HCTU, DIPEA, DMF, rt, 1 hr (c) Ac_2O, DMF, rt, 2x3 min. (*ii*) piperidine, DMF, rt, 2x10 min (*iii*) Fmoc-Cys((*RS*)-2,3-di(palmitoyloxy)-propyl)-OH, HCTU, DIPEA, DMF, DCM, rt, 24 hrs (*iv*) tetradecylisocyanate, DMF, DCM, rt, 24 hrs (*v*) TFA – H_2O – TIPS (190:5:5), rt , 3 hrs, 7.2%.

First, TentaGel S RAM **10** was elongated using six peptide coupling cycles on a Protein Technologies Tribute automated peptide synthesizer to afford resin-bound peptide **14**. Each cycle started with two treatments of 20% (v/v) piperidine in DMF for three minutes to deprotect the Fmoc group. After a series of washing steps, condensation was achieved by reacting the side-chain protected Fmoc amino acid with deprotected resin-bound peptide using HCTU as the activator and DIPEA as

the base for one hour at room temperature. Unreacted amines were capped by two treatments of 10% (v/v) Ac_2O in DMF for three minutes. The synthesis was then continued manually and the resin was subjected to two treatments of 20% (v/v) piperidine in DMF to liberate the N-terminus. Afterwards, the resin-bound peptide was coupled with Fmoc-Cys((*RS*)-2,3-di(palmitoyloxy)-propyl)-OH using HCTU as the coupling reagent and DIPEA as the base in a mixture of DMF and DCM (1:1, DMF – DCM). The resin was shaken for 24 hours and subsequently filtered and washed with DMF and DCM to give peptide **15**. After another manual Fmoc deprotection cycle, the N-terminus was reacted with tetradecylisocyanate in a mixture of DMF and DCM (1:1, DMF – DCM) for 24 hours. The resin was washed with DMF and DCM followed by treatment with a cleavage cocktail (190:5:5, TFA – TIPS – H_2O) for three hours. The suspension was filtered and the resin was washed with additional cleavage cocktail. Evaporation and subsequent purification by reversed phase HPLC afforded UPam **5** bearing an azide moiety in a yield of 7.2%.

With the TLR ligands in hand, the synthesis of RAFT scaffold **1** was attempted (*Scheme 3*). Using the procedure described in Chapter 3, the lysine ε-amine was attached to TentaGel S PHB resin with a urethane linkage to afford resin **9**. The peptide was subsequently elongated using a Protein Technologies Tribute automated peptide synthesizer with nine peptide coupling cycles. Each cycle started with two treatments of 20% (v/v) piperidine in DMF for three minutes followed by a series of washing steps to remove residual amounts of piperidine. The liberated N-terminus was then coupled to the appropriate standard Fmoc building block using HCTU and DIPEA, except for the second lysine residue, whose side chain was equipped with the monomethoxytrityl (Mmt) group. The resin was shaken for an hour at room temperature which was followed by capping of the unreacted amines by subjecting the resin to two treatments of 10% (v/v) Ac_2O in DMF for three minutes. After nine cycles, resin-bound linear peptide **8** was obtained.

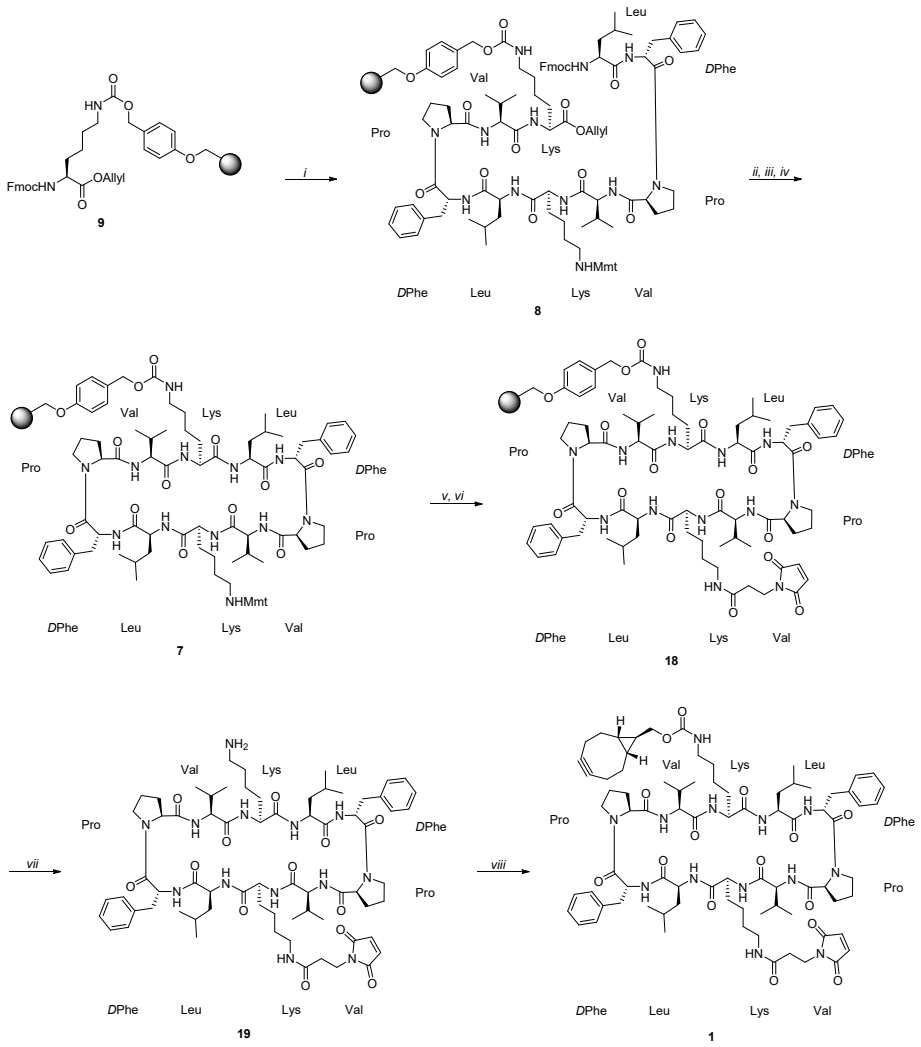

Scheme 3. Reagents and conditions: (*i*) SPPS: (a) piperidine, DMF, rt, 2x3 min. (b) Fmoc-AA-OH, HCTU, DIPEA, DMF, rt, 1 hr (c) Ac_2O, DMF, rt, 2x3 min. (*ii*) $Pd(PPh_3)_4$, $PhSiH_3$, DCM, DMF, rt, 1.5 hrs (*iii*) piperidine, DMF, rt, 2x10 min. (*iv*) benzotriazole-1-yl-oxy-tris-pyrrolidino-phosphonium hexafluorophosphate, 1-hydroxybenzotriazole hydrate, *N*-methylmorpholine, DMF, rt, 2.5 hrs (*v*) TFA – DCM (1:49), rt, 10x2 min. **(*vi*)** 3-maleimidopropionic acid NHS ester, DIPEA, DMF, rt, 4 hrs (*vii*) TFA – TIPS – H_2O (190:5:5), rt, 3 hrs (*viii*) BCN PNP ester, DIPEA, DMF.

The synthesis was continued manually by deprotecting the C-terminal allyl ester using tetrakis(triphenylphosphine) palladium(0) and phenyl silane in a mixture of DCM and DMF (1:1, DCM – DMF) for 90 minutes. After the Fmoc group was deprotected with two treatments of 20% (v/v) piperidine in DMF for ten minutes,

the resin-bound peptide was cyclized using PyBOP as the condensing agent, 1-hydroxybenzotriazole as additive and *N*-methylmorpholine as the base for 2.5 hours. Next, the removal of the Mmt group from immobilized peptide **7** was attempted. Several methods were tried, namely, treatment with TFA mixture (1:99, TFA – DCM) for 10 x 2 minutes with and without a neutralization wash with 0.5 M DIPEA in DMF afterwards as well as treatment with TFA (1:49, TFA – DCM) until no trityl cations were detected based on color.[28] However, these methods proved to be insufficiently reproducible giving fluctuating yields of crude peptide after cleavage. Therefore, a different synthetic strategy to **1** was adopted as an alternative to the exploitation of the subtle differences in the sensitivity of Mmt group and Wang linker to diluted TFA (*Scheme 3*, from **7** to **1** via **18** and **19**). Instead of utilizing two acid-sensitive functionalities in the same molecule, a change from the Mmt group to an azide was made as a means to mask the lysine ε-amine. Simultaneously, it was decided to introduce the BCN moiety first and leave the option available in a late stage to choose between a maleimide and an iodoacetamide moiety. As a consequence the more acid-labile resin TentaGel S Ac was necessary as strained octynes are more prone to decomposition at higher trifluoroacetic acid concentration.[29,30] The first step was verifying if the method used for side-chain anchoring as described in Chapter 3 was still applicable (*Scheme 4*).

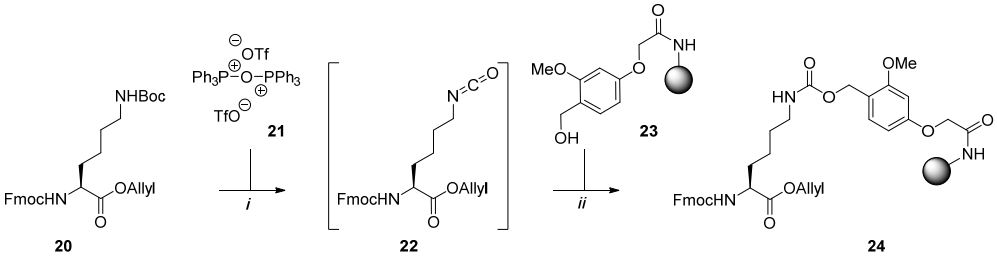

Scheme 4. Reagents and conditions: (*i*) DCM, rt, 5 min (*ii*) dibutyltin dilaurate, *N*-methylmorpholine, DCM, rt, 72 hrs, 89%.

First, Hendrickson's reagent **21** was created *in situ* by reacting two equivalents of triphenylphosphine oxide with one equivalent of triflic anhydride at 0 °C for 30 minutes. Fully protected lysine **20** was added to the mixture and stirred for five minutes to generate isocyanate **22**. Dibutyltin dilaurate and *N*-methylmorpholine were then added to the solution and the mixture was transferred to a shaker containing TentaGel S Ac **23**, which carries an additional methoxy group on the linker compared to TentaGel S PHB. The resin was shaken for 24 hours after which

the mixture was filtered and the resin washed with DCM and Et_2O. After drying the resin over N_2, loading and yield were determined in the same manner as described in Chapter 3. With a reaction time of 24 hours, side-chain anchored lysine **24** was obtained in a yield of 59% on a 0.1 mmol scale. Increasing the reaction time to 48 hours yielded product **24** in 91% yield proving that the method is applicable to TentaGel S Ac as well. The longer reaction time is likely caused by the increased steric hindrance stemming from the additional methoxy group compared to the TentaGel S PHB resin. When scaling up the synthesis to 0.5 mmol, the reaction time had to be increased to 72 hours in order to obtain resin **24** in 89% yield. With resin **24** in hand, the synthesis of RAFT scaffold **1** was attempted once more (*Scheme 5*).

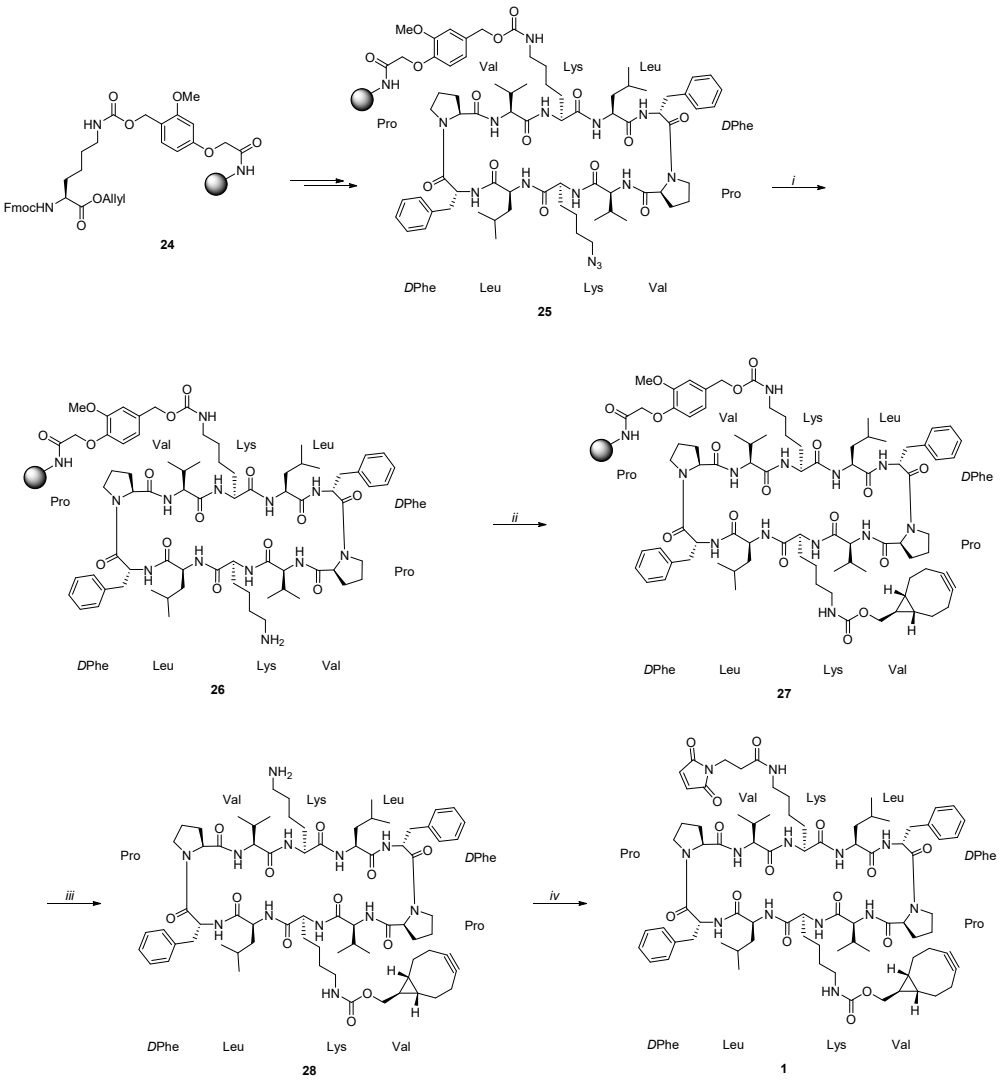

Scheme 5. Reagents and conditions: (*i*) PMe_3, toluene, 1,4-dioxane, rt, 2 hrs, then H_2O, rt, 4 hrs (*ii*) BCN PNP ester, DIPEA, DMF, rt, 1 week (*iii*) TFA – DCM (1:199), rt, 10x2 min (*iv*) 3-maleimidopropionic acid NHS ester, DIPEA, DMF, rt, 4 hrs.

Starting from functionalized resin **24**, cyclized peptide **25** was synthesized employing the same standard conditions as described above. For the reduction of the azide, the resin was treated with an excess of PMe_3 (1.0 M in toluene) diluted in 1,4-dioxane for two hours after which H_2O was added. The mixture was shaken for an additional four hours and the suspension was filtered. After rinsing the resin with

1,4-dioxane and DCM a small amount of resin (~5 mg) was treated with a cleavage cocktail (190:5:5, TFA – H_2O – TIPS) for one hour followed by filtration. Analysis of the filtrate with LC-MS indicated a clean and complete reduction of the azide to the amine. Having successfully reduced the azide on-resin, the strained cyclooctyne BCN was introduced by reacting the newly formed amine in **26** with BCN *para*-nitrophenyl carbonate and DIPEA to furnish resin **27**. Analysis of the cleavage products with LC-MS at different reaction times revealed that full conversion was achieved after one week of shaking the suspension. For the cleavage of the peptide off the resin, a mixture of TFA and DCM (1:199, TFA – DCM) was added and the suspension was shaken for two minutes. After filtration, the filtrate containing trifluoroacetic acid was immediately neutralized by a solution of pyridine in methanol. These steps were repeated ten times. To verify complete cleavage of the peptide, the resin was then treated with a higher concentration of TFA (1:99, TFA – DCM) using the same procedure followed by an even higher concentration (1:49, TFA – DCM). No additional cleavage products could be detected using LC-MS at these concentrations, indicating ten treatments with 0.5% (v/v) TFA in DCM for two minutes is sufficient for complete cleavage.

Removal of the pyridinium trifluoroacetate proved to be more troublesome however as attempts to precipitate the peptide were of no avail. To simplify the work-up and circumvent the formation of salts, a method reported by Srinivasan *et al.* was employed where the basic ion-exchange resin Amberlyst A-21 was used to neutralize TFA.[31] Before use, the Amberlyst A-21 resin was washed with methanol, dry THF and DCM and dried under high-vacuum to give a free-flowing solid. A suspension was then prepared of the Amberlyst resin (14 g per mL TFA) in DCM to which the filtrate containing the cleavage products were added. After addition of the tenth and final filtrate solution, the suspension was vigorously stirred for an additional 30 minutes followed by filtration. Evaporation of the filtrate afforded crude cleavage product **28**, which was then taken up in DMF and reacted with 3-maleimidopropionic acid NHS ester and DIPEA for four hours. Evaporation followed by purification using RP-HPLC afforded RAFT scaffold **1**. However, after evaporation of the pure fractions a byproduct was observed with LC-MS corresponding to a mass of $[M+18+H]^+$ corresponding to the addition of water. Lyophilization of the fractions using a rotor wherein the temperature increases to 35 °C saw the formation of the same byproduct. A recent report by Spangler *et al.* has shown that concentration of HPLC fractions of BCN conjugates containing 0.1% TFA

buffer under reduced pressure at 40 °C induces alkyne degradation.[32] Under these conditions, hydration of the triple bond occurs giving the vinyl alcohol which tautomerizes to the corresponding ketone. Freeze-drying the fractions without the rotor and the inherent temperature increase saw no significant by-product formation and pure scaffold **1** could ultimately be obtained in 3.7% yield.

With the procedure to generate RAFT scaffold **1** in hand, the synthesis route was then applied to afford RAFT scaffold **2** in 3.3% yield (*Scheme 6*).

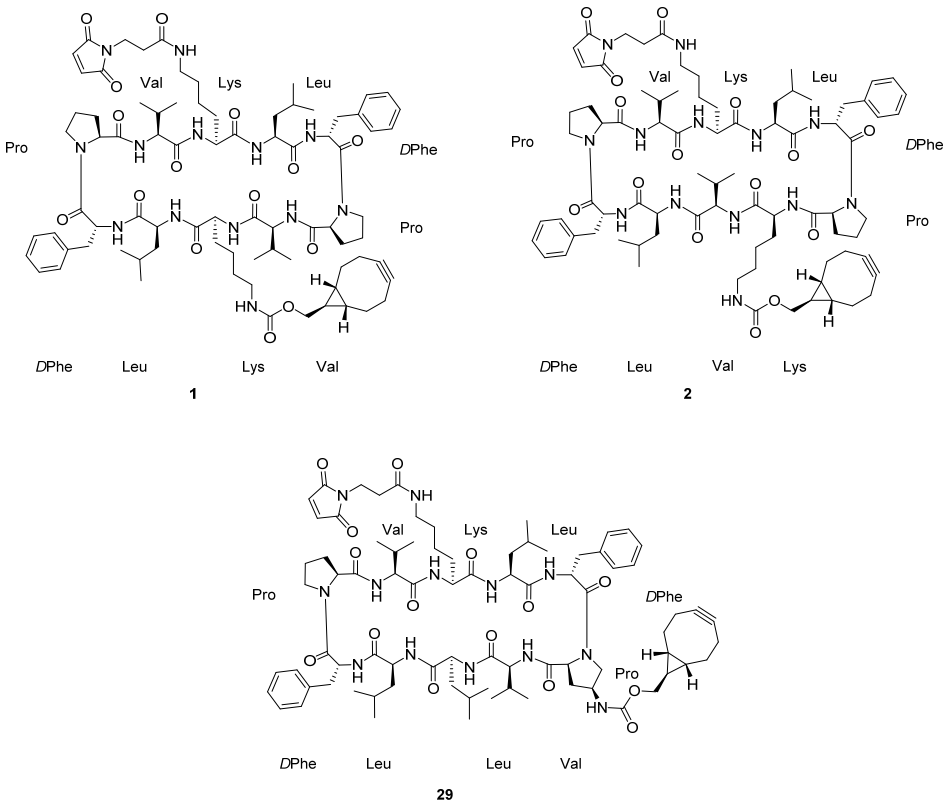

Scheme 6. RAFT scaffolds **1**, **2** and **29** all bearing the chemoselective handles in different orientations.

An advantage of masking the lysine ε-amine with an azido group is that it opens up the possibility of employing the commercially available 4-azidoproline amino acid as an additional means of inducing a different orientation of the chemoselective handles. When employing the cis-Fmoc-(2*S*, 4*S*)-4-azidoproline in place of a regular proline, RAFT scaffold **29** was obtained in 3.3% yield giving a third RAFT scaffold

with a different orientation. With these scaffolds in hand together with the synthesized TLR2, 7 and 9 ligands nine different combinations can be synthesized, which should be the focus going forward.

Conclusion

Complementing recent research efforts into synergistic effects of various TLR ligands, this Chapter is focused on synthesizing a system to study the effect of the orientation on the synergy between different TLR agonists. Inspiration was drawn from a concept introduced by Mutter termed regioselectively addressable functionalized template (RAFT) and was applied on the cyclic decapeptide gramicidin S, bearing lysine groups.[19,20] With the method described in Chapter 3 and here expanded to the TentaGel S AC resin, it was possible to differentiate between the two lysine ε-amines to install the strained cyclooctyne BCN and a maleimido moiety. The first attempted synthesis was carried out on the TentaGel S PHB resin and the Mmt group was used as the temporary lysine ε-amine protecting group, but deprotection of this group resulted in fluctuating yields. The switch to TentaGel S AC resin was made to accompany the on-resin introduction of the moderately acid-labile cyclooctyne. Simultaneously, the azide was chosen as the masking group for the lysine ε-amine and resulted in clean on-resin reduction. The cleavage procedure was simplified by using the Amberlyst A-21 basic ion-exchange resin to neutralize the trifluoroacetic acid. With this procedure three different RAFT scaffolds were synthesized. TLR2, 7 and 9 ligands were synthesized bearing complementary groups to those present on the scaffolds giving rise to nine different possible combinations of ligands and orientations which in the future could be used to study the effects of orientation of the TLR combinations on their ability to stimulate an immune response.

General information

Materials, reactions and purification

Standard Fmoc-amino acids and resins for solid-phase peptide synthesis (SPPS), amino acids for solution-phase synthesis and peptide coupling reagents 2-(6-chloro-1*H*-benzotriazole-1-yl)-1,1,3,3-tetramethyluronium hexafluorophosphate (HCTU), *N*,*N*'-diisopropylcarbodiimide (DIC), 1-ethyl-3-(3-dimethylaminopropyl) carbodiimide hydrochloride (EDC), ethyl cyano(hydroxyimino)acetate (Oxyma Pure) and 1-hydroxybenzotriazole (HOBt) were purchased from Novabiochem or Sigma-Aldrich. The resins TentaGel S PHB (0.27 mmol/g), TentaGel S AC (0.23 mmol/g) and TentaGel S RAM (0.25 mmol/g) were bought from Rapp Polymere. Fmoc-Cys((*RS*)-2,3-di(palmitoyloxy)-propyl)-OH was obtained from Bachem. Fmoc-L-Lys(N_2)-OH was purchased from Iris Biotech. 4-((6-Amino-2-butoxy-7-(tert-butoxycarbonyl)-8-oxo-7,8-dihydro-9*H*-purin-9-yl)methyl)benzoic acid and 3-maleimidopropionic acid *N*-hydroxysuccinimidyl ester were available in-house. All other chemicals were purchased from Acros, Sigma Aldrich, VWR, Fluka, Merck and Fisher Scientific and used as received unless stated otherwise. Tetrahydrofuran (THF), *N*,*N*-dimethylformamide (DMF), dichloromethane (DCM), 1,4-dioxane and toluene were stored over molecular sieves before use. Commercially available ACS grade solvents were used for column chromatography without any further purification, except for toluene and ethyl acetate which were distilled prior to use. All reactions were carried out under a nitrogen atmosphere, unless indicated otherwise. Reaction progress and chromatography fractions were monitored by thin layer chromatography (TLC) on silica-gel-coated aluminium sheets with a F254 fluorescent indicator purchased from Merck (Silica gel 60 F_{254}). Visualization was achieved by UV absorption by fluorescence quenching, permanganate stain (4 g $KMnO_4$ and 2 g K_2CO_3 in 200 mL of H_2O), ninhydrin stain (0.6 g ninhydrin and 10 mL acetic acid in 200 mL ethanol). Silica gel column chromatography was performed using Screening Devices silica gel 60 (particle size of 40 – 63 μm, pore diameter of 60 Å) with the indicated eluent. Analytical reversed-phase high-performance liquid chromatography (RP-HPLC) was performed on a Thermo Finnigan Surveyor HPLC system with a Phenomenex Gemini C_{18} column (4.6 mm x 50 mm, 3 μm particle size) with a flow rate of 1 mL/min and a solvent gradient of 10-90% solvent B over 8 min coupled to a LCQ Advantage Max (Thermo Finnigan) ion-trap spectrometer (ESI^+). Preparative RP-HPLC was performed with a GX-281 Liquid Handler and a 331 and 332-H2 primary and secondary solvent pump respectively with a Phenomenex Gemini C_{18} or C_4 column (250 x 10.0 mm, 3 μm particle size) with a flow rate of 5 mL/min and solvent gradients as described for each compound. All HPLC solvents were filtered with a Millipore filtration system equipped with a 0.22 μm nylon membrane filter prior to use. HPLC solvent compositions: solvent A is 0.1% (v/v) TFA in H_2O; solvent B is MeCN. Preparative RP-HPLC was also performed on an Agilent 1200 HPLC system coupled to a 6130 Quadrupole Mass Spectrometer using a Nucleodur C_{18} Gravity column (250 x 10.0 mm, 5 μm particle size) with a flow rate of 5 mL/min and a gradient over 12 min. as described for each compound. HPLC solvent composition: solvent A is 0.2% (v/v) TFA in H_2O and solvent B is MeCN. All HPLC solvents were filtered with a Millipore filtration system equipped with a 0.22 μm nylon membrane filter prior to use.

Characterization

Nuclear magnetic resonance (^1H and ^{13}C APT NMR) spectra were recorded on a Brüker DPX-300, Brüker AV-400, Brüker DMX-400, Brüker AV-500 or Brüker DMX-600 in the given solvent. Chemical shifts are reported in parts per million (ppm) with the residual solvent or tetramethylsilane (0 ppm) as reference. High-resolution mass spectrometry (HRMS) analysis was performed with a Thermo Finnigan LTQ Orbitrap mass spectrometer equipped with an electronspray ion source in positive mode (source voltage 3.5 kV, sheath gas flow 10 ml/min, capillary temperature 250 °C) with resolution R = 60000 at m/z 400 (mass range m/z = 150 – 2000) and dioctyl phthalate (m/z = 391.28428) as a "lock mass". The high-resolution mass spectrometer was calibrated prior to measurements with a Thermo Finnigan calibration mixture. Nominal and exact m/z values are reported in daltons.

Solid-phase peptide synthesis

General methodology

Manual solid-phase peptide synthesis

Manual amino acid couplings were carried out using a fritted reaction syringe equipped with a plunger and syringe cap or a manual reaction vessel (SHG-20260-PI, 60 mL) purchased from Peptides International. The syringe was shaken using

either a Heidolph Multi Reax vortexer set at 1000 rpm or a St. John Associates 180° Flask Shaker (model no. A5-6027). Fmoc deprotection was achieved by agitating the resin with 20% (v/v) piperidine in DMF (2 x 10 min.). After draining the reaction vessel, the resin was washed with DMF (6 x 30 sec.). The appropriately side-chain protected Fmoc-amino acid (5.0 equiv.) in DMF (5.0 mL) was pre-activated with HCTU (5.0 equiv.) and DIPEA (10 equiv.) for 5 min, then added to resin and agitated for 60 min. After draining the reaction vessel, the resin was washed with DMF (4 x 30 sec.). The completion of all couplings was assessed by a Kaiser test and double coupling was performed as needed.

Automated solid-phase peptide synthesis

The automated peptide coupling was performed on a CEM Liberty Blue microwave peptide synthesizer or a Protein Technologies Tribute peptide synthesizer using standard Fmoc protected amino acids. For the Tribute peptide synthesizer, amino acids were presented as solids and 0.20 M HCTU in DMF was used as activator, 0.50 M DIPEA in DMF as the activator base, 20% (v/v) piperidine in DMF as the deprotection agent and a 90:10, DMF – Ac_2O mixture as the capping agent. Coupling of each amino acid occurred at room temperature for 1 hr followed by a capping step (2x 3 min.) betwixt two washing steps. Subsequently, Fmoc was deprotected using the deprotection agent (2x 3 min.) followed by two more washing steps. For the Liberty Blue microwave synthesizer, amino acids were presented as a solution (0.20 M in DMF) and 0.50 M DIC in DMF was used as activator, 1.0 M Oxyma Pure in DMF as additive and 20% (v/v) piperidine in DMF as the deprotection agent. Amino acid coupling in the microwave synthesizer occurred at 90 °C for 2 min. followed by Fmoc deprotection at 90 °C using the aforementioned deprotection agent (2x 90 sec.) and two washing steps.

Loading calculation

Resin was dried before loading calculation by washing with DCM (3x 30 sec.) and Et_2O (3x 30 sec.) followed by purging with N_2. A small amount of resin (5 – 10 mg) was weighed and DMF (0.80 mL) was added and the resin was swollen for 20 min. Piperidine (0.20 mL) was then added and shaken for 20 min. Following the deprotection, the suspension was filtered and diluted with 20% (v/v) piperidine in DMF to a total volume of 10 mL in a volumetric flask. The absorption of this solution was measured against a blank 20% (v/v) piperidine in DMF solution using a Shimadzu UV-1601 UV-VIS spectrometer with a Quartz cuvette (optical pathway = 1 cm). The loading was then calculated using the following equation:

$$\text{Loading}_{\text{resin}} = \frac{A_{301.0\,\text{nm}} * 10^6\ \text{mmol mol}^{-1}\ \text{mg g}^{-1} * V * D}{\varepsilon_{301.0\,\text{nm}} * m_{\text{resin}} * l}$$

where:

$\text{Loading}_{\text{resin}}$ = Fmoc substitution in mmol/g
$A_{301.0\,\text{nm}}$ = Absorption of sample at 301.0 nm
10^6 mmol mol^{-1} mg g^{-1} = Conversion factor of mmol to mol and mg^{-1} to g^{-1}
V = Total volume in L
D = Dilution factor
$\varepsilon_{301.0\,\text{nm}}$ = Molar absorption coefficient at 301.0 nm (8021 L mol^{-1} cm^{-1})
m_{resin} = sample weight of the resin in mg
l = optical path length of the cell in cm

(*R*)-4-((6-amino-2-butoxy-8-oxo-7,8-dihydro-9*H*-purin-9-yl)methyl)-*N*-(1-amino-3-mercapto-1-oxopropan-2-yl)benzamide

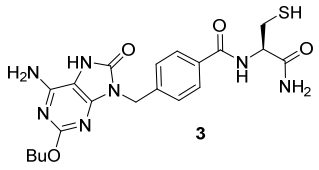

3

TentaGel S RAM (0.25 mmol/g, 0.40 g, 0.10 mmol, 1.0 equiv.) was elongated with standard cysteine building block (Fmoc-Cys(Trt)-OH) using manual peptide synthesis procedure. After Fmoc-deprotection and subsequent washing steps, a solution of 4-((6-amino-2-butoxy-7-(tert-butoxycarbonyl)-8-oxo-7,8-dihydro-9*H*-purin-9-yl)methyl)benzoic acid (69 mg, 0.15 mmol, 1.5 equiv.), HCTU (62 mg, 0.15 mmol, 1.5 equiv.) and DIPEA (52 μL, 0.30 mmol, 3.0 equiv.) in DMF (4.0 mL, 25 mM) was added to the resin and the mixture was shaken for 17 hrs. The resin was washed with DMF (4x) and DCM (4x) and a cleavage cocktail (190:5:5, TFA – H_2O – TIPS, 10 mL, 10 mM) was added and the resin was shaken for 3 hrs. The suspension was filtered and the filtrate was concentrated over a stream of N_2. Purification by RP-HPLC (GX-281, C_{18} column, 25% to 45% solvent B) followed by lyophilization afforded thiol **3** (18 mg, 39 μmol, 39%) as a white solid.

^{1}H NMR (500 MHz, DMF) δ 10.25 (s, 1H, N*H*(C=O)N), 8.47 (d, *J* = 8.0 Hz, 1H, N*H*-Cys), 8.00 – 7.93 (m, 2H, C*H*-arom), 7.69 (s, 1H, N*H*$_2$-Cys), 7.52 – 7.47 (m, 2H, C*H*-arom), 7.23 (s, 1H, N*H*$_2$-Cys), 6.70 (br s, 2H, N*H*$_2$), 5.04 (s, 2H, C*H*$_2$-benzyl), 4.69 (td, *J* = 8.2, 4.7 Hz, 1H, α-Cys), 4.21 (t, *J* = 6.6 Hz, 2H, OC*H*$_2$), 3.13 – 3.06 (m, 1H, β-Cys), 3.00 – 2.95 (m, 1H, β-Cys), 2.33 (t, *J* = 8.5 Hz, 1H, S*H*), 1.72 – 1.63 (m, 2H, OCH$_2$C*H*$_2$), 1.48 – 1.37 (m, 2H, C*H*$_2$CH$_3$), 0.93 (t, *J* = 7.4 Hz, 3H, C*H*$_3$).

^{13}C NMR (126 MHz, DMF) δ 175.0 (NH$_2$C=O), 167.6 (Ph(*C*=O)NH), 161.7 (NH$_2$*C*q), 153.9 (BuO*C*q), 150.9 (NH(*C*=O)N), 149.2 (N*C*qN), 142.0 (*C*q-arom), 134.7 (*C*q-arom), 128.8 (*C*H-arom), 128.5 (*C*H-arom), 99.8 (NH*C*q), 67.2 (O*C*H$_2$), 57.4 (α-Cys), 43.4 (*C*H$_2$-benzyl), 32.0 (OCH$_2$*C*H$_2$), 27.2 (β-Cys), 20.1 (*C*H$_2$CH$_3$), 14.4 (*C*H$_3$).

HRMS (ESI-Orbitrap) as disulfide calcd. for $C_{40}H_{49}N_{14}O_8S_2$ [M+H]$^+$ 917.32937, found 917.32989.

(*S*)-4-((6-amino-2-butoxy-8-oxo-7,8-dihydro-9*H*-purin-9-yl)methyl)-*N*-(1-amino-6-azido-1-oxohexan-2-yl)benzamide

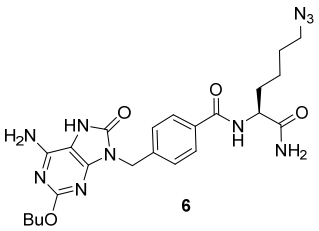

6

TentaGel S RAM (0.25 mmol/g, 0.40 g, 0.10 mmol, 1.0 equiv.) was elongated with Fmoc-L-Lys(N$_2$)-OH using manual peptide synthesis procedure. After Fmoc-deprotection and subsequent washing steps, a solution of 4-((6-amino-2-butoxy-7-(tert-butoxycarbonyl)-8-oxo-7,8-dihydro-9*H*-purin-9-yl)methyl)benzoic acid (69 mg, 0.15 mmol, 1.5 equiv.), HCTU (62 mg, 0.15 mmol, 1.5 equiv.) and DIPEA (52 μL, 0.30 mmol, 3.0 equiv.) in DMF (4.0mL, 25 mM) was added to the resin and the mixture was shaken for 17 hrs. The resin was washed with DMF (4x) and DCM (4x) and a cleavage cocktail (190:5:5, TFA – H_2O – TIPS, 10 mL, 10 mM) was added and the resin was shaken for 3 hrs. The suspension was filtered and the filtrate was concentrated over a stream of N_2. Purification by RP-HPLC (GX-281, C_{18} column, 25% to 40% solvent B) followed by lyophilization afforded azide **6** (31 mg, 61 μmol, 61%) as a white solid.

^{1}H NMR (500 MHz, DMF) δ 10.21 (s, 1H, N*H*(C=O)N), 8.36 (d, *J* = 8.1 Hz, 1H, N*H*-AzLys), 7.99 – 7.94 (m, 2H, C*H*-arom), 7.61 (s, 1H, N*H*$_2$-AzLys), 7.52 – 7.46 (m, 2H, C*H*-arom), 7.07 (s, 1H, N*H*$_2$-AzLys), 6.73 (br s, 2H, N*H*$_2$), 5.04 (s, 2H, C*H*$_2$-benzyl), 4.58 (ddd, *J* = 9.5, 8.0, 4.7 Hz, 1H, α-AzLys), 4.22 (t, *J* = 6.6 Hz, 2H, OC*H*$_2$), 3.37 (t, *J* = 6.8 Hz, 2H, ε-AzLys), 2.01 – 1.89 (m, 1H, β-AzLys), 1.89 – 1.76 (m, 1H, β-AzLys), 1.72 – 1.38 (m, 8H, OCH$_2$C*H*$_2$, δ-AzLys, γ-AzLys, C*H*$_2$CH$_3$), 0.93 (t, *J* = 7.4 Hz, 3H, C*H*$_3$).

^{13}C NMR (126 MHz, DMF) δ 175.2 (NH$_2$C=O), 167.4 (Ph(*C*=O)NH), 161.4 (NH$_2$*C*q), 153.8 (BuO*C*q), 150.9 (NH(*C*=O)N), 149.0 (N*C*qN), 141.8 (*C*q-arom), 134.9 (*C*q-arom), 128.8 (*C*H-arom), 128.5 (*C*H-arom), 99.7 (NH*C*q), 67.3 (O*C*H$_2$), 54.5 (α-AzLys), 52.0 (ε-AzLys), 43.4 (*C*H$_2$-benzyl), 32.6 (β-AzLys), 32.0 (OCH$_2$*C*H$_2$), 29.3 (δ-AzLys), 24.3 (γ-AzLys), 20.0 (*C*H$_2$CH$_3$), 14.4 (*C*H$_3$).

HRMS (ESI-Orbitrap) calcd. for $C_{23}H_{31}N_{10}O_4$ [M+H]$^+$ 511.25243, found 511.25237.

(6*R*,9*S*,12*S*,15*S*,18*S*,21*S*,24*S*)-12,15,18,21-tetrakis(4-aminobutyl)-28-azido-24-carbamoyl-9-(hydroxymethyl)-7,10,13,16,19,22-hexaoxo-6-(3-tetradecylureido)-4-thia-8,11,14,17,20,23-hexaazaoctacosane-1,2-diyl dipalmitate

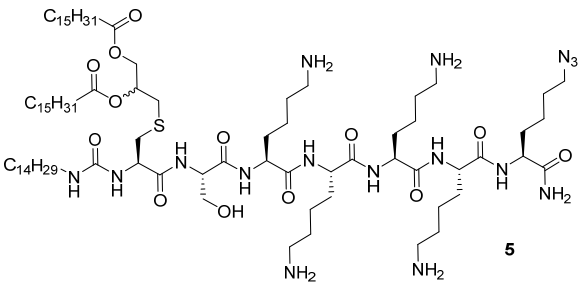

TentaGel S RAM (0.25 mmol/g, 0.40 g, 0.10 mmol, 1.0 equiv.) was elongated using the Tribute peptide synthesizer to obtain **14**. Using manual peptide chemistry, the resin was treated with piperidine in DMF (2 x 10 min) and washed with DMF (6x). A solution of Fmoc-Cys((*RS*)-2,3-di(palmitoyloxy)-propyl)-OH (0.13 g, 0.15 mmol, 1.5 equiv.), HCTU (62 mg, 0.15 mmol, 1.5 equiv.) and DIPEA (26 μL, 0.15 mmol, 1.5 equiv.) in a mixture of DCM and DMF (1:1, DMF – DCM, 4.0 mL, 25 mM) was added to the resin and the resin was shaken for 15 min. Additional DIPEA ((26 μL, 0.15 mmol, 1.5 equiv.) was added and the resin was shaken for another 24 hrs. The resin was washed with DMF (4x) and DCM (4x). After Fmoc-deprotection and subsequent washing steps, tetradecylisocyanate (0.25 mL, 0.74 mmol, 7.4 equiv.) and a mixture of DMF and DCM (1:1, DMF – DCM, 10 mL, 10 mM) were added and the mixutre was shaken for 24 hrs. The resin was washed with DMF (4x) and DCM (4x). A cleavage cocktail (190:5:5, TFA – H_2O – TIPS, 10 mL, 10 mM) was added and the resin was shaken for 3 hrs. The suspension was filtered and the filtrate was conctentrated under a stream of N_2 Purification by RP-HPLC (GX-281, C_4 column, 40% to 90% solvent B) and lyophilization afforded azide **5** (12 mg, 7.2 μmol, 7.2%) as a white solid.

^{1}H NMR (500 MHz, DMF) δ 8.49 (t, *J* = 6.9 Hz, 1H, N*H*-Lys), 8.39 (t, *J* = 7.0 Hz, 1H, N*H*-Ser), 8.16 – 8.10 (m, 1H, N*H*-Lys), 8.03 – 7.98 (m, 2H, N*H*-Lys), 7.81 (d, *J* = 7.9 Hz, 1H, N*H*-AzLys), 7.48 (s, 1H, NH_2C=O), 7.20 (s, 1H, NH_2C=O), 6.88 – 6.81 (m, 1H, N*H*-Cys), 6.79 (t, *J* = 5.8 Hz, 1H, $C_{14}H_{29}$N*H*), 5.26 – 5.15 (m, 1H, $C_{15}H_{31}$O(C=O)C*H*), 4.43 – 4.37 (m, 3H, α-Ser, α-Cys, $C_{15}H_{31}$(C=O)OCH_2), 4.37 – 4.17 (m, 6H, α-Lys, α-AzLys, $C_{15}H_{31}$(C=O)OCH_2), 3.95 (dd, *J* = 11.1, 5.3 Hz, 1H, β-Ser), 3.79 – 3.74 (m, 1H, β-Ser), 3.35 (t, *J* = 6.8 Hz, 2H, ε-AzLys), 3.21 – 3.13 (m, 2H, CH_2NH(C=O)NH), 3.13 – 2.99 (m, 10H, β-Cys, ε-Lys, β-Cys), 2.98 – 2.94 (m, 1H, CH_2S), 2.89 – 2.80 (m, 1H, CH_2S), 2.40 – 2.31 (m, 4H, CH_2(C=O)O), 1.96 – 1.70 (m, 18H, β-Lys, β-AzLys, δ-Lys), 1.64 – 1.43 (m, 18H, δ-AzLys, CH_2CH_2(C=O)O, CH_2CH_2NH(C=O)NH, γ-Lys, γ-AzLys), 1.37 – 1.22 (m, 70H, CH_2-alkyl), 0.91 – 0.85 (m, 9H, CH_3).

^{13}C NMR (126 MHz, DMF) δ 175.3 (*C*=O), 174.1 (*C*=O), 173.9 (*C*=O), 173.6 (*C*=O), 173.3 (*C*=O), 172.8 (*C*=O), 172.7 (*C*=O), 159.8 (NH(*C*=O)NH), 71.5 ($C_{15}H_{31}$(C=O)OCH), 64.7 ($C_{15}H_{31}$(C=O)OCH_2), 62.8 (β-Ser), 57.6 (α-Ser), 55.8 (α-Cys), 55.3 (α-Lys), 55.2 (α-Lys), 54.9 (α-Lys), 54.6 (α-Lys), 54.0 (α-AzLys), 52.1 (ε-AzLys), 40.9 (*C*H_2NH(C=O)NH), 40.6 (ε-Lys), 40.5 (ε-Lys), 40.5 (ε-Lys), 35.8 (β-Cys), 34.9 (*C*H_2(C=O)O), 34.6 (*C*H_2(C=O)O), 33.3 (*C*H_2S), 32.8 (*C*H_2-alkyl), 32.1 (β-Lys), 31.9 (β-Lys), 31.7 (β-Lys), 31.5 (β-Lys), 31.2 (β-AzLys), 30.6 (*C*H_2-alkyl), 30.6 (*C*H_2-alkyl), 30.5 (*C*H_2-alkyl), 30.4 (*C*H_2-alkyl), 30.3 (*C*H_2-alkyl), 30.2 (*C*H_2-alkyl), 30.2 (*C*H_2-alkyl), 30.0 (*C*H_2-alkyl), 30.0 (*C*H_2-alkyl), 29.3 (δ-AzLys), 28.0 (δ-Lys), 28.0 (δ-Lys), 27.9 (δ-Lys, *C*H_2-alkyl), 27.9 (δ-Lys, *C*H_2-alkyl), 25.9 (CH_2CH_2(C=O)O), 25.8 (CH_2CH_2(C=O)O), 24.0 (γ-AzLys), 23.8 (γ-Lys), 23.7 (γ-Lys), 23.7 (γ-Lys), 23.6 (γ-Lys), 23.5 (*C*H_2CH$_3$), 14.7 (*C*H_3).

HRMS (ESI-Orbitrap) calcd. for $C_{86}H_{169}N_{16}O_{13}S$ $[M+3H]^{3+}$ 555.42531, found 555.42457.

Fmoc-Lys(Tentagel S Ac)-OAllyl

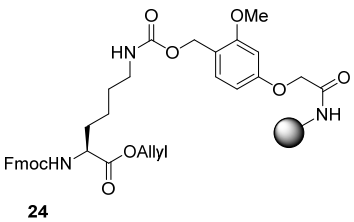

24

A solution containing triphenylphosphine oxide (1.0 g, 3.6 mmol, 7.2 equiv.) in DCM (15 mL, 0.12 M) was cooled to 0 °C and triflic anhydride (1.0 M in DCM, 1.8 mL, 1.8 mmol, 3.6 equiv.). The reaction was stirred at 0 °C for 30 min. during which a white precipitate was formed. A solution of *N*-Boc protected lysine **20** (0.77 g, 1.5 mmol, 3.0 equiv.) in DCM (2.0 mL, 0.75 M) was then added to the suspension and the cooling bath was removed. The reaction was stirred for 5 min. followed by the addition of *N*-methylmorpholine (0.41 mL, 3.8 mmol, 7.5 equiv.) and dibutyltin dilaurate (0.30 mL, 0.50 mmol, 1.0 equiv.). The solution was transferred to TentaGel S Ac resin (0.23 mmol/g, 2.2 g, 0.50 mmol, 1.0 equiv.) which was co-evaporated previously with 1,4-dioxane (3x) and the suspension was shaken for 72 hrs. The suspension was filtered and the resin was washed with DCM (4x)

and Et_2O (4x). Drying the resin over N_2 afforded functionalized resin **24** (2.3 g, 0.44 mmol, 89%) with a loading of 0.19 mmol/g.

***cyclo*(-Leu-*D*Phe-Pro-Val-Lys(N_2)-Leu-*D*Phe-Pro-Val-Lys-)**

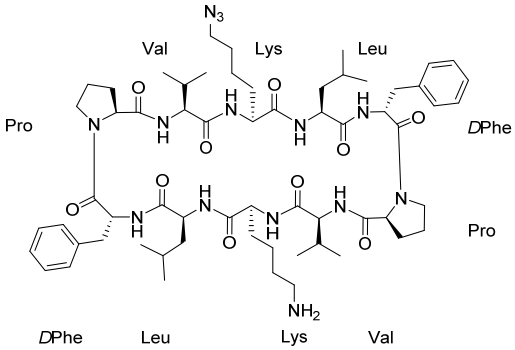

30

Functionalized resin **24** (0.53 g, 0.10 mmol, 1.0 equiv.) was elongated using the Tribute peptide synthesizer. Afterwards, the resin was washed with DCM (4x), Et_2O (4x) and dried over N_2. Resin was suspended in a mixture of DCM and DMF (1:1, DCM – DMF, 4.0 mL, 25 mM) and swollen for 20 min. Phenylsilane (31 µL, 0.25 mmol, 2.5 equiv.) and $Pd(PPh_3)_4$ (29 mg, 25 µmol, 25 mol%) were added and the resin was shaken for 90 min. while being protected from light. The suspension was filtered and the resin was washed with DCM (3x), 0.50% (w/v) sodium diethyldithiocarbamate in DMF (2x) and DMF (3x). To the resin was added 20% (v/v) piperidine in DMF (5.0 mL, 20 mM) and the mixture was shaken for 10 min. Resin was filtered and 20% (v/v) piperidine in DMF (5.0 mL, 20 mM) was added. The suspension was shaken for 10 min. Afterwards, the resin was filtered and washed with DMF (6x). DMF (4.0 mL, 25 mM) was added to the resin. Subsequently, 1-hydroxybenzotriazole hydrate (68 mg, 0.50 mmol, 5.0 equiv.), benzotriazole-1-yl-oxy-tris-pyrrolidino-phosphonium hexafluorophosphate (0.26 g, 0.50 mmol, 5.0 equiv.) and *N*-methylmorpholine (0.11 mL, 1.0 mmol, 10 equiv.) were added to the suspension and the reaction was stirred for 2.5 hrs. The suspension was filtered and the residue was washed with DMF (3x) and DCM (3x). A cleavage mixture (190:5:5, TFA – H_2O – TIPS) was added to a small amount of resin (5.0 mg) and shaken for 2 hrs. The suspension was filtered and the filtrate was analyzed by LC-MS.

LC-MS (ESI^+) calcd. for $C_{62}H_{95}N_{14}O_{10}$ $[M+H]^+$ 1195.74, observed 1195.87 with a retention time of 8.91 min.

***cyclo*(-Leu-*D*Phe-Pro-Lys(N_2)-Val-Leu-*D*Phe-Pro-Val-Lys-)**

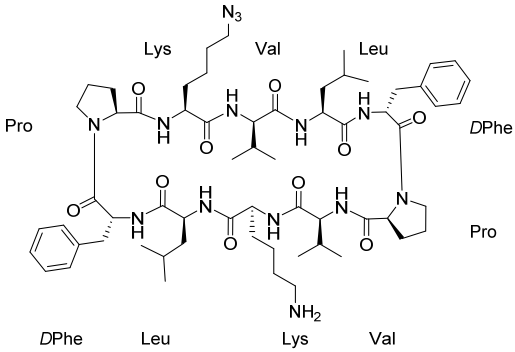

31

Functionalized resin **24** (0.53 g, 0.10 mmol, 1.0 equiv.) was elongated using the Tribute peptide synthesizer. Afterwards, the resin was washed with DCM (4x), Et_2O (4x) and dried over N_2. Resin was suspended in a mixture of DCM and DMF (1:1, DCM – DMF, 4.0 mL, 25 mM) and swollen for 20 min. Phenylsilane (31 µL, 0.25 mmol, 2.5 equiv.) and $Pd(PPh_3)_4$ (29 mg, 25 µmol, 25 mol%) were added and the resin was shaken for 90 min. while being protected from light. The suspension was filtered and the resin was washed with DCM (3x), 0.50% (w/v) sodium diethyldithiocarbamate in DMF (2x) and DMF (3x). To the resin was added 20% (v/v) piperidine in DMF (5.0 mL, 20 mM) and the mixture was shaken for 10 min. Resin was filtered and 20% (v/v) piperidine in DMF (5.0 mL, 20 mM) was added. The suspension was shaken for 10 min. Afterwards, the resin was filtered and washed with DMF (6x). DMF (4.0 mL, 25 mM) was added to the resin. Subsequently, 1-hydroxybenzotriazole hydrate (68 mg, 0.50 mmol, 5.0 equiv.), benzotriazole-1-yl-oxy-tris-pyrrolidino-phosphonium hexafluorophosphate (0.26 g, 0.50 mmol, 5.0 equiv.) and *N*-methylmorpholine (0.11 mL, 1.0 mmol, 10 equiv.) were added to the suspension and the reaction was stirred for 2.5 hrs. The suspension was filtered and the residue was washed with DMF (3x) and DCM (3x). A cleavage mixture (190:5:5, TFA – H_2O – TIPS) was added to a small amount of resin (5.0 mg) and shaken for 2 hrs. The suspension was filtered and the filtrate was analyzed by LC-MS.

LC-MS (ESI$^+$) calculated for $C_{62}H_{95}N_{14}O_{10}$ [M+H]$^+$ 1195.74, observed 1195.87 with a retention time of 8.71 min.

***cyclo*(-Leu-*D*Phe-Pro((4*S*)-4-azido)-Val-Leu-Leu-*D*Phe-Pro-Val-Lys-)**

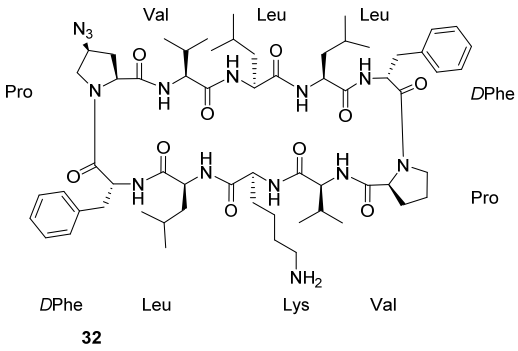

32

Functionalized resin **24** (0.53 g, 0.10 mmol, 1.0 equiv.) was elongated using the Tribute peptide synthesizer. Afterwards, the resin was washed with DCM (4x), Et_2O (4x) and dried over N_2. Resin was suspended in a mixture of DCM and DMF (1:1, DCM – DMF, 4.0 mL, 25 mM) and swollen for 20 min. Phenylsilane (31 µL, 0.25 mmol, 2.5 equiv.) and $Pd(PPh_3)_4$ (29 mg, 25 µmol, 25 mol%) were added and the resin was shaken for 90 min. while being protected from light. The suspension was filtered and the resin was washed with DCM (3x), 0.50% (w/v) sodium diethyldithiocarbamate in DMF (2x) and DMF (3x). To the resin was added 20% (v/v) piperidine in DMF (5.0 mL, 20 mM) and the mixture was shaken for 10 min. Resin was filtered and 20% (v/v) piperidine in DMF (5.0 mL, 20 mM) was added. The suspension was shaken for 10 min. Afterwards, the resin was filtered and washed with DMF (6x). DMF (4.0 mL, 25 mM) was added to the resin. Subsequently, 1-hydroxybenzotriazole hydrate (68 mg, 0.50 mmol, 5.0 equiv.), benzotriazole-1-yl-oxy-tris-pyrrolidino-phosphonium hexafluorophosphate (0.26 g, 0.50 mmol, 5.0 equiv.) and *N*-methylmorpholine (0.11 mL, 1.0 mmol, 10 equiv.) were added to the suspension and the reaction was stirred for 2.5 hrs. The suspension was filtered and the residue was washed with DMF (3x) and DCM (3x). A cleavage mixture (190:5:5, TFA – H_2O – TIPS) was added to a small amount of resin (5.0 mg) and shaken for 2 hrs. The suspension was filtered and the filtrate was analyzed by LC-MS.

LC-MS (ESI$^+$) calculated for $C_{62}H_{95}N_{14}O_{10}$ [M+H]$^+$ 1195.74, observed 1195.87 with a retention time of 8.80 min.

***cyclo*(-Leu-*D*Phe-Pro-Val-Lys(BCN)-Leu-*D*Phe-Pro-Val-Lys-)**

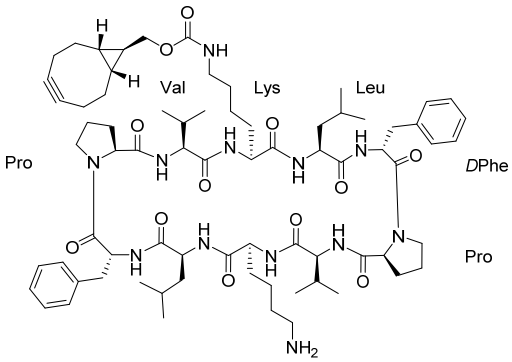

28

To functionalized resin **25** (0.10 mmol, 1.0 equiv.) was added 1,4-dioxane (10 mL, 10 mM) followed by trimethylphosphine (1.0 M in toluene, 1.6 mL, 16 equiv.) and the suspension was stirred for 2 hrs. H_2O (1.0 mL, 55 mmol, 5.5 x 10^2 equiv.) was added and the resin was shaken for an additional 4 hrs. The suspension was filtered and the resin was washed with 1,4-dioxane (3x) and DCM (3x). A solution of BCN PNP ester (63 mg, 0.20 mmol, 2.0 equiv.), DIPEA (70 µL, 0.40 mmol. 4.0 equiv.) in DMF (4.0 mL, 25 mM) was added to the resin and was subsequently shaken for 1 week. The suspension was filtered and the resin was washed with DMF (4x) and DCM (4x). The resin was treated with a cleavage cocktail (TFA – DCM, 1:199, 10 mL) for 2 min. The suspension was filtered into a vigorously stirred mixture of Amberlyst A-21 (7.0 g, previously rinsed with MeOH, THF and DCM) in DCM (20 mL) to neutralize the TFA. This procedure was repeated ten times. The Amberlyst A-21 resin was separated by filtration and rinsed with additional DCM. The filtrate was concentrated *in vacuo* and purified by RP-HPLC (Agilent 1200, 63% to 69% solvent B) to obtain alkyne **28** (4.4 mg, 3.3 µmol, 3.3%) as a white solid.

LC-MS (ESI$^+$) calcd. for $C_{73}H_{109}N_{12}O_{12}$ [M+H]$^+$ 1345.83, found 1345.87 with a retention time of 9.49 min.

***cyclo*(-Leu-*D*Phe-Pro-Val-Lys(BCN)-Leu-*D*Phe-Pro-Val-Lys(Maleimido)-)**

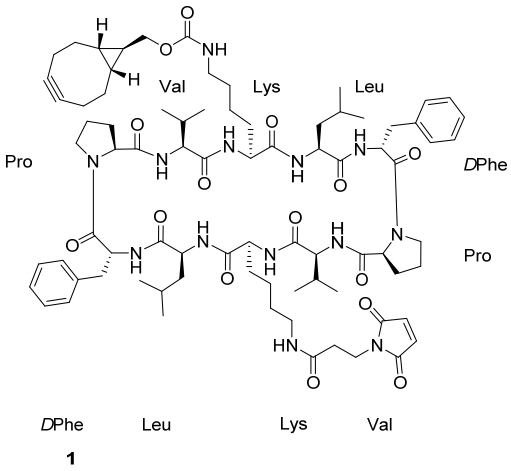

1

Crude alkyne **28** (40 mg, 30 μmol, 1.0 equiv.) was dissolved in DMF (0.50 mL, 60 mM). 3-Maleimidopropionic acid NHS ester (40 mg, 0.15 mmol, 5.0 equiv.) and *N*-methylmorpholine (17 μL, 0.15 mmol, 5.0 equiv.) were added and the reaction was stirred for 4 hrs. The mixture was concentrated *in vacuo* at room temperature. Purification by RP-HPLC (Agilent 1200, 78% to 84% solvent B) and subsequent lyophilization furnished maleimide **1** (5.6 mg, 3.7 μmol, 3.7%) as a white solid.

HRMS (ESI-Orbitrap) calcd. for $C_{80}H_{114}N_{13}O_{15}$ $[M+H]^+$ 1496.85519, found 1496.85720.

***cyclo*(-Leu-*D*Phe-Pro-Lys(BCN)-Val-Leu-*D*Phe-Pro-Val-Lys-)**

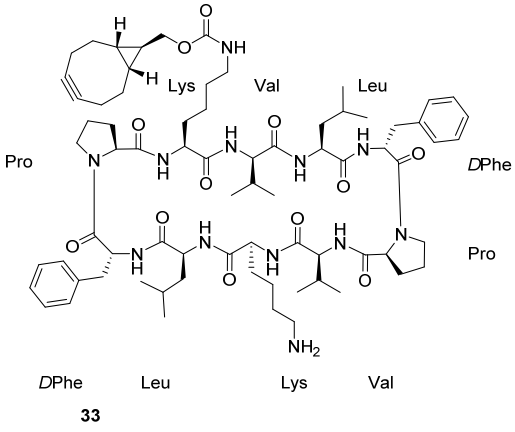

33

To functionalized resin (0.10 mmol, 1.0 equiv.) was added 1,4-dioxane (10 mL, 10 mM) followed by trimethylphosphine (1.0 M in toluene, 1.6 mL, 16 equiv.) and the suspension was stirred for 2 hrs. H_2O (1.0 mL, 55 mmol, 5.5 x 10^2 equiv.) was added and the resin was shaken for an additional 4 hrs. The suspension was filtered and the resin was washed with 1,4-dioxane (3x) and DCM (3x). A solution of BCN PNP ester (63 mg, 0.20 mmol, 2.0 equiv.), DIPEA (70 μL, 0.40 mmol. 4.0 equiv.) in DMF (4.0 mL, 25 mM) was added to the resin and was subsequently shaken for 1 week. The suspension was filtered and the resin was washed with DMF (4x) and DCM (4x). The resin was treated with a cleavage cocktail (TFA – DCM, 1:199, 10 mL) for 2 min. The suspension was filtered into a vigorously stirred mixture of Amberlyst A-21 (7.0 g, previously rinsed with MeOH, THF and DCM) in DCM (20 mL) to neutralize the TFA. This procedure was repeated ten times. The Amberlyst A-21 resin was separated by filtration and rinsed with additional DCM. The filtrate was concentrated *in vacuo* and purified by RP-HPLC (Agilent 1200, 57% to 63% solvent B) to obtain alkyne **33** (6.4 mg, 4.8 μmol, 4.8%) as a white solid.

HRMS (ESI-Orbitrap) calcd. for $C_{73}H_{109}N_{12}O_{12}$ $[M+H]^+$ 1345.82824, found 1345.82947.

***cyclo*(-Leu-*D*Phe-Pro-Lys(BCN)-Val-Leu-*D*Phe-Pro-Val-Lys(Maleimido)-)**

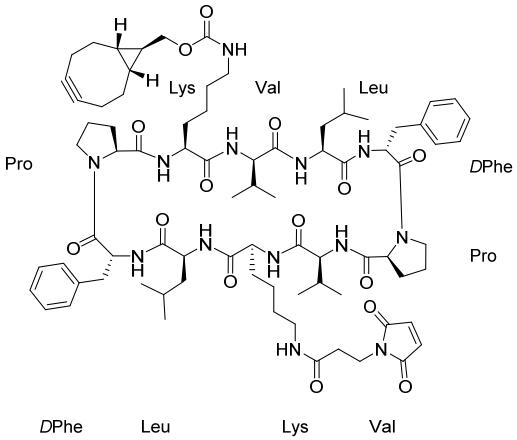

2

Crude alkyne **33** (33 mg, 25 μmol, 1.0 equiv.) was dissolved in DMF (0.50 mL, 50 mM). 3-Maleimidopropionic acid NHS ester (40 mg, 0.15 mmol, 6.0 equiv.) and *N*-methylmorpholine (17 μL, 0.15 mmol, 6.0 equiv.) were added and the reaction was stirred for 4 hrs. The mixture was concentrated *in vacuo* at room temperature. Purification by RP-HPLC (Agilent 1200, 74% to 77% solvent B) and subsequent lyophilization furnished maleimide **2** (5.0 mg, 3.3 μmol, 3.3%) as a white solid.

HRMS (ESI-Orbitrap) calcd. for $C_{88}H_{113}N_{13}O_{15}Na$ $[M+Na]^+$ 1518.83713, found 1518.83894.

***cyclo*(-Leu-*D*Phe-Pro((4*S*)-4-NHBCN)-Val-Leu-Leu-*D*Phe-Pro-Val-Lys-)**

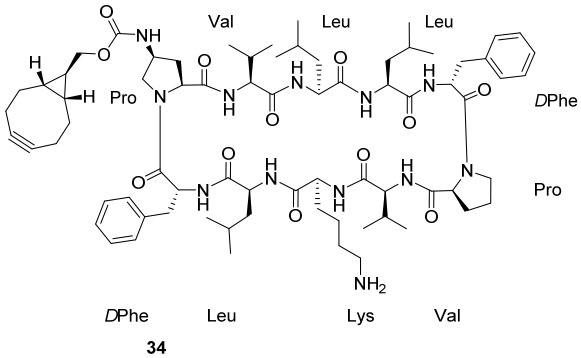

34

To functionalized resin (0.10 mmol, 1.0 equiv.) was added 1,4-dioxane (10 mL, 10 mM) followed by trimethylphosphine (1.0 M in toluene, 1.6 mL, 16 equiv.) and the suspension was stirred for 2 hrs. H_2O (1.0 mL, 55 mmol, 5.5 x 10^2 equiv.) was added and the resin was shaken for an additional 4 hrs. The suspension was filtered and the resin was washed with 1,4-dioxane (3x) and DCM (3x). A solution of BCN PNP ester (63 mg, 0.20 mmol, 2.0 equiv.), DIPEA (70 μL, 0.40 mmol. 4.0 equiv.) in DMF (4.0 mL, 25 mM) was added to the resin and was subsequently shaken for 1 week. The suspension was filtered and the resin was washed with DMF (4x) and DCM (4x). The resin was treated with a cleavage cocktail (TFA – DCM, 1:199, 10 mL) for 2 min. The suspension was filtered into a vigorously stirred mixture of Amberlyst A-21 (7.0 g, previously rinsed with MeOH, THF and DCM) in DCM (20 mL) to neutralize the TFA. This procedure was repeated ten times. The Amberlyst A-21 resin was separated by filtration and rinsed with additional DCM. The filtrate was concentrated *in vacuo* and purified by RP-HPLC (Agilent 1200, 59% to 65% solvent B) to obtain alkyne **34** (4.6 mg, 3.4 μmol, 3.4%) as a white solid.

^{1}H NMR (500 MHz, DMF) δ 8.91 (d, *J* = 4.4 Hz, 1H, N*H*-*D*Phe), 8.58 (d, *J* = 9.2 Hz, 1H, N*H*-Lys), 8.53 – 8.45 (m, 3H, N*H*-Leu), 8.40 (d, *J* = 5.8 Hz, 1H, N*H*-*D*Phe), 8.23 (br s, 3H, NH_2-Lys), 7.41 – 7.25 (m, 11H, N*H*-Val, C*H*-arom), 7.20 (d, *J* = 9.1 Hz, 1H, N*H*-Val), 6.93 (d, *J* = 13.4 Hz, 1H, N*H*BCN), 5.01 – 4.92 (m, 1H, α-Lys), 4.82 (q, *J* = 8.0 Hz, 1H, α-Leu), 4.71 – 4.56 (m, 4H, α-*D*Phe, α-Leu), 4.50 (dd, *J* = 9.2, 6.9 Hz, 1H, α-Val), 4.48 – 4.39 (m, 3H, α-Val, α-Pro, α-AmPro), 3.93 – 3.85 (m, 2H, NH(C=O)OCH_2), 3.77 – 3.71 (m, 1H, δ-Pro), 3.45 – 3.31 (m, 3H, γ-AmPro, δ-AmPro), 3.22 – 3.09 (m, 3H, ε-Lys, β-*D*Phe), 3.06 – 2.98 (m, 3H, β-*D*Phe), 2.88 – 2.81 (m, 1H, δ-Pro), 2.39 – 2.08 (m, 9H, CH_2Cp, β-AmPro, CH_2C≡C, β-Val), 2.05 – 2.02 (m, 1H, β-Pro), 2.00 – 1.92 (m, 1H, β-AmPro), 1.90 – 1.64 (m, 8H, β-Lys, δ-Lys, γ-Pro, β-Pro, γ-Leu, β-Leu), 1.62 – 1.31 (m, 12H, β-Leu, γ-Leu, β-Lys, γ-Lys, β-Leu, CH_2Cp), 0.99 – 0.81 (m, 30H, γ-Val, δ-Leu), 0.75 – 0.68 (m, 2H, C*H*-bridgehead), 0.64 – 0.60 (m, 1H, NH(C=O)OCH$_2$C*H*).

^{13}C NMR (126 MHz, DMF) δ 173.4 (NH(*C*=O)), 172.8 (NH(*C*=O)), 172.5 (NH(*C*=O)), 172.3 (NH(*C*=O)), 172.0 (NH(*C*=O)), 172.0 (NH(*C*=O)), 171.9 (NH(*C*=O)), 171.6 (NH(*C*=O)), 171.5 (NH(*C*=O)), 156.7 (NH(*C*=O)O), 138.2 (*C*q-arom), 137.7 (*C*q-

arom), 130.5 (CH-arom), 129.7 (CH-arom), 129.5 (CH-arom), 128.2 (CH-arom), 127.9 (CH-arom), 99.7 (C≡C), 69.2 (NH(C=O)OCH_2), 61.2 (α-Pro) , 60.0 (α-AmPro), 59.0 (α-Val), 58.4 (α-Val), 55.1 (α-*D*Phe), 54.8 (α-*D*Phe), 53.4 (α-Lys), 52.7 (δ-AmPro), 52.5 (α-Leu), 51.5 (α-Leu), 51.2 (α-Leu), 50.7 (γ-AmPro), 47.3 (δ-Pro), 42.4 (β-Leu), 42.3 (β-Leu), 41.9 (β-Leu), 41.1 (ε-Lys), 37.6 (β-*D*Phe), 37.3 (β-*D*Phe), 35.9 (β-AmPro), 34.2 (CH_2Cp), 34.1 (β-Lys), 32.9 (β-Val), 32.6 (β-Val), 30.3 (β-Pro), 28.8 (δ-Lys), 25.8 (γ-Leu), 25.6 (γ-Leu), 24.7 (NH(C=O)OCH_2CH), 24.7 (γ-Pro), 23.7 (δ-Leu), 23.7 (CH-bridgehead), 23.6 (δ-Leu), 23.5 (γ-Lys), 23.5 (δ-Leu), 23.5 (δ-Leu), 23.4 (δ-Leu), 23.2 (δ-Leu), 21.9 (CH_2C≡C), 20.1 (γ-Val), 20.0 (γ-Val), 19.6 (γ-Val), 19.1 (γ-Val).

HRMS (ESI-Orbitrap) calcd. for $C_{73}H_{108}N_{12}O_{12}Na$ $[M+Na]^+$ 1367.81019, found 1367.81108.

***cyclo*(-Leu-*D*Phe-Pro((4*S*)-4-NHBCN)-Val-Leu-Leu-*D*Phe-Pro-Val-Lys(Maleimido)-)**

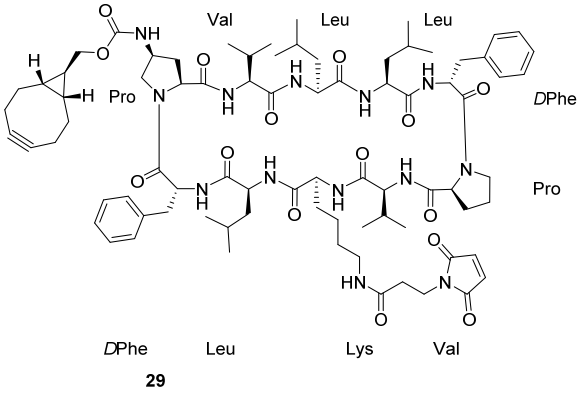

29

Crude alkyne **34** (30 mg, 22 μmol, 1.0 equiv.) was dissolved in DMF (0.50 mL, 44 mM). 3-Maleimidopropionic acid NHS ester (40 mg, 0.15 mmol, 6.8 equiv.) and *N*-methylmorpholine (17 μL, 0.15 mmol, 6.8 equiv.) were added and the reaction was stirred for 4 hrs. The mixture was concentrated *in vacuo* at room temperature. Purification by RP-HPLC (Agilent 1200, 77% to 80% solvent B) and subsequent lyophilization furnished maleimide **29** (5.0 mg, 3.3 μmol, 3.3%) as a white solid.

HRMS (ESI-Orbitrap) calcd. for $C_{73}H_{108}N_{12}O_{12}Na$ $[M+Na]^+$ 1518.83713, found 1518.83842.

References

(1) Del Giudice, G.; Rappuoli, R.; Didierlaurent, A. M. Correlates of Adjuvanticity: A Review on Adjuvants in Licensed Vaccines. *Semin. Immunol.* **2018**, *39*, 14–21. https://doi.org/10.1016/j.smim.2018.05.001.

(2) McKee, A. S.; Marrack, P. Old and New Adjuvants. *Curr. Opin. Immunol.* **2017**, *47*, 44–51. https://doi.org/10.1016/j.coi.2017.06.005.

(3) Glenny, A. T.; Pope, C. G.; Waddington, H.; Wallace, U. Immunological Notes. XVII–XXIV. *J. Pathol. Bacteriol.* **1926**, *29* (1), 31–40. https://doi.org/10.1002/path.1700290106.

(4) Marrack, P.; McKee, A. S.; Munks, M. W. Towards an Understanding of the Adjuvant Action of Aluminium. *Nat. Rev. Immunol.* **2009**, *9* (4), 287–293. https://doi.org/10.1038/nri2510.

(5) Janeway, C. A. Approaching the Asymptote? Evolution and Revolution in Immunology. *Cold Spring Harb. Symp. Quant. Biol.* **1989**, *54 Pt 1*, 1–13. https://doi.org/10.1101/sqb.1989.054.01.003.

(6) O'Neill, L. A. J.; Golenbock, D.; Bowie, A. G. The History of Toll-like Receptors - Redefining Innate Immunity. *Nat. Rev. Immunol.* **2013**, *13* (6), 453–460. https://doi.org/10.1038/nri3446.

(7) Applequist, S. E.; Wallin, R. P. A.; Ljunggren, H.-G. Variable Expression of Toll-like Receptor in Murine Innate and Adaptive Immune Cell Lines. *Int. Immunol.* **2002**, *14* (9), 1065–1074. https://doi.org/10.1093/intimm/dxf069.

(8) Botos, I.; Segal, D. M.; Davies, D. R. The Structural Biology of Toll-like Receptors. *Structure* **2011**, *19* (4), 447–459. https://doi.org/10.1016/j.str.2011.02.004.

(9) Hess, N. J.; Jiang, S.; Li, X.; Guan, Y.; Tapping, R. I. TLR10 Is a B Cell Intrinsic Suppressor of Adaptive Immune Responses. *J. Immunol.* **2017**, *198* (2), 699–707. https://doi.org/10.4049/jimmunol.1601335.

(10) Mancini, R. J.; Stutts, L.; Ryu, K. A.; Tom, J. K.; Esser-Kahn, A. P. Directing the Immune System with Chemical Compounds. *ACS Chem. Biol.* **2014**, *9* (5), 1075–1085. https://doi.org/10.1021/cb500079s.

(11) Ulrich, J. T.; Myers, K. R. Monophosphoryl Lipid A as an Adjuvant. In *Vaccine Design: The Subunit and Adjuvant Approach*; Powell, M. F., Newman, M. J., Eds.; Pharmaceutical Biotechnology; Springer US: Boston, MA, 1995; pp 495–524. https://doi.org/10.1007/978-1-4615-1823-5_21.

(12) Stadelmaier, A.; Morath, S.; Hartung, T.; Schmidt, R. R. Synthesis of the First Fully Active Lipoteichoic Acid. *Angew. Chem. Int. Ed.* **2003**, *42* (8), 916–920. https://doi.org/10.1002/anie.200390243.

(13) Trinchieri, G.; Sher, A. Cooperation of Toll-like Receptor Signals in Innate Immune Defence. *Nat. Rev. Immunol.* **2007**, *7* (3), 179–190. https://doi.org/10.1038/nri2038.

(14) Garcia-Cordero, J. L.; Nembrini, C.; Stano, A.; Hubbell, J. A.; Maerkl, S. J. A High-Throughput Nanoimmunoassay Chip Applied to Large-Scale Vaccine Adjuvant Screening. *Integr. Biol.* **2013**, *5* (4), 650–658. https://doi.org/10.1039/C3IB20263A.

(15) Kasturi, S. P.; Skountzou, I.; Albrecht, R. A.; Koutsonanos, D.; Hua, T.; Nakaya, H. I.; Ravindran, R.; Stewart, S.; Alam, M.; Kwissa, M.; Villinger, F.; Murthy, N.; Steel, J.; Jacob, J.; Hogan, R. J.; García-Sastre, A.; Compans, R.; Pulendran, B. Programming the Magnitude and Persistence of Antibody Responses with Innate Immunity. *Nature* **2011**, *470* (7335), 543–547. https://doi.org/10.1038/nature09737.

(16) Mancini, R. J.; Tom, J. K.; Esser-Kahn, A. P. Covalently Coupled Immunostimulant Heterodimers. *Angew. Chem. Int. Ed.* **2014**, *53* (1), 189–192. https://doi.org/10.1002/anie.201306551.

(17) Shukla, N. M.; Mutz, C. A.; Malladi, S. S.; Warshakoon, H. J.; Balakrishna, R.; David, S. A. Toll-Like Receptor (TLR)-7 and -8 Modulatory Activities of Dimeric Imidazoquinolines. *J. Med. Chem.* **2012**, *55* (3), 1106–1116. https://doi.org/10.1021/jm2010207.

(18) Ryu, K. A.; Slowinska, K.; Moore, T.; Esser-Kahn, A. Immune Response Modulation of Conjugated Agonists with Changing Linker Length. *ACS Chem. Biol.* **2016**, *11* (12), 3347–3352. https://doi.org/10.1021/acschembio.6b00895.

(19) Silla, U.; Mutter, M. Topological Templates as Tool in Molecular Recognition and Peptide Mimicry: Synthesis of a TASK Library. *J. Mol. Recognit.* **1995**, *8* (1–2), 29–34. https://doi.org/10.1002/jmr.300080105.

(20) Dumy, P.; Eggleston, I. M.; Cervigni, S.; Sila, U.; Sun, X.; Mutter, M. A Convenient Synthesis of Cyclic Peptides as Regioselectively Addressable Functionalized Templates (RAFT). *Tetrahedron Lett.* **1995**, *36* (8), 1255–1258. https://doi.org/10.1016/0040-4039(94)02481-P.

(21) Dumy, P.; Eggleston, I. M.; Esposito, G.; Nicula, S.; Mutter, M. Solution Structure of Regioselectively Addressable Functionalized Templates: An NMR and Restrained Molecular Dynamics Investigation. *Biopolymers* **1996**, *39* (3), 297–308. https://doi.org/10.1002/(sici)1097-0282(199609)39:3<297::aid-bip3>3.0.co;2-j.

(22) Pifferi, C.; Berthet, N.; Renaudet, O. Cyclopeptide Scaffolds in Carbohydrate-Based Synthetic Vaccines. *Biomater. Sci.* **2017**, *5* (5), 953–965. https://doi.org/10.1039/C7BM00072C.

(23) Madge, H. Y. R.; Sharma, H.; Hussein, W. M.; Khalil, Z. G.; Capon, R. J.; Toth, I.; Stephenson, R. J. Structure–Activity Analysis of Cyclic Multicomponent Lipopeptide Self-Adjuvanting Vaccine Candidates Presenting

Group A Streptococcus Antigens. *J. Med. Chem.* **2020**, *63* (10), 5387–5397. https://doi.org/10.1021/acs.jmedchem.0c00203.

(24) Llamas-Saiz, A. L.; Grotenbreg, G. M.; Overhand, M.; van Raaij, M. J. Double-Stranded Helical Twisted β-Sheet Channels in Crystals of Gramicidin S Grown in the Presence of Trifluoroacetic and Hydrochloric Acids. *Acta Crystallogr. D Biol. Crystallogr.* **2007**, *63* (3), 401–407. https://doi.org/10.1107/S0907444906056435.

(25) Asano, A.; Matsuoka, S.; Minami, C.; Kato, T.; Doi, M. [Leu2]Gramicidin S Preserves the Structural Properties of Its Parent Peptide and Forms Helically Aligned β-Sheets. *Acta Crystallogr. Sect. C Struct. Chem.* **2019**, *75* (10), 1336–1343. https://doi.org/10.1107/S2053229619011872.

(26) Willems, M. M. J. H. P.; Zom, G. G.; Khan, S.; Meeuwenoord, N.; Melief, C. J. M.; van der Stelt, M.; Overkleeft, H. S.; Codée, J. D. C.; van der Marel, G. A.; Ossendorp, F.; Filippov, D. V. N-Tetradecylcarbamyl Lipopeptides as Novel Agonists for Toll-like Receptor 2. *J. Med. Chem.* **2014**, *57* (15), 6873–6878. https://doi.org/10.1021/jm500722p.

(27) Gential, G. P. P.; Hogervorst, T. P.; Tondini, E.; van de Graaff, M. J.; Overkleeft, H. S.; Codée, J. D. C.; van der Marel, G. A.; Ossendorp, F.; Filippov, D. V. Peptides Conjugated to 2-Alkoxy-8-Oxo-Adenine as Potential Synthetic Vaccines Triggering TLR7. *Bioorg. Med. Chem. Lett.* **2019**, *29* (11), 1340–1344. https://doi.org/10.1016/j.bmcl.2019.03.048.

(28) Matysiak, S.; Böldicke, T.; Tegge, W.; Frank, R. Evaluation of Monomethoxytrityl and Dimethoxytrityl as Orthogonal Amino Protecting Groups in Fmoc Solid Phase Peptide Synthesis. *Tetrahedron Lett.* **1998**, *39* (13), 1733–1734. https://doi.org/10.1016/S0040-4039(98)00055-0.

(29) Wang, X.; Gobbo, P.; Suchy, M.; Workentin, M. S.; Hudson, R. H. E. Peptide-Decorated Gold Nanoparticles via Strain-Promoted Azide–Alkyne Cycloaddition and Post Assembly Deprotection. *RSC Adv.* **2014**, *4* (81), 43087–43091. https://doi.org/10.1039/C4RA07574A.

(30) Chigrinova, M.; McKay, C. S.; Beaulieu, L.-P. B.; Udachin, K. A.; Beauchemin, A. M.; Pezacki, J. P. Rearrangements and Addition Reactions of Biarylazacyclooctynones and the Implications to Copper-Free Click Chemistry. *Org. Biomol. Chem.* **2013**, *11* (21), 3436–3441. https://doi.org/10.1039/C3OB40683K.

(31) Srinivasan, N.; Yurek-George, A.; Ganesan, A. Rapid Deprotection of N-Boc Amines by TFA Combined with Freebase Generation Using Basic Ion-Exchange Resins. *Mol. Divers.* **2005**, *9* (4), 291–293. https://doi.org/10.1007/s11030-005-4386-8.

(32) Spangler, B.; Yang, S.; Baxter Rath, C. M.; Reck, F.; Feng, B. Y. A Unified Framework for the Incorporation of Bioorthogonal Compound Exposure Probes within Biological Compartments. *ACS Chem. Biol.* **2019**, *14* (4), 725–734. https://doi.org/10.1021/acschembio.9b00008.

4

Design and synthesis of gramicidin S-based scaffolds having three orthogonal handles to append various TLR ligands

A remarkable feat of the yellow fever vaccine is the duration of immunity it provides: up to 80% of vaccinees demonstrate immunity for as long as 40 years.[1] The vaccine was created by Theiler and Smith after the yellow fever virus was first isolated in 1927 by repeatedly propagating the virus over mouse and chicken embryos, stripped of nervous tissue, leading to an attenuated strain termed YF-17D.[2] This virus strain proved to be a safe and effective immunizing agent and since the late 1930s until 2014 has been administered approximately 540 million times.[3] Research into the immunological mechanism of the vaccine revealed the

activation of multiple dendritic cell subsets *via* TLRs 2, 7, 8, and 9 to elicit a broad spectrum of innate and adaptive immune responses leading to long-lasting immunity.[4]

The importance of engaging multiple TLRs is further demonstrated by the group of Berzofsky who found that utilizing a combination of TLR2/6, TLR3 and TLR9 agonists greatly increased the protective efficacy of vaccination with an HIV envelope peptide in mice when compared with using a mix of ligands for only two of these TLRs. Compared to the dual mixtures which amplify T cell responses by increasing the production of T cells, they found that this specific triple combination of TLR agonists augmented the quality of the T cell responses primarily by increasing their functional avidity for the antigen necessary for clearing the virus.[5]

Interestingly, Esser-Kahn and co-workers showed that covalently linking three different TLR ligands substantially alters the resulting immune response compared to the unlinked counterparts. Comparison of five constructs with a different combination of covalently linked triagonists revealed a distinct immune response for each construct with a varying T_H1/T_H2 balance.[6] This was validated in a follow-up study by Gilkes *et al*. with an *in vivo* mouse challenge model of TLR triagonists in combination with a Q fever antigen showing that spatial organization of the triagonist construct can shape immune responses toward desired outcomes.[7]

The research in this Chapter describes the expansion of the dual RAFT platform described in Chapter 4 to a triple RAFT platform. With the ultimate aim to study the effect of spatial orientation of three TLR ligands on the immune response, the three ligation handles are positioned in two manners (*Figure 1*). To achieve this goal, the availability of one additional chemoselective handle, allowing a triple orthogonal ligation strategy, is required. Sequential ligation strategies have been reported before, such as by Willems *et al.* who used a two-step procedure for simultaneous tetrazine/norbornene ligation and Staudinger-Bertozzi ligation, followed by a copper(I)-catalyzed alkyne-azide cycloaddition (CuAAC) to monitor multiple enzymatic activities by activity-based protein profiling.[8] Another ligation strategy, published by Simon *et al*. employed a tetrazine/cyclopropane ligation followed by strain-promoted alkyne-azide cycloaddition (SPAAC) and finally a CuAAC to monitor the formation of plant cell walls.[9] Thomas *et al*. established a cascade methodology for ligating four different glycosides on the RAFT scaffold, introduced by the group of Mutter.[10,11] Functionalized glycosides were ligated on the scaffold by

sequential oxime ligation, photocatalyzed thiol-ene reaction, CuAAC and finally chloroacetamide/thiol coupling.

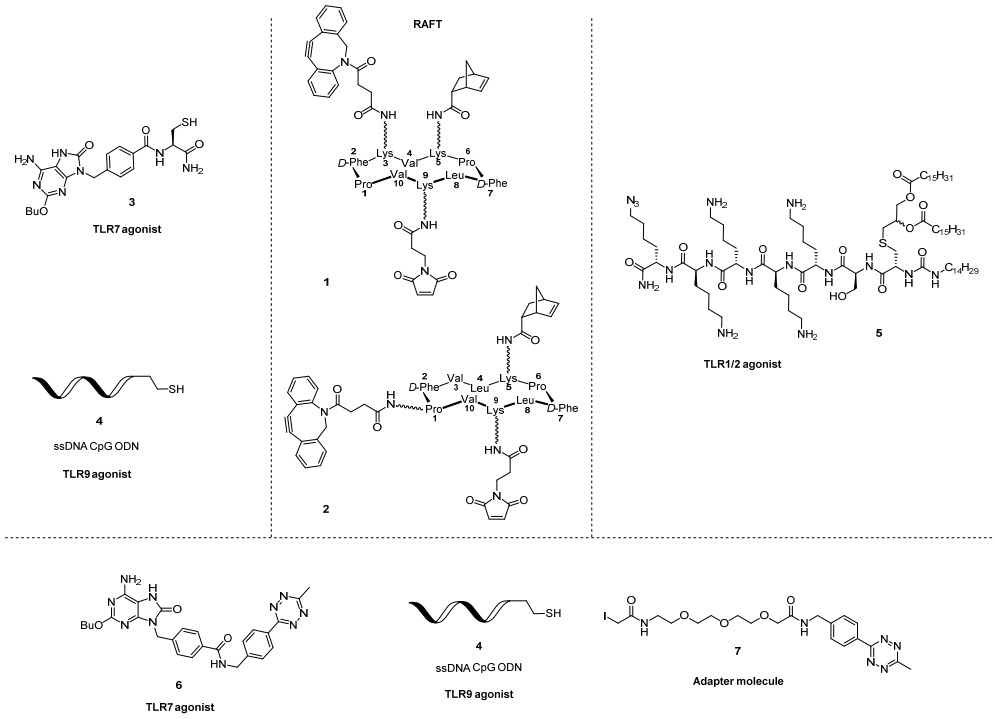

Figure 1. Design of the RAFT scaffold equipped with three orthogonal ligation handles to accommodate for three different TLR agonists.

This Chapter entails the design and synthesis of triple functionalized RAFT platforms with the focus on making the ensuing ligation as streamlined as possible by excluding additional reagents and equipment. Therefore, the choice was made to expand the thiol/maleimide coupling and SPAAC with a tetrazine/norbornene ligation. Since 1,2,4,5-tetrazines are known to react with strained cycloalkynes, the reagents and conditions had to be chosen carefully.[12] Karver and co-workers were able to mitigate this cross-reaction by employing a bulky cycloalkyne and disubstituted tetrazine to create a mutually orthogonal SPAAC and tetrazine/*trans*-cyclooctene ligation pair.[13] Therefore, the bicyclo[6.1.0]nonyne (BCN) group, which was not compatible with tetrazines, was replaced with the more bulky aza-dibenzocyclooctyne (DBCO) (*Figure 1*).[14–16]

On the basis of these considerations, RAFT scaffolds **1** and **2**, equipped with three orthogonal chemoselective handles to create TLR1/2-7-9 triagonists with the ligands in different orientations were selected as targets (*Figure 1*). The cyclic decapeptide gramicidin S will serve as the basis for the scaffold and will be suitably modified to incorporate three different amino-groups for functionalization. Gramicidin S adopts an antiparallel β sheet conformation which is closed by two type II′ β-turns and is highly stabilized by four intramolecular hydrogen bonds involving the backbone.[17] This conformational restraint presents two separate spatial domains with residues 3-5-8-10 oriented in the lower plane and residues 4-9 in the opposite plane (*Figure 1*).[18] Asano and co-workers showed that the secondary structure is not perturbed by substitution of the ornithine residues with leucine residues proving the conformation is rigid and allows for shuffling of amino acid residues 3-4-5 and 8-9-10 and helps accommodating three functionalization handles in different orientation.[19] The positioning of the handles in scaffold **2** allows for the largest possible distance between the three different ligands. In turn, scaffold **1** has two of the three attachments points at the same face of the macrocycle and one at the opposite face. To attach the TLR-agonists to scaffolds **1** and **2**, TLR7 and TLR9 ligands will be equipped with a tetrazine and in the case of TLR9 agonist this will be achieved by an adapter molecule. These functionalized ligands combined with the ones described in the previous Chapter make possible two different combinations for scaffold **1** with either the TLR7 agonist or the TLR9 ligand being the lone ligand in the plane giving a total of three different scaffolds with the inclusion of scaffold **2**.

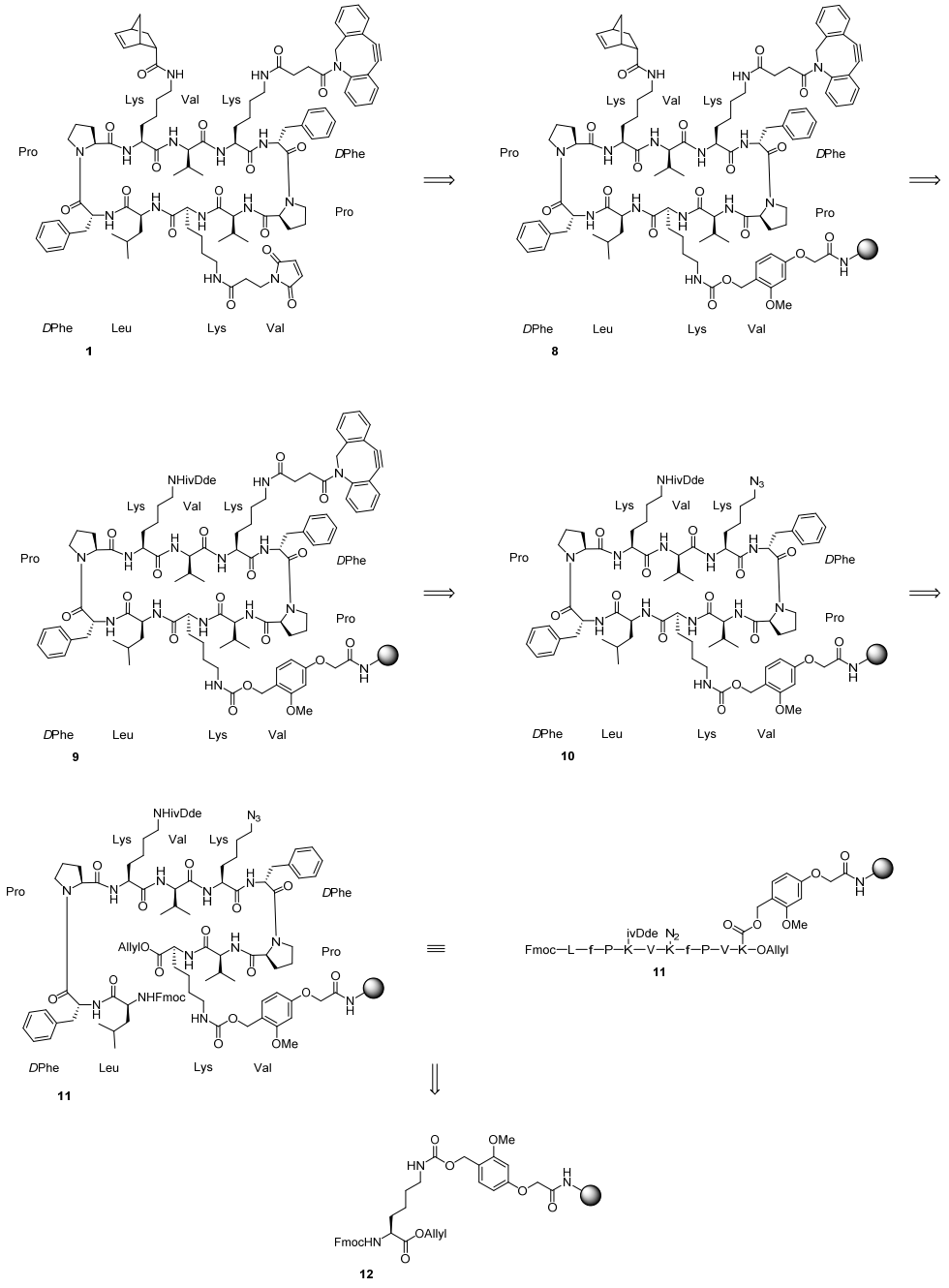

Figure 2. Retrosynthesis of RAFT scaffold **1** with three chemoselective handles.

The synthesis of RAFT scaffold **1**, and in a similar manner **2**, was envisioned to start from the TentaGel S Ac resin, allowing weakly acidic cleavage mixtures at the end of the assembly (*Figure 2*). With the procedure described in Chapter 2 and expanded in Chapter 3, the ε-amine of lysine will be attached to the resin to give functionalized resin **12**. Using an automated solid-phase peptide synthesis strategy, linear peptide **11** will be synthesized bearing four different protecting groups, which each can be removed orthogonally in the presence of the other three and the linker. To complement the allyl-, Fmoc- and azido-group, the ivDde moiety will be used as the fourth protecting group as it can be removed by treatment with hydrazine and is able to withstand Fmoc deprotection conditions. The α,β-unsaturated ketone present in the ivDde group reacts with hydrazine to form a pyrazole ring liberating the amino-group in the process.[20,21] Of the four protecting groups present, first the allyl-group will be removed using palladium(0) tetrakis(triphenylphosphine) and phenylsilane, after which the Fmoc is deprotected and the peptide cyclized with PyBOP as the condensing agent to furnish cyclic peptide **10**. The azide will then be reduced *via* a Staudinger reduction using trimethylphosphine and functionalized with a DBCO-group. The ivDde moiety will be removed with a solution of hydrazine in DMF to liberate the amine, which will then be functionalized with a norbornene moiety to give peptide **8**. The penultimate step will involve treatment of the resin to a mixture of TFA and DCM (1:199, TFA – DCM) to cleave the peptide off of the resin. Finally, the maleimide moiety will be installed to afford RAFT scaffold **1**.

Results and discussion

With the inclusion of the tetrazine/norbornene ligation as part of the triple RAFT scaffold, TLR ligands equipped with a tetrazine had to be synthesized. First, the synthesis of functionalized TLR7 ligand **6** was undertaken (*Scheme 1*).

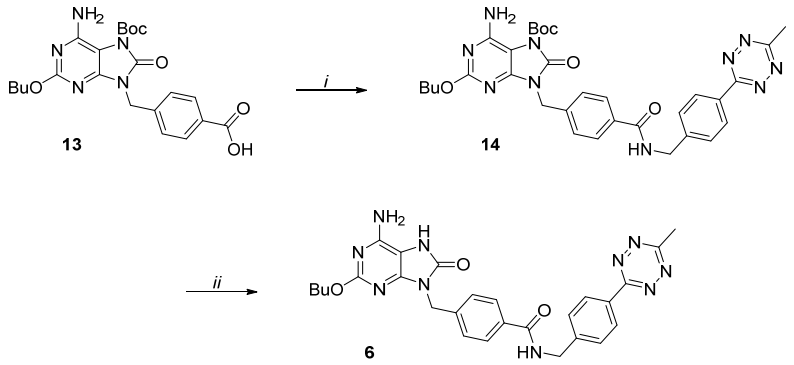

Scheme 1. Reagents and conditions: (*i*) (4-(6-methyl-1,2,4,5-tetrazin-3-yl)phenyl)methanamine hydrochloride, DIC, *N*-methylmorpholine, DCM, DMF, rt, 19 hrs, 18% (*ii*) TFA, DCM, rt, 3 hrs, quant.

The carboxylic acid in known TLR7 ligand derivative **13** (see Chapter 3) was activated by treatment with diisopropylcarbodiimide (DIC) and *N*-methylmorpholine in a DCM for one hour, followed by dropwise addition of a solution of (4-(6-methyl-1,2,4,5-tetrazin-3-yl)phenyl)methanamine hydrochloride in a mixture of DCM and DMF (1:1, DCM – DMF) to afford, after stirring for 19 hours, tetrazine **14** in 18% yield. To remove the Boc-group, a mixture of trifluoroacetic acid and DCM (1:2, TFA – DCM) was added to tetrazine **14** and the reaction was stirred for three hours to give TLR7 ligand **6** equipped with a tetrazine in a quantitative yield.

TLR9 ligand is an oligonucleotide provided with a linker functionalized with a thiol-group (*Figure 1*). To equip TLR9 ligand with a tetrazine, adapter molecule **7** was designed featuring an iodoacetamide group complementary with the thiol-group (*Scheme 2*).

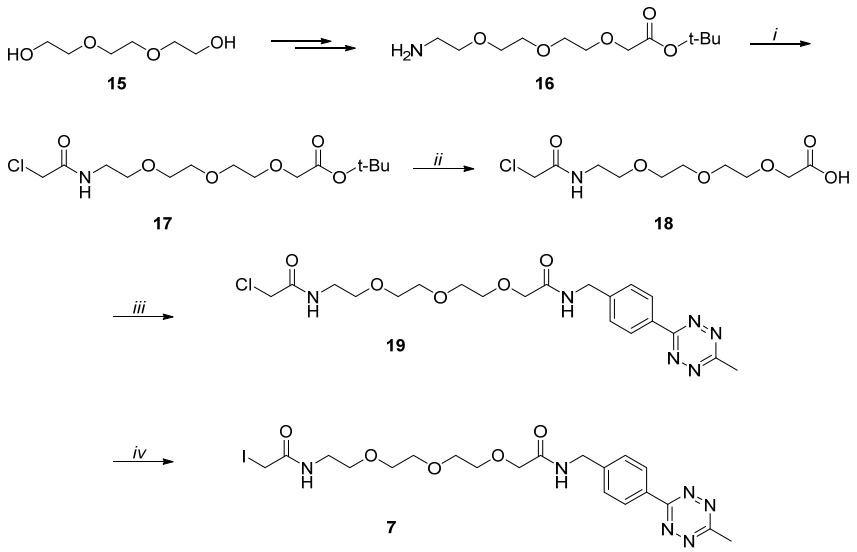

Scheme 2. Reagents and conditions: (*i*) chloroacetyl chloride, Et_3N, DCM, 0 °C, 2hrs, 44% (*ii*) TFA, DCM, rt, 17 hrs, quant. (*iii*) (4-(6-methyl-1,2,4,5-tetrazin-3-yl)phenyl)methanamine hydrochloride, DIC, *N*-methylmorpholine, DCM, DMF, rt, 19 hrs, 41% (*iv*) NaI, acetone, rt, 48 hrs, 73%.

To start, triethylene glycol **15** was transformed into amine **16** in four steps as described in Chapter 5. The amine was then dissolved in DCM after which Et_3N was added and the mixture cooled to 0 °C. Chloroacetyl chloride was added dropwise and the reaction was stirred for two hours at 0 °C to give chloroacetamide **17** in a yield of 44%. Next, the *tert*-butyl ester was removed by treatment with 10% (v/v) TFA in DCM for 17 hours to obtain carboxylic acid **18** in a quantitative yield. Carboxylic acid **18** was activated *in situ* with DIC and *N*-methylmorpholine for one hour after which a solution of (4-(6-methyl-1,2,4,5-tetrazin-3-yl)phenyl)methanamine hydrochloride in a mixture of DCM and DMF (1:1, DCM – DMF) was added dropwise to the reaction mixture. The resulting solution was stirred for 19 hours and tetrazine **19** was obtained in a yield of 41%. Finally, chloroacetamide **19** was converted into the corresponding iodoacetamide using the classic Finkelstein reaction with sodium iodide in acetone to give adapter molecule **7** in a 73% yield.[22]

The assembly of RAFT scaffold **1**, having a bulky cyclooctyne moiety incorporated, requires the availability of aza-dibenzocyclooctyne **27**, the synthesis of which is depicted in *Scheme 3*.

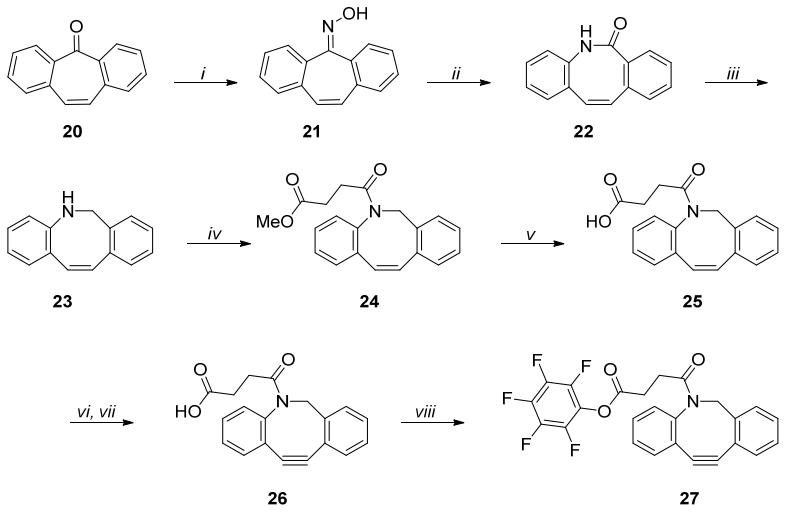

Scheme 3. Reagents and conditions: (*i*) hydroxylamine hydrochloride, pyridine, EtOH, reflux, 17 hrs, 98% (*ii*) Eaton's reagent, 100 °C, 30 min, 87% (*iii*) $LiAlH_4$, Et_2O, reflux, 19 hrs, 75% (*iv*) methyl 4-chloro-4-oxobutyrate, Et_3N, DCM, 0 °C to rt, 90 min, 68% (*v*) lithium hydroxide monohydrate, MeOH, H_2O, reflux, 20 hrs, 98% (*vi*) Br_2, DCM, 0 °C, 2 hrs (*vii*) KO^{t}Bu, THF, -45 °C, 4 hrs (*viii*) pentafluorophenol, DIC, *N*-methylmorpholine, DCM, rt, 18 hrs, 33% over 3 steps.

Although several syntheses have been reported for carboxylic acid **26**, it was decided to employ the procedure described by the group of Adronov who optimized the synthetic route for scaling up.[14,23,24] The synthesis started from 5-dibenzosuberenone **20** which was converted into oxime **21** by refluxing a solution of the ketone and hydroxylamine hydrochloride in a mixture of pyridine and ethanol. A Beckmann rearrangement was then performed at 100 °C promoted by Eaton's reagent (7.7 wt% P_2O_5 in methanesulfonic acid) to furnish lactam **22** in 87% yield. The amide was then reduced using lithium aluminium hydride in refluxing ether to give amine **23**, which was then acylated with methyl-4-chloro-4-oxobutyrate to obtain amide **24**. Afterwards, saponification of methyl ester **24** was achieved in near quantitative yield by refluxing the ester with lithium hydroxide monohydrate in a mixture of methanol and water for 20 hours. The synthesis of alkyne **26** was then realized by bromination of alkene **25** at 0 °C for two hours followed by a double elimination with potassium *tert*-butoxide at -45 °C for four hours. Lastly, carboxylic acid **26** was condensed with pentafluorophenol using DIC as the activator and *N*-methylmorpholine as the base to give activated ester **27** in 33% yield over three steps.

With the necessary building blocks in hand, the synthesis of RAFT scaffold **1** was explored (*Scheme 4*).

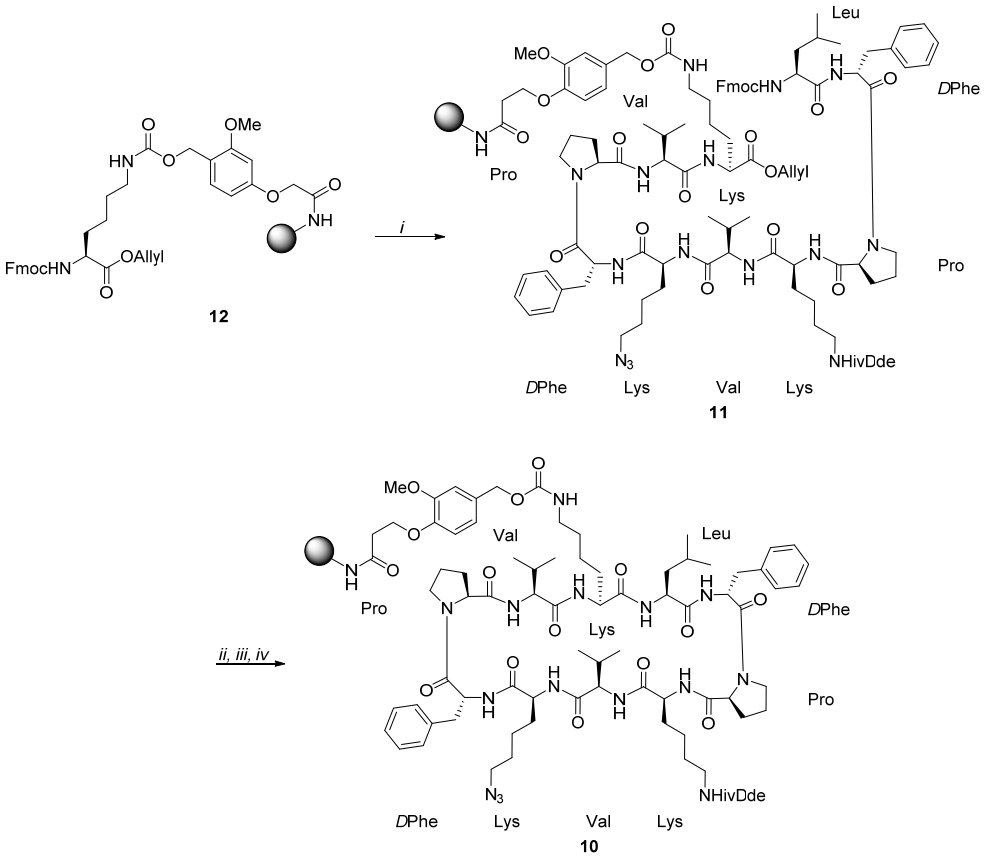

Scheme 4. Reagents and conditions: (*i*) SPPS: (a) piperidine, DMF, rt, 2x3 min. (b) Fmoc-AA-OH, HCTU, DIPEA, DMF, rt, 1 hr (c) Ac_2O, DMF, rt, 2x3 min. (*ii*) $Pd(PPh_3)_4$, $PhSiH_3$, DCM, DMF, rt, 1.5 hrs (*iii*) piperidine, DMF, rt, 2x10 min. (*iv*) benzotriazole-1-yl-oxy-tris-pyrrolidino-phosphonium hexafluorophosphate, 1-hydroxybenzotriazole hydrate, *N*-methylmorpholine, DMF, rt, 2.5 hrs.

After synthesizing side-chain functionalized resin **12**, as described in Chapter 3, the peptide chain was elongated using a Protein Technologies Tribute automated peptide synthesizer, entailing nine peptide coupling cycles. Each cycle started with two treatments of 20% (v/v) piperidine in DMF for three minutes followed by a series of washing steps to remove residual amounts of piperidine. The liberated N-terminus was then coupled to the appropriate standard Fmoc building block using HCTU and DIPEA, except for the lysine residues which were equipped with the 1-(4,4-dimethyl-2,6-dioxocyclohex-1-ylidene)-3-methylbutyl (ivDde) group or with the ε-amine masked as an azide. For the coupling the resin was shaken an hour at room temperature which was followed by capping of the unreacted amines by

subjecting the resin to two treatments of 10% (v/v) Ac_2O in DMF for three minutes. After nine cycles, resin-bound linear peptide **11** was obtained after which the synthesis was continued manually. Deallylation was achieved by treatment with $Pd(PPh_3)_4$ and phenylsilane for 90 minutes which was followed by deprotection of the Fmoc group using 20% (v/v) piperidine in DMF for 2x10 minutes. With the N- and C-termini liberated, the peptide was cyclized with PyBOP acting as the condensing agent and *N*-methylmorpholine as base to afford cyclic decapeptide **10**. Cleavage of the crude peptide off the resin and subsequent analysis by LC-MS showed the formation of the cyclic decapeptide **10** alongside substantial amount of side products, indicating a low overall yield as the deprotection and functionalization stage have yet to follow. Although ivDde is more resistant towards piperidine than the original Dde group, side product formation with the ivDde group has been reported before.[25] Even with the deliberate choice to introduce the ivDde group at the last possible position to limit the exposure to piperidine proved not to be sufficient enough to suppress the side-reactions. Therefore, it was decided to substitute the ivDde group and protect the amine as the trifluoroacetamide (*Scheme 5*).

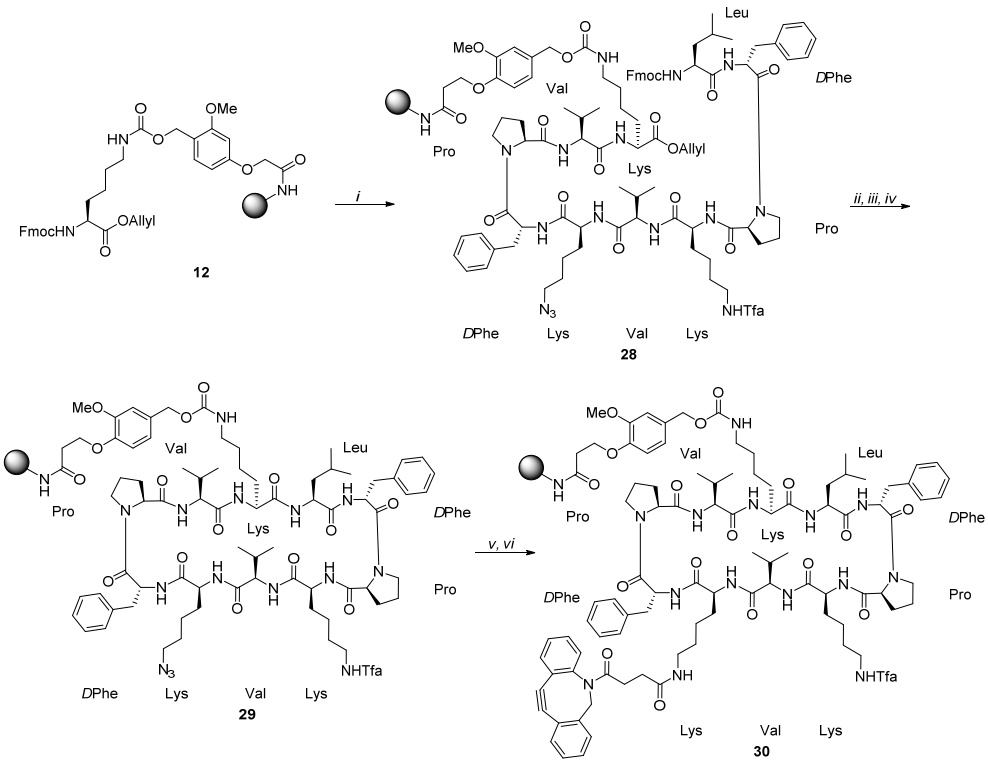

Scheme 5. Reagents and conditions: (*i*) SPPS: (a) piperidine, DMF, 90 °C, 2x90 sec (b) Fmoc-AA-OH, DIC, Oxyma Pure, DMF, 90 °C, 2 min. (*ii*) $Pd(PPh_3)_4$, $PhSiH_3$, DCM, DMF, rt, 1.5 hrs (*iii*) piperidine, DMF, rt, 2x10 min. (*iv*) benzotriazole-1-yl-oxy-tris-pyrrolidino-phosphonium hexafluorophosphate, 1-hydroxybenzotriazole hydrate, *N*-methylmorpholine, DMF, rt, 2.5 hrs (*v*) PMe_3, toluene, 1,4-dioxane, rt, 2 hrs, then H_2O, rt, 4 hrs (*vi*) **27**, DIPEA, DMF, rt, 72 hrs.

This time elongation of the peptide was performed using a CEM Liberty Blue microwave peptide synthesizer with nine peptide coupling cycles. First, the Fmoc was deprotected with two treatments of 20% (v/v) piperidine in DMF at 90 °C for 90 seconds. The resin was then washed twice with DMF before the liberated N-terminus was coupled to the appropriate standard Fmoc building block using DIC and Oxyma Pure, except for the lysine residues which were equipped with the trifluoroacetyl (Tfa) group or with the ε-amine masked as an azide. The coupling was conducted at 90 °C for two minutes. Nine such cycles furnished linear peptide **28** after which the synthesis was continued manually as before to afford cyclized peptide **29**. LC-MS analysis of the crude peptide after cleavage showed the presence of the desired cyclic peptide without significant side products. Next, the azide was reduced by treating the resin with an excess of PMe_3 (1.0 M in toluene) diluted in

1,4-dioxane for two hours after which H_2O was added and the mixture shaken for an additional four hours. The liberated amine was then functionalized with building block **27** using DIPEA to afford peptide **30** after 72 hours as observed by LC-MS analysis of the crude peptide after cleavage. Next the deprotection of the trifluoroacetamide was explored using various conditions (*Table 1*).

Table 1. Screening of conditions for the deprotection of the trifluoroacetamide group.[a]

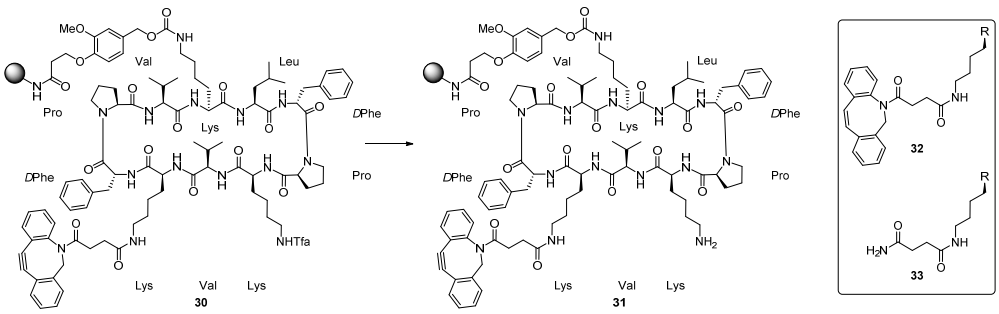

Entry	Reagent	Equivalents	Solvent	Reaction time	Product
1	–	–	0.50 M NH_3 in 1,4-dioxane	17 hours	**30**
2	25 wt% NaOMe in MeOH	5	DCM	1 hour	–[b]
3	$NaBH_4$	10	1:1, THF – EtOH –	30 min.	**32**
4	–	–	7.0 M NH_3 in MeOH	17 hours	**30/31/33**

[a] Reactions were performed at a 25 μmol scale after which the peptide was cleaved from the resin and analyzed by LC-MS. [b] No significant product could be detected.

First, 0.50 M NH_3 in dioxane was added and the resin was shaken for 17 hours. The suspension was filtered and the resin was washed with 1,4-dioxane, MeOH and DCM. The crude peptide was then cleaved off of the resin with ten treatments of 0.5% (v/v) TFA in DCM for two minutes with a filtration after each treatment. Analysis of the filtrate by LC-MS showed that the trifluoroacetamide was still intact (*Entry 1*). Next, a solution-phase procedure for Tfa deprotection reported by Snider *et al.* was tried (*Entry 2*).[26] This reaction employs sodium methoxide in methanol for the deprotection in combination with DCM as the solvent which would swell the resin significantly compared to the more polar dioxane and methanol. However, after treatment of the resin with NaOMe in DCM for one-hour LC-MS spectroscopic analysis showed apart from numerous byproducts no significant peak for either the product or starting material. Lokey and co-workers reported the quantitative

removal of the Tfa group on-resin in 30 minutes using sodium borohydride in a mixture of THF and ethanol (1:1, THF – EtOH).[27] However, employing this method did not lead to removal of the Tfa group (*Entry 3*). Instead, LC-MS analysis showed a peak with a mass two dalton higher than the mass corresponding to starting material **30** as the major product suggesting a partial reduction of the alkyne to alkene **32** had taken place. Alcohols have been shown to reduce strained alkynes.[28,29] Lastly, a solution of 7.0 M NH_3 in methanol was tried hoping that with a higher concentration of ammonia the trifluoroacetamide could be removed (*Entry 4*). After 17 hours, the crude peptide was analyzed and showed that starting material **30** and product **31** were present on the resin indicating that a partial Tfa removal had occurred. However, two other major products were detected that corresponded with the substitution of the strained cycoalkyne with ammonia (**33**) with and without Tfa deprotection. The incompatibility of the cyclooctyne with NH_3-mediated Tfa removal, urged to find out whether the order of deprotection could be reversed (Tfa removal before azide reduction) and the Tfa removal could be driven to completion with longer reaction times and/or microwave irradiation. Indeed, when peptide **29** was treated with 7.0 M NH_3 in methanol for 12 hours using microwave irradiation complete deprotection was observed (*Scheme 6*).

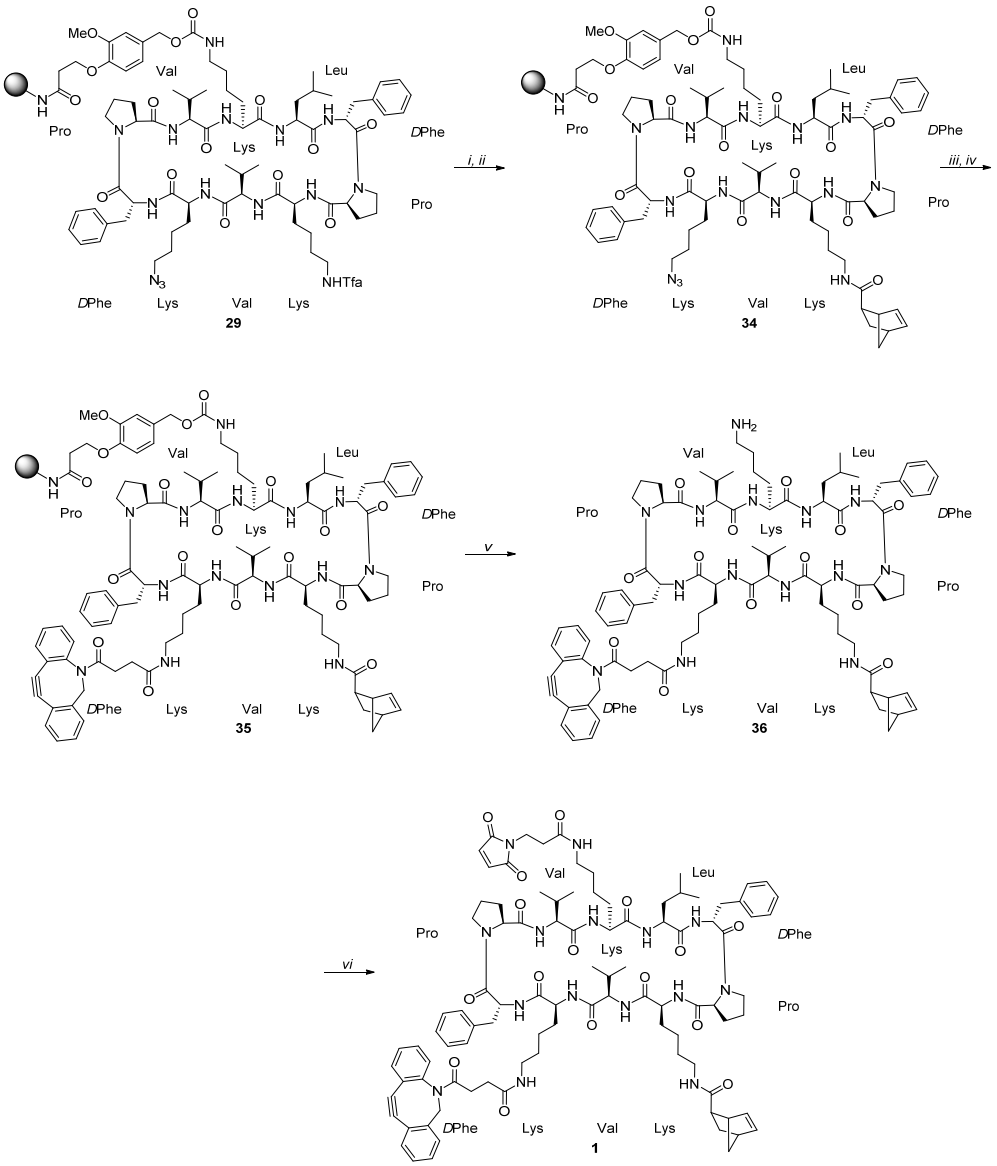

Scheme 6. Reagents and conditions: (*i*) NH_3, MeOH, μw, 90 °C, 12 hrs (*ii*) 5-norbornene carboxylic acid NHS ester, DIPEA, DMF, rt, 19 hrs (*iii*) PMe_3, toluene, 1,4-dioxane, rt, 2 hrs, then H_2O, rt, 4 hrs (*iv*) **27**, DIPEA, DMF, rt, 72 hrs (*v*) TFA – DCM (1:199), rt, 10x2 min (*vi*) 3-maleimidopropionic acid NHS ester, DIPEA, DMF, rt, 4 hrs.

After deprotection of the Tfa protection, the liberated amine was functionalized using 5-norbornene carboxylic acid NHS ester (4:1, endo – exo) and DIPEA. After 19 hours the peptide was cleaved off of the resin and analyzed by LC-MS to indicate

complete conversion to peptide **34** and the minor exo-stereoisomer. Afterwards, the resin was treated with an excess of PMe_3 (1.0 M in toluene) diluted in 1,4-dioxane for two hours after which H_2O was added and the resin shaken for four hours. Cleavage of the peptide and LC-MS analysis showed a complete and clean conversion to the amine. The amine was then reacted with DBCO building block **27** and DIPEA for 72 hours giving peptide **35** with no observable starting material. The peptide was cleaved from the resin with ten treatments of 0.5% (v/v) TFA in DCM for two minutes with a filtration after each treatment. The TFA present in the filtrate was immediately neutralized with the basic ion-exchange resin Amberlyst A-21. Filtration and subsequent concentration afforded crude peptide **36**. The crude peptide was taken up in DMF and reacted with 3-maleimidopropionic acid NHS ester and DIPEA for four hours. The reaction mixture was concentrated *in vacuo* and purified by RP-HPLC. Lyophilization of the pure fractions afforded RAFT scaffold **1** in 2.3% yield bearing three different chemoselective handles.

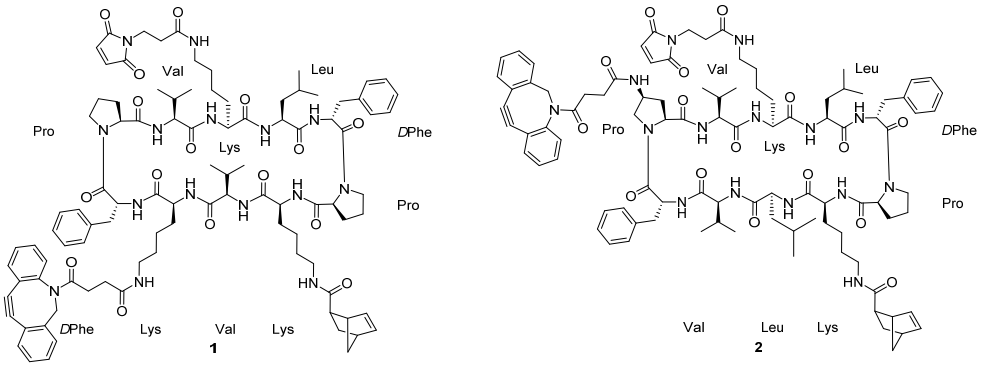

Scheme 7. RAFT scaffolds **1** and **2** bearing three chemoselective handles in different orientations.

Employing the cis-Fmoc-(2*S*, 4*S*)-4-azidoproline in the linear peptide synthesis instead of a regular proline allowed for the synthesis of RAFT scaffold **2**. RAFT scaffold **2** was synthesized in 3.3% yield using the same procedure as described for scaffold **1**. These two scaffolds in combination with the TLR ligands synthesized give rise to three different orientations of TLR ligands depending on the manner of attachment. The synthesis of these TLR1/2-7-9 constructs should be the focus going forward.

Conclusion

Recent studies reveal the importance of engaging multiple TLRs simultaneously to the immune response. Gilkes *et al.* showed that the spatial organization of TLR constructs can shape immune responses toward desired outcomes. The research outlined in this Chapter was aimed toward synthesizing a RAFT scaffold, able to accommodate three different TLR ligands in different orientations, to study the effect on the immune response. The scaffolds, allowing the adhering of two ligands, as described in Chapter 3 were expanded with a norbornene/tetrazine ligation to accommodate a third TLR ligand. The inclusion of this ligation method prompted a change in cyclooctyne from BCN to DBCO to achieve mutual orthogonality. Therefore, a DBCO building block was synthesized. The synthesis of the RAFT scaffolds was first attempted with ivDde as the additional amino protecting group. However, the purity of the cyclic peptide carrying this group was insufficient and a switch was made to trifluoroacetamide (Tfa) as the protecting group of choice. Various conditions were tried to deprotect this group on-resin and a clean conversion was shown by treating the resin with 7.0 M NH_3 in methanol under microwave irradiation for 12 hours. RAFT scaffolds **1** and **2** were ultimately obtained bearing three different chemoselective handles. To functionalize these scaffolds, a TLR7 ligand equipped with a tetrazine was synthesized as well as an adapter molecule to fit the TLR9 ligand with a tetrazine. The ligation of these TLR ligands to the scaffolds should be the focus in the future.

General information

Materials, reactions and purification

Standard Fmoc-amino acids and resins for solid-phase peptide synthesis (SPPS), amino acids for solution-phase synthesis and peptide coupling reagents 2-(6-chloro-1*H*-benzotriazole-1-yl)-1,1,3,3-tetramethyluronium hexafluorophosphate (HCTU), *N*,*N*'-diisopropylcarbodiimide (DIC), 1-ethyl-3-(3-dimethylaminopropyl) carbodiimide hydrochloride (EDC), ethyl cyano(hydroxyimino)acetate (Oxyma Pure) and 1-hydroxybenzotriazole (HOBt) were purchased from Novabiochem or Sigma-Aldrich. (4-(6-Methyl-1,2,4,5-tetrazin-3-yl)phenyl)methanamine hydrochloride was purchased from Click Chemistry Tools. Fmoc-L-Lys(N_2)-OH and Fmoc L-Lys(TFA)-OH were purchased from Iris Biotech. 4-((6-Amino-2-butoxy-7-(tert-butoxycarbonyl)-8-oxo-7,8-dihydro-9*H*-purin-9-yl)methyl)benzoic acid, 2-(6-methyl-1,2,4,5-tetrazin-3-yl)ethan-1-amine hydrochloride and 3-maleimidopropionic acid *N*-hydroxysuccinimidyl ester were available in-house.The resin TentaGel S AC (0.23 mmol/g) was bought from Rapp Polymere. All other chemicals were purchased from Acros, Sigma Aldrich, VWR, Fluka, Merck and Fisher Scientific and used as received unless stated otherwise. Tetrahydrofuran (THF), *N*,*N*-dimethylformamide (DMF), dichloromethane (DCM), 1,4-dioxane and toluene were stored over molecular sieves before use. Commercially available ACS grade solvents were used for column chromatography without any further purification, except for toluene and ethyl acetate which were distilled prior to use. All reactions were carried out under a nitrogen atmosphere, unless indicated otherwise. Reaction progress and chromatography fractions were monitored by thin layer chromatography (TLC) on silica-gel-coated aluminium sheets with a F254 fluorescent indicator purchased from Merck (Silica gel 60 F_{254}). Visualization was achieved by UV absorption by fluorescence quenching, permanganate stain (4 g $KMnO_4$ and 2 g K_2CO_3 in 200 mL of H_2O), ninhydrin stain (0.6 g ninhydrin and 10 mL acetic acid in 200 mL ethanol). Silica gel column chromatography was performed using Screening Devices silica gel 60 (particle size of 40 – 63 μm, pore diameter of 60 Å) with the indicated eluent. Analytical reversed-phase high-performance liquid chromatography (RP-HPLC) was performed on a Thermo Finnigan Surveyor HPLC system with a Phenomenex Gemini C_{18} column (4.6 mm x 50 mm, 3 μm particle size) with a flow rate of 1 mL/min and a solvent gradient of 10-90% solvent B over 8 min coupled to a LCQ Advantage Max (Thermo Finnigan) ion-trap spectrometer (ESI^+). Preparative RP-HPLC was performed with a GX-281 Liquid Handler and a 331 and 332-H2 primary and secondary solvent pump respectively with a Phenomenex Gemini C_{18} or C_4 column (250 x 10.0 mm, 3 μm particle size) with a flow rate of 5 mL/min and solvent gradients as described for each compound. HPLC solvent compositions: solvent A is 0.1% (v/v) TFA in H_2O; solvent B is MeCN. Preparative RP-HPLC was also performed on an Agilent 1200 HPLC system coupled to a 6130 Quadrupole Mass Spectrometer using a Nucleodur C_{18} Gravity column (250 x 10.0 mm, 5 μm particle size) with a flow rate of 5 mL/min and a gradient over 12 min. as described for each compound. HPLC solvent composition: solvent A is 0.2% (v/v) TFA in H_2O and solvent B is MeCN. All HPLC solvents were filtered with a Millipore filtration system equipped with a 0.22 μm nylon membrane filter prior to use.

Characterization

Nuclear magnetic resonance (^1H and ^{13}C APT NMR) spectra were recorded on a Brüker DPX-300, Brüker AV-400, Brüker DMX-400, Brüker AV-500 or Brüker DMX-600 in the given solvent. Chemical shifts are reported in parts per million (ppm) with the residual solvent or tetramethylsilane (0 ppm) as reference. High-resolution mass spectrometry (HRMS) analysis was performed with a Thermo Finnigan LTQ Orbitrap mass spectrometer equipped with an electronspray ion source in positive mode (source voltage 3.5 kV, sheath gas flow 10 ml/min, capillary temperature 250 °C) with resolution R = 60000 at m/z 400 (mass range m/z = 150 – 2000) and dioctyl phthalate (m/z = 391.28428) as a "lock mass". The high-resolution mass spectrometer was calibrated prior to measurements with a Thermo Finnigan calibration mixture. Nominal and exact m/z values are reported in daltons.

Solid-phase peptide synthesis

General methodology

Manual solid-phase peptide synthesis

Manual amino acid couplings were carried out using a fritted reaction syringe equipped with a plunger and syringe cap or a manual reaction vessel (SHG-20260-PI, 60 mL) purchased from Peptides International. The syringe was shaken using either a Heidolph Multi Reax vortexer set at 1000 rpm or a St. John Associates 180° Flask Shaker (model no. A5-6027).

Fmoc deprotection was achieved by agitating the resin with 20% (v/v) piperidine in DMF (2 x 10 min.). After draining the reaction vessel, the resin was washed with DMF (6 x 30 sec.). The appropriately side-chain protected Fmoc-amino acid (5.0 equiv.) in DMF (5.0 mL) was pre-activated with HCTU (5.0 equiv.) and DIPEA (10 equiv.) for 5 min, then added to resin and agitated for 60 min. After draining the reaction vessel, the resin was washed with DMF (4 x 30 sec.). The completion of all couplings was assessed by a Kaiser test and double coupling was performed as needed.

Automated solid-phase peptide synthesis

The automated peptide coupling was performed on a CEM Liberty Blue microwave peptide synthesizer or a Protein Technologies Tribute peptide synthesizer using standard Fmoc protected amino acids. For the Tribute peptide synthesizer, amino acids were presented as solids and 0.20 M HCTU in DMF was used as activator, 0.50 M DIPEA in DMF as the activator base, 20% (v/v) piperidine in DMF as the deprotection agent and a 90:10, DMF – Ac_2O mixture as the capping agent. Coupling of each amino acid occurred at room temperature for 1 hr followed by a capping step (2x 3 min.) betwixt two washing steps. Subsequently, Fmoc was deprotected using the deprotection agent (2x 3 min.) followed by two more washing steps. For the Liberty Blue microwave synthesizer, amino acids were presented as a solution (0.20 M in DMF) and 0.50 M DIC in DMF was used as activator, 1.0 M Oxyma Pure in DMF as additive and 20% (v/v) piperidine in DMF as the deprotection agent. Amino acid coupling in the microwave synthesizer occurred at 90 °C for 2 min. followed by Fmoc deprotection at 90 °C using the aforementioned deprotection agent (2x 90 sec.) and two washing steps.

Loading calculation

Resin was dried before loading calculation by washing with DCM (3x 30 sec.) and Et_2O (3x 30 sec.) followed by purging with N_2. A small amount of resin (5 – 10 mg) was weighed and DMF (0.80 mL) was added and the resin was swollen for 20 min. Piperidine (0.20 mL) was then added and shaken for 20 min. Following the deprotection, the suspension was filtered and diluted with 20% (v/v) piperidine in DMF to a total volume of 10 mL in a volumetric flask. The absorption of this solution was measured against a blank 20% (v/v) piperidine in DMF solution using a Shimadzu UV-1601 UV-VIS spectrometer with a Quartz cuvette (optical pathway = 1 cm). The loading was then calculated using the following equation:

$$\text{Loading}_{\text{resin}} = \frac{A_{301.0\text{ nm}} * 10^6\ \text{mmol mol}^{-1}\ \text{mg g}^{-1} * V * D}{\varepsilon_{301.0\text{ nm}} *\ m_{\text{resin}} * l}$$

where:

$\text{Loading}_{\text{resin}}$ = Fmoc substitution in mmol/g
$A_{301.0\text{ nm}}$ = Absorption of sample at 301.0 nm
10^6 mmol mol^{-1} mg g^{-1} = Conversion factor of mmol to mol and mg^{-1} to g^{-1}
V = Total volume in L
D = Dilution factor
$\varepsilon_{301.0\text{ nm}}$ = Molar absorption coefficient at 301.0 nm (8021 L mol^{-1} cm^{-1})
m_{resin} = sample weight of the resin in mg
l = optical path length of the cell in cm

5*H*-dibenzo[*a,d*][7]annulen-5-one oxime

To a solution of dibenzosuberenone **20** (5.2 g, 25 mmol, 1.0 equiv.) in ethanol (63 mL, 0.40 M) was added hydroxylamine hydrochloride (8.7 g, 0.13 mol, 5.0 equiv.) and pyridine (14 mL, 0.17 mol, 6.7 equiv.). The mixture was heated to reflux and stirred for 17 hrs. DCM was added and the organic layer was washed with 1.0 M aq. HCl (3x) and brine. The organic phase was dried ($MgSO_4$), filtered and concentrated *in vacuo* to afford **21** (5.4 g, 24 mmol, 98%) as a light brown solid.

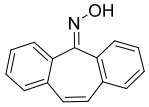

21

^{1}H NMR (400 MHz, $CDCl_3$) δ 9.07 (br s, 1H, O*H*), 7.70 – 7.62 (m, 1H, C*H*-arom), 7.62 – 7.53 (m, 1H, C*H*-arom), 7.47 – 7.35 (m, 6H, C*H*-arom), 6.90 (d, *J* = 2.9 Hz, 2H, C*H*-cycloheptene).

^{13}C NMR (101 MHz, $CDCl_3$) δ 156.7 (*C*q-oxime), 135.4 (*C*q-arom), 134.6 (*C*q-arom), 133.8 (*C*q-arom), 130.8 (*C*H-cycloheptene), 130.7 (*C*H-cycloheptene), 130.5 (*C*q-arom), 129.5 (*C*H-arom), 129.2 (*C*H-arom), 129.1 (*C*H-arom), 129.0 (*C*H-arom), 128.9 (*C*H-arom), 127.8 (*C*H-arom), 127.7 (*C*H-arom).

HRMS (ESI-Orbitrap) calcd. for $C_{15}H_{12}NO$ $[M+H]^+$ 222.09134, found 222.09112.

(*Z*)-dibenzo[*b,f*]azocin-6(5*H*)-one

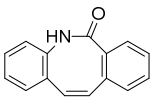

22

To oxime **21** (5.3 g, 24 mmol, 1.0 equiv.) was added Eaton's reagent (32 mL, 0.75 M). The solution turned dark red and was heated to 100 °C. After 30 min of stirring, the reaction was quenched by the addition of H_2O. After the mixture was cooled to ca. 70 °C, the product was extracted with hot EtOAc (5x). The pooled organic fractions was evaporated at 70 °C to a volume of ca. 20 mL and cooled to rt. After filtration, amide **22** (4.6 g, 21 mmol, 87%) was obtained as a brown solid.

^{1}H NMR (500 MHz, $CDCl_3$) δ 8.07 (s, 1H, N*H*), 7.48 (dd, *J* = 7.7, 1.5 Hz, 1H, C*H*-arom), 7.32 (td, *J* = 7.5, 1.5 Hz, 1H, C*H*-arom), 7.28 – 7.24 (m, 1H, C*H*-arom), 7.23 – 7.11 (m, 4H, C*H*-arom), 7.09 – 7.04 (m, 1H, C*H*-arom), 6.96 (d, *J* = 11.7 Hz, 1H, C*H*-cyclooctene), 6.85 (d, *J* = 11.6 Hz, 1H, C*H*-cyclooctene).

^{13}C NMR (126 MHz, $CDCl_3$) δ 174.0 (NHC=O), 135.2 (*C*q-arom), 135.1 (*C*q-arom), 134.3 (*C*q-arom), 134.3 (*C*q-arom), 133.1 (*C*H-cyclooctene), 129.9 (*C*H-cyclooctene), 129.9 (*C*H-arom), 129.3 (*C*H-arom), 128.4 (*C*H-arom), 128.3 (*C*H-arom), 127.8 (*C*H-arom), 127.3 (*C*H-arom), 126.4 (*C*H-arom).

HRMS (ESI-Orbitrap) calcd. for $C_{15}H_{12}NO$ $[M+H]^+$ 222.09134, found 222.09125.

(*Z*)-5,6-dihydrodibenzo[*b,f*]azocine

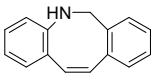

23

Et_2O (35 mL, 0.39 M) was slowly added to a mixture of amide **22** (3.0 g, 14 mmol, 1.0 equiv.) and lithium aluminium hydride (10 g, 0.27 mol, 20 equiv.). The mixture was heated to reflux and stirred for 19 hrs. DCM was added and the mixture was cooled to 0 °C. H_2O was added dropwise until the lithium aluminium hydride was quenched. The suspension was filtered over Celite and washed with DCM and H_2O. The organic layer was separated, dried ($MgSO_4$), filtered and concentrated *in vacuo* to give amine **23** (2.1 g, 10 mmol, 75%) as a yellow foam.

^{1}H NMR (500 MHz, $CDCl_3$) δ 7.26 – 7.23 (m, 1H, C*H*-arom), 7.20 – 7.11 (m, 3H, C*H*-arom), 6.96 (dd, *J* = 7.9, 1.6 Hz, 1H, C*H*-arom), 6.87 (ddd, *J* = 8.5, 7.1, 1.6 Hz, 1H, C*H*-arom), 6.59 (ddd, *J* = 7.7, 7.1, 1.2 Hz, 1H, C*H*-arom), 6.53 (d, *J* = 13.1 Hz, 1H, C*H*-cyclooctene), 6.45 (dd, *J* = 8.0, 1.2 Hz, 1H, C*H*-arom), 6.35 (d, *J* = 13.1 Hz, 1H, C*H*-cyclooctene), 4.57 (s, 2H, CH_2), 4.23 (br s, 1H, N*H*).

^{13}C NMR (126 MHz, $CDCl_3$) δ 147.2 (*C*q-arom), 139.3 (*C*q-arom), 138.3 (*C*q-arom), 134.8 (*C*H-arom), 132.9 (*C*H-cyclooctene), 130.3 (*C*H-arom), 129.0 (*C*H-arom), 128.1 (*C*H-arom), 127.8 (*C*H-arom), 127.5 (*C*H-arom), 127.5 (*C*H-cyclooctene), 121.9 (*C*q-arom), 118.1 (*C*H-arom), 117.8 (*C*H-arom), 49.7 (CH_2).

HRMS (ESI-Orbitrap) calcd. for $C_{15}H_{14}N$ $[M+H]^+$ 208.11208, found 208.11210.

methyl (*Z*)-4-(dibenzo[*b,f*]azocin-5(6*H*)-yl)-4-oxobutanoate

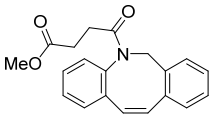

24

Amine **23** (2.0 g, 9.8 mmol, 1.0 equiv.) was dissolved in DCM (67 mL, 0.15 M). Et_3N (2.7 mL, 20 mmol, 2.0 equiv.) was added and the mixture was cooled to 0 °C. Methyl 4-chloro-4-oxobutyrate (1.8 mL, 15 mmol, 1.5 equiv.) was added dropwise over 30 min. The cooling bath was removed and the reaction was stirred at room temperature for 90 min. The solution was washed with 2.0 M aq. NaOH (3x), 2.0 M aq. HCl (3x) and brine. The organic fraction was dried ($MgSO_4$), filtered and concentrated under reduced pressure. Purification by silica gel column chromatography (1:4, EA – Pentane to 1:3, EA – Pentane) afforded methyl ester **24** (2.1 g, 6.7 mmol, 68%) as a white amorphous solid.

^{1}H NMR (500 MHz, $CDCl_3$) δ 7.28 – 7.25 (m, 5H, C*H*-arom), 7.20 – 7.08 (m, 3H, C*H*-arom), 6.79 (d, *J* = 12.9 Hz, 1H, C*H*-cyclooctene), 6.62 (d, *J* = 13.0 Hz, 1H, C*H*-cyclooctene), 5.52 (d, *J* = 15.1 Hz, 1H, CH_2), 4.26 (d, *J* = 15.1 Hz, 1H, CH_2), 3.62 (s, 3H, (C=O)OCH_3), 2.66 – 2.56 (m, 1H, CH_2(C=O)N), 2.51 – 2.38 (m, 2H, CH_2(C=O)N, CH_2(C=O)OMe), 2.06 – 1.96 (m, 1H, CH_2(C=O)OMe).

^{13}C NMR (126 MHz, $CDCl_3$) δ 173.6 (*C*=O), 171.0 (*C*=O), 140.7 (*C*q-arom), 136.6 (*C*q-arom), 136.0 (*C*q-arom), 134.7 (*C*q-arom), 132.8 (*C*H-cyclooctene), 132.0 (*C*H-arom), 131.0 (*C*H-arom), 130.3 (*C*H-arom), 128.7 (*C*H-arom), 128.4 (*C*H-arom), 128.2 (*C*H-arom), 127.5 (*C*H-arom), 127.4 (*C*H-arom), 127.1 (*C*H-cyclooctene), 54.6 (*C*H_2), 51.8 ((C=O)O*C*H_3), 29.7 (*C*H_2(C=O)OMe), 29.2 (*C*H_2(C=O)N).

HRMS (ESI-Orbitrap) calcd. for $C_{20}H_{20}NO_3$ $[M+H]^+$ 322.14377, found 322.14369.

(*Z*)-4-(dibenzo[*b*,*f*]azocin-5(6*H*)-yl)-4-oxobutanoic acid

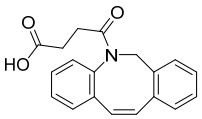

25

Methyl ester **24** (2.1 g, 6.6 mmol, 1.0 equiv.) was dissolved in a mixture of H_2O and methanol (2:1, MeOH – H_2O, 66 mL, 0.10 M). Lithium hydroxide monohydrate (1.7 g, 39 mmol, 6.0 equiv.) was added and the mixture was heated to reflux. The reaction was stirred for 20 hrs. 1.0 M aq. $NaHSO_4$ was added and the product was extracted with DCM (3x). The organic fractions were combined and washed with H_2O and brine. The organic layer was dried ($MgSO_4$), filtered and evaporated under reduced pressure to give carboxylic acid **25** (2.0 g, 6.4 mmol, 98%) as a white solid.

^{1}H NMR (500 MHz, $CDCl_3$) δ 7.32 – 7.21 (m, 5H, C*H*-arom), 7.20 – 7.09 (m, 3H, C*H*-arom), 6.80 (d, *J* = 12.8 Hz, 1H, C*H*-cyclooctene), 6.61 (d, *J* = 12.8 Hz, 1H, C*H*-cyclooctene), 5.52 (d, *J* = 15.1 Hz, 1H, CH_2), 4.29 (d, *J* = 15.1 Hz, 1H, CH_2), 2.61 (ddd, *J* = 16.8, 8.3, 5.4 Hz, 1H, CH_2(C=O)N), 2.51 (ddd, *J* = 16.8, 7.1, 5.3 Hz, 1H, CH_2(C=O)N), 2.41 (ddd, *J* = 17.0, 8.3, 5.3 Hz, 1H, CH_2(C=O)OH), 2.04 (ddd, *J* = 17.0, 7.1, 5.4 Hz, 1H, CH_2(C=O)OH).

^{13}C NMR (126 MHz, $CDCl_3$) δ 176.8 (*C*=O), 171.9 (*C*=O), 140.2 (*C*q-arom), 136.6 (*C*q-arom), 136.0 (*C*q-arom), 134.2 (*C*q-arom), 133.0 (*C*H-cyclooctene), 131.9 (*C*H-arom), 131.0 (*C*H-arom), 130.3 (*C*H-arom), 128.8 (*C*H-arom), 128.5 (*C*H-arom), 128.2 (*C*H-arom), 127.5 (*C*H-arom), 127.4 (*C*H-arom), 127.3 (*C*H-cyclooctene), 54.7 (*C*H_2), 29.8 (*C*H_2(C=O)OH), 29.7 (*C*H_2(C=O)N).

HRMS (ESI-Orbitrap) calcd. for $C_{19}H_{18}NO_3$ $[M+H]^+$ 308.12812, found 308.12801.

DIBAC-4-oxobutanoic acid

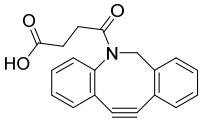

26

A solution of carboxylic acid **25** (0.92 g, 3.0 mmol, 1.0 equiv.) in DCM (40 mL, 75 mM) was cooled to 0 °C. Bromine (0.49 mL, 9.0 mmol, 3.0 equiv.) was added dropwise and the reaction was stirred at 0 °C for 2 hrs. The cooling bath was removed and bromine was quenched by addition of sat. aq. $Na_2S_2O_5$. Additional DCM was added and the layers were separated. The organic layer was washed with sat. aq. $Na_2S_2O_3$ and brine. The organic phase was dried ($MgSO_4$), filtered and concentrated *in vacuo*. The crude product was taken up in THF (50 mL, 60 mM) and cooled to -45 °C. Potassium *tert*-butoxide (1.0 M in THF, 9.0 mL, 9.0 mmol, 3.0 equiv.) was added dropwise to the solution. After 90 min, additional potassium *tert*-butoxide (1.0 M in THF, 4.0 mL, 4.0 mmol, 1.3 equiv.) was added followed by extra potassium *tert*-butoxide (1.0 M in THF, 3.0 mL, 3.0 mmol, 1.0 equiv.) after 3 hrs of stirring. The reaction was stirred in total for 4 hrs at -45 °C. The mixture was warmed to room temperature and quenched with 1.0 M aq. $NaHSO_4$ until the pH was 1. The aqueous layer was extracted with DCM (3x). The pooled organic fractions were washed with H_2O and brine. The organic phase was dried (Na_2SO_4), filtered and the volatiles were removed under reduced pressure to furnish alkyne **26** which was used immediately in the next step without further purification.

^{1}H NMR (400 MHz, $CDCl_3$) δ 7.70 (dd, *J* = 7.5, 1.3 Hz, 1H, C*H*-arom), 7.48 – 7.34 (m, 5H, C*H*-arom), 7.33 – 7.25 (m, 1H, C*H*-arom), 7.21 (dd, *J* = 7.5, 1.5 Hz, 1H, C*H*-arom), 5.19 (d, *J* = 13.8 Hz, 1H, CH_2), 3.71 (d, *J* = 13.8 Hz, 1H, CH_2), 3.02 – 2.89 (m, 1H, CH_2(C=O)N)), 2.87 – 2.69 (m, 2H, CH_2(C=O)N), CH_2(C=O)OH), 2.18 – 2.07 (m, 1H, CH_2(C=O)OH).

^{13}C NMR (101 MHz, $CDCl_3$) δ 170.9 (*C*=O), 169.0 (*C*=O), 151.2 (*C*q-arom), 147.9 (*C*q-arom), 132.4 (*C*H-arom), 129.2 (*C*H-arom), 128.7 (*C*H-arom), 128.5 (*C*H-arom), 128.5 (*C*H-arom), 127.9 (*C*H-arom), 127.4 (*C*H-arom), 125.6 (*C*H-arom), 123.1 (*C*q-arom), 122.9 (*C*q-arom), 115.1 (*C*≡*C*), 107.6 (*C*≡*C*), 55.7 (*C*H_2), 29.5 (*C*H_2(C=O)OH), 28.7 (*C*H_2(C=O)N).

HRMS (ESI-Orbitrap) calcd. for $C_{19}H_{16}NO_3$ $[M+H]^+$ 306.11247, found 306.11212.

DIBAC-4-oxobutanoic acid pentafluorophenyl ester

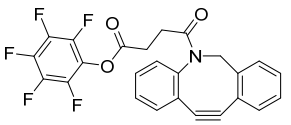

27

Crude alkyne **26** was dissolved in DCM (30 mL, 0.10 M). Pentafluorophenol (0.61 g, 3.3 mmol, 1.1 equiv.), DIC (0.51 mL, 3.3 mmol, 1.1 equiv.) and *N*-methylmorpholine (0.73 mL, 6.6 mmol, 2.2 equiv.) were added. The reaction was stirred for 18 hrs. The volatiles were removed under reduced pressure and the crude was purified by silica gel column chromatography (1:9, EA – Pentane to 1:4, EA – Pentane) to give pentaflurophenyl ester **27** (0.47 g, 0.99 mmol, 33% over 3 steps) as a white amorphous solid.

^{1}H NMR (400 MHz, $CDCl_3$) δ 7.70 – 7.65 (m, 1H, C*H*-arom), 7.48 – 7.37 (m, 4H, C*H*-arom), 7.33 (td, *J* = 7.5, 1.6 Hz, 1H, C*H*-arom), 7.30 – 7.25 (m, 1H, C*H*-arom), 7.20 (dd, *J* = 7.5, 1.6 Hz, 1H, C*H*-arom), 5.18 (d, *J* = 13.9 Hz, 1H, CH_2), 3.72 (d, *J* = 14.0 Hz, 1H, CH_2), 3.04 – 2.89 (m, 1H, CH_2(C=O)N)), 2.88 – 2.69 (m, 2H, CH_2(C=O)N), CH_2(C=O)OPfp), 2.22 – 2.10 (m, 1H, CH_2(C=O)OPfp).

^{13}C NMR (101 MHz, $CDCl_3$) δ 171.5 (*C*=O), 169.0 (*C*=O), 151.0 (*C*q-arom), 147.6 (*C*q-arom), 132.4 (*C*H-arom), 129.2 (*C*H-arom), 128.8 (*C*H-arom), 128.7 (*C*H-arom), 128.4 (*C*H-arom), 127.9 (*C*H-arom), 127.4 (*C*H-arom), 125.6 (*C*H-arom), 123.1 (*C*q-arom), 122.9 (*C*q-arom), 115.1 (*C*≡*C*), 107.5 (*C*≡*C*), 55.8 (CH_2), 29.5 (*C*H_2(C=O)OPfp), 28.7 (CH_2(C=O)N).

^{19}F NMR (471 MHz, $CDCl_3$) δ -151.38 – -153.05 (m, C*F*-arom), -158.28 (t, *J* = 21.7 Hz, C*F*-arom), -162.54 (td, *J* = 22.3, 4.8 Hz, C*F*-arom).

HRMS (ESI-Orbitrap) calcd. for $C_{25}H_{15}F_5NO_3$ [M+H]$^+$ 472.09666, found 472.09686.

***tert*-butyl 1-chloro-2-oxo-6,9,12-trioxa-3-azatetradecan-14-oate**

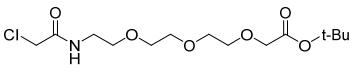

17

A solution of *tert*-butyl 2-(2-(2-(2-aminoethoxy)ethoxy)ethoxy)acetate **16** (0.47g, 1.8 mmol, 1.0 equiv.) and Et_3N (0.32 mL, 2.3 mmol, 1.3 equiv.) in DCM (18 mL, 0.10 M) was cooled to 0 °C and chloroacetyl chloride (0.18 mL, 2.3 mmol, 1.3 equiv.) was added dropwise. The reaction was stirred at 0 °C for 2 hrs. The reaction mixture was diluted with DCM and washed with sat. aq. $NaHCO_3$, H_2O and brine. The organic layer was dried ($MgSO_4$), filtered and concentrated *in vacuo*. Purification by silica gel column chromatography (1:49, MeOH – DCM to 1:19, MeOH – DCM) afforded chloroacetamide **17** (0.27 g, 0.78 mmol, 44%) as a colorless oil.

^{1}H NMR (400 MHz, $CDCl_3$) δ 7.09 (br s, 1H, N*H*), 3.97 (s, 2H, CH_2Cl), 3.94 (s, 2H, CH_2C(C=O)O^{t}Bu), 3.66 – 3.55 (m, 8H, OCH_2), 3.54 – 3.49 (m, 2H, CH_2CH$_2$NHClAc), 3.42 (q, *J* = 5.5 Hz, 2H, CH_2NHClAc), 1.42 – 1.36 (m, 9H, (C=O)O^t*Bu*).

^{13}C NMR (101 MHz, $CDCl_3$) δ 169.6 ((*C*=O)O^{t}Bu), 166.1 (NH(*C*=O)), 81.5 (*C*CH_3), 70.6 (OCH_2), 70.5 (OCH_2), 70.4 (OCH_2), 70.2 (OCH_2), 69.3 (*C*H_2CH$_2$NHClAc), 68.9 (*C*H_2(C=O)O^{t}Bu), 42.6 (*C*H_2Cl), 39.5 (*C*H_2NHClAc), 28.0 (*C*H_3).

HRMS (ESI-Orbitrap) calcd. for $C_{14}H_{26}ClNO_6Na$ [M+Na]$^+$ 362.13409, found 362.13391.

1-chloro-2-oxo-6,9,12-trioxa-3-azatetradecan-14-oic acid

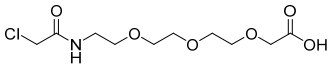

18

tert-Butyl ester **17** (71 mg, 0.21 mmol, 1.0 equiv.) was dissolved in a mixture of TFA and DCM (1:9, TFA – DCM, 2.1 mL, 0.10 M). The reaction was stirred for 17 hrs. Toluene was added and the solution was evaporated to a volume of ca. 2 mL (3x). The mixture was evaporated to dryness to obtain carboxylic acid **18** (59 mg, 0.21 mmol, quant.) as a colorless oil.

^{1}H NMR (400 MHz, $CDCl_3$) δ 8.97 (br s, 1H, COO*H*), 7.23 (br s, 1H, N*H*), 4.18 (s, 2H, CH_2(C=O)OH), 4.10 (s, 2H, CH_2Cl), 3.81 – 3.74 (m, 2H, OCH_2), 3.73 – 3.64 (m, 6H, OCH_2), 3.63 – 3.58 (m, 2H, CH_2CH$_2$NHClAc), 3.52 (q, *J* = 5.1 Hz, 2H, CH_2NHClAc).

^{13}C NMR (101 MHz, $CDCl_3$) δ 172.7 ((*C*=O)OH), 166.9 (NH(*C*=O)), 71.3 (OCH_2), 70.6 (OCH_2), 70.3 (OCH_2), 70.1 (OCH_2), 69.5 (*C*H_2CH$_2$NHClAc), 68.7 (*C*H_2(C=O)OH), 42.7 (*C*H_2Cl), 39.7 (*C*H_2NHClAc).

HRMS (ESI-Orbitrap) calcd. for $C_{10}H_{18}ClNO_6Na$ [M+Na]$^+$ 306.07149, found 306.07120.

2-chloro-*N*-(1-(4-(6-methyl-1,2,4,5-tetrazin-3-yl)phenyl)-3-oxo-5,8,11-trioxa-2-azatridecan-13-yl)acetamide

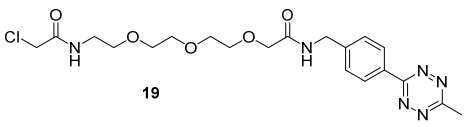

19

Carboxylic acid **18** (14 mg, 50 μmol, 1.0 equiv.) was dissolved in DCM (0.50 mL, 0.10 M) and DIC (14 μL, 0.10 mmol, 2.0 equiv.) and *N*-methylmorpholine (11 μL, 0.10 mmol, 2.0 equiv.) and the reaction was stirred. After 1 hr, a solution of (4-(6-methyl-1,2,4,5-tetrazin-3-yl)phenyl)methanamine

hydrochloride (12 mg, 50 μmol, 1.0 equiv.) and *N*-methylmorpholine (11 μL, 0.10 mmol, 2.0 equiv.) in a mixture of DCM and DMF (1:1, DCM – DMF, 1.0 mL, 50 mM) was added dropwise and the reaction was stirred for 19 hrs. The reaction mixture was washed with H_2O (5x) and the organic layer was dried ($MgSO_4$), filtered and concentrated under reduced pressure. Purification by silica gel column chromatography (1:39, MeOH – DCM) afforded tetrazine **19** (9.5 mg, 20 μmol, 41%) as a pink oil.

^{1}H NMR (500 MHz, $CDCl_3$) δ 8.56 (d, *J* = 8.0 Hz, 2H, C*H*-arom), 7.53 (d, *J* = 8.1 Hz, 3H, C*H*-arom, N*H*Bn), 7.00 (s, 1H, N*H*ClAc), 4.62 (d, *J* = 5.7 Hz, 2H, CH_2-benzyl), 4.14 (s, 2H, CH_2(C=O)NHBn), 4.03 (s, 2H, CH_2Cl), 3.74 (dd, *J* = 5.8, 2.6 Hz, 2H, OCH_2), 3.68 (dd, *J* = 5.7, 2.5 Hz, 2H, OCH_2), 3.60 (dd, *J* = 5.8, 3.1 Hz, 2H, OCH_2), 3.54 (dd, *J* = 5.8, 3.1 Hz, 2H, OCH_2), 3.50 (t, *J* = 4.9 Hz, 2H, CH_2CH$_2$NHClAc), 3.43 (q, *J* = 5.2 Hz, 2H, CH_2NHClAc), 3.10 (s, 3H, CH_3).

^{13}C NMR (126 MHz, $CDCl_3$) δ 170.4 (*C*q-tetrazine), 167.4 ((*C*=O)NHBn), 166.1 (*C*q-tetrazine), 164.0 ((*C*=O)CH$_2$Cl), 143.3 (*C*q-arom), 131.1 (*C*q-arom), 128.5 (*C*H-arom), 128.4 (*C*H-arom), 71.2 (OCH$_2$), 70.7 (CH$_2$(C=O)NHBn), 70.6 (OCH$_2$), 70.5 (OCH$_2$), 70.4 (OCH$_2$), 69.5 (CH$_2$CH$_2$NHClAc), 42.8 (CH$_2$Cl), 42.6 (CH$_2$-benzyl), 39.6 (CH$_2$NHClAc), 21.3 (CH$_3$).

HRMS (ESI-Orbitrap) calcd. for $C_{20}H_{28}ClN_6O_5$ $[M+H]^+$ 467.18042, found 467.18018.

2-iodo-*N*-(1-(4-(6-methyl-1,2,4,5-tetrazin-3-yl)phenyl)-3-oxo-5,8,11-trioxa-2-azatridecan-13-yl)acetamide

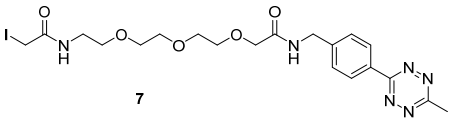

7

Chloroacetamide **19** (9.5 mg, 20 μmol, 1.0 equiv.) was dissolved in acetone (0.50 mL, 40 mM) and sodium iodide (9.0 mg, 60 μmol, 3.0 equiv.) was added. The reaction was stirred for 48 hrs and subsequently concentrated *in vacuo* and purified by silica gel column chromatography (1:39, MeOH – DCM) to give iodoacetamide **7** (8.1 mg, 15 μmol, 73%) as a pink oil.

^{1}H NMR (500 MHz, $CDCl_3$) δ 8.57 (d, *J* = 7.8 Hz, 2H, C*H*-arom), 7.54 (d, *J* = 8.0 Hz, 2H, C*H*-arom), 7.49 (s, 1H, N*H*Bn), 6.90 (s, 1H, N*H*CH$_2$I), 4.63 (d, *J* = 4.3 Hz, 2H, CH_2-benzyl), 4.22 (s, 2H, CH_2(C=O)NHBn), 3.80 – 3.65 (m, 6H, OCH_2, CH_2I), 3.63 – 3.59 (m, 2H, OCH_2), 3.57 – 3.53 (m, 2H, OCH_2), 3.51 – 3.47 (m, 2H, CH_2CH$_2$NHIAc), 3.42 – 3.38 (m, 2H, CH_2NHIAc), 3.11 (s, 3H, CH_3).

^{13}C NMR (126 MHz, $CDCl_3$) δ 170.7 (*C*q-tetrazine), 167.5 ((*C*=O)NHBn), 166.0 (*C*q-tetrazine), 164.0 ((*C*=O)CH$_2$I), 143.2 (*C*q-arom), 131.1 (*C*q-arom), 128.6 (*C*H-arom), 128.4 (*C*H-arom), 71.0 (OCH$_2$), 70.9 (CH$_2$(C=O)NHBn), 70.9 (OCH$_2$), 70.4 (OCH$_2$), 70.3 (OCH$_2$), 69.6 (CH$_2$CH$_2$NHIAc), 42.7 (CH$_2$-benzyl), 40.3 (CH$_2$NHIAc), 21.3 (CH$_3$), -0.3 (CH$_2$I).

HRMS (ESI-Orbitrap) calcd. for $C_{20}H_{28}IN_6O_5$ $[M+H]^+$ 559.11604, found 559.11582.

2,5-dioxopyrrolidin-1-yl (1*S*,4*S*)-bicyclo[2.2.1]hept-5-ene-2-carboxylate

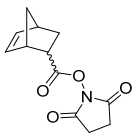

37

5-Norbornene-2-carboxylic acid (1.3 mL, 11 mmol, 1.0 equiv.) was dissolved in DCM (50 mL, 0.21 M). *N*-Hydroxysuccinimide (4.6 g, 40 mmol, 3.8 equiv.) and EDC hydrochloride (7.7 g, 40 mmol, 3.8 equiv.) were added and the reaction was stirred for 15 hrs. The reaction mixture was washed with 1.0 M aq. HCl (3x). The organic layer was dried ($MgSO_4$), filtered and concentrated *in vacuo*. Purification by silica gel column chromatography (1:9, EA – Pentane to 7:13, EA – Pentane) afforded activated ester **37** (2.5 g, 11 mmol, 99%) as a white solid.

^{1}H NMR (400 MHz, $CDCl_3$, both isomers) δ 6.28 – 6.18 (m, 1H, C*H*=C*H*), 6.18 – 6.09 (m, 1H, C*H*=C*H*), 3.44 – 3.37 (m, 0.8H, C*H*-bridgehead-endo), 3.30 – 3.20 (m, 1H, C*H*-bridghead-exo, C*H*(C=O)O-endo), 3.03 – 2.96 (m, 1H, C*H*-bridgehead-exo, C*H*-bridghead-endo), 2.89 – 2.74 (m, 4H, CH_2(C=O)N), 2.51 (ddd, *J* = 9.0, 4.5, 1.5 Hz, 0.2H, C*H*(C=O)O-exo), 2.09 – 1.97 (m, 1H, CH_2CH(C=O)O-exo, CH_2CH(C=O)O-endo), 1.58 – 1.41 (m, 2.2H, CH_2CH(C=O)O-exo, CH_2CH(C=O)O-endo, CH_2-bridge exo, CH_2-bridge endo), 1.38 – 1.31 (m, 0.8H, CH_2-bridge endo).

^{13}C NMR (101 MHz, $CDCl_3$, both isomers) δ 171.7 (*C*=O), 170.0 (C=O), 169.5 (*C*=O), 169.3 (C=O), 138.6 (CH=CH-exo), 138.2 (CH=CH-endo), 135.3 (CH=CH-exo), 132.2 (CH=CH-endo), 49.7 (CH$_2$-bridge-endo), 47.2 (CH-bridgehead-exo), 46.5 (CH-bridgehead-endo), 46.5 (CH$_2$-bridge-exo), 42.6 (CH-bridghead-endo), 41.8 (CH-bridgehead-exo), 40.7 (CH(C=O)O-endo), 40.3 (CH(C=O)O-exo), 31.0 (CH$_2$CH(C=O)O-exo), 29.6 (CH$_2$CH(C=O)O-endo), 25.7 (CH$_2$(C=O)N-exo), 25.6 (CH$_2$(C=O)N-endo).

HRMS (ESI-Orbitrap) calcd. for $C_{12}H_{14}NO_4$ $[M+H]^+$ 236.09173, found 236.04506.

***tert*-butyl 6-amino-2-butoxy-9-(4-((4-(6-methyl-1,2,4,5-tetrazin-3-yl)benzyl)carbamoyl)benzyl)-8-oxo-8,9-dihydro-7*H*-purine-7-carboxylate**

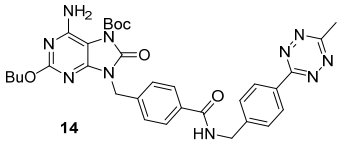

14

4-((6-amino-2-butoxy-7-(tert-butoxycarbonyl)-8-oxo-7,8-dihydro-9*H*-purin-9-yl)methyl)benzoic acid **13** (23 mg, 50 μmol, 1.0 equiv.) was dissolved in DCM (0.50 mL, 0.10 M) and DIC (14 μL, 0.10 mmol, 2.0 equiv.) and *N*-methylmorpholine (11 μL, 0.10 mmol, 2.0 equiv.) and the reaction was stirred. After 1 hr, a solution of (4-(6-methyl-1,2,4,5-tetrazin-3-yl)phenyl)methanamine hydrochloride (12 mg, 50 μmol, 1.0 equiv.) and *N*-methylmorpholine (11 μL, 0.10 mmol, 2.0 equiv.) in a mixture of DCM and DMF (1:1, DCM – DMF, 1.0 mL, 50 mM) was added dropwise and the reaction was stirred for 19 hrs. The reaction mixture was washed with H_2O (5x) and the organic layer was dried ($MgSO_4$), filtered and concentrated under reduced pressure. Purification by silica gel column chromatography (1:39, MeOH – DCM) afforded tetrazine **14** (5.6 mg, 8.9 μmol, 18%) as a pink solid.

^{1}H NMR (500 MHz, $CDCl_3$) δ 8.59 – 8.53 (m, 2H, C*H*-arom), 7.81 – 7.75 (m, 2H, C*H*-arom), 7.57 – 7.50 (m, 4H, C*H*-arom), 6.55 (t, *J* = 5.9 Hz, 1H, N*H*), 5.02 (s, 2H, CH_2N), 4.75 (d, *J* = 5.9 Hz, 2H, CH_2NH), 4.27 (t, *J* = 6.7 Hz, 2H, OCH_2), 3.10 (s, 3H, CH_3), 1.79 – 1.70 (m, 2H, OCH$_2$CH_2), 1.62 (s, 9H, N(C=O)O^t*Bu*), 1.53 – 1.42 (m, 2H, CH_2CH$_3$), 0.96 (t, *J* = 7.4 Hz, 3H, CH$_2$CH_3).

^{13}C NMR (126 MHz, $CDCl_3$) δ 167.4 (NH(*C*=O), 167.2 (*C*q-tetrazine), 164.0 (*C*q-tetrazine), 162.0 (NH$_2$*C*q), 150.9 (BuO*C*q), 150.4 (N(*C*=O)N), 150.2 (N(*C*=O)O^{t}Bu), 149.7 (N*C*qN), 143.2 (*C*q-arom), 139.7 (*C*q-arom), 133.8 (*C*q-arom), 131.2 (*C*q-arom), 129.1 (*C*H-arom), 128.6 (*C*H-arom), 128.5 (*C*H-arom), 127.5 (*C*H-arom), 97.2 (*C*qNBoc), 86.4 (*C*CH$_3$), 67.5 (O*C*H$_2$), 43.9 (*C*H$_2$NH), 43.4 (*C*H$_2$N), 31.1 (OCH$_2$*C*H$_2$), 28.1 (N(C=O)O^t*Bu*), 21.3 (*C*H$_3$), 19.3 (CH$_2$*C*H$_3$), 14.0 (CH$_2$*C*H$_3$).

HRMS (ESI-Orbitrap) calcd. for $C_{32}H_{37}N_{10}O_5$ $[M+H]^+$ 641.29429, found 641.29470.

4-((6-amino-2-butoxy-8-oxo-7,8-dihydro-9*H*-purin-9-yl)methyl)-N-(4-(6-methyl-1,2,4,5-tetrazin-3-yl)benzyl)benzamide

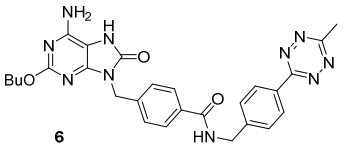

6

Tetrazine **14** (5.6 mg, 8.9 μmol, 1.0 equiv.) was dissolved in a mixture of TFA and DCM (1:2, TFA – DCM, 0.50 mL, 18 mM). The reaction was stirred for 3 hrs. Toluene was added and the solution was evaporated to a volume of ca. 1 mL (3x). The mixture was evaporated to dryness to obtain tetrazine **6** (4.8 mg, 8.9 μmol, quant.) as a pink solid.

^{1}H NMR (500 MHz, DMF) δ 10.21 (s, 1H, N*H*(C=O)N), 9.15 (t, *J* = 6.0 Hz, 1H, N*H*Bn), 8.51 – 8.46 (m, 2H, C*H*-arom), 8.02 – 7.99 (m, 2H, C*H*-arom), 7.70 – 7.65 (m, 2H, C*H*-arom), 7.54 – 7.48 (m, 2H, C*H*-arom), 6.67 (br s, 2H, NH_2), 5.04 (s, 2H, CH_2N), 4.72 (d, *J* = 6.0 Hz, 2H, CH_2NH), 4.19 (t, *J* = 6.6 Hz, 2H, OCH_2), 3.04 (s, 3H, CH_3), 1.71 – 1.62 (m, 2H, OCH$_2$CH_2), 1.47 – 1.36 (m, 2H, CH_2CH$_3$), 0.92 (t, *J* = 7.4 Hz, 3H, CH$_2$CH_3).

^{13}C NMR (126 MHz, DMF) δ 168.5 NH(*C*=O)Ph, 167.4 (*C*q-tetrazine), 164.7 (*C*q-tetrazine), 161.7 (NH$_2$*C*q), 153.9 (BuO*C*q), 150.9 (NH(*C*=O)N), 149.2 (N*C*qN), 145.8 (*C*q-arom), 142.0 (*C*q-arom), 134.9 (*C*q-arom), 131.9 (*C*q-arom), 129.3 (*C*H-arom), 128.6 (*C*H-arom), 128.6 (*C*H-arom), 128.5 (*C*H-arom), 99.7 (NH*C*q), 67.2 (O*C*H$_2$), 43.9 (NH*C*H$_2$), 43.4 (N*C*H$_2$), 32.0 (OCH$_2$*C*H$_2$), 21.4 (*C*H$_3$), 20.1 (*C*H$_2$CH$_3$), 14.4 (CH$_2$*C*H$_3$).

HRMS (ESI-Orbitrap) calcd. for $C_{27}H_{29}N_{10}O_3$ $[M+H]^+$ 541.24186, found 541.24211.

***cyclo*(-Leu-*D*Phe-Pro-Lys(N_2)-Val-Lys(TFA)-*D*Phe-Pro-Val-Lys-)**

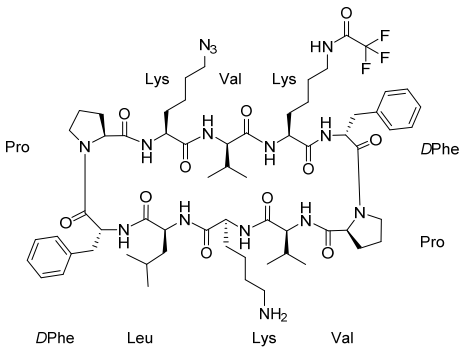

38

Functionalized resin **12** (0.53 g, 0.10 mmol, 1.0 equiv.) was elongated using the Liberty Blue peptide synthesizer. Afterwards, the resin was washed with DCM (4x), Et_2O (4x) and dried over N_2. Resin was suspended in a mixture of DCM and DMF (1:1, DCM – DMF, 4.0 mL, 25 mM) and swollen for 20 min. Phenylsilane (31 μL, 0.25 mmol, 2.5 equiv.) and $Pd(PPh_3)_4$ (29 mg, 25 μmol, 25 mol%) were added and the resin was shaken for 90 min. while being protected from light. The suspension was filtered and the resin was washed with DCM (3x), 0.50% (w/v) sodium diethyldithiocarbamate in DMF (2x) and DMF (3x). To the resin was added 20% (v/v) piperidine in DMF (5.0 mL, 20 mM) and the mixture was shaken for 10 min. Resin was filtered and 20% (v/v) piperidine in DMF (5.0 mL, 20 mM) was added. The suspension was shaken for 10 min. Afterwards, the resin was filtered and washed with DMF (6x). DMF (4.0 mL, 25 mM) was added to the resin. Subsequently, 1-hydroxybenzotriazole hydrate (68 mg, 0.50 mmol, 5.0 equiv.), benzotriazole-1-yl-oxy-tris-pyrrolidino-phosphonium hexafluorophosphate (0.26 g, 0.50 mmol, 5.0 equiv.) and *N*-methylmorpholine (0.11 mL, 1.0 mmol, 10 equiv.) were added to the suspension and the reaction was stirred for 2.5 hrs. The suspension was filtered and the residue was washed with DMF (3x) and DCM (3x). A cleavage mixture (190:5:5, TFA – H_2O – TIPS) was added to a small amount of resin (5.0 mg) and shaken for 2 hrs. The suspension was filtered and the filtrate was analyzed by LC-MS.

LC-MS (ESI^+) calcd. for $C_{64}H_{95}F_3N_{15}O_{11}$ $[M+H]^+$ 1306.73, observed 1306.67 with a retention time of 7.90 min.

***cyclo*(-Leu-*D*Phe-Pro((4*S*)-4-azido)-Val-Leu-Lys(TFA)-*D*Phe-Pro-Val-Lys-)**

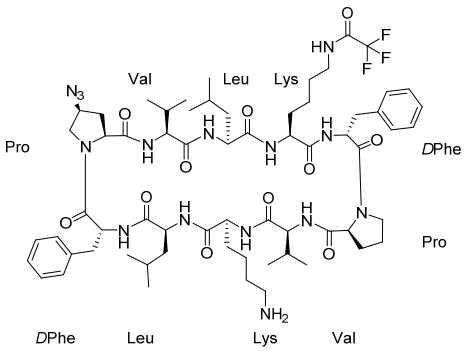

39

Functionalized resin **12** (0.53 g, 0.10 mmol, 1.0 equiv.) was elongated using the Liberty Blue peptide synthesizer. Afterwards, the resin was washed with DCM (4x), Et_2O (4x) and dried over N_2. Resin was suspended in a mixture of DCM and DMF (1:1, DCM – DMF, 4.0 mL, 25 mM) and swollen for 20 min. Phenylsilane (31 μL, 0.25 mmol, 2.5 equiv.) and $Pd(PPh_3)_4$ (29 mg, 25 μmol, 25 mol%) were added and the resin was shaken for 90 min. while being protected from light. The suspension was filtered and the resin was washed with DCM (3x), 0.50% (w/v) sodium diethyldithiocarbamate in DMF (2x) and DMF (3x). To the resin was added 20% (v/v) piperidine in DMF (5.0 mL, 20 mM) and the mixture was shaken for 10 min. Resin was filtered and 20% (v/v) piperidine in DMF (5.0 mL, 20 mM) was added. The suspension was shaken for 10 min. Afterwards, the resin was filtered and washed with DMF (6x). DMF (4.0 mL, 25 mM) was added to the resin. Subsequently, 1-hydroxybenzotriazole hydrate (68 mg, 0.50 mmol, 5.0 equiv.), benzotriazole-1-yl-oxy-tris-pyrrolidino-phosphonium hexafluorophosphate (0.26 g, 0.50 mmol, 5.0 equiv.) and *N*-methylmorpholine (0.11 mL, 1.0 mmol, 10 equiv.) were added to the suspension and the reaction was stirred for 2.5 hrs. The suspension was filtered and the residue was washed with DMF (3x) and DCM (3x). A cleavage mixture (190:5:5, TFA – H_2O – TIPS) was added to a small amount of resin (5.0 mg) and shaken for 2 hrs. The suspension was filtered and the filtrate was analyzed by LC-MS.

LC-MS (ESI^+) calcd. for $C_{64}H_{95}F_3N_{15}O_{11}$ $[M+H]^+$ 1306.73, observed 1306.87 with a retention time of 7.74 min.

***cyclo*(-Leu-*D*Phe-Pro-Lys(N_2)-Val-Lys-*D*Phe-Pro-Val-Lys-)**

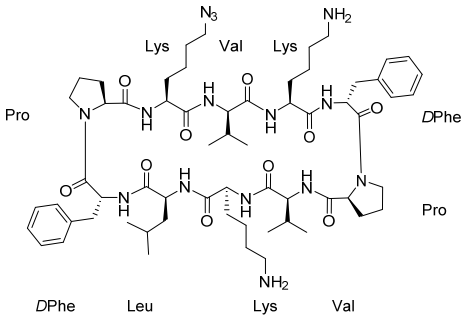

40

Resin **29** (0.10 mmol, 1.0 equiv.) was suspended in 7.0 M NH_3 in MeOH (8.0 mL, 13 mM). The suspension was irradiated in a microwave to 90 °C and stirred at 90 °C for 12 hrs. The suspension was filtered and the resin was washed with MeOH (4x), DMF (3x) and DCM (3x). A cleavage mixture (190:5:5, TFA – H_2O – TIPS) was added to a small amount of resin (5.0 mg) and shaken for 2 hrs. The suspension was filtered and the filtrate was analyzed by LC-MS.

LC-MS (ESI^+) calcd. for $C_{62}H_{96}F_3N_{15}O_{10}$ $[M+H]^+$ 1210.75, observed 1210.67 with a retention time of 6.38 min.

***cyclo*(-Leu-*D*Phe-Pro-Lys(N_2)-Val-Lys(Norb)-*D*Phe-Pro-Val-Lys-)**

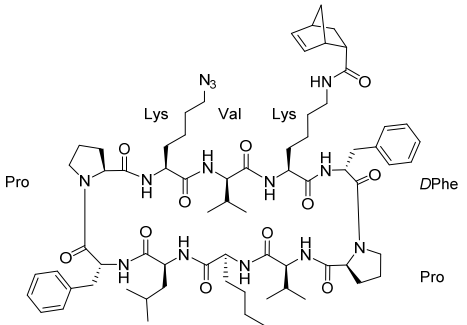

41

To the resin with the free lysine ε-amine (0.10 mmol, 1.0 equiv.) was added activated ester **37** (47 mg, 0.20 mmol, 2.0 equiv.) and DMF (4.0 mL, 25 mM) followed by DIPEA (70 μL, 0.40 mmol, 4.0 equiv.). The suspension was shaken for 19 hrs followed by filtration. The resin was washed with DMF (4x) and DCM (4x). A cleavage mixture (1:199, TFA – DCM) was added to a small amount of resin (5.0 mg) and shaken for 2 min followed by filtration (10x). The filtrate was analyzed by LC-MS.

LC-MS (ESI^+) calcd. for $C_{70}H_{104}N_{15}O_{11}$ $[M+H]^+$ 1330.80, observed 1330.93 with a retention time of 8.21 min.

***cyclo*(-Leu-*D*Phe-Pro-Lys(DIBAC)-Val-Lys(Norb)-*D*Phe-Pro-Val-Lys-)**

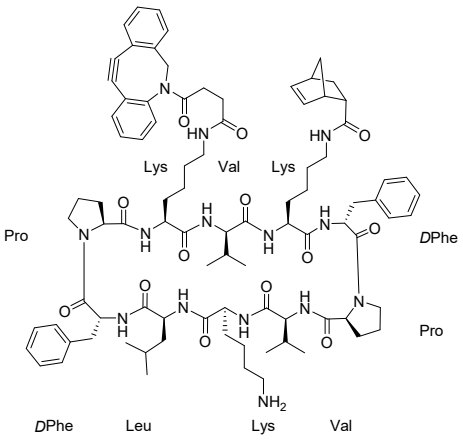

36

To functionalized resin **34** (0.10 mmol, 1.0 equiv.) was added 1,4-dioxane (10 mL, 10 mM) followed by trimethylphosphine (1.0 M in toluene, 1.6 mL, 16 equiv.) and the suspension was stirred for 2 hrs. H_2O (1.0 mL, 55 mmol, 5.5 x 10^2 equiv.) was added and the resin was shaken for an additional 4 hrs. The suspension was filtered and the resin was washed with 1,4-dioxane (3x) and DCM (3x). A solution of activated ester **27** (71 mg, 0.15 mmol, 1.5 equiv.), DIPEA (52 μL, 0.30 mmol. 3.0 equiv.) in DMF (4.0 mL, 25 mM) was added to the resin and was subsequently shaken for 72 hrs. The suspension was filtered and the resin was washed with DMF (4x) and DCM (4x). The resin was treated with a cleavage cocktail (TFA – DCM, 1:199, 10 mL) for 2 min. The suspension was filtered into a vigorously stirred mixture of Amberlyst A-21 (7.0 g, previously rinsed with MeOH, THF and DCM) in DCM (20 mL) to neutralize the TFA. This procedure was repeated ten times. The Amberlyst A-21 resin was separated by filtration and rinsed with additional DCM. The filtrate was concentrated *in vacuo* and purified by RP-HPLC (Agilent 1200, 53% to 59% solvent B) to obtain alkyne **36** (4.0 mg, 2.5 μmol, 2.5%) as a white solid.

HRMS (ESI-Orbitrap) calcd. for $C_{89}H_{120}N_{14}O_{13}$ $[M+2H]^{2+}$ 796.45742, found 796.45703.

***cyclo*(-Leu-*D*Phe-Pro((4*S*)-4-NHDIBAC)-Val-Leu-Lys(Norb)-*D*Phe-Pro-Val-Lys-)**

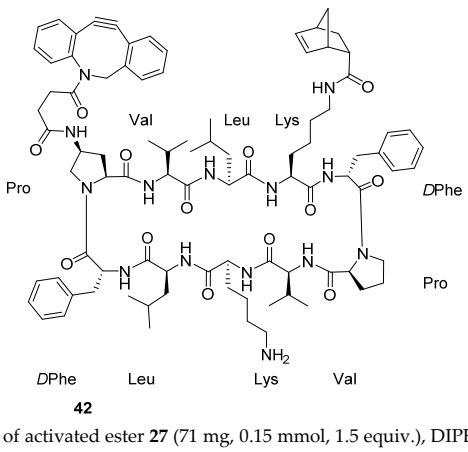

42

The resin bearing the cyclopeptide (0.10 mmol, 1.0 equiv.) was suspended in 7.0 M NH_3 in MeOH (8.0 mL, 13 mM). The suspension was irradiated in a microwave to 90 °C and stirred at 90 °C for 12 hrs. The suspension was filtered and the resin was washed with MeOH (4x), DMF (3x) and DCM (3x). To the resin was then added activated ester **37** (47 mg, 0.20 mmol, 2.0 equiv.) and DMF (4.0 mL, 25 mM) followed by DIPEA (70 μL, 0.40 mmol, 4.0 equiv.). The suspension was shaken for 19 hrs followed by filtration. The resin was washed with DMF (4x) and DCM (4x) and to the resin was added 1,4-dioxane (10 mL, 10 mM) followed by trimethylphosphine (1.0 M in toluene, 1.6 mL, 16 equiv.) and the suspension was stirred for 2 hrs. H_2O (1.0 mL, 55 mmol, 5.5 x 10^2 equiv.) was added and the resin was shaken for an additional 4 hrs. The suspension was filtered and the resin was washed with 1,4-dioxane (3x) and DCM (3x). A solution of activated ester **27** (71 mg, 0.15 mmol, 1.5 equiv.), DIPEA (52 μL, 0.30 mmol. 3.0 equiv.) in DMF (4.0 mL, 25 mM) was added to the resin and was subsequently shaken for 72 hrs. The suspension was filtered and the resin was washed with DMF (4x) and DCM (4x). The resin was treated with a cleavage cocktail (TFA – DCM, 1:199, 10 mL) for 2 min. The suspension was filtered into a vigorously stirred mixture of Amberlyst A-21 (7.0 g, previously rinsed with MeOH, THF and DCM) in DCM (20 mL) to neutralize the TFA. This procedure was repeated ten times. The Amberlyst A-21 resin was separated by filtration and rinsed with additional DCM. The filtrate was concentrated *in vacuo* and purified by RP-HPLC (Agilent 1200, 55% to 61% solvent B) to obtain alkyne **42** (6.2 mg, 3.9 μmol, 3.9%) as a white solid.

HRMS (ESI-Orbitrap) calcd. for $C_{89}H_{120}N_{14}O_{13}$ $[M+2H]^{2+}$ 796.45742, found 796.45711.

***cyclo*(-Leu-*D*Phe-Pro-Lys(DIBAC)-Val-Lys(Norb)-*D*Phe-Pro-Val-Lys(Mal)-)**

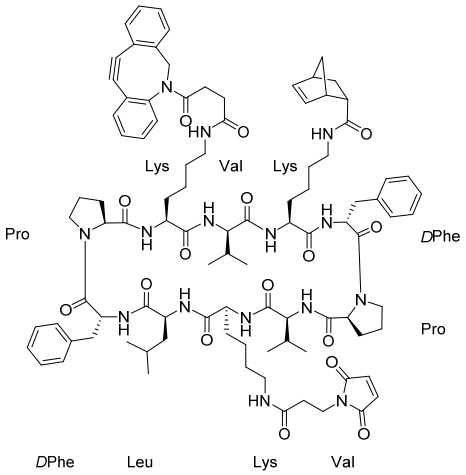

1

Crude alkyne **36** (30 mg, 17 μmol, 1.0 equiv.) was dissolved in DMF (0.50 mL, 34 mM). 3-Maleimidopropionic acid NHS ester (40 mg, 0.15 mmol, 8.8 equiv.) and *N*-methylmorpholine (17 μL, 0.15 mmol, 8.8 equiv.) were added and the reaction was stirred for 4 hrs. The mixture was concentrated *in vacuo* at room temperature. Purification by RP-HPLC (Agilent 1200, 69% to 71% solvent B) and subsequent lyophilization furnished maleimide **1** (4.0 mg, 2.3 μmol, 2.3%) as a white solid.

HRMS (ESI-Orbitrap) calcd. for $C_{96}H_{125}N_{15}O_{16}$ $[M+2H]^{2+}$ 871.97089, found 871.97109.

***cyclo*(-Leu-*D*Phe-Pro((4*S*)-4-NHDIBAC)-Val-Leu-Lys(Norb)-*D*Phe-Pro-Val-Lys(Mal)-)**

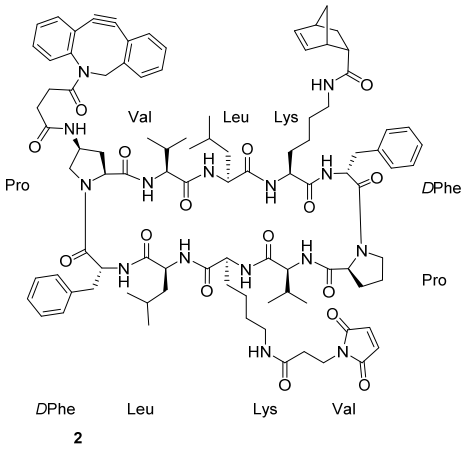

2

Crude alkyne **42** (30 mg, 17 μmol, 1.0 equiv.) was dissolved in DMF (0.50 mL, 34 mM). 3-Maleimidopropionic acid NHS ester (40 mg, 0.15 mmol, 8.8 equiv.) and *N*-methylmorpholine (17 μL, 0.15 mmol, 8.8 equiv.) were added and the reaction was stirred for 4 hrs. The mixture was concentrated *in vacuo* at room temperature. Purification by RP-HPLC (Agilent 1200, 68% to 70% solvent B) and subsequent lyophilization furnished maleimide **2** (5.8 mg, 3.3 μmol, 3.3%) as a white solid.

HRMS (ESI-Orbitrap) calcd. for $C_{96}H_{125}N_{15}O_{16}$ $[M+2H]^{2+}$ 871.97089, found 871.97098.

References

(1) Gotuzzo, E.; Yactayo, S.; Córdova, E. Efficacy and Duration of Immunity after Yellow Fever Vaccination: Systematic Review on the Need for a Booster Every 10 Years. *Am. J. Trop. Med. Hyg.* **2013**, *89* (3), 434–444. https://doi.org/10.4269/ajtmh.13-0264.

(2) Theiler, M.; Smith, H. H. The Use of Yellow Fever Virus Modified by in Vitro Cultivation for Human Immunization. *J. Exp. Med.* **1937**, *65* (6), 787–800.

(3) Orenstein, R. W. *Plotkin's Vaccines*; Elsevier, 2017.

(4) Querec, T.; Bennouna, S.; Alkan, S.; Laouar, Y.; Gorden, K.; Flavell, R.; Akira, S.; Ahmed, R.; Pulendran, B. Yellow Fever Vaccine YF-17D Activates Multiple Dendritic Cell Subsets via TLR2, 7, 8, and 9 to Stimulate Polyvalent Immunity. *J. Exp. Med.* **2006**, *203* (2), 413–424. https://doi.org/10.1084/jem.20051720.

(5) Zhu, Q.; Egelston, C.; Gagnon, S.; Sui, Y.; Belyakov, I. M.; Klinman, D. M.; Berzofsky, J. A. Using 3 TLR Ligands as a Combination Adjuvant Induces Qualitative Changes in T Cell Responses Needed for Antiviral Protection in Mice. *J. Clin. Invest.* **2010**, *120* (2), 607–616. https://doi.org/10.1172/JCI39293.

(6) Albin, T. J.; Tom, J. K.; Manna, S.; Gilkes, A. P.; Stetkevich, S. A.; Katz, B. B.; Supnet, M.; Felgner, J.; Jain, A.; Nakajima, R.; Jasinskas, A.; Zlotnik, A.; Pearlman, E.; Davies, D. H.; Felgner, P. L.; Burkhardt, A. M.; Esser-Kahn, A. P. Linked Toll-Like Receptor Triagonists Stimulate Distinct, Combination-Dependent Innate Immune Responses. *ACS Cent. Sci.* **2019**, *5* (7), 1137–1145. https://doi.org/10.1021/acscentsci.8b00823.

(7) Gilkes, A. P.; Albin, T. J.; Manna, S.; Supnet, M.; Ruiz, S.; Tom, J.; Badten, A. J.; Jain, A.; Nakajima, R.; Felgner, J.; Davies, D. H.; Stetkevich, S. A.; Zlotnik, A.; Pearlman, E.; Nalca, A.; Felgner, P. L.; Esser-Kahn, A. P.; Burkhardt, A. M. Tuning Subunit Vaccines with Novel TLR Triagonist Adjuvants to Generate Protective Immune Responses against Coxiella Burnetii. *J. Immunol.* **2020**, *204* (3), 611–621. https://doi.org/10.4049/jimmunol.1900991.

(8) Willems, L. I.; Li, N.; Florea, B. I.; Ruben, M.; van der Marel, G. A.; Overkleeft, H. S. Triple Bioorthogonal Ligation Strategy for Simultaneous Labeling of Multiple Enzymatic Activities. *Angew. Chem. Int. Ed.* **2012**, *51* (18), 4431–4434. https://doi.org/10.1002/anie.201200923.

(9) Simon, C.; Lion, C.; Spriet, C.; Baldacci-Cresp, F.; Hawkins, S.; Biot, C. One, Two, Three: A Bioorthogonal Triple Labelling Strategy for Studying the Dynamics of Plant Cell Wall Formation In Vivo. *Angew. Chem. Int. Ed.* **2018**, *57* (51), 16665–16671. https://doi.org/10.1002/anie.201808493.

(10) Thomas, B.; Fiore, M.; Daskhan, G. C.; Spinelli, N.; Renaudet, O. A Multi-Ligation Strategy for the Synthesis of Heterofunctionalized Glycosylated Scaffolds. *Chem. Commun.* **2015**, *51* (25), 5436–5439. https://doi.org/10.1039/C4CC05451B.

(11) Dumy, P.; Eggleston, I. M.; Cervigni, S.; Sila, U.; Sun, X.; Mutter, M. A Convenient Synthesis of Cyclic Peptides as Regioselectively Addressable Functionalized Templates (RAFT). *Tetrahedron Lett.* **1995**, *36* (8), 1255–1258. https://doi.org/10.1016/0040-4039(94)02481-P.

(12) Sauer, J.; Heldmann, D. K.; Hetzenegger, J.; Krauthan, J.; Sichert, H.; Schuster, J. 1,2,4,5-Tetrazine: Synthesis and Reactivity in [4+2] Cycloadditions. *Eur. J. Org. Chem.* **1998**, *1998* (12), 2885–2896. https://doi.org/10.1002/(SICI)1099-0690(199812)1998:12<2885::AID-EJOC2885>3.0.CO;2-L.

(13) Karver, M. R.; Weissleder, R.; Hilderbrand, S. A. Bioorthogonal Reaction Pairs Enable Simultaneous, Selective, Multi-Target Imaging. *Angew. Chem. Int. Ed.* **2012**, *51* (4), 920–922. https://doi.org/10.1002/anie.201104389.

(14) Debets, M. F.; Berkel, S. S. van; Schoffelen, S.; Rutjes, F. P. J. T.; Hest, J. C. M. van; Delft, F. L. van. Aza-Dibenzocyclooctynes for Fast and Efficient Enzyme PEGylation via Copper-Free (3+2) Cycloaddition. *Chem. Commun.* **2010**, *46* (1), 97–99. https://doi.org/10.1039/B917797C.

(15) Borrmann, A.; Milles, S.; Plass, T.; Dommerholt, J.; Verkade, J. M. M.; Wießler, M.; Schultz, C.; van Hest, J. C. M.; van Delft, F. L.; Lemke, E. A. Genetic Encoding of a Bicyclo[6.1.0]Nonyne-Charged Amino Acid Enables Fast Cellular Protein Imaging by Metal-Free Ligation. *ChemBioChem* **2012**, *13* (14), 2094–2099. https://doi.org/10.1002/cbic.201200407.

(16) Lang, K.; Davis, L.; Wallace, S.; Mahesh, M.; Cox, D. J.; Blackman, M. L.; Fox, J. M.; Chin, J. W. Genetic Encoding of Bicyclononynes and Trans-Cyclooctenes for Site-Specific Protein Labeling in Vitro and in Live Mammalian Cells via Rapid Fluorogenic Diels–Alder Reactions. *J. Am. Chem. Soc.* **2012**, *134* (25), 10317–10320. https://doi.org/10.1021/ja302832g.

(17) Llamas-Saiz, A. L.; Grotenbreg, G. M.; Overhand, M.; van Raaij, M. J. Double-Stranded Helical Twisted β-Sheet Channels in Crystals of Gramicidin S Grown in the Presence of Trifluoroacetic and Hydrochloric Acids. *Acta Crystallogr. D Biol. Crystallogr.* **2007**, *63* (3), 401–407. https://doi.org/10.1107/S0907444906056435.

(18) Dumy, P.; Eggleston, I. M.; Esposito, G.; Nicula, S.; Mutter, M. Solution Structure of Regioselectively Addressable Functionalized Templates: An NMR and Restrained Molecular Dynamics Investigation. *Biopolymers* **1996**, *39* (3), 297–308. https://doi.org/10.1002/(sici)1097-0282(199609)39:3<297::aid-bip3>3.0.co;2-j.

(19) Asano, A.; Matsuoka, S.; Minami, C.; Kato, T.; Doi, M. [Leu2]Gramicidin S Preserves the Structural Properties of Its Parent Peptide and Forms Helically Aligned β-Sheets. *Acta Crystallogr. Sect. C Struct. Chem.* **2019**, *75* (10), 1336–1343. https://doi.org/10.1107/S2053229619011872.

(20) Bycroft, B. W.; Chan, W. C.; Chhabra, S. R.; Hone, N. D. A Novel Lysine-Protecting Procedure for Continuous Flow Solid Phase Synthesis of Branched Peptides. *J. Chem. Soc. Chem. Commun.* **1993**, No. 9, 778–779. https://doi.org/10.1039/C39930000778.

(21) Chhabra, S. R.; Hothi, B.; Evans, D. J.; White, P. D.; Bycroft, B. W.; Chan, W. C. An Appraisal of New Variants of Dde Amine Protecting Group for Solid Phase Peptide Synthesis. *Tetrahedron Lett.* **1998**, *39* (12), 1603–1606. https://doi.org/10.1016/S0040-4039(97)10828-0.

(22) Finkelstein, H. Darstellung Organischer Jodide Aus Den Entsprechenden Bromiden Und Chloriden. *Berichte Dtsch. Chem. Ges.* **1910**, *43* (2), 1528–1532. https://doi.org/10.1002/cber.19100430257.

(23) Chadwick, R. C.; Gyzen, S. V.; Liogier, S.; Adronov, A. Scalable Synthesis of Strained Cyclooctyne Derivatives. *Synthesis* **2014**, *46* (5), 669–677. https://doi.org/10.1055/s-0033-1340509.

(24) Kuzmin, A.; Poloukhtine, A.; Wolfert, M. A.; Popik, V. V. Surface Functionalization Using Catalyst-Free Azide−Alkyne Cycloaddition. *Bioconjug. Chem.* **2010**, *21* (11), 2076–2085. https://doi.org/10.1021/bc100306u.

(25) Xu, Y.; Wang, T.; Guan, C.-J.; Li, Y.-M.; Liu, L.; Shi, J.; Bierer, D. Dmab/IvDde Protected Diaminodiacids for Solid-Phase Synthesis of Peptide Disulfide-Bond Mimics. *Tetrahedron Lett.* **2017**, *58* (17), 1677–1680. https://doi.org/10.1016/j.tetlet.2017.03.024.

(26) Snider, B. B.; Ahn, Y.; O'Hare, S. M. Total Synthesis of (±)-Martinellic Acid. *Org. Lett.* **2001**, *3* (26), 4217–4220. https://doi.org/10.1021/ol016884o.

(27) Turner, R. A.; Hauksson, N. E.; Gipe, J. H.; Lokey, R. S. Selective, On-Resin N-Methylation of Peptide N-Trifluoroacetamides. *Org. Lett.* **2013**, *15* (19), 5012–5015. https://doi.org/10.1021/ol402341u.

(28) Krebs, A.; Colberg, H. Untersuchungen über gespannte cyclische Acetylene, VIII. Hydrierung winkelgespannter Siebenring-Acetylene mit Alkoholen. *Chem. Ber.* **1980**, *113* (5), 2007–2014. https://doi.org/10.1002/cber.19801130534.

(29) Spang, W.; Hanack, M. Notizen. Hydrierung von Achtringacetylenen Mit Alkoholen. *Chem. Ber.* **1980**, *113* (5), 2025–2027. https://doi.org/10.1002/cber.19801130536.

5

Towards the synthesis of a fusion protein *via* a synthetic chemical ligation approach

Fusion proteins integrate two or more domains originating from different proteins into a single polypeptide chain. Such proteins are abundant in nature and scientists have copied nature's strategy to create synthetic fusion proteins that combine separate functions of the corresponding domains into a single entity.[1] Amongst the earliest examples are the polypeptide affinity tags fused to a protein of interest to simplify purification, or to enable its detection and monitoring, with minimal perturbation to its tertiary structure and biological activity. A prominent example is green fluorescent protein (GFP) that has been frequently used as a fusion

partner to act either as a tag to monitor the target's localization and fate or as an indicator, in which the GFP-fluorescence can be modulated post-translationally by its chemical environment or by protein-protein interactions.[2] Besides efforts to increase reaction rates in consecutive enzymatic reactions and to construct bifunctional enzymes, fusion proteins have also become an important class of therapeutic agents.[3–8] Fusion proteins have for instance found use in targeted drug delivery where the therapeutic protein can be linked to an antibody targeting a specific cell type or fused to a cell-penetrating peptide to efficiently transport the drug across the cell membrane.[9–11] In the context of biopharmaceuticals, fusion proteins, in which the biologically active protein is connected to Fc domains of antibodies or carrier proteins, have prolonged plasma half-lives and improved therapeutic efficacy compared to the unconjugated protein.[12,13] For instance, etanercept (tumor necrosis factor fused with Fc domain of IgG1) and aflibercept (extracellular domains of VEGF receptors 1 and 2 fused with Fc domain of IgG1) have found considerable success in the clinic, and both are listed in the ten top-selling biopharmaceuticals in 2017.[14]

Three main approaches exist for the construction of fusion peptides. The first one concerns domain insertion and entails insertion of the DNA-sequence encoding a domain of one protein into the gene of the second protein to establish the fusion. Tandem fusion is an approach in which the multiple domains are genetically connected end-to-end, usually via a linker peptide. Finally, post-translation conjugation comprises fusion of two proteins through (bio)chemical means after the proteins are individually expressed separating the fusion and expression step. Although the extra step in the latter approach inherently complicates the synthesis, this approach allows for modular pairing and assembly of the domains after expression in optimal hosts.[15] The conjugation of the domains can either be performed chemically through, for instance, lysine or thiol modifications, enzymatically by employing the frequently used sortase A or through split intein-mediated protein ligation (*Figure 1*).[16–18]

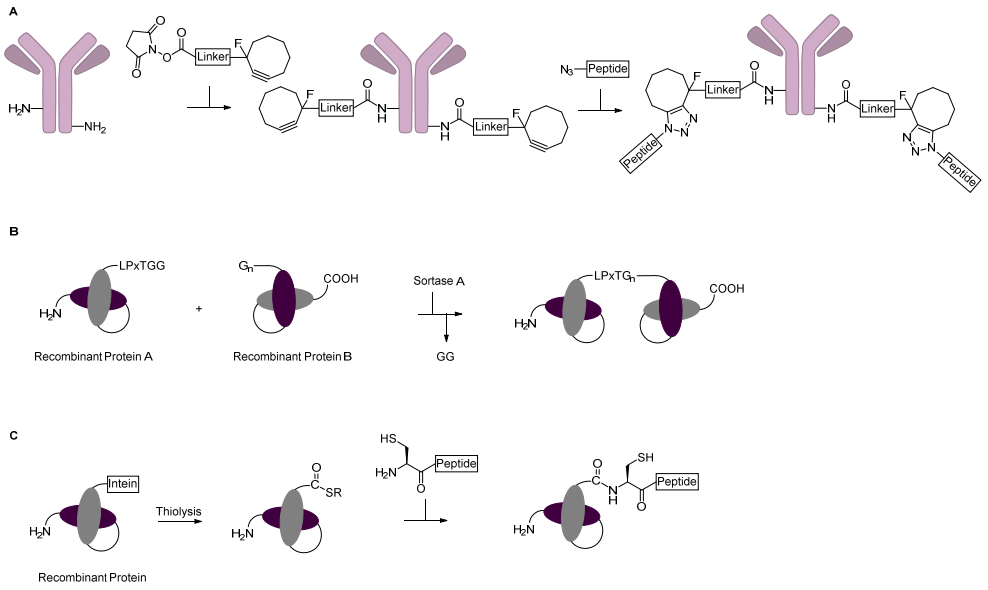

Figure 1. A. Chemical conjugation of multiple peptides to an antibody employing a copper-free conjugation strategy. *B.* Enzymatic fusion of two proteins by Sortase A. *C.* Split intein-mediated protein ligation with the generation of a C-terminal thioester.

The research described in this Chapter entails the synthesis of a fusion protein employing a chemical conjugation strategy with the emphasis on the late-stage derivatization of the individual proteins (*Figure 2*). For this purpose, both proteins will be genetically engineered with a thiol group for functionalization as this will allow for a variety of protein combinations to be assembled. Due to their unique characteristics, camelid single-domain antibodies were selected as a model system. Their good expression in microbial systems in combination with their beneficial biochemical properties (small size, good stability and solubility, high affinity and specificity for their antigen and strict monomeric behavior) makes VHH antibodies, also called nanobodies, well suited for the role of model proteins.[19] Nanobodies against PD-1 and CD4 are useful therapeutics, because $CD4^+$ T lymphocytes expressing PD-1 play a significant role in HIV persistence and T cell dysfunction and exhaustion in tumors. Hypothetically, a fusion protein of anti-PD-1 and anti-CD4 may accomplish a more selective targeting and restore antitumor response.[20–22] The respective nanobodies were genetically engineered to be equipped with a histidine tag for purification purposes and a C-terminal cysteine for conjugation purposes.

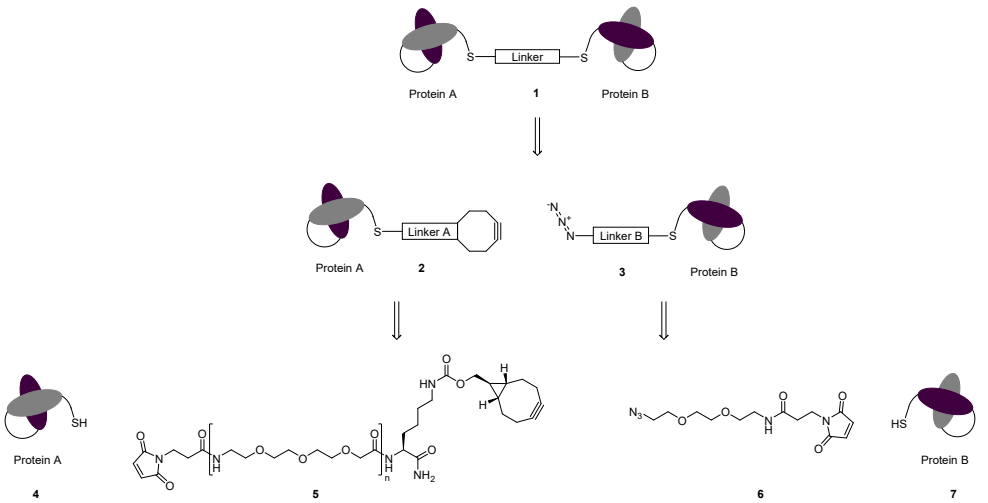

Figure 2. Design of a fusion protein with a late-stage conjugation strategy using a two-component linker system.

To construct the fusion protein, a two-component linker system was envisioned to facilitate late-stage fusion (*Figure 2*). First, bifunctional scaffold **5** equipped with a maleimide will be conjugated to the free thiol present on the anti-CD4 nanobody in a Michael addition reaction. Separately, the other VHH antibody (anti-PD-1) will be conjugated with bifunctional linker **6** in a similar fashion to construct derivatized protein **3**. With both nanobodies now bearing complementary conjugation partners (strained cyclooctyne and alkyl azide), the fusion will be achieved by a strain-promoted alkyne-azide cycloaddition (SPAAC) to furnish fusion protein **1**. The SPAAC was selected over the copper(I)-catalyzed Huisgen cycloaddition as the His-tag present on the VHH antibodies would hinder the reaction. The standard method with copper(II)sulfate and sodium ascorbate relies on the *in situ* reduction to the active copper(I) species, but bis(histidine)copper(II) complexes show negligible reduction to copper(I) by ascorbate in the presence of oxygen or argon.[23,24]

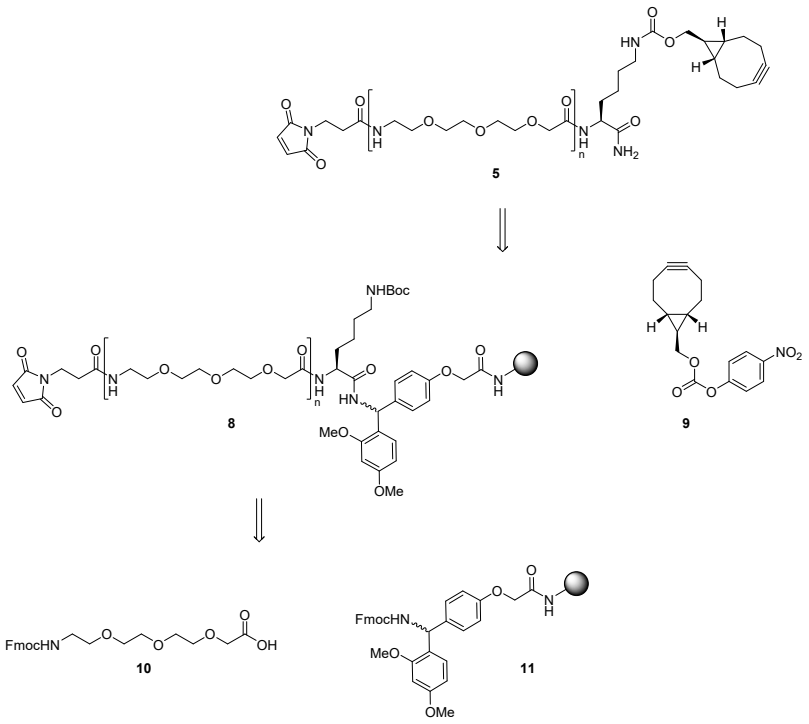

Figure 3. Retrosynthesis of bifunctional linker **5**.

Linkers play a crucial role in the fusion protein design providing an appropriate distance between the two domains in order to exhibit biological activity.[25] With that in mind, scaffold **5** was designed to allow for linker length variation by inserting ethylene glycol building block **10** multiple times (*Figure 3*). The synthesis of bifunctional linker **5** was envisioned using a solid-phase peptide chemistry approach. First, Rink amide resin **11** will be elongated with Fmoc-Lys(Boc)-OH for later functionalization. Then ethylene glycol building block **10** synthesized for use in an Fmoc-based solid-phase approach will be installed. The length of the linker can be varied at this stage based on the number of cycles with building block **10**. As an initial step, two ethylene glycol linkers will be installed. After installation of the maleimide functionality to furnish compound **8**, the linker will be cleaved from the resin liberating the ε-amine of the lysine. Reacting activated carbonate **9** with the free amine will finally give bifunctional linker **5**. The utility of linkers **5** and **6** is then demonstrated by the fusion of an anti-PD1 and anti-CD4 nanobody in the proposed manner (*Figure 2*). After conjugation of the linkers to either the anti-PD1 or anti-CD4

VHH antibody, the two differently functionalized proteins are fused through the strain-promoted alkyne-azide cycloaddition.

Results and discussion

First attention was focused on the synthesis of bifunctional linker **6** bearing an azide and maleimide moiety (*Scheme 1*). Starting from triethylene glycol **12**, tosylation of the diol with 4-toluenesulfonyl chloride and sodium hydroxide as the base furnished the corresponding ditosylate in 91% yield.

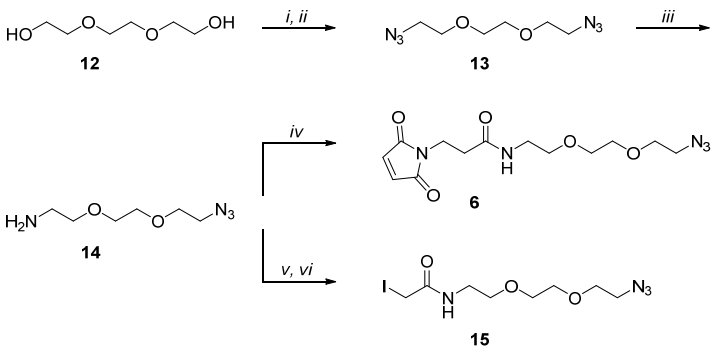

Scheme 1. Reagents and conditions: (*i*) TsCl, NaOH, DCM, 0 °C, 3 hrs, 91% (*ii*) NaN_3, TBAI, DMF, 80 °C, 17 hrs, 91% (*iii*) PPh_3, Et_2O, THF, 1.0 M aq. HCl, rt, 24 hrs, 71% (*iv*) (a) 3-maleimidopropionic acid NHS ester, DIPEA, THF, rt, 4 hrs, 10% (b) 3-maleimidopropionic acid, 1-(3-dimethylaminopropyl)-3-ethylcarbodiimide hydrochloride, DIPEA, DCM, rt, 17 hrs, <5% (*v*) chloroacetyl chloride, Et_3N, DCM, 0 °C, 2 hrs, 68% (*vi*) NaI, acetone, rt, 48 hrs, 84%.

Overnight substitution of the ditosylate with sodium azide at elevated temperatures gave diazide **13** in 91% yield. At this stage in the synthesis desymmetrization of the molecule was achieved by employing a biphasic system. Diazide **13** was dissolved in a mixture of diethyl ether and 1.0 M aq. HCl solution with tetrahydrofuran added as a phase transfer reagent and a solution of triphenylphosphine in ether was added dropwise. Upon formation of the iminophosphorane, hydrolysis and protonation of the resultant amine in the acidic, aqueous layer prevented the reduction of the second azide. After vigorously stirring the mixture for 24 hours, amine **14** was isolated in a yield of 71%. Next the installation of the maleimide moiety was attempted but the synthesis thereof proved to be abortive. Neither 3-maleimidopropionic acid and peptide coupling reagents (diisopropylcarbodiimide and 1-ethyl-3-(3-dimethylaminopropyl)carbodiimide were tried) nor the maleimide activated ester and a base gave satisfactory results. The yields were low and the isolation of maleimide derivative **6** was always accompanied with impurities. After a literature search it was found that this compound degrades in a matter of hours,

hence commercial products of this kind are sold as a two-component kit. It is hypothesized that the instability is in part caused by a [2+3] dipolar cycloaddition between the azide and maleimide. Usually this reaction occurs at elevated temperatures, but Constant and co-workers reported the formation of the dihydrotriazole at room temperature.[26–28]

With the maleimide being incompatible in the designed conjugation strategy, an alternative linker was synthesized bearing the iodoacetamide capable of alkylating the sulfhydryl group. First, amine **14** and triethylamine were dissolved in DMF and chloroacetyl chloride was added dropwise at 0 °C to obtain the corresponding chloroacetamide. The chloroacetamide was converted into iodoacetamide **15** in a classic Finkelstein reaction with sodium iodide in acetone in a yield of 84%.[29]

With one component of the designed linker system in hand, attention was shifted to bifunctional linker **5** equipped with a strained cyclooctyne and maleimide moiety. To control the overall length of the linker, the core of **5** consists of several repeats of ethylene glycol building block **10**, which was synthesized first (*Scheme 2*). The functional groups of **10** resemble a standard amino acid building block featuring an Fmoc-protected N-terminus and an unprotected C-terminus. The synthesis started from the symmetrical triethylene glycol **12** leaving two options for desymmetrization; starting the synthesis from the C-terminus and installing the N-terminus later or *vice versa*. Both options were investigated.

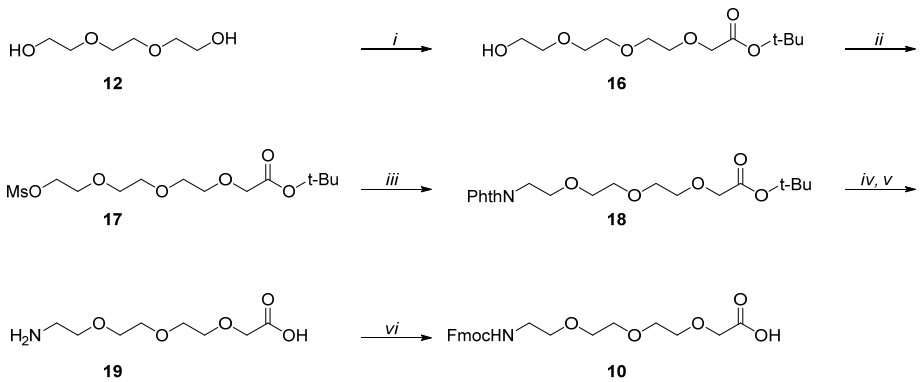

Scheme 2. Reagents and conditions: (*i*) NaH, TBAI, *tert*-butylbromoacetate, THF, 0 °C to rt, 17 hrs, 46% (*ii*) MsCl, Et_3N, DCM, 0 °C, 3 hrs, 88% (*iii*) KPhth, DMF, 110 °C, 3 hrs, 97% (*iv*) TFA, DCM, 1 hr (*v*) hydrazine hydrate, MeOH, 90 min., 70% (*vi*) Fmoc NHS ester, *N*-methylmorpholine, H_2O, 1,4-dioxane, 0 °C to rt, 17 hrs, 11%.

Triethylene glycol **12** was alkylated using sodium hydride and *tert*-butylbromoacetate in THF with TBAI acting as a catalyst giving *tert*-butyl ester **16** in a 46% yield (*Scheme 2*). The remaining alcohol was then mesylated with methanesulfonyl chloride and triethylamine in DCM with a yield of 88%. Reaction of mesylate ester **17** with potassium phthalimide in DMF at an elevated temperature furnished phthalimide-protected amine **18** in a 97% yield. Deprotection of the phthalimide **18** with hydrazine in methanol would convert the *tert*-butyl ester into an acylhydrazide. Therefore, the *tert*-butyl ester was deprotected first using trifluoroacetic acid in DCM followed by treatment with hydrazine in methanol to furnish zwitterion **19** in a yield of 70% over two steps. Finally, Fmoc-protected amine **10** was obtained by reacting zwitterion **19** with Fmoc NHS ester and *N*-methylmorpholine in a mixture of THF and water in 11% yield. The reaction was accompanied by a number of byproducts presumably due to the formation of the asymmetric anhydride and subsequent side-reactions.

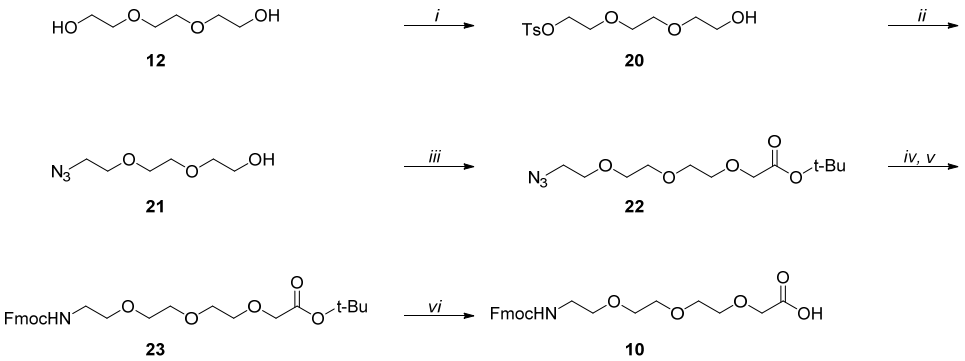

Scheme 3. Reagents and conditions: (*i*) TsCl, Et_3N, DCM, 0 °C to rt, 17 hrs, 98% (*ii*) NaN_3, DMF, 90 °C, 4 hrs, 82% (*iii*) KO^{t}Bu, *tert*-butyl bromoacetate, ^{t}BuOH, 30 °C to 50 °C, 6 hrs, 80% (*iv*) PPh_3, H_2O, THF, 0 °C to rt, 41 hrs, 89% (*v*) Fmoc NHS ester, *N*-methylmorpholine, DCM, 0 °C, 6 hrs, 96% (*vi*) 85% wt% aq. H_3PO_4, toluene, 4 hrs, 98%.

To first install the N-terminus, one alcohol was selectively tosylated by reaction with tosyl chloride and triethylamine in DCM giving tosylate **20** in a yield of 98% (*Scheme 3*). The azide group was employed as a masked amine instead of the phthalimido group to allow for milder deprotection conditions. Therefore, tosylate ester **20** was reacted with sodium azide in DMF at an elevated temperature to furnish azido **21** in 82% yield. The following installation of the C-terminus was achieved using different conditions than before as the quenching of the sodium hydride with water or methanol would lead to partial hydrolysis or transesterification of the *tert*-butyl

ester. Instead, a procedure by Heller and co-workers was followed where alcohol **21** was treated with potassium *tert*-butoxide as the base in *tert*-butanol at 30 °C followed by the addition of *tert*-butylbromoacetate and increasing the temperature to 50 °C.[30] After stirring for six hours, *tert*-butyl ester **22** was obtained in a yield of 80%.

Hydrogenation of azide **22** with 10 mol% Pd/C and 1.0 equivalent of 1.0 M aq. HCl in ethanol for four hours furnished the corresponding amine in a yield of 79%. It should be noted that when 2.0 equivalents of 1.0 M aq. HCl was used premature cleavage of the *tert*-butyl group was observed. Moreover, when performing the reaction on a large scale partial cleavage was also observed with only 1.0 equivalent of 1.0 M aq. HCl prompting a change in the deprotection method.

As an alternative, Staudinger reduction was employed to deprotect the azide functionality. Azide **22** was dissolved in THF and triphenylphosphine was added. After 20 hours, water was added and the reaction was stirred an additional 21 hours. The mixture was then diluted with DCM and washed three times with sat. aq. $NaHCO_3$. However, this work-up method led to low yields as a significant portion of the amine remained in the aqueous layer. Therefore, a revised work-up was employed where the reaction mixture was diluted with toluene and the organic layer extracted three times with water. Evaporation of the combined aqueous layers afforded the free amine in 89% yield. The free amine was then taken up in DCM and Fmoc NHS ester was added portion wise at 0 °C followed by addition of *N*-methylmorpholine. The reaction was stirred for six hours at 0 °C affording Fmoc-protected amine **23** in a yield of 96%. The final step comprised deprotection of the *tert*-butyl group to give building block **10**. The common method for this deprotection is treatment with trifluoroacetic acid in DCM, but on a large-scale evaporation of trifluoroacetic acid is troublesome. Therefore, a different procedure was sought with a more convenient work-up. The group of Hamilton describes the use of zinc bromide in DCM as a mild reagent for the deprotection of *tert*-butyl esters.[31] The subsequent isolation of the free carboxylic acid would only require washing the organic layer with water. Employing this procedure, *tert*-butyl ester **23** was dissolved in DCM and treated with 5.0 equivalents of zinc bromide. After 24 hours, the deprotection was still incomplete and adding extra zinc bromide did not lead to full deprotection. In another report by Li and co-workers aqueous phosphoric acid is used for deprotecting *tert*-butyl esters where isolation of the free carboxylic acid was also achieved using only washing steps.[32] Therefore, *tert*-butyl ester **23** was dissolved in toluene and 5.0 equivalents of 85% aq. H_3PO_4 was added slowly. After

stirring for four hours, water and ethyl acetate were added and the layers were separated. The aqueous phase was extracted two times with ethyl acetate and the combined organic layers were evaporated to successfully give free carboxylic acid **10** in a 98% yield.

Comparing the two methods for desymmetrization, alkylation of triethylene glycol **12** with *tert*-butylbromoacetate was accompanied by the formation of byproducts hampering the isolation, especially in large scale reactions. On the other hand, tosylation of triethylene glycol **12** proceeded cleanly and tosylate ester **20** could be isolated by extraction, which was not possible for *tert*-butyl ester **16**. This allowed a larger excess of triethylene glycol to be used, thereby increasing the yield of the mono-substituted product. This made the installation of the N-terminus first the preferred strategy.

With building block **10** in hand, attention was focused on the synthesis of a strained cyclooctyne needed for bifunctional scaffold **5**. The bicyclo[6.1.0]non-4-yne group was chosen because of its relative ease of synthesis combined with its ability to add to alkyl azides with fast reaction rates (*Scheme 4*). An additional advantage is the symmetrical nature of the molecule which leads to the formation of a single regioisomer upon cycloaddition.[33]

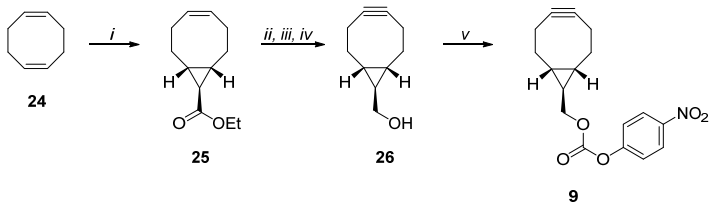

*Scheme 4.*Reagents and conditions: (*i*) ethyl diazoacetate, copper(II)acetylacetonate, EtOAc, reflux, 17 hrs, 44% (*ii*) $LiAlH_4$, Et_2O, rt, 15 min. (*iii*) Br_2, DCM, 0 °C, 5 min. (*iv*) KO^{t}Bu, THF, reflux, 2 hrs, 56% over 3 steps (*v*) *p*-nitrophenyl chloroformate, pyridine, DCM, rt, 15 min, 69%.

The first step was the cyclopropanation of 1,5-cyclooctadiene **24**. Instead of using rhodium acetate as the catalyst as was advocated in the first literature report on the synthesis of **25**, the less expensive copper acetylacetonate was employed.[33,34] Ethyl diazoacetate was slowly added to a solution of the copper catalyst and a large excess of 1,5-cyclooctadiene **24** in ethyl acetate after which the reaction was refluxed for 17 hours. Purification by silica gel column chromatography furnished *exo*-adduct **25** and the *endo*-adduct in a yield of 44% and 12% respectively. Continuing the synthesis, *exo*-adduct **25** was treated with lithium aluminum hydride in ether to give

the corresponding alcohol and bromination of the alkene followed by double elimination using potassium *tert*-butoxide in refluxing tetrahydrofuran afforded alkynol **26** in a yield of 56% over three steps. Finally, alcohol **26** was reacted with *p*-nitrophenyl chloroformate and pyridine in DCM to obtain activated carbonate ester **9** in a 69% yield.

Having both building blocks **9** and **10** now available, the synthesis of bifunctional scaffold **5** was undertaken next. To accommodate the option to vary the length of the linker, a solid-phase synthesis strategy was designed (*Scheme 5*). The choice was made for a C-terminal carboxamide over a carboxylic acid to simplify the synthesis and purification. To that end, the synthesis was started from TentaGel S RAM **27** and the amine was liberated by treatment with piperidine in DMF followed by six washing steps with DMF to remove any traces of piperidine.

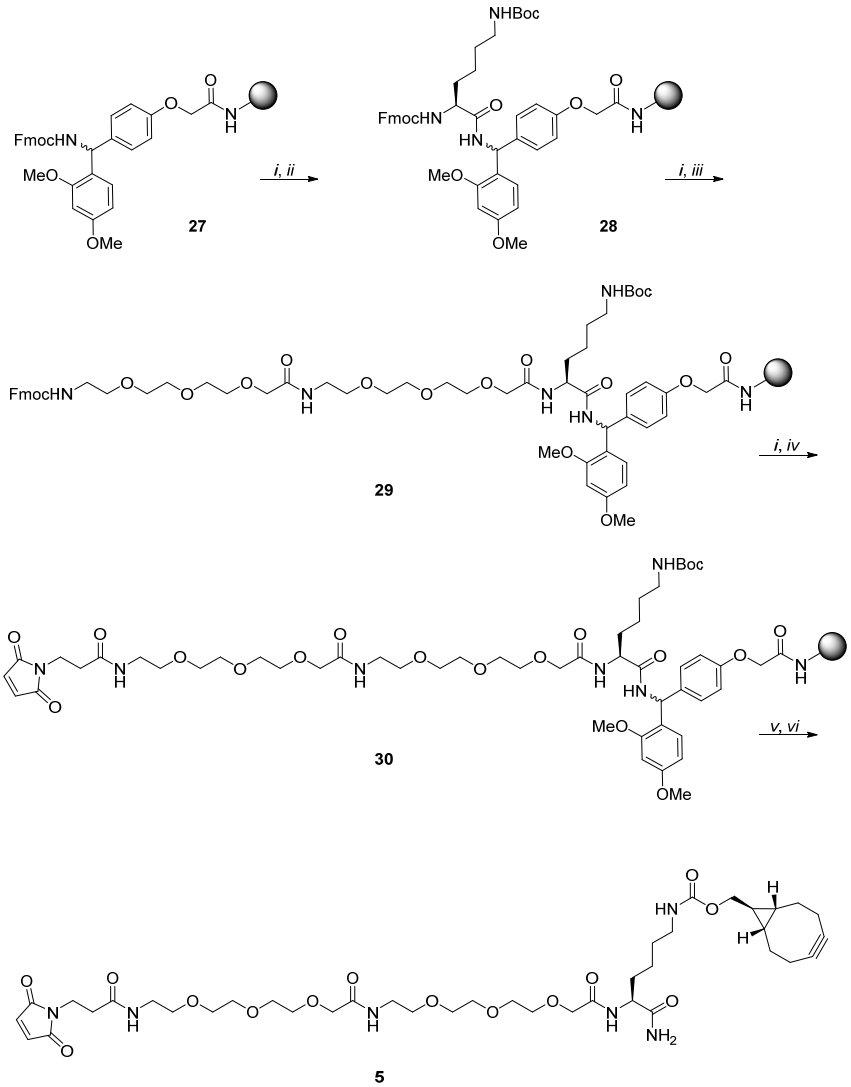

Scheme 5. Reagents and conditions: (*i*) piperidine, DMF, rt, 20 min (*ii*) Fmoc-Lys(Boc)-OH, HCTU, DIPEA, DMF, rt, 1 hr (*iii*) **10**, HCTU, DIPEA, DMF, rt, 1 hr (*iv*) 3-maleimidopropionic acid NHS ester, DIPEA, DMF, rt, 4 hrs (*v*) TFA – H_2O – TIPS (190:5:5), rt, 3 hrs (*vi*) **9**, DIPEA, DMF, rt, 4 hrs, 25%.

Standard peptide condensation conditions were employed to attach Fmoc-Lys(Boc)-OH to the resin. The lysine building block was dissolved in DMF and pre-activated for five minutes with HCTU and DIPEA before the solution was added to the resin. The reaction was shaken for one hour after which the resin was washed with DMF and the Fmoc group was deprotected using piperidine in DMF. The resin was

washed with DMF (6 x 30 sec.) and two entities of building block **10** were then installed using the same procedure as for the lysine building block. After liberation of the amine, the resin was elongated with a maleimide moiety by treatment of 3-maleimidopropionic acid NHS ester and DIPEA in DMF for four hours. At this stage, the compound was liberated from the resin using a cleavage cocktail (190:5:5, TFA – TIPS – H_2O) for three hours while simultaneously removing the Boc-group exposing a functionalization handle for the strained cyclooctyne. The suspension was filtered and the resin was washed with additional cleavage cocktail and the filtrate was evaporated. The crude product was taken up in DMF and the strained cyclooctyne was installed by treatment with activated carbonate ester **9** and DIPEA for four hours. Purification by preparative reversed-phase HPLC was attempted, but the formation of a byproduct was observed during either evaporation of the aqueous mixture or lyophilization. Instead, bifunctional scaffold **5** was purified by size exclusion chromatography followed by silica gel column chromatography yielding **5** in 25% yield.

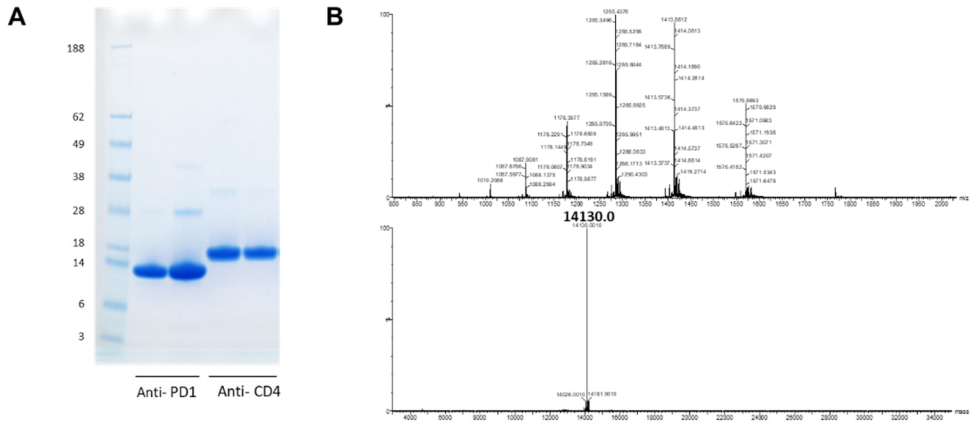

Figure 4.A. Visualization of the purified anti-PD1 and anti-CD4 VHH antibodies using SDS-PAGE. *B.* ESI-TOF spectrum of the anti-PD1 VHH antibody (upper panel), and deconvoluted mass spectrum (lower panel) with a calculated molecular weight of 14131.7 Da.

After having attained both bifunctional scaffold **5** and adapter **15** the feasibility of the protein conjugation chemistry was assessed. Towards that end the anti-PD1 (**4**) and anti-CD4 VHH antibodies equipped with a cysteine residue have been expressed and purified to near homogeneity (*Figure 4*). To test the conjugation approach, a homodimer of anti-PD1 antibodies was targeted. Nanobody **4** was first

reacted at its cysteine residue with an excess of scaffold **5** to provide protein **2** modified with the strained cyclooctyne and thus capable to react with alkyl azides under ambient and copper-free conditions. (*Figure 5*) The reaction was performed in aqueous buffer in the presence of TCEP to inhibit formation of unreactive disulfide bonded dimers from starting protein **4**. Progress of the reaction was monitored by MALDI-TOF spectrometry and complete conversion was observed after reacting the mixture at 0 °C for 30 minutes. Gel filtration of the solution afforded cyclooctyne-tagged protein **2**.

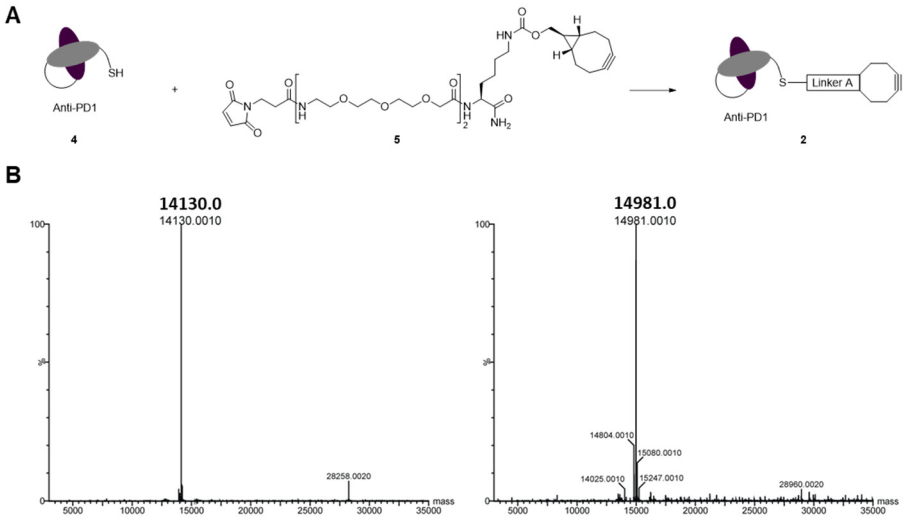

Figure 5.A. Reagents and conditions: compound **5** (30 equiv.), TCEP (1 mM), 0 °C, 30 min. *B.* Deconvoluted mass spectrum of anti-PD1 VHH antibody **4** (left panel) and deconvoluted mass spectrum of purified anti-PD1 nanobody conjugated to compound **5** (right panel) with a calculated molecular weight of 14982.6 Da.

Next, the anti-PD1 nanobody **3** equipped with an alkyl azide was prepared by a site-specific derivatization of the cysteine residue in protein **4** with iodoacetamide **15** (*Figure 6*). Compared to the previously performed thiol-maleimide conjugation, reaction of the iodoacetamide with the thiol proceeded at a slower rate. Optimization of the conjugation included increasing the equivalents of linker **15** and performing the reaction at room temperature. Under these conditions, complete conversion was achieved in two hours as observed by mass spectrometry. Lastly, purification by gel filtration furnished azido-tagged VHH antibody **3**.

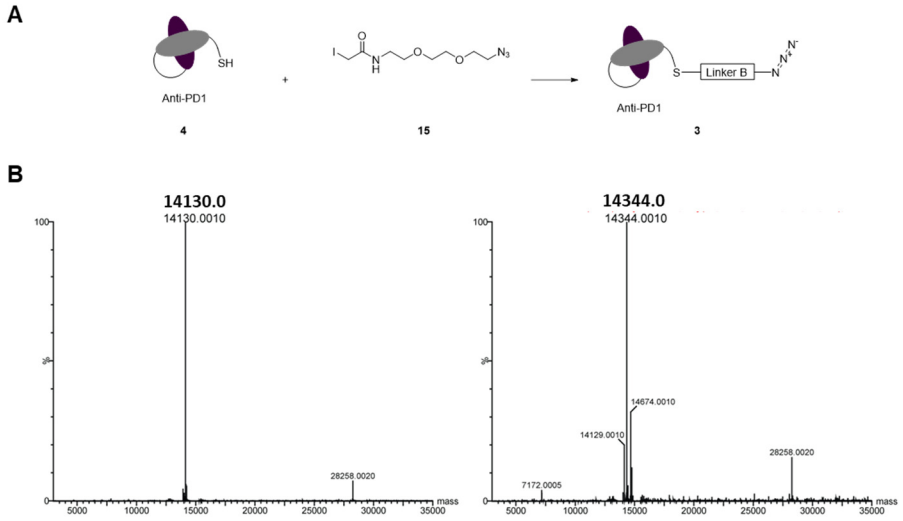

Figure 6.A. Reagents and conditions: compound **15** (50 equiv.), TCEP (1 mM), rt, 2 hrs. *B.* Deconvoluted mass spectrum of anti-PD1 VHH antibody **4** (left panel) and deconvoluted mass spectrum of purified anti-PD1 nanobody conjugated to compound **15** (right panel) with a calculated molecular weight of 14345.9 Da.

With both azido- and alkyne-tagged nanobodies **2** and **3** in hand, the preparation of a model fusion protein **1** by strain promoted cycloaddition reaction was attempted on a test scale following the reaction by mass spectrometry (*Figure 7*). Functionalized proteins **2** and **3** were mixed in aqueous buffer in a ratio of 1:2 (alkyne – azide). After 17 hours of incubation at room temperature showed the formation of expected fusion protein **1**. As a proof of principle, this result demonstrates the feasibility of fusing two VHH antibodies *via* the here-proposed synthetic chemical ligation. However, the reaction has not reached completion and to ensure synthesis of the bifunctional anti-CD4 and anti-PD1 fusion protein in the future further optimization is needed to gain access to suitable amounts of material that also need to be purified down the line. Performing the reaction at an elevated temperature and/or increasing the reaction time would be a reasonable starting point.

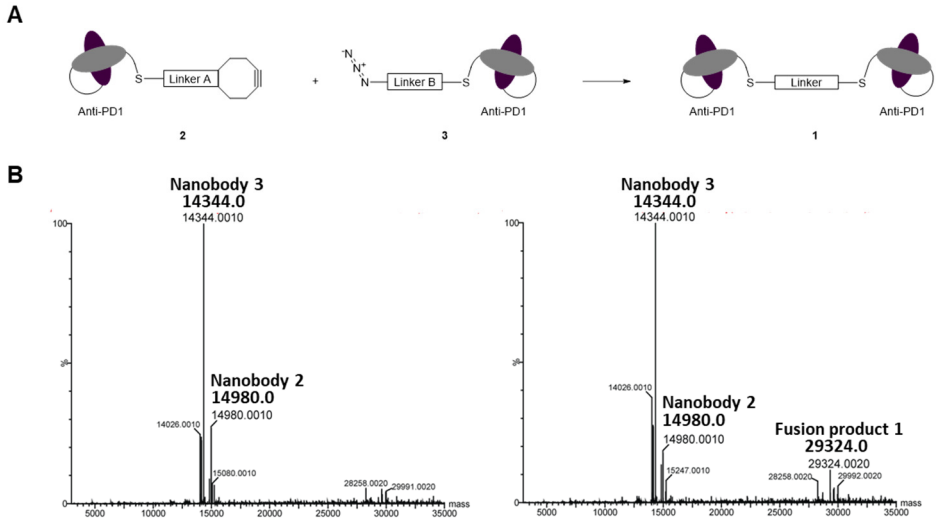

Figure 7.A. Reagents and conditions: nanobody **2** (1.0 equivalent), nanobody **3** (2.0 equivalent), rt, 17 hrs. *B.* Deconvoluted mass spectrum of reaction mixture at the start (left panel), and deconvoluted mass spectrum of the mixture after 17 hrs (right panel) showing formation of the fusion protein with a calculated molecular weight of 29328.5 Da.

Conclusion

This chapter demonstrates the feasibility of chemical conjugation of nanobodies *via* a new synthetic chemical ligation procedure. The designed approach focused on late-stage derivatization of the individual proteins necessitating a two-component linker system. Anti-CD4 and anti-PD1 VHH antibodies equipped with a C-terminal cysteine residue were expressed and purified to near homogeneity. Two linkers were envisioned equipped with a maleimide group to allow for ligation to the cysteine residue present on the nanobodies and either the strained cyclooctyne BCN or the complementary azido moiety. The linker equipped with the cyclooctyne and maleimide group was synthesized using a solid-phase approach. Separation between the two functionalities was achieved by an ethylene glycol building block which allowed for facile elongation during the on-resin synthesis. Purification by reversed-phase HPLC saw the formation of a single byproduct during either evaporation of the aqueous mixture or lyophilization. Instead, size exclusion chromatography followed by silica gel column chromatography proved successful in isolating the linker. As for the complementary linker, the combination of azide and maleimide functionalities proved to be incompatible and a switch was made to the iodoacetamide group. The conjugation of both linkers to anti-PD1 nanobodies

were readily achieved with the iodoacetamide-thiol ligation requiring additional equivalents of the linker and elevated reaction temperatures. A preliminary investigation was then conducted on the SPAAC ligation between the two anti-PD1 nanobodies, which demonstrated that fusion proteins can be formed in the proposed manner. Future research will demonstrate whether the procedure can be made more efficient in terms of scale at which it can be executed, yields and purities in terms of suppressing side reactions. Finally, the methodology can be utilized to produce homodimers, as shown here, but would be particularly attractive in the generation of heterodimers in a controlled fashion, yielding structurally homogeneous bioconjugates in which the nature, specifically also the size, of the spacer linking the two proteins can be controlled, simply through variation in the SPPS procedure as brought to bear in the construction of **5**, with respect to the number and nature of amino acids that are introduced at this stage.

General information

Materials, reactions and purification

Standard Fmoc-amino acids and resins for solid-phase peptide synthesis (SPPS), amino acids for solution-phase synthesis and peptide coupling reagents 2-(6-chloro-1*H*-benzotriazole-1-yl)-1,1,3,3-tetramethyluronium hexafluorophosphate (HCTU), *N*,*N*'-diisopropylcarbodiimide (DIC), 1-ethyl-3-(3-dimethylaminopropyl) carbodiimide hydrochloride (EDC), ethyl cyano(hydroxyimino)acetate (Oxyma Pure) and 1-hydroxybenzotriazole (HOBt) were purchased from Novabiochem or Sigma-Aldrich. The resin TentaGel S RAM (0.25 mmol/g) was bought from Rapp Polymere. 3-Maleimidopropionic acid NHS ester was available in-house. All other chemicals were purchased from Acros, Sigma Aldrich, VWR, Fluka, Merck and Fisher Scientific and used as received unless stated otherwise. Tetrahydrofuran (THF), *N*,*N*-dimethylformamide (DMF), dichloromethane (DCM), 1,4-dioxane and toluene were stored over molecular sieves before use. Commercially available ACS grade solvents were used for column chromatography without any further purification, except for toluene and ethyl acetate which were distilled prior to use. All reactions were carried out under a nitrogen atmosphere, unless indicated otherwise. Reaction progress and chromatography fractions were monitored by thin layer chromatography (TLC) on silica-gel-coated aluminium sheets with a F254 fluorescent indicator purchased from Merck (Silica gel 60 F_{254}). Visualization was achieved by UV absorption by fluorescence quenching, permanganate stain (4 g $KMnO_4$ and 2 g K_2CO_3 in 200 mL of H_2O), ninhydrin stain (0.6 g ninhydrin and 10 mL acetic acid in 200 mL ethanol). Silica gel column chromatography was performed using Screening Devices silica gel 60 (particle size of 40 – 63 μm, pore diameter of 60 Å) with the indicated eluent. Analytical reversed-phase high-performance liquid chromatography (RP-HPLC) was performed on a Thermo Finnigan Surveyor HPLC system with a Phenomenex Gemini C_{18} column (4.6 mm x 50 mm, 3 μm particle size) with a flow rate of 1 mL/min and a solvent gradient of 10-90% solvent B over 8 min coupled to a LCQ Advantage Max (Thermo Finnigan) ion-trap spectrometer (ESI^+). Preparative RP-HPLC was performed with a GX-281 Liquid Handler and a 331 and 332-H2 primary and secondary solvent pump respectively with a Phenomenex Gemini C_{18} or C_4 column (250 x 10.0 mm, 3 μm particle size) with a flow rate of 5 mL/min and solvent gradients as described for each compound. HPLC solvent compositions: solvent A is 0.1% (v/v) TFA in H_2O; solvent B is MeCN. Preparative RP-HPLC was also performed on an Agilent 1200 HPLC system coupled to a 6130 Quadrupole Mass Spectrometer using a Nucleodur C_{18} Gravity column (250 x 10.0 mm, 5 μm particle size) with a flow rate of 5 mL/min and a gradient over 12 min. as described for each compound. HPLC solvent composition: solvent A is 0.2% (v/v) TFA in H_2O and solvent B is MeCN. All HPLC solvents were filtered with a Millipore filtration system equipped with a 0.22 μm nylon membrane filter prior to use.

Characterization

Nuclear magnetic resonance (^1H and ^{13}C APT NMR) spectra were recorded on a Brüker DPX-300, Brüker AV-400, Brüker DMX-400, Brüker AV-500 or Brüker DMX-600 in the given solvent. Chemical shifts are reported in parts per million (ppm) with the residual solvent or tetramethylsilane (0 ppm) as reference. High-resolution mass spectrometry (HRMS) analysis was performed with a Thermo Finnigan LTQ Orbitrap mass spectrometer equipped with an electronspray ion source in positive mode (source voltage 3.5 kV, sheath gas flow 10 ml/min, capillary temperature 250 °C) with resolution R = 60000 at m/z 400 (mass range m/z = 150 – 2000) and dioctyl phthalate (m/z = 391.28428) as a "lock mass". The high-resolution mass spectrometer was calibrated prior to measurements with a Thermo Finnigan calibration mixture. Nominal and exact m/z values are reported in daltons.

Solid-phase peptide synthesis

General methodology

Manual solid-phase peptide synthesis

Manual amino acid couplings were carried out using a fritted reaction syringe equipped with a plunger and syringe cap or a manual reaction vessel (SHG-20260-PI, 60 mL) purchased from Peptides International. The syringe was shaken using either a Heidolph Multi Reax vortexer set at 1000 rpm or a St. John Associates 180° Flask Shaker (model no. A5-6027). Fmoc deprotection was achieved by agitating the resin with 20% (v/v) piperidine in DMF (2 x 10 min.). After draining the reaction vessel, the resin was washed with DMF (6 x 30 sec.). The appropriately side-chain protected Fmoc-amino acid (5.0 equiv.) in DMF (5.0 mL) was pre-activated with HCTU (5.0 equiv.) and DIPEA (10 equiv.) for 5 min, then added

to resin and agitated for 60 min. After draining the reaction vessel, the resin was washed with DMF (4 x 30 sec.). The completion of all couplings was assessed by a Kaiser test and double coupling was performed as needed.

Automated solid-phase peptide synthesis

The automated peptide coupling was performed on a CEM Liberty Blue microwave peptide synthesizer or a Protein Technologies Tribute peptide synthesizer using standard Fmoc protected amino acids. For the Tribute peptide synthesizer, amino acids were presented as solids and 0.20 M HCTU in DMF was used as activator, 0.50 M DIPEA in DMF as the activator base, 20% (v/v) piperidine in DMF as the deprotection agent and a 90:10, DMF – Ac_2O mixture as the capping agent. Coupling of each amino acid occurred at room temperature for 1 hr followed by a capping step (2x 3 min.) betwixt two washing steps. Subsequently, Fmoc was deprotected using the deprotection agent (2x 3 min.) followed by two more washing steps. For the Liberty Blue microwave synthesizer, amino acids were presented as a solution (0.20 M in DMF) and 0.50 M DIC in DMF was used as activator, 1.0 M Oxyma Pure in DMF as additive and 20% (v/v) piperidine in DMF as the deprotection agent. Amino acid coupling in the microwave synthesizer occurred at 90 °C for 2 min. followed by Fmoc deprotection at 90 °C using the aforementioned deprotection agent (2x 90 sec.) and two washing steps.

Loading calculation

Resin was dried before loading calculation by washing with DCM (3x 30 sec.) and Et_2O (3x 30 sec.) followed by purging with N_2. A small amount of resin (5 – 10 mg) was weighed and DMF (0.80 mL) was added and the resin was swollen for 20 min. Piperidine (0.20 mL) was then added and shaken for 20 min. Following the deprotection, the suspension was filtered and diluted with 20% (v/v) piperidine in DMF to a total volume of 10 mL in a volumetric flask. The absorption of this solution was measured against a blank 20% (v/v) piperidine in DMF solution using a Shimadzu UV-1601 UV-VIS spectrometer with a Quartz cuvette (optical pathway = 1 cm). The loading was then calculated using the following equation:

$$\text{Loading}_{\text{resin}} = \frac{A_{301.0\,\text{nm}} * 10^6\ \text{mmol mol}^{-1}\ \text{mg g}^{-1} * V * D}{\varepsilon_{301.0\,\text{nm}} * m_{\text{resin}} * l}$$

where:

$\text{Loading}_{\text{resin}}$ = Fmoc substitution in mmol/g
$A_{301.0\,\text{nm}}$ = Absorption of sample at 301.0 nm
10^6 mmol mol^{-1} mg g^{-1} = Conversion factor of mmol to mol and mg^{-1} to g^{-1}
V = Total volume in L
D = Dilution factor
$\varepsilon_{301.0\,\text{nm}}$ = Molar absorption coefficient at 301.0 nm (8021 L mol^{-1} cm^{-1})
m_{resin} = sample weight of the resin in mg
l = optical path length of the cell in cm

***tert*-Butyl 2-(2-(2-(2-hydroxyethoxy)ethoxy)ethoxy)acetate**

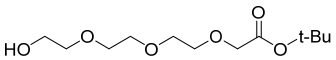

16

To a solution of triethylene glycol **12** (5.3 mL, 40 mmol, 2.0 equiv.) in THF (0.20 L, 0.10 M) at 0 °C was added sodium hydride (0.88 g, 22 mmol, 1.1 equiv.). After 5 min., Tetrabutylammonium iodide (0.74 g, 2.0 mmol, 10 mol%) and *tert*-butyl bromoacetate (3.0 mL, 20 mmol, 1.0 equiv.) were added and the reaction was stirred at room temperature. After 17 hrs, the reaction mixture was filtered. The filtrate was concentrated and purified by silica gel column chromatography (EA) obtaining ester **16** (2.4 g, 9.2 mmol, 46%) as a pale yellow oil.

^{1}H NMR (400 MHz, $CDCl_3$) δ 4.03 (s, 2H, CH_2COO^{t}Bu), 3.76 – 3.65 (m, 10H, OCH_2, CH_2OH), 3.63 – 3.60 (m, 2H, OCH_2), 2.69 (br s, 1H, O*H*), 1.48 (s, 9H, COO^t*Bu*).

^{13}C NMR (101 MHz, $CDCl_3$) δ 169.7 (*C*OO^{t}Bu), 81.7 (*C*CH$_3$), 72.6 (OCH$_2$), 70.8 (OCH$_2$), 70.7 (OCH$_2$), 70.7 (OCH$_2$), 70.4 (OCH$_2$), 69.1 (*C*H$_2$COO^{t}Bu), 61.8 (*C*H$_2$OH), 28.2 (*C*H$_3$).

***tert*-Butyl 2-(2-(2-(2-((methylsulfonyl)oxy)ethoxy)ethoxy)ethoxy)acetate**

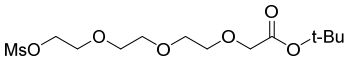

17

Ester **16** (2.0 g, 7.6 mmol, 1.0 equiv.) and Et_3N (2.1 mL, 15 mmol, 2.0 equiv.) were dissolved in DCM (77 mL, 0.10 M) and the solution was cooled to 0 °C. MsCl (0.67 mL, 8.7 mL, 1.2 equiv.) was slowly added and the reaction was stirred for 3 hrs at 0 °C gradually warming to room temperature. The solution was diluted with DCM and subsequently washed with 10% aq. $KHSO_4$ (3x), 10% aq. $NaHCO_3$ (3x) and brine (1x). The organic layer was dried (Na_2SO_4), filtered and concentrated *in vacuo*. After silica gel column chromatography (2:3, EA – Pentane to 4:1, EA – Pentane), mesylate **17** (2.3 g, 6.7 mmol, 88%) was furnished as a colorless oil.

^{1}H NMR (400 MHz, $CDCl_3$) δ 4.42 – 4.35 (m, 2H, CH_2OMs), 4.01 (s, 2H, CH_2COO^{t}Bu), 3.81 – 3.74 (m, 2H, CH_2CH$_2$OMs), 3.72 – 3.64 (m, 8H, OCH_2), 3.08 (s, 3H, CH_3SO$_2$), 1.48 (s, 9H, COO^t*Bu*).

^{13}C NMR (101 MHz, $CDCl_3$) δ 169.7 (*C*OO^{t}Bu), 81.7 (*C*CH$_3$), 70.8 (OCH$_2$), 70.8 (OCH$_2$), 70.7 (OCH$_2$), 70.7 (OCH$_2$), 69.4 (OCH$_2$), 69.2 (*C*H$_2$OMs), 69.1 (*C*H$_2$COO^{t}Bu), 37.9 (*C*H$_3$SO$_2$), 28.2 (*C*H$_3$).

***tert*-Butyl 2-(2-(2-(2-(1,3-dioxoisoindolin-2-yl)ethoxy)ethoxy)ethoxy)acetate**

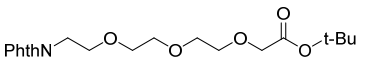

18

A solution of mesylate **17** (0.26 g, 0.75 mmol, 1.0 equiv.) and potassium phthalimide (0.18 g, 0.98 mmol, 1.3 equiv.) in DMF (3.0 mL, 0.25 M) was heated to 110 °C and stirred for 3 hrs. DMF was evaporated and the resulting residue was dissolved in DCM and H_2O. The layers were separated and the organic layer was dried ($MgSO_4$), filtered and concentrated *in vacuo*. The concentrate was purified by silica gel column chromatography (1:9, EA – Pentane to 1:1, EA – Pentane) giving phthalimidate **18** (0.29 g, 0.73 mmol, 97%) as a yellow-green oil.

^{1}H NMR (400 MHz, $CDCl_3$) δ 7.89 – 7.80 (m, 2H, C*H*-arom), 7.76 – 7.69 (m, 2H, C*H*-arom), 3.99 (s, 2H, CH_2COO^{t}Bu), 3.90 (t, J = 5.8 Hz, 2H, PhthNCH_2), 3.75 (t, J = 5.8 Hz, 2H, PhthNCH$_2$CH_2), 3.71 – 3.58 (m, 8H, OCH_2), 1.47 (s, 9H, COO^t*Bu*).

^{13}C NMR (101 MHz, $CDCl_3$) δ 169.7 (*C*OO^{t}Bu), 168.2 (*C*O-Phth), 133.9 (*C*H-arom), 132.1 (*C*q-arom), 123.2 (*C*H-arom), 81.4 (*C*CH$_3$), 70.7 (OCH$_2$), 70.6 (OCH$_2$), 70.6 (OCH$_2$), 70.0 (OCH$_2$), 69.0 (*C*H$_2$COO^{t}Bu), 67.9 (PhthNCH$_2$CH$_2$), 37.2 (PhthNCH$_2$), 28.1 (*C*H$_3$).

2-(2-(2-(2-Aminoethoxy)ethoxy)ethoxy)acetic acid

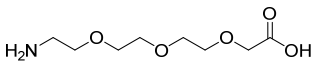

19

Phthalimidate **18** (0.20 g, 0.51 mmol, 1.0 equiv.) was dissolved in a mixture of DCM and TFA (1:1, TFA – DCM, 5.1 mL, 0.10 M) and the reaction was stirred at room temperature. After 1 hr, toluene was added and the solution was concentrated. The crude product was taken up in methanol (5.1 mL, 0.10 M) and hydrazine hydrate (0.25 mL, 5.1 mmol, 10 equiv.) was added. After stirring for 90 min. at room temperature, the solution was evaporated. Methanol was added, the resulting suspension filtered and the filtrate concentrated (15x) giving amine **19** (74 mg, 0.36 mmol, 70%) as a colorless oil.

^{1}H NMR (400 MHz, MeOD) δ 3.91 (s, 2H, CH_2COOH), 3.79 – 3.74 (m, 2H, H$_2$NCH$_2$CH_2), 3.74 – 3.61 (m, 8H, OCH_2), 3.16 – 3.08 (m, 2H, H$_2$NCH_2).

^{13}C NMR (101 MHz, MeOD) δ 178.0 (*C*OOH), 71.9 (OCH$_2$), 71.4 (OCH$_2$), 71.2 (OCH$_2$), 70.9 (OCH$_2$), 70.8 (OCH$_2$), 68.2 (*C*H$_2$COOH), 40.0 (NH$_2$*C*H$_2$).

1-(9*H*-Fluoren-9-yl)-3-oxo-2,7,10,13-tetraoxa-4-azapentadecan-15-oic acid

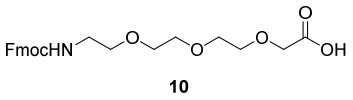

10

To a mixture of 1,4-dioxane and H_2O (2:1, 1,4-dioxane – H_2O, 21 mL, 0.13 M) were added amine **19** (0.55 g, 2.7 mmol, 1.0 equiv.) and *N*-methylmorpholine (0.88 mL, 8.0 mmol, 3.0 equiv.) and the solution was cooled to 0 °C. Fmoc *N*-hydroxysuccinimide ester (1.4 g, 4.0 mmol, 1.5 equiv.) was added portionwise and the reaction was stirred for 17 hours, gradually warming to room temperature. DCM and 1.0 M aq. HCl were added and the layers were separated. The organic phase was dried ($MgSO_4$), filtered and evaporated to dryness. Purification by silica gel column chromatography (3:97, MeOH – DCM to 1:9, MeOH – DCM) afforded title compound **10** (0.13 g, 0.29 mmol, 11%) as a pale yellow oil.

^{1}H NMR (400 MHz, MeOD) δ 7.76 (d, *J* = 7.5 Hz, 2H, C*H*-arom), 7.62 (d, *J* = 7.5 Hz, 2H, C*H*-arom), 7.37 (td, *J* = 7.5, 1.2 Hz, 2H, C*H*-arom), 7.29 (td, *J* = 7.4, 1.2 Hz, 2H, C*H*-arom), 4.33 (d, *J* = 6.9 Hz, 2H, CH_2-Fmoc), 4.17 (t, *J* = 6.9 Hz, 1H, C*H*-Fmoc), 3.97 (s, 2H, CH_2COOH), 3.64 – 3.55 (m, 8H, OCH_2), 3.51 (t, *J* = 5.4 Hz, 2H, FmocHNCH$_2$CH_2), 3.33 – 3.24 (m, 2H, FmocHNCH_2).

^{13}C NMR (101 MHz, MeOD) δ 176.6 (*C*OOH), 159.1 (NH*C*OO), 145.3 (*C*q-arom), 142.5 (*C*q-arom), 128.8 (*C*H-arom), 128.1 (*C*H-arom), 126.2 (*C*H-arom), 120.9 (*C*H-arom), 71.5 (FmocHNCH$_2$*C*H$_2$), 71.1 (O*C*H$_2$), 71.0 (O*C*H$_2$), 70.9 (O*C*H$_2$), 70.8 (*C*H$_2$COOH), 67.7 (*C*H$_2$-Fmoc), 48.4 (*C*H-Fmoc), 41.5 (FmocHN*C*H$_2$).

2-(2-(2-Hydroxyethoxy)ethoxy)ethyl 4-methylbenzenesulfonate

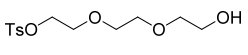

20

Triethylene glycol **12** (0.13 L, 1.0 mol, 10 equiv.) was dissolved in DCM (0.13 L, 0.80 M). The solution was cooled to 0 °C and Et_3N (21 mL, 0.15 mol, 1.5 equiv.) was added. Subsequently tosyl chloride (19 g, 0.10 mol, 1.0 equiv.) was added portionwise over 90 min. and the reaction was stirred for an additional 17 hrs gradually warming to room temperature. The mixture was washed with H_2O (3x) with each aqueous layer being back-extracted with DCM. The pooled organic layers were washed with 10% aq. citric acid (3x), dried ($MgSO_4$), filtered and concentrated *in vacuo* giving tosylate **20** (30 g, 98 mmol, 98%) as a pale yellow oil.

^{1}H NMR (500 MHz, $CDCl_3$) δ 7.82 – 7.77 (m, 2H, C*H*-arom), 7.37 – 7.33 (m, 2H, C*H*-arom), 4.18 – 4.15 (m, 2H CH_2OTs), 3.72 – 3.68 (m, 4H, CH_2OH, CH_2CH$_2$OTs), 3.60 (s, 4H, OCH_2), 3.58 – 3.55 (m, 2H, CH_2CH$_2$OH), 2.79 (br s, 1H, O*H*), 2.45 (s, 3H, CH_3).

^{13}C NMR (126 MHz, $CDCl_3$) δ 144.9 (*C*q-arom), 132.8 (*C*q-arom), 129.9 (*C*H-arom), 127.9 (*C*H-arom), 72.5 (CH$_2$CH$_2$OH), 70.7 (OCH$_2$), 70.2 (OCH$_2$), 69.2 (CH$_2$CH$_2$OTs), 68.6 (CH$_2$OTs), 61.6 (CH$_2$OH), 21.6 (CH$_3$).

HRMS (ESI-Orbitrap) calcd. for $C_{13}H_{21}O_6S$ $[M+H]^+$ 305.10534, found 305.10515.

2-(2-(2-Azidoethoxy)ethoxy)ethan-1-ol

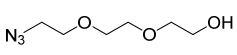

21

To a solution of tosylate **20** (0.12 kg, 0.40 mol, 1.0 equiv.) in DMF (0.18 L, 2.3 M) was added sodium azide (26 g, 0.40 mol, 1.0 equiv.) and the suspension was heated to 90 °C and stirred for 4 hrs. The mixture was filtered and the precipitate was washed with DMF. The filtrate was concentrated and the residue co-evaporated with toluene (2x). DCM was added, suspension was filtered and concentrated under reduced pressure (2x) affording azide **21** (58 g, 0.33 mol, 82%) as a yellow oil.

^{1}H NMR (500 MHz, $CDCl_3$) δ 3.74 (t, *J* = 4.3 Hz, 2H, CH_2OH), 3.71 – 3.67 (m, 6H, OCH_2), 3.64 – 3.60 (m, 2H, CH_2CH$_2$OH), 3.41 (t, *J* = 5.1 Hz, 2H, CH_2N$_3$), 2.75 (br s, 1H, O*H*).

^{13}C NMR (126 MHz, $CDCl_3$) δ 72.5 (CH$_2$CH$_2$OH), 70.6 (OCH$_2$), 70.4 (OCH$_2$), 70.0 (OCH$_2$), 61.7 (CH$_2$OH), 50.6 (CH$_2$N$_3$).

HRMS (ESI-Orbitrap) calcd. for $C_6H_{13}N_3O_3Na$ $[M+Na]^+$ 198.08491, found 198.08491.

***tert*-Butyl 2-(2-(2-(2-azidoethoxy)ethoxy)ethoxy)acetate**

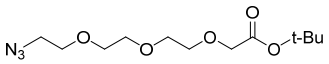

22

tert-Butanol (50 mL, 0.58 M) was warmed to 30 °C and azide **21** (5.0 g, 29 mmol, 1.0 equiv.) and potassium *tert*-butoxide (6.5 g, 58 mmol, 2.0 equiv.) were added. The reaction was stirred for 1hr after which *tert*-butyl bromoacetate (8.5 mL, 58 mmol, 2.0 equiv.) was slowly added. The suspension was further warmed to 50 °C and stirred for 5 hrs. The volatiles were removed under reduced pressure and the residue was taken up in DCM and H_2O. The layers were separated and the aqueous layer was back-extracted with DCM (3x). The pooled organic fractions were washed with brine, dried ($MgSO_4$), filtered and concentrated *in vacuo*. Purification by silica gel column chromatography (1:4, EA – Pentane to 3:2, EA – Pentane) furnished *tert*-butyl ester **22** (6.7 g, 23 mmol, 80%) as a yellow oil.

^{1}H NMR (500 MHz, $CDCl_3$) δ 4.03 (s, 2H, CH_2COO^tBu), 3.75 – 3.65 (m, 10H, OCH_2), 3.39 (t, *J* = 5.1 Hz, 2H, CH_2N_3), 1.48 (s, 9H, COO^tBu).
^{13}C NMR (126 MHz, $CDCl_3$) δ 169.7 (COO^tBu), 81.6 (CCH_3), 70.8 (OCH_2), 70.7 (OCH_2), 70.7 (OCH_2), 70.7 (OCH_2), 70.1 (OCH_2), 69.1 (CH_2COO^tBu), 50.7 (CH_2N_3), 28.1 (CH_3).
HRMS (ESI-Orbitrap) calcd. for $C_{12}H_{23}N_3O_5Na$ $[M+Na]^+$ 312.15299, found 312.15277.

***tert*-Butyl 2-(2-(2-(2-aminoethoxy)ethoxy)ethoxy)acetate**

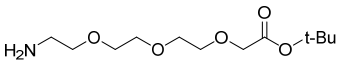

30

tert-Butyl ester **22** (0.50 g, 1.7 mmol, 1.0 equiv.) was dissolved in THF (13 mL, 0.13 M) and the solution was cooled to 0 °C. Triphenylphosphine (0.59 g, 2.3 mmol, 1.3 equiv.) was added portionwise and the reaction was stirred for 17 hrs slowly warming to room temperature. H_2O (81 μL, 4.5 mmol, 2.6 equiv.) was added and the reaction was stirred for an additional 24 hrs. Toluene and H_2O were added and the layers were separated. The organic layer was extracted with H_2O (2x) and the combined aqueous layers were concentrated under reduced pressure furnishing amine **30** (0.41 g, 1.5 mmol, 89%) as a yellow oil.
^{1}H NMR (400 MHz, $CDCl_3$) δ 4.03 (s, 2H, CH_2COO^tBu), 3.75 – 3.61 (m, 8H, OCH_2), 3.54 (t, *J* = 5.2 Hz, 2H, $CH_2CH_2NH_2$), 2.89 (t, *J* = 5.2 Hz, 2H, CH_2NH_2), 2.54 (s, 2H, NH_2), 1.48 (s, 9H, COO^tBu).
^{13}C NMR (101 MHz, $CDCl_3$) δ 169.7 (COO^tBu), 81.6 (CCH_3), 72.8 ($CH_2CH_2NH_2$), 70.6 (OCH_2), 70.5 (OCH_2), 70.5 (OCH_2), 70.2 (OCH_2), 69.0 (CH_2COO^tBu), 41.5 (CH_2NH_2), 28.1 (CH_3).
HRMS (ESI-Orbitrap) calcd. for $C_{12}H_{26}NO_5$ $[M+H]^+$ 264.18055, found 264.18045.

***tert*-Butyl 1-(9*H*-fluoren-9-yl)-3-oxo-2,7,10,13-tetraoxa-4-azapentadecan-15-oate**

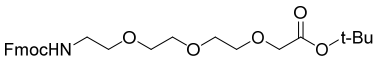

23

At 0 °C, DCM (2.5 mL, 0.15 M) was added to amine **30** (0.10 g, 0.38 mmol, 1.0 equiv.) and Fmoc *N*-hydroxysuccinimide ester (0.14 g, 0.42 mmol, 1.1 equiv.) was added portionwise. The reaction was stirred at 0 °C for 1 hr before *N*-methylmorpholine (42 μL, 0.38 mmol, 1.0 equiv.) was added. After stirring for another hr, additional *N*-methylmorpholine (42 μL, 0.38 mmol, 1.0 equiv.) was added and the solution was allowed to stir for 4 more hrs at 0 °C. The solution was washed with H_2O and the aqueous layer was back-extracted with DCM. The pooled organic layers were dried ($MgSO_4$), filtered and the volatiles were removed under reduced pressure. The crude was purified by silica gel column chromatography (1:4, EA – Pentane to 1:1, EA – Pentane) obtaining Fmoc-protected amine **23** (0.18 g, 0.37 mmol, 96%) as a light yellow oil.
^{1}H NMR (500 MHz, $CDCl_3$) δ 7.76 (dt, J = 7.6, 0.9 Hz, 2H, C*H*-arom), 7.61 (d, J = 7.5 Hz, 2H, C*H*-arom), 7.40 (td, J = 7.5, 0.9 Hz, 2H, C*H*-arom), 7.31 (td, J = 7.5, 1.2 Hz, 2H, C*H*-arom), 5.43 (t, J = 5.7 Hz, 1H, N*H*Fmoc), 4.39 (d, J = 7.1 Hz, 2H, CH_2-Fmoc), 4.22 (t, J = 7.0 Hz, 1H, C*H*-Fmoc), 4.00 (s, 2H, CH_2COO^tBu), 3.74 – 3.61 (m, 8H, OCH_2), 3.58 (t, J = 5.0 Hz, 2H, $CH_2CH_2NHFmoc$), 3.40 (q, J = 5.3 Hz, 2H, $CH_2NHFmoc$), 1.46 (s, 9H, COO^tBu).
^{13}C NMR (126 MHz, $CDCl_3$) δ 169.8 (COO^tBu) , 156.7 (NHCOO), 144.1 (*C*q-arom), 141.4 (*C*q-arom), 127.8 (*C*H-arom), 127.2 (*C*H-arom), 125.2 (*C*H-arom), 120.1 (*C*H-arom), 81.7 (CCH_3), 70.8 (OCH_2), 70.7 (OCH_2), 70.7 (OCH_2), 70.4 (OCH_2), 70.2 ($CH_2CH_2NHFmoc$), 69.1 (CH_2COO^tBu) , 66.7 (CH_2-Fmoc), 47.4 (*C*H-Fmoc), 41.0 ($CH_2NHFmoc$), 28.2 (CH_3).
HRMS (ESI-Orbitrap) calcd. for $C_{27}H_{35}NO_7Na$ $[M+Na]^+$ 508.23057, found 508.23016.

1-(9*H*-Fluoren-9-yl)-3-oxo-2,7,10,13-tetraoxa-4-azapentadecan-15-oic acid

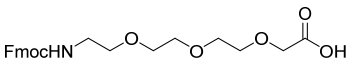

10

tert-Butyl ester **23** (39 g, 81 mmol, 1.0 equiv.) was dissolved in toluene (20 mL, 4.0 M) and 85% wt. aq. H_3PO_4 (28 mL, 0.40 mol, 5.0 equiv.) was slowly added. The reaction was stirred at room temperature for 4 hrs after which EA and H_2O were added. The layers were separated and the aqueous phase was extracted with EA (2x). The pooled organic fractions were dried ($MgSO_4$), filtered and concentrated under reduced pressure to furnish carboxylic acid **10** (34 g, 79 mmol, 98%) as a pale yellow oil.
^{1}H NMR (500 MHz, $CDCl_3$) δ 7.75 (d, *J* = 7.6 Hz, 2H, C*H*-arom), 7.60 (d, *J* = 7.5 Hz, 2H, C*H*-arom), 7.38 (t, *J* = 7.5 Hz, 2H, C*H*-arom), 7.30 (td, *J* = 7.5, 1.2 Hz, 2H, C*H*-arom), 7.06 (br s, 1H, COO*H*), 5.58 (t, *J* = 5.9 Hz, 1H, Fmoc*H*N), 4.39 (d, *J* = 7.0 Hz, 2H, CH_2-Fmoc), 4.21 (t, *J* = 7.0 Hz, 1H, C*H*-Fmoc), 4.12 (s, 2H, CH_2COOH), 3.79 – 3.59 (m, 8H, OCH_2), 3.55 (t, *J* = 5.1 Hz, 2H, $CH_2CH_2NHFmoc$), 3.39 (q, *J* = 5.3 Hz, 2H, $CH_2NHFmoc$).

^{13}C NMR (126 MHz, $CDCl_3$) δ 172.7 (*C*OOH), 156.8 (NH*C*OO), 144.1 (Cq-arom), 141.4 (Cq-arom), 127.7 (*C*H-arom), 127.1 (*C*H-arom), 125.2 (*C*H-arom), 120.0 (*C*H-arom), 71.2 (OCH_2), 70.5 (OCH_2), 70.3 (OCH_2), 70.2 (OCH_2), 70.1 (OCH_2), 68.7 (CH_2COOH), 66.7 (CH_2-Fmoc), 47.3 (*C*H-Fmoc), 40.9 (CH_2NHFmoc).
HRMS (ESI-Orbitrap) calcd. for $C_{23}H_{28}NO_7$ $[M+H]^+$ 430.18603, found 430.18607.

(1*R*,8*S*,9*r*,*Z*)-Ethyl bicyclo[6.1.0]non-4-ene-9-carboxylate

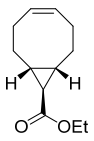

25

Cyclooctadiene **24** (0.20 L, 1.6 mol, 8.0 equiv.) and copper(II)acetylacetonate (1.1 g, 4.0 mmol, 2.0 mol%) were dissolved in EA (0.10 L, 2.0 M). A solution of ethyl diazoacetate (20 mL, 0.20 mol, 1.0 equiv.) in EA (0.10 L, 2.0 M) was added dropwise over 3 hrs and the reaction mixture was refluxed for 17 hrs. EA was removed under reduced pressure. Excess cyclooctadiene was removed by flushing the crude over silica (1:200, EA – Pentane) after which the product was eluted with EA. The solution was concentrated *in vacuo* and purified by silica gel column chromatography (toluene) to afford *exo*-product **25** (17 g, 88 mmol, 44%) and *endo*-product (4.6 g, 24 mmol, 12%) as light yellow oils.

Exo-product **25**
^{1}H NMR (400 MHz, $CDCl_3$) δ 5.66 – 5.56 (m, 2H, C*H*=C*H*), 4.09 (q, J = 7.1 Hz, 2H, CH_2-Ethyl), 2.32 – 2.24 (m, 2H, CH_2Cp), 2.22 – 2.13 (m, 2H, CH_2CH=CH), 2.11 – 2.00 (m, 2H, CH_2CH=CH), 1.61 – 1.52 (m, 2H, C*H*-bridgehead), 1.51 – 1.40 (m, 2H, CH_2Cp), 1.23 (t, J = 7.2 Hz, 3H, CH_3-ethyl), 1.17 (t, J = 4.6 Hz, 1H, C*H*).
^{13}C NMR (101 MHz, $CDCl_3$) δ 174.5 (*C*OOEt), 130.0 (*C*H=CH), 60.3 (OCH_2CH_3), 28.3 (CH_2CH=CH), 27.9 (*C*H), 27.8 (*C*H-Bridgehead), 26.7 (CH_2Cp), 14.4 (OCH_2CH_3).
Endo-product
^{1}H NMR (400 MHz, $CDCl_3$) δ 5.67 – 5.53 (m, 2H, C*H*=C*H*), 4.11 (q, *J* = 7.1 Hz, 2H, CH_2-Ethyl), 2.57 – 2.42 (m, 2H, CH_2Cp), 2.26 – 2.16 (m, 2H, CH_2CH=CH), 2.13 – 1.96 (m, 2H, CH_2CH=CH), 1.90 – 1.76 (m, 2H, CH_2Cp), 1.70 (t, *J* = 8.8 Hz, 1H, C*H*), 1.46 – 1.32 (m, 2H, C*H*-bridgehead), 1.26 (t, *J* = 7.1 Hz, 3H, CH_3-Ethyl).
^{13}C NMR (101 MHz, $CDCl_3$) δ 172.4 (*C*OOEt), 129.5 (*C*H=*C*H), 59.8 (OCH_2CH_3), 27.2 (CH_2CH=CH), 24.3 (*C*H-Bridgehead), 22.8 (CH_2Cp), 21.3 (*C*H), 14.5 (OCH_2CH_3).

((1*R*,8*S*,9*r*)-bicyclo[6.1.0]non-4-yn-9-yl)methanol

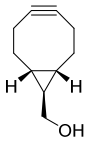

26

$LiAlH_4$ (0.24 g, 6.3 mmol, 0.90 equiv.) was added to Et_2O (26 mL, 0.27 M) and the suspension was cooled to 0 °C. A solution of ethyl ester **25** (1.4 g, 7.0 mmol, 1.0 equiv) in Et_2O (26 mL, 0.27 M) was added dropwise over 30 min. The suspension was stirred for 15 min. at room temperature, then cooled down to 0 °C. H_2O was added slowly until the grey solid had turned white. The suspension was dried (Na_2SO_4), filtered and the residue washed with copious amounts of Et_2O. The filtrate was concentrated under reduced pressure. The crude was dissolved in DCM (55 mL, 0.13 M) and cooled to 0 °C. Bromine (0.40 mL, 7.7 mmol, 1.1 equiv.) was added dropwise until the yellow color persisted. The excess bromine was quenched with sat. aq. Na_2SO_3 and the mixture was extracted with DCM (2x). The pooled organic fractions were dried (Na_2SO_4), filtered and concentrated *in vacuo*. The crude dibromide was taken up in THF (65 mL, 0.11 M) and cooled to 0 °C. To this solution was added KO^{t}Bu (1.0 M in THF, 23 mL, 23 mmol, 3.3 equiv.) dropwise and the mixture was heated to reflux and stirred for 2 hrs. After the reaction was cooled, the mixture was quenched with sat. aq. NH_4Cl and subsequently extracted with DCM (3x). The combined organic layers were dried (Na_2SO_4), filtered and concentrated under reduced pressure. Purification by silica gel column chromatography (1:9, EA – Pentane to 2:3, EA – Pentane) afforded strained alkyne **26** (0.59 g, 3.9 mmol, 56%) as a white solid.
^{1}H NMR (300 MHz, $CDCl_3$) δ 3.55 (d, *J* = 6.3 Hz, 2H, CH_2OH), 2.47 – 2.37 (m, 2H, CH_2Cp), 2.36 – 2.22 (m, 2H, CH_2C≡C), 2.21 – 2.11 (m, 2H, CH_2C≡C), 2.09 (s, 1H, O*H*), 1.47 – 1.32 (m, 2H, CH_2Cp), 0.77 – 0.60 (m, 3H, C*H*-bridgehead, C*H*CH_2OH).
^{13}C NMR (75 MHz, $CDCl_3$) δ 98.9 (*C*≡*C*), 67.1 (*C*H_2OH), 33.5 (CH_2C≡C), 27.3 ($CHCH_2$OH), 22.6 (*C*H-Bridgehead), 21.5 (CH_2Cp).

((1*R*,8*S*,9*r*)-bicyclo[6.1.0]non-4-yn-9-yl)methyl (4-nitrophenyl) carbonate

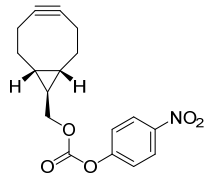

9

Alcohol **26** (2.7 g, 18 mmol, 1.0 equiv.) was dissolved in DCM (0.43 L, 43 mM) and pyridine (3.7 mL, 46 mmol, 2.5 equiv.) and *p*-nitrophenyl chloroformate (4.6 g, 23 mmol, 1.3 equiv.) were added. The solution was stirred at room temperature for 15 min after which the mixture was quenched with sat. aq. NH_4Cl. The mixture was subsequently extracted with DCM (3x) and the pooled organic layers were dried (Na_2SO_4), filtered and concentrated *in vacuo*. After silica gel column chromatography (1:9, EA – Pentane to 1:4, EA – Pentane), carbonate **9** (3.9 g, 13 mmol, 69%) was obtained as a white solid.

^{1}H NMR (400 MHz, $CDCl_3$) δ 8.32 – 8.26 (m, 2H, C*H*-arom), 7.44 – 7.35 (m, 2H, C*H*-arom), 4.23 (d, *J* = 6.8 Hz, 2H, CH_2O), 2.51 – 2.41 (m, 2H, CH_2Cp), 2.38 – 2.25 (m, 2H, CH_2C≡C), 2.23 – 2.13 (m, 2H, CH_2C≡C), 1.51 – 1.35 (m, 2H, CH_2Cp), 0.93 – 0.78 (m, 3H, C*H*-bridgehead, C*H*CH_2O).

^{13}C NMR (101 MHz, $CDCl_3$) δ 155.7 (*C*=O), 152.7 (*C*q-arom), 145.4 (*C*q-arom), 125.4 (CH-arom), 121.9 (*C*H-arom), 98.7 (*C*≡*C*), 74.0 (CH$_2$O), 33.2 (*C*H$_2$C≡C), 23.3 (*C*H-Bridgehead), 23.0 (*C*HCH$_2$O), 21.4 (CH$_2$Cp).

HRMS (ESI-Orbitrap) calcd. for $C_{17}H_{18}NO_5$ [M+H]$^+$ 317.12130, found 317.19331.

((1*R*,8*S*,9*r*)-bicyclo[6.1.0]non-4-yn-9-yl)methyl ((*S*)-29-carbamoyl-1-(2,5-dioxo-2,5-dihydro-1*H*-pyrrol-1-yl)-3,15,27-trioxo-7,10,13,19,22,25-hexaoxa-4,16,28-triazatritriacontan-33-yl)carbamate

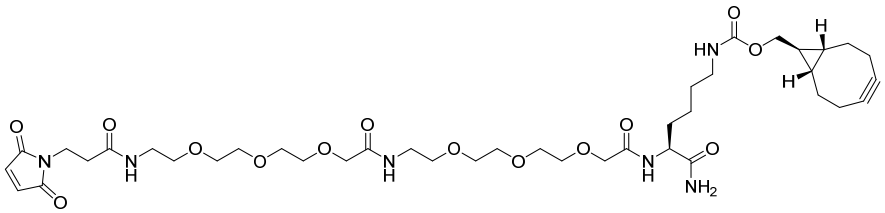

5

Using the procedure for manual peptide synthesis, Tentagel S RAM (0.25 mmol/g, 0.40 g, 0.10 mmol, 1.0 equiv.) was elongated with standard lysine building block and triethylene building block **10** to afford resin **28**. After Fmoc deprotection, a solution of 3-maleimido propionic acid NHS ester (68 mg, 0.30 mmol, 3.0 equiv.) and Hünig's base (52 μL, 0.30 mmol, 3.0 equiv.) in DMF (4.0 mL, 25 mM) was added to the resin and the resulting suspension was shaken for 4 hrs. The resin was washed with DMF (4x) and DCM (4x). A cleavage cocktail (190:5:5, TFA – H_2O – TIPS, 10 mL, 10 mM) was added and shaken for 3 hrs. The suspension was filtered and the filtrate was concentrated under a stream of N_2. The crude product was taken up in DMF (1.0 mL, 0.10 M) and Hünig's base (19 μL, 0.11 mmol, 1.1 equiv.) and BCN PNP carbonate **9** (35 mg, 0.11 mmol, 1.1 equiv.) were added. The reaction mixture was stirred for 4 hrs and subsequently evaporated at 20 °C. The crude product was purified by size exclusion chromatography (Sephadex LH-20, 1:1, MeOH – DCM) followed by silica gel column chromatography (1:99, MeOH – DCM to 7:93, MeOH – DCM) to afford linker **5** (21 mg, 25 μmol, 25%) as a colorless oil.

^{1}H NMR (500 MHz, $CDCl_3$) δ 7.43 (d, *J* = 8.5 Hz, 1H, N*H*-Lys), 7.32 (t, *J* = 6.0 Hz, 1H, *N*HCH$_2$CH$_2$O), 7.05 (t, *J* = 5.3 Hz, 1H, *N*HCH$_2$CH$_2$O), 6.71 (s, 2H, C*H*-Maleimide), 6.67 (s, 1H, N*H*$_2$), 6.02 (s, 1H, N*H*$_2$), 5.04 (t, *J* = 5.7 Hz, 1H, N*H*-BCN), 4.49 (td, *J* = 8.4, 5.7 Hz, 1H, α-Lys), 4.08 – 4.03 (m, 4H, OC*H*$_2$C=O), 3.95 (d, *J* = 6.9 Hz, 2H, C*H*$_2$OC=O), 3.83 (t, *J* = 7.2 Hz, 2H, C*H*$_2$N(C=O)$_2$), 3.73 – 3.60 (m, 16H, OC*H*$_2$), 3.60 – 3.56 (m, 2H, NHCH$_2$C*H*$_2$O), 3.53 (t, *J* = 5.1 Hz, 2H, NHCH$_2$C*H*$_2$O), 3.49 – 3.42 (m, 2H, NHC*H*$_2$), 3.42 – 3.36 (m, 2H, NHC*H*$_2$), 3.20 – 3.13 (m, 2H, ε-Lys), 2.52 (t, *J* = 7.2 Hz, 2H, C*H*$_2$CH$_2$N(C=O)$_2$), 2.42 – 2.36 (m, 2H, C*H*$_2$Cp), 2.31 – 2.24 (m, 2H, C*H*$_2$C≡C), 2.17 – 2.10 (m, 2H, C*H*$_2$C≡C), 1.96 – 1.87 (m, 1H, β-Lys)), 1.75 – 1.65 (m, 1H, β-Lys)), 1.58 – 1.52 (m, 2H, δ-Lys)), 1.43 – 1.31 (m, 4H, γ-Lys, C*H*$_2$C≡C), 0.77 – 0.70 (m, 2H, C*H*-bridgehead), 0.69 – 0.55 (m, 1H, C*H*CH$_2$OC=O).

^{13}C NMR (126 MHz, $CDCl_3$) δ 174.0 (NH$_2$*C*=O), 170.7 (*C*=O), 170.5 (*C*=O), 170.4 (*C*=O), 170.2 (*C*=O), 157.0 (*C*=O-urethane), 134.3 (*C*H-maleimide), 98.9 (*C*≡*C*), 71.2 (OCH$_2$), 70.8 (OCH$_2$), 70.7 (OCH$_2$), 70.6 (OCH$_2$), 70.5 (OCH$_2$), 70.4 (OCH$_2$), 70.3 (OCH$_2$), 70.3 (OCH$_2$), 70.1 (OCH$_2$), 70.0 (OCH$_2$), 70.0 (OCH$_2$), 69.7 (OCH$_2$), 69.0 (*C*H$_2$OC=O), 52.2 (α-Lys), 40.6 (ε-Lys), 39.3 (CH$_2$NHC=O), 38.7 (CH$_2$NHC=O), 34.5 (*C*H$_2$N(C=O)$_2$), 34.5 (*C*H$_2$CH$_2$N(C=O)$_2$), 33.4 (*C*H$_2$Cp), 31.5 (β-Lys), 29.5 (δ-Lys), 23.8 (CHCH$_2$OC=O), 22.9 (*C*H-bridgehead), 22.8 (γ-Lys), 21.5 (*C*H$_2$C≡C).

HRMS (ESI-Orbitrap) calcd. for $C_{40}H_{63}N_6O_{14}$ [M+H]$^+$ 851.43968, found 851.43964.

Triethylene glycol ditosylate

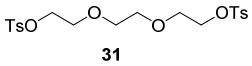

31

Triethylene glycol **12** (2.0 mL, 15 mmol, 1.0 equiv.) and *p*-toluenesulfonyl chloride (5.7 g, 30 mmol, 2.0 equiv.) were dissolved in DCM (75 mL, 0.20 M) and the solution was cooled to 0 °C. Powdered sodium hydroxide (4.8 g, 0.12 mol, 8.0 equiv.) was added portionwise and the mixture was stirred for 3 hrs at 0 °C. H_2O was added and the layers were separated. The aqueous phase was back-extracted with DCM (2x) and the combined organic layers were dried ($MgSO_4$), filtered and concentrated under reduced pressure. Purification by silica gel column chromatography (1:1, EA – Pentane) afforded ditosylate **31** (6.3 g, 14 mmol, 91%) as a white solid.

^{1}H NMR (400 MHz, $CDCl_3$) δ 7.84 – 7.75 (m, 4H, C*H*-arom), 7.38 – 7.30 (m, 4H, C*H*-arom), 4.15 – 4.12 (m, 4H, CH_2OTs), 3.67 – 3.63 (m, 4H, CH_2CH_2OTs), 3.52 (s, 4H, OCH_2), 2.44 (s, 6H, PhCH_3).

^{13}C NMR (101 MHz, $CDCl_3$) δ 145.0 (*C*q-arom), 133.0 (*C*q-arom), 130.0 (*C*H-arom), 128.0 (*C*H-arom), 70.7 (OCH_2), 69.3 (CH_2OTs), 68.8 (CH_2CH_2OTs), 21.7 (PhCH_3).

Triethylene glycol diazide

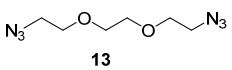

13

Ditosylate **31** (6.3 g, 14 mmol, 1.0 equiv.) and tetrabutylammonium iodide (0.25 g, 0.68 mmol, 5.0 mol%) were dissolved in DMF (20 mL, 0.70 M). Sodium azide (3.6 g, 55 mmol, 4.0 equiv.) was added and the mixture was heated to 80 °C and stirred for 17 hrs. The mixture was concentrated and further co-evaporation with *n*-heptane was performed to remove all traces of DMF. Et_2O was added, the resulting suspension was filtered and the filtrate concentrated (3x). Purification of the filtrate by silica gel column chromatography (2:3, EA – Pentane to 1:0, EA – Pentane) gave diazide **13** (2.5 g, 12 mmol, 91%) as a pale yellow oil.

^{1}H NMR (400 MHz, $CDCl_3$) δ 3.72 – 3.66 (m, 8H, OCH_2), 3.40 (t, *J* = 5.0 Hz, 4H, CH_2N_3).

^{13}C NMR (101 MHz, $CDCl_3$) δ 70.8 (OCH_2), 70.2 ($CH_2CH_2N_3$), 50.7 (CH_2N_3).

2-(2-(2-azidoethoxy)ethoxy)ethan-1-amine

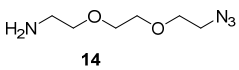

14

To diazide **13** (1.3 g, 6.3 mmol, 1.0 equiv.) was added a mixture of Et_2O, THF and 1.0 M aq. HCl (5:1:4, Et_2O – THF – 1.0 M aq. HCl, 19 mL, 0.32 M). A solution of PPh_3 (2.0 g, 9.3 mmol, 1.5 equiv.) in Et_2O (25 mL, 0.37 M) was added dropwise and the mixture was stirred vigorously for 24 hrs. To the mixture was added 4.0 M aq. HCl and the layers were separated. The aqueous layer was washed with Et_2O (2x) and subsequently brought to pH 14 by adding sodium hydroxide. The aqueous layer was then extracted with DCM (3x). The pooled organic fractions were dried ($MgSO_4$), filtered and concentrated *in vacuo* to furnish amine **14** (0.77 g, 4.4 mmol, 71%) as a yellow oil.

^{1}H NMR (400 MHz, $CDCl_3$) δ 3.66 – 3.53 (m, 6H, OCH_2), 3.46 (t, *J* = 5.2 Hz, 2H, C$H_2CH_2NH_2$), 3.33 (t, *J* = 5.0 Hz, 2H, CH_2N_3), 2.80 (t, *J* = 5.2 Hz, 2H, CH_2NH_2), 1.60 (br s, 2H, NH_2).

^{13}C NMR (101 MHz, $CDCl_3$) δ 73.4 ($CH_2CH_2NH_2$), 70.6 (OCH_2), 70.3 (OCH_2), 70.0 (OCH_2), 50.6 (CH_2N_3), 41.7 (CH_2NH_2).

***N*-(2-(2-(2-azidoethoxy)ethoxy)ethyl)-2-chloroacetamide**

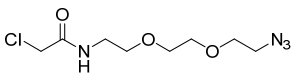

32

Amine **14** (35 mg, 0.20 mmol, 1.0 equiv.) and Et_3N (36 µL, 0.26 mmol, 1.3 equiv.) were dissolved in DCM (1.0 mL, 0.20 M) and the solution was cooled to 0 °C. Chloroacetyl chloride (21 µL, 0.26 mmol, 1.3 equiv.) was added dropwise and the reaction was stirred for 2 hrs at 0 °C. Additional DCM was added and the mixture was washed with sat. aq. $NaHCO_3$ (2x), H_2O and brine. The organic layer was dried ($MgSO_4$), filtered and the volatiles were removed under reduced pressure. Purification by silica gel column chromatography (1:49, MeOH – DCM) afforded chloroacetamide **32** (34 mg, 0.14 mmol, 68%) as a colorless oil.

^{1}H NMR (300 MHz, $CDCl_3$) δ 7.01 (br s, 1H, N*H*), 4.06 (s, 2H, CH_2Cl), 3.73 – 3.57 (m, 8H, OCH_2), 3.55 – 3.48 (m, 2H, CH_2NHClAc), 3.45 – 3.36 (m, 2H, CH_2N_3).

^{13}C NMR (75 MHz, $CDCl_3$) δ 166.1 (*C*=O), 70.7 (OCH_2), 70.5 (OCH_2), 70.2 (OCH_2), 69.6 (CH_2CH_2NHClAc), 50.8 (CH_2N_3), 42.7 (CH_2Cl), 39.7 (CH_2NHClAc).

_N_-(2-(2-(2-azidoethoxy)ethoxy)ethyl)-2-iodoacetamide

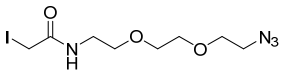

15

Chloroacetamide **32** (34 mg, 0.14 mmol, 1.0 equiv.) was dissolved in acetone (1.0 mL, 0.14 M) and sodium iodide (61 mg, 0.41 mmol, 3.0 equiv.) was added. The reaction was stirred for 48 hrs and subsequently concentrated *in vacuo* and purified by silica gel column chromatography (1:39, MeOH – DCM) to give iodoacetamide **15** (39 mg, 0.11 mmol, 84%) as a pale yellow oil.

^{1}H NMR (400 MHz, $CDCl_3$) δ 6.57 (s, 1H, N*H*), 3.75 – 3.64 (m, 8H, OCH_2, CH_2I), 3.61 – 3.55 (m, 2H, CH_2CH_2N$_3$), 3.51 – 3.46 (m, 2H, CH_2NHIAc), 3.42 (t, *J* = 4.9 Hz, 2H, CH_2N$_3$).

^{13}C NMR (101 MHz, $CDCl_3$) δ 167.3 (*C*=O), 70.6 (OCH_2), 70.4 (OCH_2), 70.3 (OCH_2), 69.5 (CH_2CH_2NHIAc), 50.8 (CH_2N_3), 40.2 (CH_2NHIAc), -0.5 (CH_2I).

Strained cyclooctyne-functionalized anti-PD1 nanobody

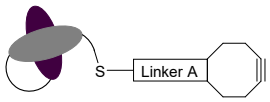

anti-PD1 **2**

A solution of anti-PD1 VHH antibody **4** (0.30 mg, 21 nmol, 1.0 equiv.) and tris(2-carboxyethyl)phosphine (57 µg, 0.20 µmol, 9.5 equiv.) in aqueous buffer (0.20 mL, 0.11 mM) was cooled to 0 °C and compound **5** (0.54 mg, 0.64 µmol, 30 equiv.) was added. The reaction was stirred for 30 min. at 0 °C after which conjugated nanobody **2** was purified by gel filtration.

MS (ESI-TOF) calcd. 14982.6 (MW), found 14981.0.

Azide-functionalized anti-PD1 nanobody

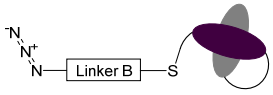

3 anti-PD1

To a solution of anti-PD1 VHH antibody **4** (0.30 mg, 21 nmol, 1.0 equiv.) and tris(2-carboxyethyl)phosphine (57 µg, 0.20 µmol, 9.5 equiv.) in aqueous buffer (0.20 mL, 0.11 mM) was added compound **15** (0.36 mg, 1.1 µmol, 50 equiv.) was added. The reaction was stirred for 2 hrs at room temperature after which conjugated nanobody **3** was purified by gel filtration.

MS (ESI-TOF) calcd. 14345.9 (MW), found 14344.0.

Anti-PD1 VHH antibody homodimer

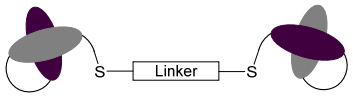

anti-PD1 **1** anti-PD1

To a solution of cyclooctyne-functionalized nanobody **2** (10 µg, 0.67 nmol, 1.0 equiv.) in aqueous buffer (6.7 µL, 0.10 mM) was added azide-functionalized VHH antibody **3** (19 µg, 1.3 nmol, 2.0 equiv.). The reaction was stirred for 17 hrs at room temperature.

MS (ESI-TOF) calcd. 29328.5 (MW), found 29324.0.

References

(1) Aroul-Selvam, R.; Hubbard, T.; Sasidharan, R. Domain Insertions in Protein Structures. *J. Mol. Biol.* **2004**, *338* (4), 633–641. https://doi.org/10.1016/j.jmb.2004.03.039.

(2) Tsien, R. Y. The Green Fluorescent Protein. *Annu. Rev. Biochem.* **1998**, *67* (1), 509–544. https://doi.org/10.1146/annurev.biochem.67.1.509.

(3) Nixon, A. E.; Ostermeier, M.; Benkovic, S. J. Hybrid Enzymes: Manipulating Enzyme Design. *Trends Biotechnol.* **1998**, *16* (6), 258–264. https://doi.org/10.1016/S0167-7799(98)01204-9.

(4) Lindbladh, C.; Persson, M.; Bülow, L.; Mosbach, K. Characterization of a Recombinant Bifunctional Enzyme, Galactose Dehydrogenase/Bacterial Luciferase, Displaying an Improved Bioluminescence in a Three-Enzyme System. *Eur. J. Biochem.* **1992**, *204* (1), 241–247. https://doi.org/10.1111/j.1432-1033.1992.tb16630.x.

(5) Fan, Z.; Werkman, J. R.; Yuan, L. Engineering of a Multifunctional Hemicellulase. *Biotechnol. Lett.* **2009**, *31* (5), 751–757. https://doi.org/10.1007/s10529-009-9926-3.

(6) Xue, Y.; Peng, J.; Wang, R.; Song, X. Construction of the Trifunctional Enzyme Associating the Thermoanaerobacter Ethanolicus Xylosidase-Arabinosidase with the Thermomyces Lanuginosus Xylanase for Degradation of Arabinoxylan. *Enzyme Microb. Technol.* **2009**, *45* (1), 22–27. https://doi.org/10.1016/j.enzmictec.2009.03.010.

(7) Berger, S.; Lowe, P.; Tesar, M. Fusion Protein Technologies for Biopharmaceuticals: Applications and Challenges. *mAbs* **2015**, *7* (3), 456–460. https://doi.org/10.1080/19420862.2015.1019788.

(8) Baldo, B. A. Chimeric Fusion Proteins Used for Therapy: Indications, Mechanisms, and Safety. *Drug Saf.* **2015**, *38* (5), 455–479. https://doi.org/10.1007/s40264-015-0285-9.

(9) Kreitman, R. J.; Pastan, I. Immunotoxins for Targeted Cancer Therapy. *Adv. Drug Deliv. Rev.* **1998**, *31* (1), 53–88. https://doi.org/10.1016/S0169-409X(97)00094-X.

(10) Guidotti, G.; Brambilla, L.; Rossi, D. Cell-Penetrating Peptides: From Basic Research to Clinics. *Trends Pharmacol. Sci.* **2017**, *38* (4), 406–424. https://doi.org/10.1016/j.tips.2017.01.003.

(11) Ghosh, D.; Peng, X.; Leal, J.; Mohanty, R. Peptides as Drug Delivery Vehicles across Biological Barriers. *J. Pharm. Investig.* **2018**, *48* (1), 89–111. https://doi.org/10.1007/s40005-017-0374-0.

(12) Weimer, T.; Wormsbächer, W.; Kronthaler, U.; Lang, W.; Liebing, U.; Schulte, S. Prolonged In-Vivo Half-Life of Factor VIIa by Fusion to Albumin. *Thromb. Haemost.* **2008**, *99* (4), 659–667. https://doi.org/10.1160/TH07-08-0525.

(13) Dumont, J. A.; Low, S. C.; Peters, R. T.; Bitonti, A. J. Monomeric Fc Fusions: Impact on Pharmacokinetic and Biological Activity of Protein Therapeutics. *BioDrugs Clin. Immunother. Biopharm. Gene Ther.* **2006**, *20* (3), 151–160. https://doi.org/10.2165/00063030-200620030-00002.

(14) Walsh, G. Biopharmaceutical Benchmarks 2018. *Nat. Biotechnol.* **2018**, *36* (12), 1136–1145. https://doi.org/10.1038/nbt.4305.

(15) Yu, K.; Liu, C.; Kim, B.-G.; Lee, D.-Y. Synthetic Fusion Protein Design and Applications. *Biotechnol. Adv.* **2015**, *33* (1), 155–164. https://doi.org/10.1016/j.biotechadv.2014.11.005.

(16) Tsukiji, S.; Nagamune, T. Sortase-Mediated Ligation: A Gift from Gram-Positive Bacteria to Protein Engineering. *ChemBioChem* **2009**, *10* (5), 787–798. https://doi.org/10.1002/cbic.200800724.

(17) Zhang, Y.; Park, K.-Y.; Suazo, K. F.; Distefano, M. D. Recent Progress in Enzymatic Protein Labelling Techniques and Their Applications. *Chem. Soc. Rev.* **2018**, *47* (24), 9106–9136. https://doi.org/10.1039/c8cs00537k.

(18) Thompson, R. E.; Muir, T. W. Chemoenzymatic Semisynthesis of Proteins. *Chem. Rev.* **2020**, *120* (6), 3051–3126. https://doi.org/10.1021/acs.chemrev.9b00450.

(19) Muyldermans, S.; Baral, T. N.; Retamozzo, V. C.; De Baetselier, P.; De Genst, E.; Kinne, J.; Leonhardt, H.; Magez, S.; Nguyen, V. K.; Revets, H.; Rothbauer, U.; Stijlemans, B.; Tillib, S.; Wernery, U.; Wyns, L.; Hassanzadeh-Ghassabeh, Gh.; Saerens, D. Camelid Immunoglobulins and Nanobody Technology. *Vet. Immunol. Immunopathol.* **2009**, *128* (1), 178–183. https://doi.org/10.1016/j.vetimm.2008.10.299.

(20) Waldman, A. D.; Fritz, J. M.; Lenardo, M. J. A Guide to Cancer Immunotherapy: From T Cell Basic Science to Clinical Practice. *Nat. Rev. Immunol.* **2020**, 1–18. https://doi.org/10.1038/s41577-020-0306-5.

(21) Damouche, A.; Pourcher, G.; Pourcher, V.; Benoist, S.; Busson, E.; Lataillade, J.-J.; Van, M. L.; Lazure, T.; Adam, J.; Favier, B.; Vaslin, B.; Müller-Trutwin, M.; Lambotte, O.; Bourgeois, C. High Proportion of PD-1-Expressing CD4+ T Cells in Adipose Tissue Constitutes an Immunomodulatory Microenvironment That May Support HIV Persistence. *Eur. J. Immunol.* **2017**, *47* (12), 2113–2123. https://doi.org/10.1002/eji.201747060.

(22) Wang, W.; Lau, R.; Yu, D.; Zhu, W.; Korman, A.; Weber, J. PD1 Blockade Reverses the Suppression of Melanoma Antigen-Specific CTL by CD4+CD25Hi Regulatory T Cells. *Int. Immunol.* **2009**, *21* (9), 1065–1077. https://doi.org/10.1093/intimm/dxp072.

(23) Scarpa, M.; Vianello, F.; Signor, L.; Zennaro, L.; Rigo, A. Ascorbate Oxidation Catalyzed by Bis(Histidine)Copper(II). *Inorg. Chem.* **1996**, *35* (18), 5201–5206. https://doi.org/10.1021/ic9600644.

(24) Qiu, S.; Miao, M.; Wang, T.; Lin, Z.; Guo, L.; Qiu, B.; Chen, G. A Fluorescent Probe for Detection of Histidine in Cellular Homogenate and Ovalbumin Based on the Strategy of Clickchemistry. *Biosens. Bioelectron.* **2013**, *42*, 332–336. https://doi.org/10.1016/j.bios.2012.10.039.

(25) Chen, X.; Zaro, J. L.; Shen, W.-C. Fusion Protein Linkers: Property, Design and Functionality. *Adv. Drug Deliv. Rev.* **2013**, *65* (10), 1357–1369. https://doi.org/10.1016/j.addr.2012.09.039.

(26) Sinclair, A. J.; Amo, V. del; Philp, D. Structure–Reactivity Relationships in a Recognition Mediated [3+2] Dipolar Cycloaddition Reaction. *Org. Biomol. Chem.* **2009**, *7* (16), 3308–3318. https://doi.org/10.1039/B908072D.

(27) Dürüst, Y.; Karakuş, H.; Kaiser, M.; Tasdemir, D. Synthesis and Anti-Protozoal Activity of Novel Dihydropyrrolo[3,4-d][1,2,3]Triazoles. *Eur. J. Med. Chem.* **2012**, *48*, 296–304. https://doi.org/10.1016/j.ejmech.2011.12.028.

(28) Constant, C.; Albert, S.; Zivic, N.; Baczko, K.; Fensterbank, H.; Allard, E. Orthogonal Functionalization of a Fullerene Building Block through Copper-Catalyzed Alkyne–Azide and Thiol–Maleimide Click Reactions. *Tetrahedron* **2014**, *70* (18), 3023–3029. https://doi.org/10.1016/j.tet.2014.02.086.

(29) Finkelstein, H. Darstellung Organischer Jodide Aus Den Entsprechenden Bromiden Und Chloriden. *Berichte Dtsch. Chem. Ges.* **1910**, *43* (2), 1528–1532. https://doi.org/10.1002/cber.19100430257.

(30) Heller, K.; Ochtrop, P.; Albers, M. F.; Zauner, F. B.; Itzen, A.; Hedberg, C. Covalent Protein Labeling by Enzymatic Phosphocholination. *Angew. Chem. Int. Ed.* **2015**, *54* (35), 10327–10330. https://doi.org/10.1002/anie.201502618.

(31) Wu, Y.; Limburg, D. C.; Wilkinson, D. E.; Vaal, M. J.; Hamilton, G. S. A Mild Deprotection Procedure for Tert-Butyl Esters and Tert-Butyl Ethers Using ZnBr2 in Methylene Chloride. *Tetrahedron Lett.* **2000**, *41* (16), 2847–2849. https://doi.org/10.1016/S0040-4039(00)00300-2.

(32) Li, B.; Berliner, M.; Buzon, R.; Chiu, C. K.-F.; Colgan, S. T.; Kaneko, T.; Keene, N.; Kissel, W.; Le, T.; Leeman, K. R.; Marquez, B.; Morris, R.; Newell, L.; Wunderwald, S.; Witt, M.; Weaver, J.; Zhang, Z.; Zhang, Z. Aqueous Phosphoric Acid as a Mild Reagent for Deprotection of Tert-Butyl Carbamates, Esters, and Ethers. *J. Org. Chem.* **2006**, *71* (24), 9045–9050. https://doi.org/10.1021/jo061377b.

(33) Dommerholt, J.; Schmidt, S.; Temming, R.; Hendriks, L. J. A.; Rutjes, F. P. J. T.; van Hest, J. C. M.; Lefeber, D. J.; Friedl, P.; van Delft, F. L. Readily Accessible Bicyclononynes for Bioorthogonal Labeling and Three-Dimensional Imaging of Living Cells. *Angew. Chem. Int. Ed.* **2010**, *49* (49), 9422–9425. https://doi.org/10.1002/anie.201003761.

(34) Gential, G. P. P.; Ho, N. I.; Chiodo, F.; Meeuwenoord, N.; Ossendorp, F.; Overkleeft, H. S.; van der Marel, G. A.; Filippov, D. V. Synthesis and Evaluation of Fluorescent Pam3Cys Peptide Conjugates. *Bioorg. Med. Chem. Lett.* **2016**, *26* (15), 3641–3645. https://doi.org/10.1016/j.bmcl.2016.05.094.

6

Summary and future prospects

Cyclic peptides encompass a major class of macrocylic compounds, varying widely in structure, ring size, functional group patterns and biological activities. The defining characteristic of macrocycles are their cyclic structure consisting of twelve or more atoms. During the early days of antibiotic research extensive investigations were conducted on cyclic peptides leading to a vast resource of antimicrobial compounds. In recent years, interest in peptidic macrocycles as therapeutics has been renewed as these compounds occupy a middle space between small-molecule drugs and large pharmaceutical agents (biologicals) such as proteins

and antibody-drug conjugates. Cyclic peptides have also seen widespread usage as a multifunctional platform by utilizing a peptide template that serves as a structural motif onto which several molecular entities can be attached.

Macrocyclization is the key step in the synthesis of cyclic peptides and **Chapter 1** provides an overview of the main strategies employed. To exemplify, syntheses of several bioactive peptides are described utilizing these strategies. The applications of cyclic peptides as multifunctional platforms are discussed as well and representative examples are given.

The attachment of lysine ε-amines or ornithine δ-amines to resins most commonly involve the usage or synthesis of an activated electrophilic resin. **Chapter 2** describes the establishment of a method to anchor the lysine and ornithine side-chains using the nucleophilic para-hydroxymethylphenyloxy (Wang) linker on a TentaGel resin through a carbamate linkage. When compared to the linkage of the respective C-terminus, the properties of the linker remain unaffected as exposure to trifluoroacetic acid liberates the amine accompanied by the formation of carbon dioxide. The method involves the formation of an isocyanate which was achieved through treatment of the *N*-Boc carbamate with the oxaphilic Hendrickson's reagent. The coupling of the isocyanate to Wang-type resins was found to be efficiently catalyzed by dibutyltin dilaurate and zirconium(IV) acetylacetonate. With these methods, four head-to-tail cyclic peptides were synthesized in yields and purities comparable to those reported in literature.

It would be of interest to widen the scope of this method to paint a more complete picture. Since the equivalents of the catalysts has not yet been varied, it would be interesting to find out the minimum amounts of catalysts that could still efficiently catalyze the reaction. As the choice of base was also found to be influential, investigating different bases would be a logical next step as well. The two tested bases, *N*-methylmorpholine and 1-methylimidazole, were reported to be catalysts itself for the transformation and attempting the coupling with a non-catalytic base might achieve better synergy. Possible bases are limited to ensure Fmoc compatibility, but the sterically hindered 2,6-lutidine would be an interesting candidate. Additionally, the number of different resins can be increased. The method has been only tested on TentaGel resins, which is a graft copolymer of weakly cross-linked polystyrene and linear polyethylene glycol.[1] Polystyrene-based resins as well as resins comprised of only polyethylene glycol, such as the PEGA and

ChemMatrix resins, would be valuable additions.[2–4] The inclusion of additional amines, such as 2,4-diaminobutyric acid, would open up the possibility of synthesizing a wider variety of cyclic peptides. Interesting peptides include the head-to-side-chain cyclic peptide polymyxin B2 **1** and the cyclic tetradecapeptide murepavadin **2** (*Figure 1*).

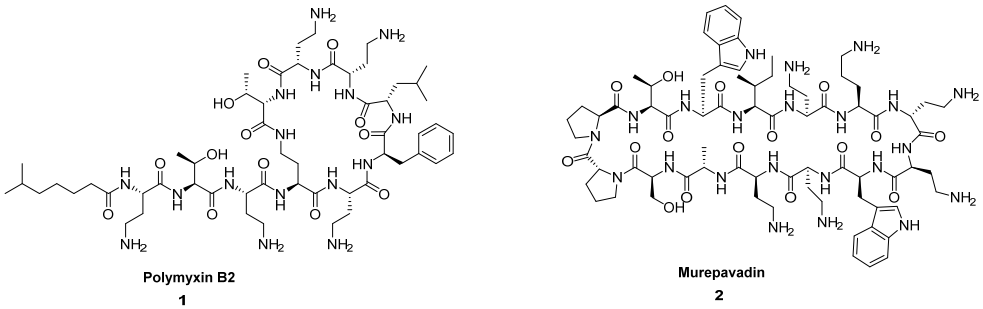

Figure 1. A wider variety of cyclic peptides that could be synthesized include polymyxin B2 **1** and murepavadin **2**.

There have been recent reports investigating the synergystic effects of various (conjugated) Toll-like receptor (TLR) ligands. **Chapter 3** describes the synthesis of a platform to probe the influence of the spatial positioning of a pair of TLR agonists on their immunogenicity. Advantage was taken of the cyclodecapeptide gramicidin S which presents amino acid side-chains into opposite planes owing to its secondary structure. Three gramicidin S scaffolds were synthesized that orient the amine functionalities into different directions. To facilitate swift and clean attachment of the TLR ligands, the amines were equipped with a maleimide group and a BCN moiety. TLR2, 7 and 9 ligands were synthesized with a complementary reactive group (thiol or azide) creating nine possible combinations of ligands and orientation. To accommodate on-resin installation of the BCN moiety, the method developed in Chapter 2 was expanded to the TentaGel S AC resin and the peptide cleavage and purification method were optimized. In the future, RP-HPLC purification of the cyclopeptides carrying the BCN group should be carried out with ammonium acetate instead of TFA to avoid alkyne hydration.

Chapter 4 describes the expansion of the platform in Chapter 3 to allow presentation of three different TLR ligands. Adjustments were made to install the third ligand *via* tetrazine/norbornene ligation by substituting the BCN group with the bulky DBCO moiety preventing cross-reaction of the tetrazine. Two gramicidin S-based scaffolds were synthesized carrying three amino functionalities in different orientations. The

norbornene and DBCO groups were installed on-resin which required an additional protected amine during synthesis of the peptide. The Tfa group proved effective and could be removed by treatment with ammonia in methanol under microwave irradiation at elevated temperatures. To accompany the new ligation, a TLR7 ligand carrying a tetrazine was synthesized as well as an adapter molecule for the TLR9 agonist. With these molecules in hand, three combinations of ligands and orientations are possible.

The main priority moving forward is conjugation of the TLR agonists to the scaffolds. As there have been several reports of cross-reactivity between the thiol and alkyne functionalities, the best option would be sequential conjugation.[5,6] Counterintuitively, the group of Plückthun achieved higher yields of protein-protein ligation when performing the thiol-maleimide ligation first which they attribute to the longer reaction times required for the azide-alkyne cycloaddition leading to maleimide hydrolysis and other side-reactions.[7] Since these molecules are several magnitudes smaller, both sequences should be attempted. Following literature precedent, the alkyne-azide cycloaddition and tetrazine/norbornene ligation could be performed simultaneously as they are mutually orthogonal.[8–10] As for the biological evaluation of the linked TLR agonists, it would be of interest to follow the example set by the group of Esser-Kahn to allow for comparison.[11] In their evaluation of linked triagonists, they examined activation of the transcription factor NF-κB, which leads to cytokine production, as a measure of synergistic activity as well as activation of interferon stimulatory genes. They also build a cytokine profile by analyzing cytokine concentrations, in particular IL-12p70, TNF-α, IFN-γ, IL-6, IL-10 and CCL2.

To create a more diverse library, it would be of interest to increase the number of TLR ligands. The most sensible additions would be the pyrimido[5,4-*b*]indole **3**, a TLR4 ligand, and the diacylated Pam_2Cys **4** that is an agonist for TLR2/6 (*Figure* 2).[12,13] It would also be interesting to widen the scope to more ligands of pattern recognition receptors. The NOD2 agonist muramyl dipeptide **5** would be a valuable addition as there have been promising results with TLR2/NOD2 dual ligands.[14,15] Benzothiazole compound **6** was found by Gale and co-workers to activate the transcription factor interferon regulatory factor 3 (IRF3) in the RIG-I-like receptor (RLR) signaling pathway and would be an interesting addition in the future.[16] Lastly, diamidobenzimidazole **7** has been recently identified as an agonist for stimulator of

interferon genes (STING) eliciting a type-I interferon response and would make an interesting inclusion in the library.[17]

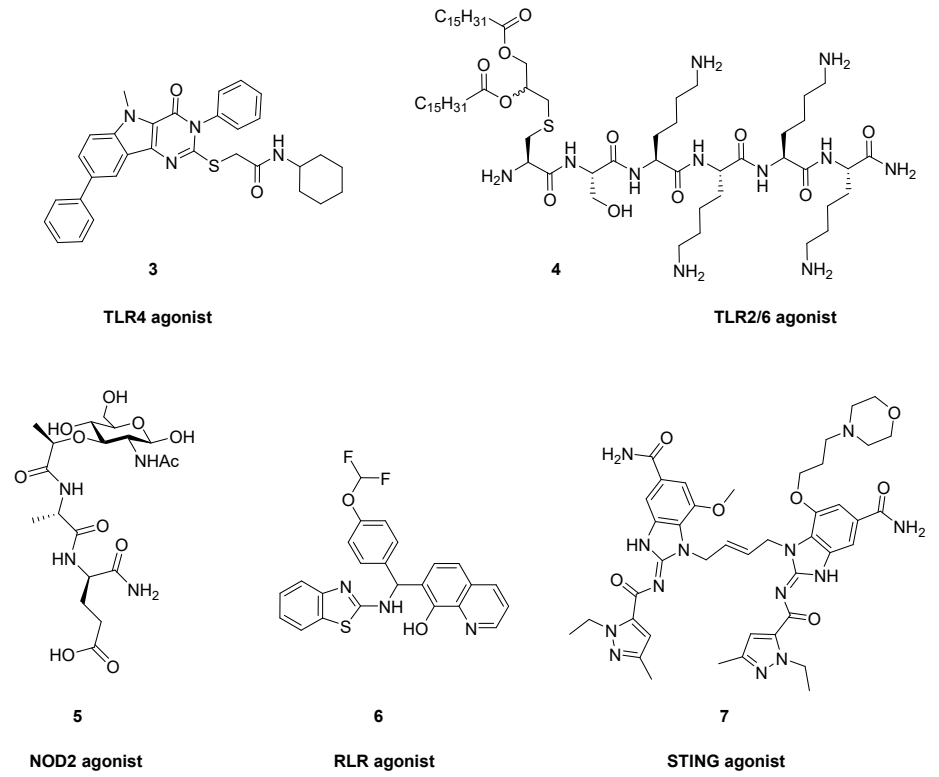

Figure 2. Possible agonists of pattern recognition receptors to expand the library created in Chapters 3 and 4.

Chapter 5 describes the synthesis of a fusion protein utilizing a chemical conjugation strategy. A linker system was designed that placed the emphasis on late-stage derivatization of the individual proteins. Anti-PD1 and anti-CD4 VHH antibodies were genetically engineered with a C-terminal cysteine for conjugation purposes and were obtained in good purities. A two-component linker system was synthesized to facilitate late-stage fusion. One linker consisted of an iodoacetamide group as a complement to the thiol group and an azide moiety for a SPAAC ligation. The complementary linker was equipped with a maleimide for thiol conjugation and the strained cycloalkyne BCN as the ligation partner for the azide and were linked together by an ethylene glycol spacer. The linkers were successfully conjugated to anti-PD1 VHH antibodies and a preliminary investigation was conducted on the

SPAAC ligation which saw formation of the fusion protein, but further optimization is needed.

The first step for optimization could be to apply the optimal conditions found by Schiffelers and co-workers for conjugating a 20 kDa poly-ethylene glycol to a VHH antibody *via* a SPAAC ligation, which includes a higher temperature (50 °C) and a 3:1 ratio of alkyne to azide.[18] Another adjustment that could be made is increasing the length of the linkers. The design of the BCN linker allows for facile prolongation by incorporating more ethylene glycol spacers during the solid-phase synthesis. Increasing the length of the azido linker requires more attention, but has been achieved as well (*Figure 3*). After obtaining amine **8**, the compound was reacted with the ethylene glycol spacer utilizing Castro's reagent and DIPEA to afford Fmoc-protected amine **9** in 44% yield. Fmoc deprotection was achieved with 1,8-diazabicyclo[5.4.0]undec-7-ene (DBU) and *n*-octanethiol as the scavenger giving amine **10** in 96% yield. The iodoacetamide was installed in a similar manner as described in Chapter 2 and compound **11** was obtained in 56% yield over two steps.

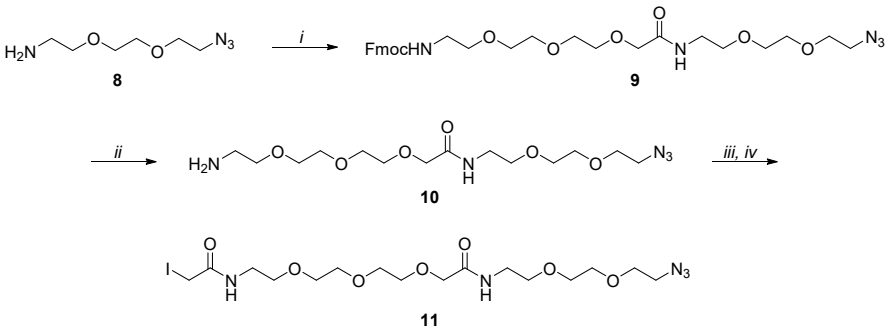

Figure 3. Reagents and conditions: (*i*) Ethylene glycol building block, BOP, DIPEA, DMF, rt, 4 hrs, 44% (*ii*): DBU, *n*-octanethiol, THF, rt, 36 hrs, 96% (*iii*) Chloroacetyl chloride, Et_3N, DMF, 0 °C, 2.5 hrs, 77% (*iv*): NaI, acetone, rt, 48 hrs, 73%.

A limitation of the current approach is the reliance on cysteine for the conjugation of the linkers to the protein. When additional cysteines are present on the protein selectivity cannot be guaranteed. An alternative would be the utilization of ligation enzymes, such as sortase A and butelase.[19,20] However, that would require the engineering of different linkers on each protein hampering the goal of late-stage derivatization. Another option would be the site-specific cysteine conjugation developed by the group of Pentelute (*Figure 4*).[21] A four-amino-acid sequence (Phe-Cys-Pro-Phe) tunes the reactivity of the cysteine thiol enabling site-selective

conjugation with perfluoroaromatic reagents and the addition of ammonium sulfate accelerates the reaction.[22] This motif could be engineered at the C-termini of the antibodies while the perfluoroaromatic group could be installed instead of the maleimide and iodoacetamide functionalities. The use of this conjugation could be the basis of a more general fusion protein approach.

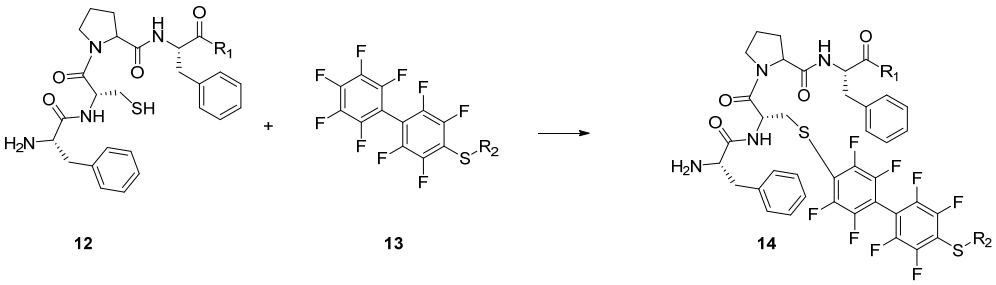

Figure 4. The site-selective cysteine conjugation of a four-amino-acid sequence with perfluoroaromatic reagents developed by the group of Pentelute.

General information

Materials, reactions and purification

Standard Fmoc-amino acids and resins for solid-phase peptide synthesis (SPPS), amino acids for solution-phase synthesis and peptide coupling reagents 2-(6-chloro-1*H*-benzotriazole-1-yl)-1,1,3,3-tetramethyluronium hexafluorophosphate (HCTU), *N*,*N*'-diisopropylcarbodiimide (DIC), 1-ethyl-3-(3-dimethylaminopropyl) carbodiimide hydrochloride (EDC), ethyl cyano(hydroxyimino)acetate (Oxyma Pure) and 1-hydroxybenzotriazole (HOBt) were purchased from Novabiochem or Sigma-Aldrich. The resin TentaGel S RAM (0.25 mmol/g) was bought from Rapp Polymere. All other chemicals were purchased from Acros, Sigma Aldrich, VWR, Fluka, Merck and Fisher Scientific and used as received unless stated otherwise. Tetrahydrofuran (THF), *N*,*N*-dimethylformamide (DMF), dichloromethane (DCM), 1,4-dioxane and toluene were stored over molecular sieves before use. Commercially available ACS grade solvents were used for column chromatography without any further purification, except for toluene and ethyl acetate which were distilled prior to use. All reactions were carried out under a nitrogen atmosphere, unless indicated otherwise. Reaction progress and chromatography fractions were monitored by thin layer chromatography (TLC) on silica-gel-coated aluminium sheets with a F254 fluorescent indicator purchased from Merck (Silica gel 60 F_{254}). Visualization was achieved by UV absorption by fluorescence quenching, permanganate stain (4 g $KMnO_4$ and 2 g K_2CO_3 in 200 mL of H_2O), ninhydrin stain (0.6 g ninhydrin and 10 mL acetic acid in 200 mL ethanol). Silica gel column chromatography was performed using Screening Devices silica gel 60 (particle size of 40 – 63 μm, pore diameter of 60 Å) with the indicated eluent. Analytical reversed-phase high-performance liquid chromatography (RP-HPLC) was performed on a Thermo Finnigan Surveyor HPLC system with a Phenomenex Gemini C_{18} column (4.6 mm x 50 mm, 3 μm particle size) with a flow rate of 1 mL/min and a solvent gradient of 10-90% solvent B over 8 min coupled to a LCQ Advantage Max (Thermo Finnigan) ion-trap spectrometer (ESI^+). Preparative RP-HPLC was performed with a GX-281 Liquid Handler and a 331 and 332-H2 primary and secondary solvent pump respectively with a Phenomenex Gemini C_{18} or C_4 column (250 x 10.0 mm, 3 μm particle size) with a flow rate of 5 mL/min and solvent gradients as described for each compound. HPLC solvent compositions: solvent A is 0.1% (v/v) TFA in H_2O; solvent B is MeCN. Preparative RP-HPLC was also performed on an Agilent 1200 HPLC system coupled to a 6130 Quadrupole Mass Spectrometer using a Nucleodur C_{18} Gravity column (250 x 10.0 mm, 5 μm particle size) with a flow rate of 5 mL/min and a gradient over 12 min. as described for each compound. HPLC solvent composition: solvent A is 0.2% (v/v) TFA in H_2O and solvent B is MeCN. All HPLC solvents were filtered with a Millipore filtration system equipped with a 0.22 μm nylon membrane filter prior to use.

Characterization

Nuclear magnetic resonance (^1H and ^{13}C APT NMR) spectra were recorded on a Brüker DPX-300, Brüker AV-400, Brüker DMX-400, Brüker AV-500 or Brüker DMX-600 in the given solvent. Chemical shifts are reported in parts per million (ppm) with the residual solvent or tetramethylsilane (0 ppm) as reference. High-resolution mass spectrometry (HRMS) analysis was performed with a Thermo Finnigan LTQ Orbitrap mass spectrometer equipped with an electronspray ion source in positive mode (source voltage 3.5 kV, sheath gas flow 10 ml/min, capillary temperature 250 °C) with resolution R = 60000 at m/z 400 (mass range m/z = 150 – 2000) and dioctyl phthalate (m/z = 391.28428) as a "lock mass". The high-resolution mass spectrometer was calibrated prior to measurements with a Thermo Finnigan calibration mixture. Nominal and exact m/z values are reported in daltons.

(9*H*-fluoren-9-yl)methyl (1-azido-10-oxo-3,6,12,15,18-pentaoxa-9-azaicosan-20-yl)carbamate

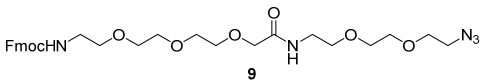

9

An oven-dried 50 mL flask was charged with ethylene glycol spacer bearing the carboxylic acid (1.1 g, 2.5 mmol, 1.0 equiv.). Benzotriazol-1-yloxytris(dimethylamino)phosphonium hexafluorophosphate (BOP) (1.4 g, 3.2 mmol, 1.3 equiv.) was added and the mixture was dissolved in anhydrous DMF (13 mL, 0.20 M). DIPEA (1.3 mL, 7.5 mmol, 3.0 equiv.) and 2-(2-(2-azidoethoxy)ethoxy)ethan-1-amine (0.57 g, 3.3 mmol, 1.3 equiv.) were added and the mixture was stirred for 4 hours. The mixture was concentrated by co-evaporation with *n*-heptane and purified by silica gel column chromatography (7:3, DCM – MeCN) to yield compound **9** (0.64 g, 1.1 mmol, 44%) as a colourless oil.

^{1}H NMR (400 MHz, $CDCl_3$) δ 7.66 (d, *J* = 7.5 Hz, 2H, C*H*-arom), 7.52 (d, *J* = 7.5 Hz, 2H, C*H*-arom), 7.29 (t, *J* = 7.5 Hz, 2H, C*H*-arom), 7.21 (t, *J* = 7.4 Hz, 2H, C*H*-arom), 7.14 (t, *J* = 5.8 Hz, 1H, N*H*), 5.81 (t, J = 5.7 Hz, 1H, N*H*Fmoc), 4.32 (d, *J* = 6.9 Hz, 2H, CH_2-Fmoc), 4.11 (t, *J* = 6.8 Hz, 1H, C*H*-Fmoc), 3.92 (s, 2H, CH_2(C=O)), 3.59 – 3.25 (m, 24H, OCH_2, CH_2N_3, CH_2NH). ^{13}C NMR (101 MHz, $CDCl_3$) δ 169.9 (*C*=O), 156.3 (*C*=O), 143.71 (*Cq*-arom), 141.0 (*Cq*-arom), 127.4 (*C*H-arom), 126.8 (*C*H-arom), 124.8 (*C*H-arom), 119.7 (*C*H-arom), 70.5 (OCH_2), 70.2 (OCH_2), 70.1 (OCH_2), 70.1 (OCH_2), 70.0 (OCH_2), 69.9 (OCH_2), 69.7 (OCH_2), 69.6 (OCH_2), 69.5 (CH_2(C=O)), 66.1 (CH_2-Fmoc), 50.3 (CH_2N_3), 47.0 (CH-Fmoc), 40.6 (CH_2NH), 38.3 (CH_2NH).

***N*-(1-azido-10-oxo-3,6,12,15,18-pentaoxa-9-azaicosan-20-yl)-2-chloroacetamide**

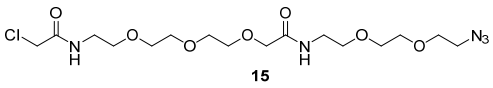

15

Compound **9** (0.52 g, 0.89 mmol, 1.0 equiv.) was dissolved in anhydrous THF (7.7 mL, 0.12 M). *n*-Octanethiol (1.5 mL, 8.8 mmol, 10 equiv.) was added followed by dropwise addition of 1,8-diazabicyclo[5.4.0]undec-7-ene (DBU) in THF (1.0 mL, 88 mM). The mixture was allowed to stir for 36 hours. The mixture was evaporated and the residue was dissolved in toluene (5.0 mL). H_2O (5.0 mL) was added and the aqueous layer was separated. The organic layer was extracted with water (3x 5.0 mL) and the combined aqueous layers were washed with toluene (6x 10 mL). The combined aqueous layers were concentrated to yield amine **10** (0.31 g, 0.85 mmol, 96%) as a colourless oil. DMF (2.1 mL, 0.20 M) and Et_3N (76 μL, 0.55 mmol, 1.3 equiv.) were added and the solution was cooled to 0 °C. Chloroacetyl chloride (44 μL, 0.55 mmol, 1.3 equiv.) was added dropwise and the mixture was stirred for 140 min. The mixture was evaporated to obtain an orange crude and purification by silica gel column chromatography (1:9, MeOH – DCM) yielded chloroacetamide **15** (0.14 g, 0.32 mmol, 77%) as pale yellow oil.

^{1}H NMR (400 MHz, $(CD_3)_2CO$) δ 7.72 (s, 1H, N*H*), 7.43 (s, 1H, N*H*), 4.08 (s, 2H, CH_2Cl), 3.96 (s, 2H, CH_2(C=O)), 3.70 – 3.52 (m, 18H, OCH_2), 3.43 – 3.37 (m, 6H, CH_2N_3, CH_2NH).

^{13}C NMR (101 MHz, $(CD_3)_2CO$) δ 170.6 (*C*=O), 166.8 (*C*=O), 71.4 (OCH_2), 71.3 (OCH_2), 71.1 (OCH_2), 71.0 (OCH_2), 71.0 (OCH_2), 70.9 (OCH_2), 70.8 (OCH_2), 70.6 (OCH_2), 70.6 (OCH_2), 70.4 (OCH_2), 70.2 (OCH_2), 69.9 (CH_2(C=O)), 51.2 (CH_2N_3), 43.3 (CH_2Cl), 40.2 (CH_2NH), 39.1 (CH_2NH).

***N*-(1-azido-10-oxo-3,6,12,15,18-pentaoxa-9-azaicosan-20-yl)-2-iodoacetamide**

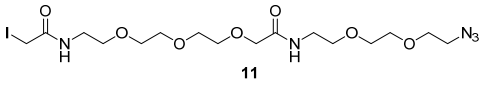

11

Chloroacetamide **15** (0.13 g, 0.30 mmol, 1.0 equiv.) was dissolved in acetone (2.9 mL, 0.10 M) and sodium iodide (0.14 g, 0.90 mmol, 3.0 equiv.) was added. The mixture was stirred for 48 hrs. The mixture was concentrated and purification by silica column chromatography (1:9, MeOH – DCM) yielded iodoacetamide **11** (0.11 g, 0.22 mmol, 72%) as pale yellow oil.

^{1}H NMR (500 MHz, $(CD_3)_2CO$) δ 7.79 (s, 1H, N*H*), 7.41 (s, 1H, N*H*), 3.99 (s, 2H, CH_2(C=O)), 3.76 (s, 2H, CH_2I), 3.70 – 3.59 (m, 14H, OCH_2), 3.56 (t, *J* = 5.7 Hz, 2H, CH_2CH$_2$NH), 3.52 (t, *J* = 5.5 Hz, 2H, CH_2CH$_2$NH), 3.45 – 3.38 (m, 4H, CH_2N_3, CH_2NH), 3.36 (q, *J* = 5.5 Hz, 2H, CH_2NH).

^{13}C NMR (126 MHz, $(CD_3)_2CO$) δ 170.7 (*C*=O), 168.4 (*C*=O), 71.4 (OCH_2), 71.2 (OCH_2), 71.2 (OCH_2), 71.0 (OCH_2), 71.0 (OCH_2), 70.9 (OCH_2), 70.6 (OCH_2), 70.2 (OCH_2), 70.0 (CH_2(C=O)), 51.3 (CH_2N_3), 40.5 (CH_2NH), 39.2 (CH_2NH), -0.2 (CH_2I).

References

(1) Bayer, E. Towards the Chemical Synthesis of Proteins. *Angew. Chem. Int. Ed. Engl.* **1991**, *30* (2), 113–129. https://doi.org/10.1002/anie.199101133.

(2) Merrifield, R. B. Solid Phase Peptide Synthesis. I. The Synthesis of a Tetrapeptide. *J. Am. Chem. Soc.* **1963**, *85* (14), 2149–2154. https://doi.org/10.1021/ja00897a025.

(3) Meldal, M. Pega: A Flow Stable Polyethylene Glycol Dimethyl Acrylamide Copolymer for Solid Phase Synthesis. *Tetrahedron Lett.* **1992**, *33* (21), 3077–3080. https://doi.org/10.1016/S0040-4039(00)79604-3.

(4) García-Ramos, Y.; Paradís-Bas, M.; Tulla-Puche, J.; Albericio, F. ChemMatrix® for Complex Peptides and Combinatorial Chemistry. *J. Pept. Sci.* **2010**, *16* (12), 675–678. https://doi.org/10.1002/psc.1282.

(5) van Geel, R.; Pruijn, G. J. M.; van Delft, F. L.; Boelens, W. C. Preventing Thiol-Yne Addition Improves the Specificity of Strain-Promoted Azide-Alkyne Cycloaddition. *Bioconjug. Chem.* **2012**, *23* (3), 392–398. https://doi.org/10.1021/bc200365k.

(6) Fairbanks, B. D.; Sims, E. A.; Anseth, K. S.; Bowman, C. N. Reaction Rates and Mechanisms for Radical, Photoinitated Addition of Thiols to Alkynes, and Implications for Thiol−Yne Photopolymerizations and Click Reactions. *Macromolecules* **2010**, *43* (9), 4113–4119. https://doi.org/10.1021/ma1002968.

(7) Merten, H.; Schaefer, J. V.; Brandl, F.; Zangemeister-Wittke, U.; Plückthun, A. Facile Site-Specific Multiconjugation Strategies in Recombinant Proteins Produced in Bacteria. *Methods Mol. Biol. Clifton NJ* **2019**, *2033*, 253–273. https://doi.org/10.1007/978-1-4939-9654-4_17.

(8) Karver, M. R.; Weissleder, R.; Hilderbrand, S. A. Bioorthogonal Reaction Pairs Enable Simultaneous, Selective, Multi-Target Imaging. *Angew. Chem. Int. Ed.* **2012**, *51* (4), 920–922. https://doi.org/10.1002/anie.201104389.

(9) Patterson, D. M.; Nazarova, L. A.; Xie, B.; Kamber, D. N.; Prescher, J. A. Functionalized Cyclopropenes As Bioorthogonal Chemical Reporters. *J. Am. Chem. Soc.* **2012**, *134* (45), 18638–18643. https://doi.org/10.1021/ja3060436.

(10) Späte, A.-K.; Bußkamp, H.; Niederwieser, A.; Schart, V. F.; Marx, A.; Wittmann, V. Rapid Labeling of Metabolically Engineered Cell-Surface Glycoconjugates with a Carbamate-Linked Cyclopropene Reporter. *Bioconjug. Chem.* **2014**, *25* (1), 147–154. https://doi.org/10.1021/bc4004487.

(11) Albin, T. J.; Tom, J. K.; Manna, S.; Gilkes, A. P.; Stetkevich, S. A.; Katz, B. B.; Supnet, M.; Felgner, J.; Jain, A.; Nakajima, R.; Jasinskas, A.; Zlotnik, A.; Pearlman, E.; Davies, D. H.; Felgner, P. L.; Burkhardt, A. M.; Esser-Kahn, A. P. Linked Toll-Like Receptor Triagonists Stimulate Distinct, Combination-Dependent Innate Immune Responses. *ACS Cent. Sci.* **2019**, *5* (7), 1137–1145. https://doi.org/10.1021/acscentsci.8b00823.

(12) Chan, M.; Kakitsubata, Y.; Hayashi, T.; Ahmadi, A.; Yao, S.; Shukla, N. M.; Oyama, S.; Baba, A.; Nguyen, B.; Corr, M.; Suda, Y.; Carson, D. A.; Cottam, H. B.; Wakao, M. Structure–Activity Relationship Studies of Pyrimido[5,4-b]Indoles as Selective Toll-Like Receptor 4 Ligands. *J. Med. Chem.* **2017**, *60* (22), 9142–9161. https://doi.org/10.1021/acs.jmedchem.7b00797.

(13) Kang, J. Y.; Nan, X.; Jin, M. S.; Youn, S.-J.; Ryu, Y. H.; Mah, S.; Han, S. H.; Lee, H.; Paik, S.-G.; Lee, J.-O. Recognition of Lipopeptide Patterns by Toll-like Receptor 2-Toll-like Receptor 6 Heterodimer. *Immunity* **2009**, *31* (6), 873–884. https://doi.org/10.1016/j.immuni.2009.09.018.

(14) Pavot, V.; Rochereau, N.; Rességuier, J.; Gutjahr, A.; Genin, C.; Tiraby, G.; Perouzel, E.; Lioux, T.; Vernejoul, F.; Verrier, B.; Paul, S. Cutting Edge: New Chimeric NOD2/TLR2 Adjuvant Drastically Increases Vaccine Immunogenicity. *J. Immunol.* **2014**, *193* (12), 5781–5785. https://doi.org/10.4049/jimmunol.1402184.

(15) Zom, G. G.; Willems, M. M. J. H. P.; Meeuwenoord, N. J.; Reintjens, N. R. M.; Tondini, E.; Khan, S.; Overkleeft, H. S.; van der Marel, G. A.; Codee, J. D. C.; Ossendorp, F.; Filippov, D. V. Dual Synthetic Peptide Conjugate Vaccine Simultaneously Triggers TLR2 and NOD2 and Activates Human Dendritic Cells. *Bioconjug. Chem.* **2019**, *30* (4), 1150–1161. https://doi.org/10.1021/acs.bioconjchem.9b00087.

(16) Pattabhi, S.; Wilkins, C. R.; Dong, R.; Knoll, M. L.; Posakony, J.; Kaiser, S.; Mire, C. E.; Wang, M. L.; Ireton, R. C.; Geisbert, T. W.; Bedard, K. M.; Iadonato, S. P.; Loo, Y.-M.; Gale, M. Targeting Innate Immunity for Antiviral Therapy through Small Molecule Agonists of the RLR Pathway. *J. Virol.* **2016**, *90* (5), 2372–2387. https://doi.org/10.1128/JVI.02202-15.

(17) Ramanjulu, J. M.; Pesiridis, G. S.; Yang, J.; Concha, N.; Singhaus, R.; Zhang, S.-Y.; Tran, J.-L.; Moore, P.; Lehmann, S.; Eberl, H. C.; Muelbaier, M.; Schneck, J. L.; Clemens, J.; Adam, M.; Mehlmann, J.; Romano, J.; Morales, A.; Kang, J.; Leister, L.; Graybill, T. L.; Charnley, A. K.; Ye, G.; Nevins, N.; Behnia, K.; Wolf, A. I.; Kasparcova, V.; Nurse, K.; Wang, L.; Puhl, A. C.; Li, Y.; Klein, M.; Hopson, C. B.; Guss, J.; Bantscheff, M.; Bergamini, G.; Reilly, M. A.; Lian, Y.; Duffy, K. J.; Adams, J.; Foley, K. P.; Gough, P. J.; Marquis, R. W.; Smothers, J.; Hoos, A.; Bertin, J. Design of Amidobenzimidazole STING Receptor Agonists with Systemic Activity. *Nature* **2018**, *564* (7736), 439–443. https://doi.org/10.1038/s41586-018-0705-y.

(18) van Moorsel, M. V. A.; Urbanus, R. T.; Verhoef, S.; Koekman, C. A.; Vink, M.; Vermonden, T.; Maas, C.; Pasterkamp, G.; Schiffelers, R. M. A Head-to-Head Comparison of Conjugation Methods for VHHs: Random Maleimide-Thiol Coupling versus Controlled Click Chemistry. *Int. J. Pharm. X* **2019**, *1*, 100020. https://doi.org/10.1016/j.ijpx.2019.100020.

(19) Tsukiji, S.; Nagamune, T. Sortase-Mediated Ligation: A Gift from Gram-Positive Bacteria to Protein Engineering. *ChemBioChem* **2009**, *10* (5), 787–798. https://doi.org/10.1002/cbic.200800724.

(20) Nguyen, G. K. T.; Wang, S.; Qiu, Y.; Hemu, X.; Lian, Y.; Tam, J. P. Butelase 1 Is an Asx-Specific Ligase Enabling Peptide Macrocyclization and Synthesis. *Nat. Chem. Biol.* **2014**, *10* (9), 732–738. https://doi.org/10.1038/nchembio.1586.

(21) Zhang, C.; Welborn, M.; Zhu, T.; Yang, N. J.; Santos, M. S.; Van Voorhis, T.; Pentelute, B. L. π -Clamp-Mediated Cysteine Conjugation. *Nat. Chem.* **2016**, *8* (2), 120–128. https://doi.org/10.1038/nchem.2413.

(22) Dai, P.; Zhang, C.; Welborn, M.; Shepherd, J. J.; Zhu, T.; Van Voorhis, T.; Pentelute, B. L. Salt Effect Accelerates Site-Selective Cysteine Bioconjugation. *ACS Cent. Sci.* **2016**, *2* (9), 637–646. https://doi.org/10.1021/acscentsci.6b00180.

Samenvatting

In de jaren 1940 zorgde de ontdekking en isolatie van het antibioticum streptomycine uit de bacterie *Streptomyces griseus* voor een grootschalige zoektocht naar nieuwe bioactieve stoffen uit de natuur. Deze zoektocht leverde een scala aan verbindingen op, waaronder naast antibiotica ook antikanker medicijnen, afweerremmers, antimycotica en anthelminthica. Onder deze moleculen bevindt zich een belangrijke familie van macrocyclische peptiden, welke een keten van aminozuren zijn die een gesloten ring vormen van meer dan twaalf atomen via verbinding van de

zijketens en/of de termini. Antibiotische peptiden hebben voornamelijk gebruik gevonden tegen plaatselijke infecties vanwege verschillende beperkingen voor inwendig gebruik, zoals slechte orale opname of ernstige bijwerkingen. In recente jaren is er met hernieuwde interesse naar cyclische peptiden gekeken als potentiële geneesmiddelen en zijn er meerdere nieuwe macrocyclische peptiden klinisch onderzoek belandt. Een andere toepassing die cyclische peptiden hebben gevonden is als multifunctioneel platform waarin het peptide zorgt voor een structureel motief waaraan verschillende moleculaire entiteiten kunnen worden vastgemaakt.

Hoofdstuk 1 behandelt de voornaamste strategieën die zijn toegepast om cyclische peptiden te synthetiseren waarvan de moeilijkste stap de macrocyclisatie is. Ter illustratie worden de synthese van enkele bioactieve peptiden besproken die gebruikmaken van deze strategieën. Daarnaast wordt de toepassing van cyclische peptiden als multifunctioneel platform bediscussieerd en worden er representatieve voorbeelden gegeven.

Bij het vastmaken van de lysine ε-amines of ornithine δ-amines aan vaste dragers wordt in het algemeen gebruik gemaakt van een geactiveerde electrofiele vaste drager, welke vatbaar is voor degradatie. **Hoofdstuk 2** beschrijft de totstandkoming van een methode om de zijketen van lysines en ornithines te verankeren aan een nucleofiele hydoxymethylfenyloxy (Wang) linker op een TentaGel vaste drager door middel van een urethaan verbinding. Wanneer deze verbinding vergeleken wordt met de standaard C-terminale verankering blijven de eigenschappen van de linker hetzelfde en kan het amine worden verlost van de vaste drager met de gebruikelijke behandeling met trifluorazijnzuur, waarbij ook koolstofdioxide gevormd wordt. De beschreven methode omvat de formatie van een isocyanaat, welke verkregen kan worden door de *N*-Boc urethaan te reageren met een dehydraterend reagens. Dibutyltin dilauraat en zirconium(IV) acetylacetonaat bleken de koppeling tussen het isocyanaat en de vaste drager efficiënt te katalyseren. Deze methode werd vervolgens gebruikt om vier verschillende cyclische peptiden te synthetiseren waarvan de opbrengsten en zuiverheid vergelijkbaar waren met eerder beschreven methodes.

Er zijn recentelijk bevindingen gerapporteerd waar de versterkende werking tussen diverse (geconjugeerde) Toll-like receptor (TLR) liganden is onderzocht. **Hoofdstuk 3** beschrijft de synthese van een platform dat bedoeld

is om de invloed van de ruimtelijke ordening van een paar van TLR-liganden op de immunogeniciteit te onderzoeken. Er is gebruik gemaakt van het cyclodecapeptide gramicidine S, dat zijn aminozuur zijketens aan de tegenovergestelde kanten presenteert dankzij zijn secundaire structuur. Drie verschillende gramicidine S structuren zijn gesynthetiseerd die van elkaar verschillen in dat ze hun twee amine functionaliteiten in verschillende richtingen positioneren. De amines zijn uitgerust met een maleimide- en een BCN-groep om een snelle en schone conjugatie met TLR-liganden te kunnen bewerkstelligen. TLR2, 7 en 9 agonisten zijn gesynthetiseerd die uitgerust zijn met de complementaire reactieve groep (thiol of azide) voor een totaal van negen verschillende combinaties van liganden en oriëntaties. Om het mogelijk te maken de BCN-groep, die een gespannen alkyn bevat, te introduceren op de vaste drager is de methode die beschreven is in Hoofdstuk 2 uitgebreid naar de extreem zuurgevoelige TentaGel S AC hars en is de methode om de peptide van de vaste drager te verwijderen en te zuiveren geoptimaliseerd.

Hoofdstuk 4 beschrijft de uitbreiding van het platform beschreven in Hoofdstuk 3 om het presenteren van drie verschillende TLR-agonisten mogelijk te maken. De keuze voor tetrazine/norborneen ligatie is gemaakt voor de introductie van het derde ligand welke leidde tot de nodige aanpassingen in het originele ontwerp. The BCN-groep werd verruild voor de loggere DBCO-groep om kruisreacties van de tetrazine te voorkomen. Twee gramicidine S platforms zijn gesynthetiseerd met drie amine functionaliteiten in verschillende oriëntaties. De norborneen- en DBCO-groepen zijn geïnstalleerd op de vaste drager waarvoor een extra beschermgroep nodig was tijdens de peptide synthese. De trifluoroacetamide groep bleek een effectieve beschermgroep en kon ontschermd worden na behandeling van ammonia in methanol op hogere temperaturen en met behulp van microgolfbestraling. Om gebruik te kunnen maken van de derde ligatiemethode was er een TLR7-ligand gesynthetiseerd die uitgerust was met een tetrazine en was er een adapter molecuul gesynthetiseerd voor de TLR9-agonist. Met deze moleculen zijn er drie verschillende combinaties van liganden en oriëntaties mogelijk.

Hoofdstuk 5 beschrijft de synthese van een fusie eiwit door middel van een chemische conjugatie strategie. Een linker systeem is ontworpen dat de focus

legde op het functionaliseren van het eiwit in een zo laat mogelijk stadium. Anti-PD1 en anti-CD4 VHH antilichamen zijn genetisch gemodificeerd met een C-terminale cysteïne als aangrijppunt voor de conjugaties en deze antilichamen waren verkregen in goede opbrengsten. Een linker systeem bestaande uit twee componenten zijn gesynthetiseerd voor de fusie van de twee antilichamen. De ene linker bestond uit een iodoacetamide groep voor de conjugatie met het cysteïne residue en een azidegroep voor een SPAAC reactie. De complementaire linker was uitgerust met een maleimide groep die kan reageren met de thiol aanwezig op het antilichaam en de gespannen cycloalkyn BCN als tegenhanger van de azide. De linkers bleken succesvol geconjugeerd aan anti-PD1 VHH antilichamen en een testligatie tussen de alkyn en azide is uitgevoerd waarin de vorming van het fusie eiwit was geobserveerd.

Aansluitend op de inleiding en de vier experimentele hoofdstukken biedt het proefschrift tenslotte een blik naar de toekomst, in het licht van de behaalde en beschreven resultaten, en waarin – nu de constructen en bioorthogonale platforms gereed zijn – kort aangestipt wordt voor welk type bioconjugaten, en in het verlengde daarvan voor welk biologisch onderzoek dan wel biomedische toepassingen, het onderzoek beschreven in dit proefschrift van nut zou kunnen zijn.

About the author

Evert Peterse was born in Wageningen in 1991. After finishing his secondary education (VWO) at the Hendrik Pierson College in 2009, he commenced his studies in Chemistry at the Radboud Universiteit Nijmegen. He received his bachelor's degree in 2012 after completing his research internship in the group of prof. dr. Floris P.J.T. Rutjes. As part of his continuing studies culminating in a master degree in Chemistry in 2015, he conducted a research internship in the group of prof. dr. Floris P.J.T. Rutjes focusing on multivalent presentation of carbohydrates, followed by an internship abroad at the University of Illinois at Urbana-Champaign in the group of prof. dr. Wilfred A. van der Donk investigating the mechanism of lanthionine cyclization. In 2015, he started his PhD studies at the Universiteit Leiden under the supervision of dr. Dmitri V. Filippov and prof. dr. Hermen S. Overkleeft.